ASTRONAUTICA ACTA

OFFIZIELLES ORGAN DER INTERNATIONALEN ASTRONAUTISCHEN FÖDERATION

OFFICIAL JOURNAL OF THE INTERNATIONAL ASTRONAUTICAL FEDERATION

ORGANE OFFICIEL DE LA FÉDÉRATION INTERNATIONALE D'ASTRONAUTIQUE

VOL. II

MIT 69 ABBILDUNGEN / WITH 69 FIGURES / AVEC 69 FIGURES

SPRINGER-VERLAG · WIEN

I. R. MAXWELL & CO. LTD. · LONDON/PARIS/NEW YORK

1956

Inhalt — Contents — Sommaire

Buchbesprechungen — Book Reviews — Comptes rendus

Aero-Thermodynamics of Descending Orbital Vehicles

By

Krafft A. Ehricke[1], ARS, IAS

(With 5 Figures)

(*Received September 30th, 1954*[2])

Abstract. The theory of laminar and turbulent friction and heat transfer in the compressible boundary layer with and without dissociation is discussed with respect to the descent of orbital vehicles through the atmosphere. Equations for the REYNOLDS number and heat transfer coefficients are derived in terms of parameters of significance for the descent problem, using the reference temperature method as well as the reference enthalpy method. The approximate REYNOLDS number variation across oblique and normal shock waves is given as function of flight velocity, assuming an isothermal atmosphere. An analysis is carried out for simplified computation of properties across normal and oblique shock waves in a dissociated gas.

Zusammenfassung. Die laminare und turbulente Reibungs- und Wärmeübergangs-Theorie in der kompressiblen Grenzschicht mit und ohne Dissoziation wird behandelt im Hinblick auf die Rückkehr eines Satellitenflugzeuges durch die Atmosphäre. Gleichungen werden entwickelt für REYNOLDS-Zahl und Wärmeübergangskoeffizienten unter Benutzung von Parametern, die bei Behandlung von zurückkehrenden Satellitengleitern von Bedeutung sind, wobei sowohl die Referenz-Temperatur-Methode als auch die Referenz-Enthalpie-Methode angewandt werden. Die ungefähre Variation der REYNOLDS-Zahl im Strömungsfeld vor und nach senkrechten und schrägen Schockwellen ist angegeben als Funktion der Fluggeschwindigkeit unter Annahme einer isothermen Atmosphäre. Eine Analyse zur vereinfachten Berechnung von Zustandsdaten beim Durchgang durch senkrechte und schräge Schockwellen in einem dissoziierten Gas wird durchgeführt.

Résumé. La théorie du frottement laminair et turbulent ainsi que la transmission de la chaleur dans la couche limite compressible avec et sans dissociation sont traitées en relation avec la descente des véhicules orbitaux à travers l'atmosphère. Des équations gouvernant le nombre des REYNOLDS et le coefficient de transmission de chaleur sont dérivées en fonction des paramètres pertinents au problème de la descente en utilisant la méthode de référence de la température ainsi que la méthode de référence d'enthalpie. Les variations approximatives du nombre de REYNOLDS à travers les ondes de choc obliques et normales sont présentées, en fonction de la vitesse du vol, pour une atmosphère isotherme. Le calcul des conditions que présentent les ondes de choc normales et obliques dans un gaz dissocié est l'objet d'une analyse simplificatrice.

---

[1] Convair, Guided Missile Group, San Diego Division, California, USA.

[2] A supplement was received October 4, 1955.

Nomenclature

a	local sound velocity (ft/sec)	v	gas velocity (ft/sec)
C_f	mean skin friction coefficient	x	length measured from leading edge (ft)
c_f	local skin friction coefficient	y	distance normal to the wall (ft)
c_p	specific heat at constant pressure (Btu/lb °R)	Z	ratio of molecular weight of undissociated air to that of dissociated air
E	internal energy	β	flow deflection angle
H	enthalpy (Btu/lb or cal/g)	γ	ratio of specific heats
h	heat transfer coefficient (Btu/ft² sec °R)	δ	boundary layer thickness
k	heat conductivity (Btu/hr ft °R)	η	recovery factor
(MW)	molecular weight	θ	shock angle with respect to free stream direction
p	pressure (lb/ft²)	λ	mean free molecular path
q	heat transfer rate per unit area (Btu/ft² sec)	μ	dynamic viscosity (lb sec/ft²)
q	dynamic pressure (lb/ft²)	ϱ	density (slug/ft³ = lb sec²/ft⁴)
R	Universal gas constant (1,987 18 Btu/lb °R or cal/gm °K)	σ	density ratio ϱ_0/ϱ_{00}
T	absolute static temperature (°R)	τ	shear force
T'	reference temperature [Eqs. (14)—(16)] (°R)		

$M = v/a$ MACH number
$Nu = h\,x/k$ NUSSELT number
$Pr = g\,c_p\,\mu/k$ PRANDTL number
$Re = \varrho\,x\,v/\mu$ REYNOLDS number
$St = h/c_p\,v = Nu/Re\,Pr$ STANTON number

Subscripts

b	base value	w	wall conditions
c	convective	x	in direction parallel to the wall
i	insulated wall conditions	y	in direction normal to the wall
l	laminar	δ	conditions just outside the boundary layer
NS	normal shock	00	surface (sea level) conditions
OS	oblique shock	0	free stream conditions
st	stagnation conditions	1	conditions behind shock wave
t	turbulent		

Superscripts

evaluated at reference temperature	*	ratio of property variable at temperature to variable at base enthalpy (e.g. $\varrho^* = \varrho_T/\varrho_b$)

I. Introduction

In a preceding paper [1] the atmospheric environmental flight conditions of a descending orbital glider were discussed on the basis of the lift parameter, defined as ratio of lift coefficient over lifting area load, $C_L/(W/S)$. In this paper aerothermodynamic aspects of the descent are considered, based on the continuum flow concept.

Aerothermodynamics is a new field of applied research which is being developed as the aeronautical technology advances toward very high speed and very high altitude flight. It combines aerodynamic with thermodynamic analysis, thereby taking into account frictional heating phenomena occurring in high speed compressible flow.

Compression through shock waves and in the boundary layer leads to a significant increase in air temperature. The heat produced by conversion from kinetic to thermal energy of the gas will be conducted, in part, into the skin and the interior of the vehicle. It is therefore of importance to find the amount of heat (heat transfer rate) transported into the skin, convectively and in extreme cases also by radiation. These investigations are carried out using the theory of friction and heat transfer. The heat transfer rate is, among other parameters, a function of flight speed and strength of the shock wave(s) preceding the flow field near the skin. These features, in turn, are determined by aerodynamic parameters such as angle of attack, profile of wings and body, and lift parameter $C_L/(W/S)$ which relates flight speed and flight altitude (i.e. free stream pressure). Thus aerodynamic qualifications, evaluated by means of the impact theory, have a controlling influence over the thermodynamic characteristics of a hypersonic glider; and from the viewpoint of the aerothermodynamicist, the winged orbital vehicle belongs to the extreme end of the class of hypersonic gliders.

Vol. 2 1956

The maximum permissible temperature of the vehicle, or of individual components is determined by the physical characteristics and the function of the components. The temperature must be kept sufficiently low so as not to affect adversely the structural strength of load carrying members, impair the accuracy of automatic equipment, possibly to prevent vaporization of propellants or auxiliary fluids, and to maintain reasonably comfortable living conditions for the human crew.

A measure of the amount of aerodynamic heating is the convective heat transfer rate per unit area per second, determined by the heat transfer coefficient h_c, and by the difference between insulated wall temperature T_i and actual wall temperature T_w,

$$q = h_c\,(T_i - T_w) \qquad \frac{\text{Btu}}{\text{ft}^2\,\text{sec}}. \tag{1}$$

The heat transfer coefficient depends upon boundary layer condition (laminar or turbulent), pressure in the boundary layer, gas composition in the boundary layer, flight velocity, and upon the mechanics of the boundary layer flow, that is, the length of the molecular mean free path in relation to the boundary layer thickness. All these parameters, except gas composition, are decisively influenced by the lift parameter.

II. Laminar Friction and Heat Transfer

1. Incompressible Case

Two-dimensional boundary layer flow at constant pressure and steady state is described by the following well-known fundamental equations,

Conservation of energy,

$$\varrho\, v_x \frac{\partial H}{\partial x} + \varrho\, v_y \frac{\partial H}{\partial y} = \frac{\partial}{\partial y}\left(\frac{H}{Pr}\frac{\partial H}{\partial y}\right) + \mu\left(\frac{\partial v_x}{\partial y}\right) \tag{2}$$

where the energy is given in terms of the gas enthalpy H rather than gas temperature $T = dH/c_p$ to include the case of gas dissociation,

Conservation of momentum,

$$\varrho\, v_x \frac{\partial v_x}{\partial x} + \varrho\, v_y \frac{\partial v_x}{\partial y} = \frac{\partial}{\partial y}\left(\mu \frac{\partial v_x}{\partial y}\right), \tag{3}$$

Conservation of mass,

$$\frac{\partial(\varrho v_x)}{\partial x} + \frac{\partial(\varrho v_y)}{\partial y} = 0. \tag{4}$$

In the simplest case, characterized by constant gas properties and constant temperature normal to the wall (*incompressible case*), a stream function can be defined which satisfies Eq. (4) and permits to solve Eq. (3). The resulting solution, known as BLASIUS solution, yields for the local skin friction coefficient,

$$c_f = 0{,}664\,(Re)^{-1/2}, \tag{5}$$

and for the NUSSELT number,

$$Nu = \frac{h_c\, x}{k} = \frac{c_f\,(Re)^{1/2}}{2}\,(Re)^{1/2}\,(Pr)^{1/3} = 0{,}332\,(Re)^{1/2}\,(Pr)^{1/3}. \tag{6}$$

The insulated wall temperature in Eq. (1) is related to the total or stagnation temperature by the recovery factor η as pointed out in [1]. In the incompressible case

$$\eta = (Pr)^{1/2}. \tag{7}$$

The STANTON number, another important parameter in heat transfer calculations is defined as

$$St = \frac{Nu}{Re\,Pr} = \frac{h}{c_p\, v} \tag{8}$$

or, in the incompressible case,

$$St = \frac{c_f}{2}\,Pr^{-2/3}. \tag{9}$$

This is known as the modified REYNOLDS analogy between skin friction and heat transfer, the usual REYNOLDS analogy being $St = c_f/2$ for $Pr = 1$.

2. *Compressible Case*

With increasing flight velocity, the assumption of constancy of the gas properties in the boundary layer (normal to the wall) is no longer justified, because of the temperature gradient across the boundary layer (*compressible case*). Therefore the variation of dynamic viscosity μ, thermal conductivity k, specific heat c_p and PRANDTL number Pr in the boundary layer should be taken into account. This is too cumbersome to be done by hand calculations. However, the mechanical differential analyzer (e.g. at the University of California) was used successfully for integrating the boundary layer equations (2) through (4), feeding the variation with temperature of all above named properties and of the density into the analyzer during the computation process. YOUNG and JANSSEN [2] obtained in this manner solutions of the boundary layer equations, assuming the ideal gas equation for relating density, pressure and temperature, and using exponential equations for expressing the variation of c_p, μ, and k with temperature

$$c_p = c_{p_0}\left(\frac{T}{T_0}\right)^{\varphi} \tag{10}$$

$$\mu = \mu_0\left(\frac{T}{T_0}\right)^{\omega} \tag{11}$$

$$k = k_0\left(\frac{T}{T_0}\right)^{\varkappa} \tag{12}$$

where φ, ω, and $\varkappa$ as used by YOUNG and JANSSEN are shown in Fig. 1 as function of temperature. Aside from the machine work it should be mentioned that VAN DRIEST [3], by modifying CROCCO's solution, succeeded in obtaining a closed solution which includes the variation of all air properties with temperature. However, the solution must be obtained iteratively and therefore involves more work.

The results of the machine computations of compressible boundary layer flow can be summarized briefly as follows: Eq. (7) for the recovery factor remains valid; however the PRANDTL number varies now. Skin friction $c_f (Re)^{1/2}$ and $St(Re)^{1/2}$ are a function of MACH number M, ratio of wall temperature to temperature just outside the boundary layer, T_w/T_δ, dynamic viscosity, and of T_δ itself, as well as of the PRANDTL number. However, skin friction and heat transfer remain related by the modified REYNOLDS analogy, Eq. (9), except that the PRANDTL number varies.

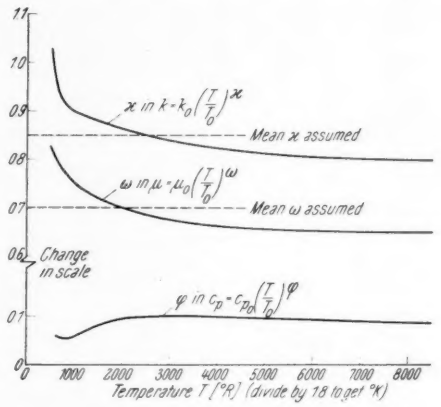

Fig. 1. Variation of exponents of power terms for k, μ and c_p with absolute temperature

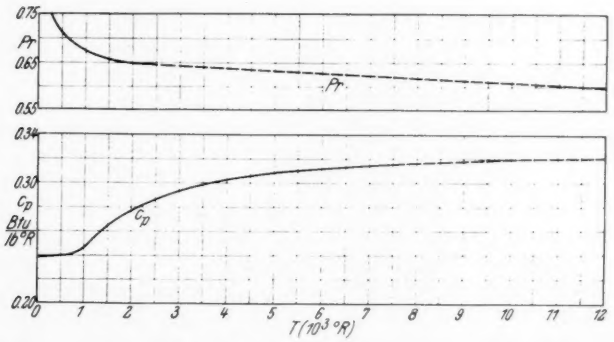

Fig. 2. Variation of specific heat and PRANDTL number of air with temperature

Fortunately, a simplification of the treatment of the compressible boundary layer problem is possible, because c_p and Pr vary much less with temperature (Fig. 2, ref. [8] for c_p and [9] for Pr) than do μ and k, as long as there is no dissociation. The variation of the viscosity is shown in Fig. 3 for several values of ω and for the SUTHERLAND equation,

$$\mu = \mu_0 \left(\frac{T}{T_0}\right)^{3/2} \frac{1 + \theta}{T/T_0 + \theta} \tag{13}$$

where $\theta = 0{,}522$ [2].

It is therefore possible in the first approximation to set c_p and Pr constant. By doing this, the viscosity-temperature relations can also be applied to the thermal conductivity — temperature variation. Thereby, and by assuming a power law

Vol. 2 1956

for μ (i.e. selecting a constant ω-value), the solution of Eqs. (2) through (4) is simplified, can be done manually, and still takes at least the main aspects of the temperature effect in compressible boundary layer flow into account. Approximate solutions of this type have been obtained by v. KÁRMÁN and TSIEN, COPE and HARTREE, HANTZSCHE and WENDT, VAN DRIEST and others [4], [5]. Their results established of course the same trend as the differential analyzer work, except for the dependency on Pr and c_p. Since the appropriate selection of exponents for μ and c_p and of Pr, is not obvious, different values have been used by the different authors, producing somewhat varying numerical results. VAN DRIEST [6] increased the accuracy of his method by using the SUTHERLAND equation.

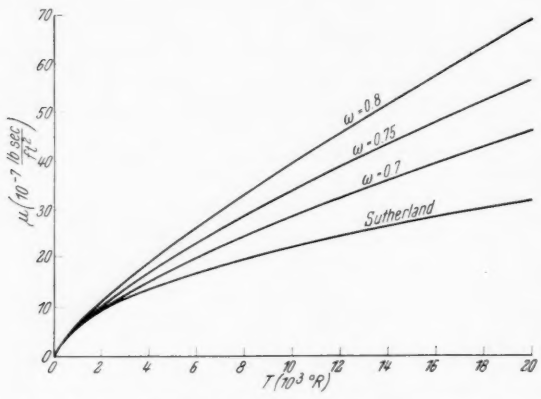

Fig. 3. Viscosity of air (perfect gas). SUTHERLAND:

$$\mu = \mu_0 \left(\frac{T}{T_0}\right)^{3/2} \frac{1+\theta}{T/T_0+\theta}, \qquad \frac{\mu}{\mu_0} = \left(\frac{T}{T_0}\right)^{\omega}$$

Note: at $T_0 = 470^0$ R, $\mu_0 = 3{,}51 \cdot 10^{-7}$ lb sec/ft²

Of main interest in the results of the exact as well as the approximate work was the fact that the incompressible relations can be used in the compressible case, if the properties, or at least μ and k vary proportionally to the absolute temperature. In fact, for $\omega = 1$ the friction coefficient becomes independent of M and T_w/T_δ, thereby approaching the incompressible case even further.

These conditions suggested the introduction of a reference temperature $T' = f(M, T_w/T_\delta)$ which could be defined in such a manner that $c_f(Re)$ and $St(Re)$ would be always (not only when $\omega = 1$) independent of M and T_w/T_δ. This then would permit outright use of the incompressible solution in determining compressible friction and heat transfer characteristics.

RUBESIN and JOHNSON were the first to introduce this method [5] and to propose an empirical T'-formula such that with the incompressible equations the same values for skin friction coefficient and heat transfer coefficient were obtained as with an established compressible solution (CROCCO). Thereafter the computational work is simplified, since the T'-method, having been checked against a compressible solution, can from then on be applied immediately. RUBESIN and JOHNSON's equation which applies up to about $M = 5{,}5$, has the form

$$\frac{T'}{T_\delta} = 0{,}42 + 0{,}032\, M_\delta^2 + 0{,}58\, \frac{T_w}{T_\delta}. \tag{14}$$

Later, YOUNG and JANSSEN [2] established for the region $M > 5{,}5$ the relation

$$\frac{T'}{T_\delta} = 0{,}70 + 0{,}023\, M_\delta^2 + 0{,}58\, \frac{T_w}{T_\delta}. \tag{15}$$

The variation of T'/T_δ with MACH number and T_w/T_δ according to Eq. (15) is shown in Fig. 4.

ECKERT [7] later combined the two MACH number regions in one equation which fits the differential analyzer data of YOUNG and JANSSEN up to $M = 30$ and in which he introduced a variable recovery factor, as indicated by the term $(Pr')^{1/2}$,

$$\frac{T'}{T} = 0{,}5 + 0{,}044\,(Pr')^{1/2}\,M^2 + 0{,}50\,\frac{T_w}{T}. \tag{16}$$

It can be seen that the use of a recovery factor which must be evaluated at reference temperature implies that Eq. (16) must be solved by iteration. However, for moderate PRANDTL number variation with temperature, the convergence is rapid.

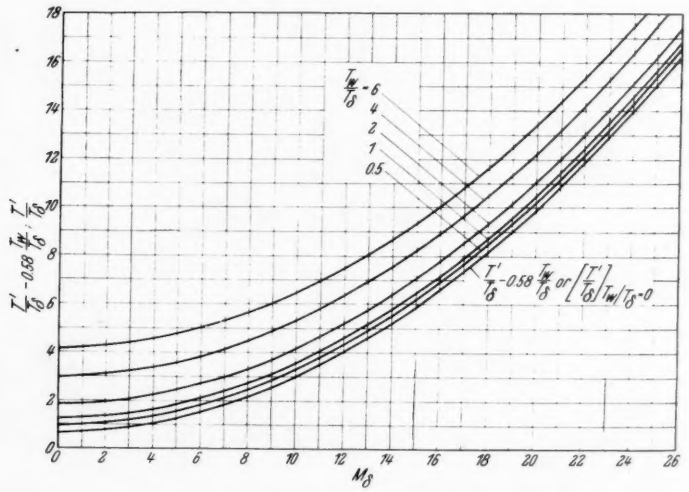

Fig. 4. Variation of T'/T_δ with MACH number

In using the reference temperature method, Eq. (5) becomes

$$c_{f'\,\text{incomp}} = 0{,}664\,(Re')^{-1/2} \tag{17}$$

where $Re' = \varrho'\,v\,x/\mu'$.

The shear force τ follows from

$$\tau = c_f\,q = c_{f'\,\text{incomp}}\,q' = 0{,}332\left(\frac{\varrho'\,v\,x}{\mu'}\right)^{1/2}\varrho'\,v^2. \tag{18}$$

This shear force must be equal to the shear force obtained in the compressible case, $c_{f\delta}\,q_\delta$,

$$c_{f\delta}\,q_\delta = c_{f'\,\text{incomp}}\,q' = 0{,}332\left(\frac{\mu_\delta}{\varrho_\delta\,v\,x}\right)^{1/2}\varrho_\delta\,v^2\left(\frac{\varrho'\,\mu'}{\varrho_\delta\,\mu_\delta}\right)^{1/2}$$

which yields

$$\frac{c_{f\delta}}{c_{f'\,\text{incomp}}} = \left(\frac{\varrho'\,\mu'}{\varrho_\delta\,\mu_\delta}\right)^{1/2} \tag{19 a}$$

or

$$c_f\,(Re)^{1/2} = 0{,}664\left(\frac{\varrho'\,\mu'}{\varrho_\delta\,\mu_\delta}\right)^{1/2}. \tag{19 b}$$

The mean skin friction coefficient $C_{f'\,\text{incomp}}$ in the incompressible case equals $2\,c_{f'\,\text{incomp}}$, whence for the reference temperature method

$$\frac{C_{f\,\delta}}{C_{f'\,\text{incomp}}} = \left(\frac{\varrho'\,\mu'}{\varrho_\delta\,\mu_\delta}\right)^{1/2}. \tag{19 c}$$

The equations (19) thus yield the local and mean skin friction coefficient in compressible flow, based on density and dynamic viscosity which are evaluated at the reference temperature T' and the stream temperature T_δ just outside the boundary layer.

Based on the NUSSELT number, one obtains for the convective laminar heat transfer coefficient in compressible flow

$$(h_{c,l})_\delta = 0{,}332\,\frac{k'}{x}\,(Re')^{1/2}\,(Pr')^{1/3}. \tag{20}$$

On the basis of the STANTON number one finds

$$(h_{c,l})_\delta = St'\,c_{p'}\,\varrho'\,v = \frac{c_{f'}}{2}\,(Pr')^{-2/3}\,c_{p'}\,\varrho'\,v \tag{21 a}$$

which can be transformed, using the preceding analysis, into

$$(h_{c,l})_\delta = 0{,}332\,c_{p'}\,(Pr')^{-2/3}\left(\frac{\varrho'\,\mu'\,v}{x}\right)^{1/2}. \tag{21 b}$$

For the ratio of compressible to incompressible STANTON number, ECKERT [7] finds

$$\frac{St_\delta}{St_{\text{incomp}}} = \left(\frac{\varrho'\,\mu'}{\varrho_\delta\,\mu_\delta}\right)^{1/2}\left(\frac{Pr_\delta}{Pr'}\right)^{2/3}. \tag{22}$$

Likewise, for the NUSSELT number ratio one can derive

$$\frac{Nu_\delta}{Nu_{\text{incomp}}} = \left(\frac{\varrho'\,\mu'}{\varrho_\delta\,\mu_\delta}\right)^{1/2}\left(\frac{Pr_\delta}{Pr'}\right)^{1/3} = \frac{St_\delta}{St_{\text{incomp}}}\left(\frac{Pr_\delta}{Pr'}\right)^{-1/3}. \tag{23}$$

The insulated wall temperature in the incompressible case follows from

$$T_i = T_0 + \eta\,\frac{{v_0}^2}{2\,g\,J\,c_p} \tag{24}$$

in the compressible case with variable specific heat

$$T_i = T_\delta + \eta\,\frac{{v_\delta}^2}{2\,g\,J\,[\overline{c}_p]_{T_\delta}^{T_i}} \tag{25}$$

and when using the reference temperature method (ECKERT [7])

$$T_i = T_\delta + \eta\,\frac{{v_\delta}^2}{2\,g\,J\,[\overline{c}_p]_{T_\delta}^{T'}}. \tag{26}$$

J is the mechanical energy equivalent. In all these cases the subscript δ means that the property is evaluated at the temperature and pressure of the flow just outside the boundary layer while the prime indicates evaluation at reference temperature. The term η in Eq. (25) varies as function of MACH number, PRANDTL number and temperature, while with the reference temperature method, Eq. (26), the recovery factor is $\eta = (Pr')^{1/2}$. The use of v_0 in Eq. (24) and of v_δ in the two subsequent equations indicates that in the compressible case the conditions just outside the boundary layer are not necessarily equal to the free stream conditions (e.g. behind a shock wave).

3. Dissociated Air

It is not exactly clear up to what MACH number incompressible relations together with the reference temperature may actually be used. There exist no experimental data on heat transfer under very high speed and high temperature conditions. RUBESIN and JOHNSON [5] indicated good agreement with the CROCCO method for the compressible case up to $M=5$ and approximate agreement up to $M = 10$. YOUNG and JANSSEN's relation [2] extends the applicability of the reference temperature method to higher MACH numbers. However, it yields somewhat higher heat transfer coefficients than obtained with the VAN DRIEST method [6]; so does ECKERT's reference temperature relation, as a few check points indicated. In fact, the latter method appears to yield even somewhat more conservative values, compared to VAN DRIEST, than YOUNG and JANSSEN. For this reason, Eq. (19) has been used in the present investigation for the compressible case without dissociation.

At very high speeds a new effect enters the picture: dissociation of the air in the boundary layer or already behind the shock wave. This affects the applicability of the previous methods. Characteristic for a dissociating gas is the rapid increase in specific heat which is due to the amount of dissociation energy which is being absorbed in addition to the thermal energy. Therefore the temperature is no longer a correct measure for the energy content of the gas and must be replaced by the enthalpy as a more general parameter. For this reason the energy equation (2) has been expressed in terms of the enthalpy. Likewise, the insulated wall temperature must be replaced by the insulated wall enthalpy. The insulated wall temperature is equal to the maximum temperature in the boundary layer, by definition, and as the boundary layer gas becomes dissociated it is again preferable to introduce the corresponding enthalpy term,

Vol. 2 1956

$$H_i = H_\delta + \eta \frac{v_\delta^2}{2\,g\,J}. \tag{27}$$

Here H_δ is the enthalpy of the air just outside the boundary layer. Depending on flight speed and strength of the shock wave, H_δ may already represent dissociated air. The reference enthalpy replaces the reference temperature. ECKERT [7] by evaluating the data of ref. [2] found the relation

$$H' = 0{,}5\,(H_w + H_\delta) + 0{,}044\,(Pr')^{1/2}\,M_\delta^2 \tag{28}$$

where M_δ is the MACH number of the dissociated air just outside the boundary layer. Its value follows from the gas speed v_δ and the local speed of sound

$$a_\delta^2 = g\,\gamma_\delta\,J\,\frac{R}{(MW)_\delta}\,T \tag{29}$$

where $(MW)_\delta$ is the molecular weight of the gas just outside the boundary layer. If the gas is dissociated, the molecular weight is related to the molecular weight of the non-dissociated gas by a factor Z,

$$(MW)_\delta = \frac{(MW)}{Z} \tag{30}$$

which is a function of temperature and pressure and is given in Table 1 below; γ_δ is the ratio of specific heats of the dissociated gas outside the boundary layer. This value can not be determined accurately without knowing the gas composition. Fortunately, γ_δ will be small, between 1,15 and 1,05, approximately. The square root of these values can be

put equal to unity without much error. The MACH number is then in good approximation given by

$$M_\delta \cong \frac{v_\delta}{(g\,J\,Z\,T_\delta\,R/(MW))^{1/2}}. \tag{31}$$

III. Turbulent Friction and Heat Transfer

There exists no accurate solution of the turbulent boundary layer equations. JOHNSON and RUBESIN assumed that the reference temperature method would also be applicable to the turbulent case. Subsequently, the method was applied to this problem by YOUNG and JANSSEN [2]. A comparison of their results with VAN DRIEST's turbulent compressible boundary layer solution [8] shows that the reference temperature method yields lower values for the local friction coefficient, hence, also for the heat transfer coefficient. However, the friction coefficient is larger than the value obtained by v. KÁRMÁN under the assumption that wall conditions apply throughout the boundary layer.

For the incompressible case, the BLASIUS solution (1/7th power law) for the turbulent boundary layer equations is in good agreement with experimental evidence at or below a REYNOLDS number of 10^7. For this case the local skin friction coefficient is

$$\frac{c_f}{2} = 0{,}029\,(Re)^{-1/5}. \tag{32}$$

For the compressible case one obtains in analogy to the laminar case

$$c_{f\delta}\,q_\delta = \tau = c_{f'\,\mathrm{incomp}}\,q' = 0{,}029\,(Re)^{-1/5}\left(\frac{\mu'}{\mu_\delta}\right)^{1/5}\left(\frac{\varrho'}{\varrho_\delta}\right)^{4/5}\varrho_\delta\,v_\delta^2 \tag{33}$$

$$\frac{c_f}{c_{f'\,\mathrm{incomp}}} = \frac{C_{f\delta}}{C_{f'\,\mathrm{incomp}}} = \left[\frac{\mu'}{\mu_\delta}\left(\frac{\varrho'}{\varrho_\delta}\right)^4\right]^{1/5}. \tag{34}$$

For the calculation of the turbulent heat transfer, the incompressible NUSSELT number can be used,

$$Nu = 0{,}029\,(Re)^{0,8}\,(Pr)^{1/3}. \tag{35}$$

Using the reference temperature method one can write for the convective turbulent heat transfer coefficient in compressible flow,

$$(h_{c,t})_\delta = 0{,}029\,\frac{k'}{x}\,(Re')^{0,8}\,(Pr')^{1/3}. \tag{36}$$

IV. Evaluation of Methods

1. Discussion

Accurate treatment of the compressible, non-dissociated case with variation of all properties, as well as of the dissociated case (MOORE [9]) must rely on machine computation. Therefore, the reference methods, based on temperature or enthalpy, are the most attractive tools for a preliminary aerothermodynamic analysis.

The reference temperature method is applicable to the laminar as well as the turbulent compressible non-dissociated case. The method can be extended into the dissociated flow regime on the premise that the increase in apparent heat transfer coefficient (due to re-association near the comparatively cool wall) approximately balances the decrease in apparent temperature T_i due to dissocia-

tion, compared to the much higher value of T_i if the air were not dissociated. Thus, by neglecting the dissociation effects in T_i as well as in h, the heat transfer rate q in Eq. (1) could be calculated by means of the reference temperature method also for the dissociated case. That this scheme is attractive becomes apparent if one considers the labor required to compute the equilibrium composition of the dissociated gas for a great variety of pressures and densities and, on this basis, to compute all the other required information. However, application of this method yields conservative results if compared to the dissociated case as presented in ref. [9].

ECKERT's reference enthalpy method is inherently more versatile, since it is of general nature and can be applied to both, the dissociated and the non-dissociated case. It can also potentially be extended to include relaxation effects and energy transport phenomena across the shock. This method, however, requires much more special information, namely knowledge of the gas composition, gas enthalpy and the properties of the dissociated gas (cf. section IV,3 below).

The subsequent evaluation of the two methods is based on the following ground rules and data:

(a) isothermal atmosphere, $T_0 = T_{00} = 470\ ^0\mathrm{R} = 261\ ^0\mathrm{K}$,
(b) because of (a), dynamic viscosity and thermal conductivity are also constant; $\mu_0 = 3{,}51 \cdot 10^{-7}$ lb sec/ft^2, $k_0 = 0{,}0133$ Btu/hr ft ^{0}R,
(c) the surface density is $\varrho_{00} = 0{,}002\,378$ slug/ft^3,
(d) the surface pressure is $p_{00} = 2\,116$ lb/ft^2,
(e) the ratio of specific heats of the ambient air is $\gamma_0 = 1{,}4$.

Vol. 2 1956

2. *Reference Temperature Method*

The T'-method for the laminar case can be evaluated on the basis of the STANTON number,

$$h_{c,l} = St\, c_p\, \varrho\, v \tag{27}$$

and for the laminar and turbulent case on the basis of the NUSSELT number [Eq. (20) and (36), respectively]. Presently the NUSSELT number will be used, because this procedure leads to convenient equations involving the REYNOLDS number. This parameter is of interest in evaluating the possibility of laminar-turbulent boundary layer transition which is accompanied by a sharp rise in the heat transfer rate. Although at the flight conditions under consideration here the REYNOLDS number is no longer the dominant parameter for transition, as pointed out in [1], it is still of interest if greater body lengths are involved. Furthermore, the KNUDSEN number λ/δ can be expressed in terms of MACH number and REYNOLDS number [10]. The KNUDSEN number is of importance for the determination of the aerodynamic or superaerodynamic flow regime behind the shock wave. The nature of the flow affects the heat transfer rate. This has been discussed in [1] and the flow regimes applied to free-stream conditions in Fig. 6 of [1].

The REYNOLDS number can be written in the form

$$Re = \frac{x\,\varrho\,v}{\mu} = \frac{x\,\varrho}{\mu} M\,a = \frac{x}{\mu} M\,p \sqrt{\gamma \frac{\varrho}{p}}. \tag{38}$$

For free-stream conditions this can be transformed into

$$Re_0 = \frac{x}{\mu} M_0\, p_0 \sqrt{\gamma \frac{p_{00}}{\varrho_{00}}} \sqrt{\frac{\sigma}{p_0/p_{00}}}. \tag{39 a}$$

In an isothermal atmosphere the last square root term is equal to one. Furthermore, using γ_0, ϱ_{00} and p_{00} as given in section IV,1 the first square root term becomes $1{,}254 \cdot 10^{-3}$ sec/ft, so that

$$Re_0 = 1{,}254 \cdot 10^{-3} \frac{x M_0 p_0}{\mu_0} . \tag{39 b}$$

For the conditions behind a plane shock wave which are equal to those just outside the boundary layer, one can write, designating the conditions behind the shock by the subscript 1,

$$Re_1 = \frac{x}{\mu_1} M_1 p_1 \sqrt{\gamma_1 \frac{\varrho_1}{p_1}} , \tag{40 a}$$

where

$$p_1 = \frac{p_1}{p_0} \frac{p_0}{p_{00}} p_{00}$$

$$\varrho_1 = \frac{\varrho_1}{\varrho_0} \sigma \varrho_{00}$$

$$M_1 = \frac{M_1}{M_0} M_0$$

$$\frac{M_1}{M_0} = \frac{v_1}{v_0} \frac{\gamma_0}{\gamma_1} \sqrt{\frac{p_0}{p_1} \frac{\varrho_1}{\varrho_0}} .$$

Considering that $\sqrt{\sigma/(p_0/p_{00})} = 1$, one obtains finally

$$Re_1 = 1{,}254 \cdot 10^{-3} \frac{x}{\mu_1} p_0 M_0 \frac{v_1}{v_0} \frac{\varrho_1}{\varrho_0} . \tag{40 b}$$

In the case of a normal shock wave the equation is simplified, because in this case $(v_1/v_0)\,(\varrho_1/\varrho_0) = 1{,}0$. The viscosity behind the shock μ_1 can be expressed in terms of μ_0 by means of Eq. (11) or (13). The REYNOLDS number ratio across the shock wave becomes then, using Eq. (11), for the normal shock

$$\frac{Re_1}{Re_0} = \frac{\mu_0}{\mu_1} = \left(\frac{T_0}{T_1}\right)^{\omega} \tag{41}$$

and for the oblique shock

$$\frac{Re_1}{Re_0} = \frac{\varrho_1}{\varrho_0} \frac{v_1}{v_0} \left(\frac{T_1}{T_0}\right)^{\omega} \tag{42}$$

where

$$\frac{\varrho_1}{\varrho_0} = \frac{\tan \theta}{\tan (\theta - \beta)} \tag{43}$$

$$\frac{v_1}{v_0} = \frac{\cos \theta}{\cos (\theta - \beta)} \tag{44}$$

$$\tan \beta = \frac{M_0^2 \sin 2\theta - 2 \cot \theta}{2 + M_0^2 (\gamma + 2 \cot \theta)} . \tag{45}$$

Stagnation temperature

$$T_{st,o} = T_0 \left(1 + \frac{\gamma - 1}{2} M_0^2\right) \tag{46}$$

$$T_1 = \frac{T_{St,0}}{1 + \frac{\gamma - 1}{2} M_1^2} \tag{47}$$

$$M_1^2 = \frac{2}{(\gamma + 1)(\varrho_1/\varrho_0) - (\gamma - 1)} \operatorname{cosec}^2(\theta - \beta) \,. \tag{48}$$

The computation proceeds by assuming θ and M_0 whence everything else can be calculated. For ω a mean value of 0,7 is sometimes used (cf. Fig. 1). The value of γ should be smaller than 1,4 when a large MACH number range is considered. However, in the present analysis, where the trend is more significant than the actual numerical value, $\gamma = 1{,}4$ has been used so that existing oblique

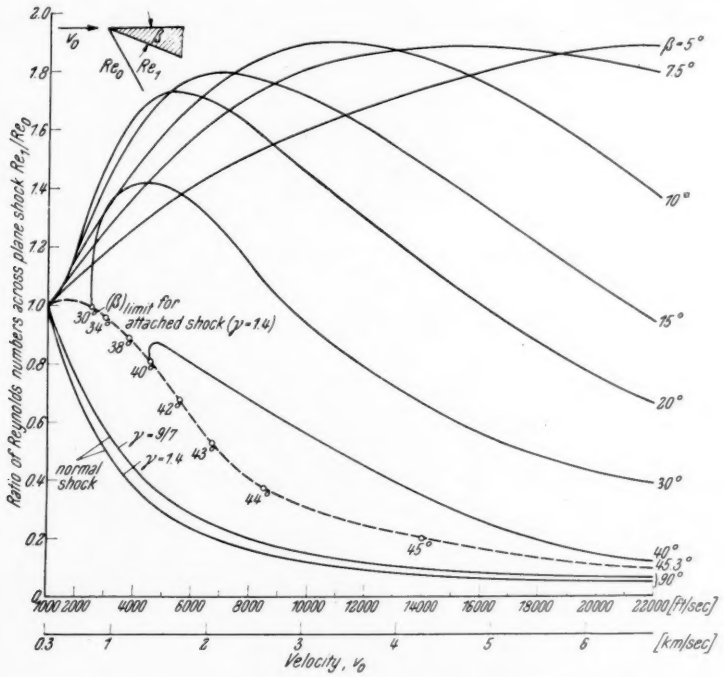

Fig. 5. REYNOLDS number ratio across plane shock as function of flight velocity ($T_0 = 470^0$ R)

shock computations (e.g. [11] through [13]) could be applied, either directly, or by adding a few points at high MACH numbers and interpolating. The result is shown in Fig. 5, for oblique shock waves as function of flight velocity at different deflection angles. For the normal shock condition the values found with $\gamma = 1{,}4$ were compared with those for $\gamma = 9/7 = 1{,}2857$, in order to give an impression of the effect of this difference in γ. It can be seen that in order to obtain low REYNOLDS numbers in the flow field behind the shock (i.e. outside the boundary layer), the descending orbital glider should operate at large angles of attack in the high-velocity region, and at small angles at flight velocities below 6000 ft/sec (roughly $M = 6$). This requirement for large angles of attack on these grounds adds a supporting argument to the demand for high drag due to lift rather than

form drag (bluntness) which was stated in [1] for reasons of obtaining high glide altitude.

The relation for the free-stream REYNOLDS number (i.e. no shock), evaluated at T', can be written in the convenient form (for isothermal atmosphere),

$$Re_0' = \frac{x \varrho_0' v_0}{\mu_0'} = (Re_{00})_{v_0} \frac{p_0}{p_{00}} \left(\frac{T_0}{T_0'}\right)^{1+\omega}, \tag{49}$$

where $(Re_{00})_{v_0}$ is the surface REYNOLDS number, evaluated at free stream velocity

$$(Re_{00})_{v_0} = \frac{x \varrho_{00} v_0}{\mu_{00}} = 6{,}775\, x\, v_0 \tag{50}$$

based on the data given in section IV,1. In an isothermal atmosphere p_0/p_{00} can be exchanged for σ.

For the REYNOLDS number behind an oblique shock one obtains in convenient and pertinent parameters

$$(Re_1')_{OS} = (Re_{00})_{v_0} \frac{v_1}{v_0} \sigma \frac{p_1}{p_0} \left(\frac{T_1}{T_1'}\right)^{1+\omega} \left(\frac{T_0}{T_1}\right)^{1+\omega} \tag{51}$$

and for the normal shock

$$(Re_1')_{NS} = (Re_{00})_{v_0} \frac{p_0}{p_{00}} \left(\frac{T_0}{T_1}\right)^{\omega} \left(\frac{T_1}{T_1'}\right)^{1+\omega}. \tag{52}$$

The laminar heat transfer coefficient for the flow field behind a plane shock wave is given by

$$h_{c,l} = 0{,}332 \frac{k_1'}{x} (Re_1')^{1/2} (Pr_1')^{1/3} \tag{53 a}$$

or, using Eq. (12)

$$h_{c,l} = 0{,}332 \frac{k_0}{x} (Pr_1')^{1/3} (Re_1')^{1/2} \left(\frac{T_1'}{T_1}\right)^{\varkappa} \left(\frac{T_1}{T_0}\right)^{\varkappa}. \tag{53 b}$$

For the oblique shock case one obtains, using Eq. (51)

$$(h_{c,l})_{OS} = 0{,}332\, k_0 (Pr_1')^{1/3} \left(\frac{(Re_{00})_{v_0}}{x}\right)^{1/2} \left(\frac{v_1}{v_0} \frac{p_1}{p_0} \sigma\right)^{1/2} \left(\frac{T_1'}{T_1}\right)^{\frac{1+\omega-2\varkappa}{2}} \left(\frac{T_1}{T_0}\right)^{\frac{1+\omega-2\varkappa}{2}}. \tag{54 a}$$

Inserting the numerical value for k_0 and using $\omega = 0{,}7$, $\varkappa = 0{,}85$ yields the temperature independent relation

$$(h_{c,l})_{OS} = 0{,}004\,41 \left(\frac{(Re_{00})_{v_0}}{x}\right)^{1/2} \left(\frac{v_1}{v_0} \frac{p_1}{p_0} \sigma\right)^{1/2} (Pr_1')^{1/3}. \tag{54 b}$$

For the flow behind a normal shock wave one finds

$$(h_{c,l})_{NS} = 0{,}003\,828 \left(\frac{(Re_{00})_{v_0}}{x}\right)^{1/2} \sigma^{1/2} \left(\frac{T_1}{T_0}\right)^{1/2} \tag{55}$$

replacing σ by p_0/p_{00} if desired.

Turbulent heat transfer behind a plane shock is given by

$$h_{c,t} = 0{,}029 \frac{k_1'}{x} (Re_1')^{0,8} (Pr_1')^{1/3} \tag{56}$$

yielding, by means of a similar operation as before, for the oblique shock field

$$(h_{c,t})_{OS} = 0{,}000\,386 (Pr_1')^{1/3} \frac{\left((Re_{00})_{v_0}\right)^{0,8}}{x^{0,2}} \left(\frac{v_1}{v_0} \frac{p_1}{p_0} \sigma\right)^{0,8} \left(\frac{T_1}{T_1'}\right)^{0,8(1+\omega)-\varkappa} \left(\frac{T_0}{T_1}\right)^{0,8(1+\omega)-\varkappa} \tag{57 a}$$

or, after inserting the numerical values

$$(h_{c,t})_{OS} = 0{,}000\,386 \frac{\left((Re_{00})_{v_0}\right)^{0,8}}{x^{0,2}} \left(\frac{v_1}{v_0}\frac{p_1}{p_0}\sigma\right)^{0,8} \left(\frac{T_1}{T_1'}\right)^{0,51} \left(\frac{T_0}{T_1}\right)^{0,51} (Pr_1')^{1/3} \qquad (57\text{ b})$$

and for the normal shock case

$$(h_{c,t})_{NS} = 0{,}000\,386 \frac{\left((Re_{00})_{v_0}\right)^{0,8}}{x^{0,2}} \sigma^{0,8} \left(\frac{T_1}{T_1'}\right)^{0,51} \left(\frac{T_1}{T_0}\right)^{0,29}. \qquad (58)$$

In applying these relations, $(Re_{00})_{v_0}$ can be computed once and for all, T_1/T_0 follows from the oblique shock data, Eqs. (43) through (48), and T_1' is obtained from Eq. (15) for a constant PRANDTL number.

3. Reference Enthalpy Method and Shock Wave Relations for a Dissociated Gas

In the reference enthalpy method the gas properties must be known as function of the enthalpy rather than the temperature. From Eqs. (8) and (9) it follows for the incompressible case

$$h = St_{incomp}\, c_p\, \varrho\, v = \frac{c_{f\,incomp}}{2} (Pr)^{-2/3}. \qquad (59)$$

In relating the compressible to the incompressible case, one finds again

$$St_\delta\, c_{p\delta}\, \varrho_\delta\, v = h_\delta = \frac{c_{f'\,incomp}}{2} (Pr')^{-2/3}\, c_p'\, \varrho'\, v$$

or, using Eq. (17) one finds for the laminar convective heat transfer coefficient in compressible flow

$$h_{c,l} = 0{,}332\, (Re')^{-1/2}\, (Pr')^{-2/3}\, c_p'\, \varrho'\, v. \qquad (60\text{ a})$$

It has been found practical to make the property data dimensionless, by expressing them in terms of a base value, designated by the subscript b. Designating the dimensionless value by an asterisk, e.g. $\varrho^* = \varrho'/\varrho_b$, one can write the resulting equation in the form

$$h_{c,l} = \frac{0{,}332}{x^{1/2}} (\varrho_b \mu_b)^{1/2}\, c_{pb}\, (\varrho^* \mu^*)^{1/2}\, c_p^*\, (Pr')^{-2/3}. \qquad (60\text{ b})$$

These base values can be taken, for example, at an enthalpy of $H_b = 112{,}3$ Btu/lb $= 62{,}38$ cal/g, corresponding to $T_b = 470\ ^0\mathrm{R} = 261{,}1\ ^0\mathrm{K}$. The dimensionless density follows then from

$$\varrho^* = \frac{\varrho'}{\varrho_b} = \frac{(MW)_T}{(MW)_{T_b}} \frac{T_b}{T'} = \frac{1}{Z} \frac{T_b}{T'}. \qquad (61)$$

The viscosity μ' can be computed according to [14], the PRANDTL number by means of ref. [15]. These methods will be applied in a subsequent paper. The specific heat c_p' follows in the conventional manner from the specific heat at the given temperature of the individual constituents of the gas in equilibrium composition.

It is realized that the computational effort for obtaining the background data is considerably greater than for the reference temperature method. However, the results are more accurate if compared with exact computations on the differential analyzer. Unfortunately much of the existing work (e.g. [9]) has been invalidated to a certain extent in view of the recently established higher value

Table I. *Properties of dissociated air* (National Bureau of Standards Rep. 3991, 1955)[1]

$\log_{10}\left(\frac{\varrho_1}{\varrho_{00}}\right)$	$T = 2000\,^0\mathrm{K} = 3600\,^0\mathrm{R}$		$T = 3000\,^0\mathrm{K} = 5400\,^0\mathrm{R}$		$T = 4000\,^0\mathrm{K} = 7200\,^0\mathrm{R}$		$T = 5000\,^0\mathrm{K} = 9000\,^0\mathrm{R}$		$T = 6000\,^0\mathrm{K} = 10\,800\,^0\mathrm{R}$		$T = 7000\,^0\mathrm{K} = 12\,600\,^0\mathrm{R}$		$T = 8000\,^0\mathrm{K} = 14\,400\,^0\mathrm{R}$	
	Z (—)	E (cal/g)	Z (—)	E (cal/g)	Z (—)	E (cal/g)	Z (—)	E (cal/g)	Z (—)	E (cal/g)	Z (—)	E (cal/g)	Z (−)	E (cal/g)
0	1,000	410,6	1,007	705,8	1,063	1203	1,146	1780	1,199	2287	1,271	3039	1,401	4284
−0,4	1,000	410,6	1,011	722,1	1,089	1301	1,172	1875	1,224	2421	1,323	3400	1,500	5035
−0,8	1,000	411,0	1,018	747,1	1,120	1414	1,192	1954	1,252	2596	1,391	3910	1,619	5961
—1,0	1,000	411,3	1,022	764,0	1,135	1471	1,200	1990	1,268	2708	1,434	4232	1,683	6460
−1,4	1,000	411,6	1,034	810,1	1,162	1573	1,215	2065	1,309	3004	1,536	5022	1,804	7418
−1,8	1,000	412,3	1,050	876,6	1,183	1649	1,230	2155	1,366	3432	1,658	5966	1,899	8175
—2,0	1,001	412,7	1,061	918,9	1,191	1676	1,239	2213	1,402	3710	1,721	6457	1,933	8442
—2,4	1,001	414,1	1,087	1023	1,202	1718	1,260	2364	1,493	4408	1,835	7353	1,977	8803
—2,8	1,001	416,2	1,118	1144	1,209	1750	1,291	2597	1,606	5286	1,918	8006	2,001	9018
—3,0	1,002	417,5	1,135	1207	1,212	1766	1,311	2751	1,668	5768	1,946	8227	2,010	9104
—3,2	1,002	419,3	1,150	1267	1,215	1783	1,336	2939	1,730	6251	1,966	8390	2,018	9188
—3,4	1,003	421,7	1,164	1320	1,218	1802	1,365	3164	1,789	6711	1,981	8510	2,026	9278
—3,6	1,004	424,3	1,176	1366	1,222	1824	1,400	3434	1,842	7122	1,992	8598	2,035	9381

$$Z = \frac{(M\,W)_{Tb}}{(M\,W)_T} \qquad E = \text{Internal energy} = H\,(\text{cal/g}) - \frac{Z\,R\,T}{(M\,W)_{Tb}}$$

[1] $Z = Z(\rho_1/\rho_{00}, T)$ has been taken from Rep. 3991; E has been computed as described in this paper

for the dissociation energy of nitrogen (revised from 7,373 electron volts per molecule = 170 kcal/gm-mole to 9,758 e.v./molecule = 225 kcal/gm-mole)[1]. The only data of dissociated air, using the higher value for N_2, which seem to be available presently are given in [16], of which an excerpt is presented in Table 1.

Like in the reference temperature case, the conditions behind the shock wave must be known before the above information can be applied. These conditions are computed for the normal shock wave case and thereafter can be used for respective oblique shock wave condition.

The normal shock wave calculation uses the well-known fundamental equations (cf. e.g. [17]) for the conservation of energy, momentum and mass, respectively,

$$\frac{v_0^2}{2} + E_0 - \frac{p_0}{\varrho_0} = \frac{v_1^2}{2} - E_1 - \frac{p_1}{\varrho_1} \tag{62}$$

$$p_0 + \varrho_0 v_0^2 = p_1 + \varrho_1 v_1^2 \tag{63}$$

$$\varrho_1 v_1 = \varrho_2 v_2. \tag{64}$$

Eliminating the velocity and pressure terms, one obtains from these equations, using the ideal gas equation in the form $p_1 = Z_1 \varrho_1 \frac{R}{(MW)} T_1$,

$$\left(\frac{p_0}{\varrho_0} - Z_1 \frac{g\,R}{(MW)} T_1\right) - \left(\frac{p_0}{\varrho_1} - \frac{\varrho_1}{\varrho_0} Z_1 \frac{g\,R}{(MW)} T_1\right) = 2\,(E_1 - E_0). \tag{65}$$

Strictly, this equation must be solved by way of iteration. However, if one solves for ϱ_1/ϱ_0,

$$\frac{\varrho_1}{\varrho_0} = \frac{2\,(E_1 - E_0) + Z_1 \frac{g\,R}{(MW)} T_1 - \frac{p_0}{\varrho_0}}{Z_1 \frac{g\,R}{(MW)} T_1} + \frac{\frac{p_0}{\varrho_1}}{Z_1 \frac{g\,R}{(MW)} T_1} \tag{66}$$

and inserts values in consistent units, one finds that the first term which does not contain ϱ_1 is of the order of 10 to 17, while the second term which contains ϱ_1 in the denominator is only of the order of 0,2 or smaller. In the first approximation the second term can therefore be neglected (or considered later as correction), whereby the density ratio across the normal shock can be obtained directly without iteration. The altitude follows from the identity $\sigma \equiv \varrho_0/\varrho_{00} \equiv \equiv (\varrho_1/\varrho_{00})/(\varrho_1/\varrho_0)$ which is equal to p_0/p_{00} in an isothermal atmosphere. The ratio ϱ_1/ϱ_{00} is an independent variable, selected from Table 1 together with the temperature T_1, which in turn yield E_1 and Z_1. The static pressure ratio across the shock follows from the ideal gas equation

$$\frac{p_1}{p_0} = Z_1 \frac{\varrho_1}{\varrho_0} \frac{T_1}{T_0}. \tag{67}$$

---

[1] KRIEGER and WHITE [19] still used the smaller value. MOORE's work [9] is based on the resulting equilibrium composition and so is Fig. 11 in [1]. It is of interest to note that a British author, GAYDON [20], in 1950 already suspected a value of 9,8 ± 0,5 e. v. which he deduced from the BIRGE-SPONER extrapolation for the ground state of the nitrogen atom, using observed vibration levels up to 6,33 e. v. In a table GAYDON presents a variety of proposed values, ranging from > 17 e. v. to 5,2 e. v.

The velocities finally are found to be, from Eqs. (63) and (64),

$$v_0 = \left[\frac{\dfrac{\underline{p}_1}{\underline{p}_0} - 1}{\dfrac{\underline{p}_0}{\varrho_0}\left(1 - \dfrac{1}{\varrho_1/\varrho_0}\right)} \right]^{1/2} \tag{68}$$

$$v_1 = \left[\frac{1 - \dfrac{\underline{p}_1}{\underline{p}_0}}{\dfrac{\underline{p}_0}{\varrho_0}\left(\dfrac{\varrho_1}{\varrho_0} - \left(\dfrac{\varrho_1}{\varrho_0}\right)^2\right)} \right]^{1/2} . \tag{69}$$

In order to apply these results to oblique shock waves, one starts with a given density ratio ϱ_1/ϱ_0 from the previous calculations, and selects a deflection angle β (which may be the sum of wedge half angle and angle of attack); by iteration one determines then the oblique shock wave angle θ from Eq. (43). The velocities v_0 and v_1 from the normal shock calculation must now be regarded as the velocity components normal to the oblique shock, $v_{n,0}$ and $v_{n,1}$. The components tangential (parallel) to the shock do not change theoretically, hence are the same on either side of the oblique shock wave. They can now be determined, knowing θ and β, by the relations

$$v_{t,0} = v_{n,0} \cot \theta \tag{70}$$

$$v_{t,1} = v_{n,1} \cot (\theta - \beta) \tag{71}$$

whence the gas velocity after the shock and the flight velocity are found from

$$v_1 = \left[v_{n,1}^2 + v_{t,1}^2 \right]^{1/2} \tag{72}$$

$$v_0 = \left[v_{n,0}^2 + v_{t,0}^2 \right]^{1/2} . \tag{73}$$

It should be pointed out that this oblique and normal shock wave analysis is based on the classical assumption of no energy transport across the shock and, for the oblique shocks, of an attached shock wave at the leading edge. This latter requirement places the region of applicability of the above analysis somewhat behind the leading edge, since a technically practical radius of curvature of the leading edge plus the rapid growth of the boundary layer thickness right behind the leading edge whereby the apparent profile bluntness is increased, make an attached shock wave unlikely at the flight conditions under consideration. Consideration of energy transport across the shock wave (by means of radiation, for instance) would tend to soften the "jump" since in this case the process is no longer truly adiabatic (it is, of course, never isentropic). Neglecting the energy transport should therefore yield conservative results. In general, it must be kept in mind that these calculations are only approximations of the true conditions which must be explored in ground and flight tests to obtain a better understanding of the phenomens involved.

A numerical evaluation of the above analysis and application to the descending orbital glider will be presented in a subsequent paper.

References

1. K. A. EHRICKE, On the Descent of Winged Orbital Vehicles. Astronaut. Acta **1**, 137 (1955).
2. G. B. W. YOUNG and E. JANSSEN, The Compressible Boundary Layer. J. Aeronaut. Sci. **19**, 229 (1952).
3. E. R. VAN DRIEST, The Laminar Boundary Layer with Variable Fluid Properties. North Amer. Aviat. Rep. AL-1866, 19 Jan., 1954.

4. H. A. Johnson and M. W. Rubesin, A Summary of Skin Friction and Heat Transfer Solutions of the Laminar Boundary Layer of a Flat Plate. Univ. California Rep. No. 12, Ser. 2, Iss. 5, 24 Feb., 1948.
5. M. W. Rubesin and H. A. Johnson, A Critical Review of Skin Friction and Heat Transfer Solutions of the Laminar Boundary Layer of a Flat Plate. Trans. Amer. Soc. Mech. Engrs. **71**, 383 (1949).
6. E. R. Van Driest, Investigation of Laminar Boundary Layer in Compressible Fluids, Using the Crocco Method. N.A.C.A. Techn. Note No. 2597, Washington, January, 1952.
7. E. R. G. Eckert, Survey in Heat Transfer at High Speeds. Wright Air Development Center Techn. Rep. 54-70, April, 1954.
8. E. R. Van Driest, Turbulent Boundary Layer in Compressible Fluids. J. Aeronaut. Sci. **18**, 145 (1951).
9. L. L. Moore, A Solution of the Laminar Boundary Layer Equations for a Compressible Fluid with Variable Properties, Including Dissociation. J. Aeronaut. Sci. **19**, 1 (1952).
10. H. S. Tsien, Superaerodynamics, Mechanics of Rarified Gases. J. Aeronaut. Sci. **13**, 653 (1946).
11. C. C. Dailey and F. C. Wood, Computation Curves for Compressible Fluid Problems. New York: J. Wiley & Sons, Inc., 1949.
12. Notes and Tables for the Use in the Analysis of Supersonic Flow, Staff of the 1 × 3 foot Supersonic Wind Tunnel Section, Ames Aeronautical Laboratory. N.A.C.A. Techn. Note No. 1428, 1947.
13. Handbook of Supersonic Aerodynamics, NAVORD Report 1488, Vol. 2. Washington 25, D.C.: Navy Department, Bureau of Ordnance, October, 1950.
14. F. J. Krieger, Calculation of the Viscosity of Gas Mixtures. Project RAND, Rep. RM-649, July, 1951.
15. C. F. Hansen, Note of the Prandtl Number of Dissociated Air. Reader's Forum, J. Aeronaut. Sci. **20**, 11 (1953).
16. J. Hilsenrath and Ch. W. Beckett, Thermodynamic Properties of Argon-free Air (0,78847 N_2, 0.211153 O_2) to 15 000° K. National Bureau of Standards Rep. 3991, April, 1955.
17. A. Ferri, Elements of Aerodynamics of Supersonic Flows. New York: MacMillan Comp., 1949.
18. H. J. Keenan and J. Kaye, Gas Tables. New York: J. Wiley & Sons, Inc., 1948.
19. F. J. Krieger and W. B. White, The Composition and Thermodynamic Properties of Air at Temperatures from 500 to 8000° K and Pressures from 0,000 01 to 100 Atmospheres. Project RAND, The RAND Corporation, R-149, Santa Monica, California, April, 1949.
20. A. G. Gaydon, Dissociation Energies and Spectra of Diatomic Molecules. New York: Dover Publications, Inc., 1950.

Some Considerations in Regard to the Physiology of Space Flight[1]

By

F. A. Hitchcock[2], ARS

Abstract. The physiological stresses that will be encountered in space flight are considered. Exposure to barometric pressures lower than 47 mm Hg (63,000 feet) will produce all of the harmful effects that would occur in a vacuum. Therefore from a physiological viewpoint any flight above 63,000 feet may be considered as space flight. In such flights sealed cabins provided with an air conditioned artificial atmosphere must be used. While compressed, liquid or chemical oxygen might be satisfactory for flights of short duration the biological method of providing such atmospheres is probably the best. Thermal stresses, accelerative forces and cosmic radiation are some of the other factors which must be considered. The physiological responses of living animals to a vacuum are discussed. It is concluded that none of these physiological problems is unsurmountable.

Zusammenfassung. Es werden die physiologischen Beanspruchungen betrachtet, die man im freien Raum antreffen wird. Die Einwirkung barometrischer Drucke, die geringer als 47 mm Hg sind (in einer Höhe von 19 000 Meter), wird alle jene schädlichen Folgen hervorrufen, die in einem Vakuum auftreten würden. Aus diesem Grund können von einem physiologischen Standpunkt Flüge oberhalb 19 000 Meter Höhe als Weltraumflug angesehen werden. Bei solchen Flügen müssen luftdichte Kabinen verwendet werden, die mit einer von einer automatischen Klimaanlage gelieferten künstlichen Atmosphäre versehen sind. Während komprimierter, flüssiger oder chemisch erzeugter Sauerstoff für Flüge von kurzer Dauer ausreichend sein dürfte, ist wahrscheinlich die biologische Methode zur Herstellung solcher Atmosphären am besten. Thermische Beanspruchung, Beschleunigungskräfte und kosmische Strahlung sind einige der übrigen Faktoren, die in Betracht gezogen werden müssen. Die physiologischen Reaktionen lebender Tiere gegen ein Vakuum werden erörtert. Es wird der Schluß gezogen, daß keines dieser physiologischen Probleme unübersteigbare Schwierigkeiten bereitet.

Résumé. Les facteurs de tension physiologique accompagnant le vol interplanétaire sont examinés. Une exposition à des pressions barométriques inférieures à 47 mm. de mercure a tous les effets nocifs du vide absolu. Par conséquent tout vol à des altitudes supérieures à 19 000 mètres peut être considéré comme interplanétaire. Il faut alors utiliser des cabines étanches pourvues d'une atmosphère artificiellement conditionnée. Si l'oxygène comprimé, liquide, ou produit par voie chimique fournit une solution satisfaisante pour les vols de faible durée, les procédés biologiques de constitution de l'atmosphère sont probablement les meilleurs. Les tensions d'origine thermique, les accélérations et les radiations cosmiques sont d'autres facteurs à prendre en considération. Le comportement physiologique des animaux dans le vide est discuté. En conclusion il semble qu' aucun de ces problèmes physiologiques ne soit insurmontable.

The medical and physiological problems involved in space flight are not unlike those concerned with flight in the higher regions of the atmosphere. We

[1] This paper was presented at the Sixth I.A.F. Congress at Copenhagen, August 3, 1955.

[2] Laboratory of Aviation Physiology, Ohio State University, Columbus/O., USA.

can, however, set up certain limits within which particular physiological problems become acute. Thus the use of oxygen by aviators is not necessary at altitudes below 10,000 feet. At the altitude of 38,000 feet it is necessary to breath 100% oxygen in order to avoid the effects of hypoxia or oxygen lack. Above 40,000 feet it is necessary to use some method of increasing pressure in the lungs. This may be done by so called pressure breathing or by pressurization of the cabin or cockpit of the aircraft. At the altitude of 50,000 feet the total barometric pressure is approximately equal to the sum of the tension of carbon dioxide and water vapor in the lungs. Therefore at this altitude no oxygen could reach the blood in the absence of pressurization, even though the aviator inhales 100% oxygen. At 63,000 feet the total barometric pressure is approximately 47 mm Hg which is the vapor pressure of blood and body fluids at body temperature (37° C). Therefore at any altitude higher than this the body fluids boil. For this reason we have reached the conclusion that the physiological and pathological effects of exposure to altitude in excess of 63,000 feet are equivalent to those that would be experienced in a complete vacuum. Therefore it has been our contention that from a physiological and medical angle flights at altitude in excess of 63,000 feet are to all intents and purposes space flights. The present ceiling for jet engines and for the conventional methods of pressurizating cabins and cockpits of aircraft is of considerable interest. Some engineers feel that by improvement and modification of existing systems the service ceilings of jet aircraft can be extended as high as 100,000 feet. Flights have already been made to altitudes as high as 90,000 feet although these have as a rule been accomplished by the use of rocket engines and the maximal altitude attained is the top of an arc. Cruising at such extreme altitudes is not yet possible. We are justified, therefore, in saying that from a physiological and medical angle space flights are already being made. It is obvious that at some point probably in the neighborhood of 90,000 or 100,000 feet the pressurization of the ambient atmosphere for use in the cabin and cockpit of the aircraft will become impracticable. It will then become necessary to resort to completely sealed cabins provided with artificial atmospheres. Here at Ohio State University we are currently engaged in the study of the best methods of providing such artificial atmosphere. In its simplest terms the problem is as follows: We must create in the cabin of the aircraft an artificial environment which will maintain human life under conditions that will provide a reasonable degree of comfort. For flights of relatively short duration this might be accomplished by the use of compressed oxygen, chemical oxygen or liquid oxygen. The system would require a method which would provide adequate pressure in the cabin as well as a sufficient tension of oxygen. It would also be necessary to provide for the absorption of carbon dioxide and water vapor. Existing knowledge as to the tolerance of human beings for carbon dioxide indicates that this gas should not be allowed to exceed a partial pressure of 8 to 10 mm Hg. It is also desirable to maintain a relative humidity not greater than 40%. It is the custom in the United States in flights to high altitudes to provide oxygen to the pilot by means of a conventional oxygen mask while the pressure in the cabin is supplied in some cases by air bled from the engine. Such air often contains toxic substances. In other cases the cockpit is pressurized by nitrogen. This represents a considerable hazard to the crew in that the removal or the leaking of the oxygen masks would result in almost immediate asphyxiation. In the study which we are conducting at the present time we aim to provide an atmosphere in the cabin which would make it unnecessary for the pilot to wear an oxygen mask and would also relieve him of the necessity of wearing a pressure suit. Emergency escape would, under these conditions, be accomplished by the

ejection of a sealed capsule in which the pilot would be separated from his ship in case of serious impairment to the aircraft.

We are investigating the possibility of providing a simple air conditioning system for sealed cabins which would consist of a container filled with liquid oxygen through which the air of the cabin would periodically be circulated. The low temperature of the liquid oxygen would freeze out both the carbon dioxide and the water vapor and provide an atmosphere that would not only be adequate in its oxygen content but would also be free from excess carbon dioxide and water vapor. It is believed that this system would be adequate for flights lasting as long as several days. The pressure in the cabin could be maintained by the evaporation of the liquid oxygen and could be controlled by an escape valve which could be set to vent air at any desired pressure. It is our opinion that this pressure should be maintained at a value of approximately 500 mm Hg (10 psi) if the duration of the flight is to be more than an hour or so. This would prevent the occurrence of any type of decompression sickness such as the bends or chokes.

In the meantime we should begin investigations of the biological method of air conditioning sealed cabins. This method would consist of the establishment of a balance between some form of plant lift and the human occupants of the sealed cabin. It seems likely that the plants to be used under such conditions would be some species of algae. Many of these minute organisms are extremely efficient in their photosynthetic processes. Investigation of the possibility of using such organism to furnish oxygen and absorb CO_2 in sealed cabins is already being carried on in the United States. The chief difficulty that is anticipated is the energy required in supplying adequate light for the photosynthetic processes carried on by the algae. However, this difficulty would be removed if sunlight were used and this seems to us the logical method.

There are many problems to be solved in the establishment of such a balanced system but none of these are insurmountable. Another subject which has been intensively studied in our laboratories is the reactions of living animals to a vacuum. These briefly may be described as follows: Immediately following exposure to an ambient pressure of 30 mm Hg or less respiration becomes deep and rapid. This hyperventilation lasts for a matter of seconds. Marked abdominal distension occurs immediately. This is, of course, due to the expansion of gases present in the intestinal tract. The animal collapses in about 8 seconds. Mild convulsions generally occurred in from 10 to 12 seconds and last for several seconds. Following this the animal is quiescent except for occasional respiratory gasps which are ineffective in ventilating the lungs. Usually lacrimation, salivation and urination occur. All fluids bubble in the tank. Thirty to fourty seconds following the reduction of pressure a secondary swelling begins. This swelling usually first occurs in the hind limbs and lower abdomen and progresses headward. The animal usually survived and showed complete recovery if the exposure to 30 mm Hg was for less than 90 seconds. Exposures of 2 minutes or longer are almost always fatal. With the exception of the swelling of the body all of these effects are believed to be the results of anoxia. The initial swelling which occurred chiefly in the abdominal region, as has already been pointed out, is due to the expansion of gas already present in the body but the secondary swelling is believed to be the result of the vaporization of tissue fluids and is a chief line of evidence in support of the belief that blood and body fluids actually do boil at these low barometric pressures. This secondary swelling was at first believed to be entirely subcutaneous. However, in later experiments incisions were made in the abdominal wall and the skin removed from the limbs in order to make direct observations on the effects of such low barometric pressure on the abdominal viscera, skeletal

muscles and fascia. In these experiments we observed that there was marked distension not only in the gas filled viscera such as the stomach and intestine but also in the bladder. This was no doubt due to the release of dissolved gases from the urine and perhaps also the rapid evaporation of this liquid. The edges of the liver were also observed to become rounded and it increased in size and became turgid. The skeletal muscles were observed to swell and bubbles of gas were observed issuing from the tissue and from the tissue fluids. This sometimes gives the appearance of conventional boiling. Considerable gas is sometimes trapped in subcutaneous fascia forming large blisters. The brain herniates through trephined openings in the cranium. It should be pointed out that there are probably three factors involved in this type of swelling. The first of these is the expansion of gas already present in the body. This occurs only in gas filled viscera. The second cause is the release of dissolved gas from the body fluids and the subsequent expansion of such gas. The third factor is the rapid vaporization or boiling of blood and body fluids.

There are of course many other factors which will produce severe physiological stresses that the crew of a space ship must endure. Some of these are briefly discussed below:

First let us consider accelerative forces. Linear acceleration during take off would undoubtedly be the most serious hazard of this type. From studies on human tolerance to stresses of this type there is ample experimental evidence indicating that normal human males in either the prone or supine position can tolerate an accelerative force of as much as 7 g for 10 minutes or more while forces up to 10 g can be tolerated for as long as 100 seconds. It is doubtful if these values would be exceeded by a rocket space ship either in take off or landing, and it therefore appears that intolerable accelerative forces would not be encountered during space flight.

Once the space ship has attained escape velocity and the rocket engines are shut off the crew will of course be in a gravity free state. No animal or man has yet been in this condition for more than a few seconds at a time and it is therefore impossible to predict all of the objective and subjective effects of such a condition. However, such evidence as we do have indicates that no serious consequences will result from exposure to the gravity free state. The worst that could happen would be an inability to orient ones self in space and the occurrance of perhaps a mild form of motion sickness. This latter might result from the absence of stimulation to the vestibular receptors in the middle ear. Presumably, however, it would be possible to substitute centrifugal force for ordinary gravity and thus largely mitigate any adverse effects of the absence of gravity.

Thermal stresses should also be considered. During escape from the atmosphere the skin temperature of the ship would undoubtedly be very high and even though the cabin is insulated, uncomfortably high temperatures would undoubtedly occur in the cabin. It seems unlikely, however, that these would exceed human tolerance. This is especially true since the duration of adiabatic compression of the ambient atmosphere, the chief cause of the high skin temperatures would probably be quite brief. Once out of the atmosphere it seems likely that comfortable temperatures could be maintained within the ship by the adjustment of the relative amounts of absorbing and reflecting areas on the surface of the space ship.

One of the minor although increasingly important stresses in conventional aircraft is noise and vibration. These would be completely eliminated in space travel except during take off and landing. Another stress which is at present impossible to evaluate is the effects of cosmic rays and ultra violet light. In order

to make life possible in a space ship it would be absolutely necessary to shield it from the excessive amount of ultra violet light present outside the earth's atmosphere. In view of the fact, however, that most glass and plastics absorb ultra violet light such shielding would probably be easily accomplished. The matter of shielding from cosmic rays is much more difficult if not impossible. Experiments are currently underway to determine the effects of cosmic rays on animals. These experiments consist of exposing small animals to regions in the upper atmosphere where cosmic radiation is at a maximum. When results of such experiments are available we will be better able to evaluate the hazards of cosmic radiation.

The matter of illumination and visibility both inside and outside the ship should be given serious consideration. In this case it is interesting to note that American test pilots who have flown to altitudes as high as 90,000 feet report that visibility was not noticeably changed. These pilots say that they were able to orient themselves by reference to the horizon and to recognize geographical land marks on the surface of the earth such as mountain ranges, deserts, etc. It has been predicted that light inside the cockpit at these high altitudes would produce strong contrasts due to the lack of an atmosphere to diffuse the light. Again the experience of test pilots who have flown in the upper atmosphere indicates that this is not altogether true. The atmosphere within the cockpit is sufficient to produce adequate diffusion of light and the illumination of instrument as well as other portions of the cockpit is perfectly adequate.

The matter of ozone and other toxic substances such as atomic clouds through which the ship might pass is of no serious importance since the cabin would be sealed and provided with an artificial atmosphere and would therefore be impenetrable to any gaseous substances through which the flight might pass.

In conclusion let me say that while there are many physiological problems in relation to space flight still to be solved nevertheless in the light of current investigations none of these seems to be insurmountable.

Relativistische Zeitdilatation eines künstlichen Satelliten

Von

F. Winterberg[1], GfW

(*Eingelangt am 10. August 1955*)

Zusammenfassung. Bei Berücksichtigung der Relativitätstheorie treten meßbare Zusatzglieder zum DOPPLER-Effekt auf, die in unmittelbarem Zusammenhang mit der EINSTEINschen Zeitdilatation stehen. Beim vorliegenden Problem darf jedoch nicht die spezielle Relativitätstheorie, sondern muß entsprechend dem Vorhandensein von Gravitationsfeldern die allgemeine Relativitätstheorie zugrunde gelegt werden. Die Überlegungen, die für den DOPPLER-Effekt maßgebend sind, übertragen sich dabei sinngemäß auf Uhren auf dem Satelliten und auf der Erde, deren Gang verglichen wird. Die Messung der Abweichung des Uhrenganges und damit die Messung der Zeitdilatation wird ermöglicht durch Vergleich zweier mit Molekülresonanzlinien gesteuerter Quarzuhren (sog. Atomuhren) auf dem künstlichen Satelliten und auf der Erdoberfläche. Es zeigt sich dabei, daß die auf einem künstlichen Satelliten befindliche Uhr gegenüber einer auf der Erdoberfläche aufgestellten im Laufe eines Jahres um einige tausendstel Sekunden und damit um einen meßbaren Betrag nachgeht.

Abstract. Considering the theory of relativity there come forth measurable supplement limbs of the DOPPLER effect which are closely connected with EINSTEIN's dilatation of time. In the problem at hand the basic element is not the Special Theory of Relativity but, according to the existence of fields of gravitation, it is the General Theory of Relativity. The considerations which are competent for the DOPPLER-effect are transferred logically to clocks on the satellite and on the earth, the motion of which is compared. The measuring of the divergence of the motion of the clock and thus the measuring of the time dilatation is made possible through comparison of two quartz-clocks (so-called atomic clocks) with molecule resonance lines on the artificial satellite and on the surface of the earth. Thereby it shows that the clock on the artificial satellite compared with a clock placed on the surface of the earth, in the course of a year will lose several thousandths of a second, that is, a measurable amount.

Résumé. La théorie de la relativité introduit dans l'effet DOPPLER des termes additionnels mesurables qui sont en relation avec la dilatation du temps. En raison de la présence d'un champ de gravitation il faut appliquer la théorie de la relativité généralisée. Les considérations pertinentes à l'effet DOPPLER s'appliquent aussi bien à la mesure du temps à la surface d'un satellite et à la surface de la terre. En utilisant des horloges à quartz, asservies à une fréquence de résonance moléculaire, le faible écart que présente la comparaison pourrait être décelé. Le calcul montre en effet que sur une période d' un an l'horloge du satellite artificiel doit retarder de quelques millièmes de secondes.

---

[1] Stuttgart, Frauenkopfstraße 3, Bundesrepublik Deutschland.

I. Einleitung

Aus der elementaren Theorie des DOPPLER-Effekts ergibt sich bekanntlich eine Frequenzänderung der Strahlung eines relativ zu einem ruhenden Beobachter bewegten Senders, wobei die Frequenzänderung proportional dem Verhältnis v/c ist. Dabei ist v die Komponente der Geschwindigkeit des Senders in Richtung auf den Beobachter hin und c die Lichtgeschwindigkeit.

Die relativistische Behandlung des DOPPLER-Effekts führt neben diesem sogenannten longitudinalen DOPPLER-Effekt noch auf den transversalen DOPPLER-Effekt, der in erster Näherung proportional $(v/c)^2$ ist, wobei v aber jetzt der Absolutbetrag der Geschwindigkeit sein soll. Dieser sogenannte transversale DOPPLER-Effekt hängt eng mit der EINSTEINschen Zeitdilatation zusammen und ist von der Bewegungsrichtung des Senders relativ zum Beobachter unabhängig.

Die Überlegungen, die für den DOPPLER-Effekt maßgebend sind, übertragen sich auf die Frage nach dem Gang von zwei Uhren im System des bewegten Senders und in demjenigen des Beobachters.

Setzen wir eine periodische Bewegung des Senders relativ zum Beobachter voraus, wie sie beim künstlichen Satelliten gegeben ist, so wird beim Vergleich des Ganges der Uhr auf dem Satelliten mit dem Gang der Uhr des Beobachters der gewöhnliche DOPPLER-Effekt (longitudinaler Effekt) ein periodisch schwankendes Vor- und Nachgehen der Uhr des Satelliten gegenüber der Uhr des Beobachters bewirken. Anders beim transversalen DOPPLER-Effekt, der zu einem stetigen Anwachsen des Gangunterschiedes der auf dem Satelliten befindlichen Uhr gegenüber der Uhr des Beobachters führen wird.

Zur Messung des hierbei auftretenden Gangunterschiedes sind gewöhnliche Quarzuhren noch zu ungenau und daher ungeeignet. Neuerdings sind aber Quarzuhren von unerhörter Genauigkeit entwickelt worden, bei denen die Temperatur des Steuerquarzes mit einer Molekülresonanzlinie geregelt wird. Diese sogenannten Atomuhren haben die Genauigkeit von 10^{-12} in ihrem Gang. Sie werden sich zur Nachprüfung des hier beschriebenen Effekts eignen.

In Verbindung mit dem Bau eines künstlichen Satelliten ergibt sich damit eine neue Möglichkeit zur Nachprüfung der allgemeinen Relativitätstheorie.

II. Allgemeine Theorie des Doppler-Effekts von zwei in einem Gravitationsfeld sich bewegenden Körpern

Die hier erläuterte allgemeine DOPPLER-Formel findet sich in dem bekannten Buch von TOLMAN[1].

Als Lösung der EINSTEINschen Feldgleichungen der Gravitation ergibt sich allgemein eine nichteuklidische Form des vierdimensionalen Linienelements

$$ds^2 = g_{\mu\nu}\, dx_\mu\, dx_\nu; \qquad (\mu, \nu = 1, 2 \ldots 4), \tag{1}$$

wobei über doppelt vorkommende griechische Indizes nach Vereinbarung zu summieren ist. Die Lage von Sender und Empfänger sind Funktionen der Zeit, wobei dem Sender der Index 1 und dem Beobachter der Index 2 gegeben werde. Weiters sei angenommen, daß zur Zeit t_1 ein Signal den Sender verläßt und zur Zeit t_2 den Beobachter erreicht. Zwischen beiden Zeiten besteht eine Abhängigkeit der Form

$$t_2 = f(t_1), \tag{2}$$

---

[1] R. C. TOLMAN, Relativity, Thermodynamics and Cosmology, S. 288. Oxford: Clarendon Press.

die sich aus der Ausbreitungsbedingung des Lichtes $ds = 0$ errechnet. Mit diesen Festsetzungen ergibt sich dann als allgemeine DOPPLER-Formel:

$$\frac{\Delta t_2}{\Delta t_1} = \frac{(g_{\mu\nu}\,\dot{x}_\mu\,\dot{x}_\nu)_2^{1/2}}{(g_{\mu\nu}\,\dot{x}_\mu\,\dot{x}_\nu)_1^{1/2}} \frac{d}{dt_1} f(t_1). \tag{3}$$

Durch Gl. (3) ist das Verhältnis eines Zeitintervalls von zwei gleichen, im System des Senders und des Beobachters befindlichen Uhren festgelegt.

III. Spezialisierung auf ein zentralsymmetrisches Gravitationsfeld

Gl. (3) soll nun auf den Fall eines zentralsymmetrischen Gravitationsfeldes angewandt werden, wie er bei einem im Erdkraftfeld sich bewegenden Satelliten vorliegt.

Die Lösung der Feldgleichungen ist dabei durch das SCHWARZSCHILDsche Linienelement gegeben, das in sphärischen Polarkoordinaten lautet:

$$ds^2 = g_r\,dr^2 + g_\vartheta\,d\vartheta^2 + g_\varphi\,d\varphi^2 + g_t dt^2, \tag{4}$$

wobei

$$g_r = \frac{1}{1 - \frac{2\alpha}{r}}; \qquad g_\vartheta = r^2$$
$$g_\varphi = r^2 \sin^2\vartheta; \qquad g_t = -c^2\left(1 - \frac{2\alpha}{r}\right) \tag{5}$$

ist, mit der Abkürzung $\alpha = G\,M/c^2$, wo G die Gravitationskonstante, M die Erdmasse und c die Lichtgeschwindigkeit ist. Zur Aufstellung der Abhängigkeit (2) setzen wir

$$t_2 = t_1 + \frac{s}{c}; \tag{6}$$

dabei ist s der Abstand des Satelliten vom Beobachter zur Zeit t_1. Gl. (6) gilt näherungsweise, wenn die Geschwindigkeit des Satelliten relativ zum Beobachter klein gegen die Lichtgeschwindigkeit ist. Zur Berechnung von s setzen wir außerdem $g_r = 1$, was einer Vernachlässigung der Raumkrümmung gleichkommt.

Wir erhalten zunächst an Stelle von Gl. (3):

$$\frac{\Delta t_2}{\Delta t_1} = \frac{(g_r\,\dot{r}^2 + g_\vartheta\,\dot{\vartheta}^2 + g_\varphi\,\dot{\varphi}^2 + g_t)_2^{1/2}}{(g_r\,\dot{r}^2 + g_\vartheta\,\dot{\vartheta}^2 + g_\varphi\,\dot{\varphi}^2 + g_t)_1^{1/2}} \frac{d}{dt_1} f(t_1). \tag{7}$$

Mit Gl. (6) ergibt sich:

$$\frac{df(t_1)}{dt_1} = 1 + \frac{d}{dt_1}\left(\frac{s}{c}\right) = 1 + \frac{1}{c}\frac{ds}{dt_1} = 1 + P(t_1), \tag{8}$$

wo $P(t)$ eine periodische Funktion der Zeit ist. Somit erhalten wir statt (7):

$$\frac{\Delta t_2}{\Delta t_1} = \big(1 + P(t_1)\big)\,\frac{(g_r\,\dot{r}^2 + g_\vartheta\,\dot{\vartheta}^2 + g_\varphi\,\dot{\varphi}^2 + g_t)_2^{1/2}}{(g_r\,\dot{r}^2 + g_\vartheta\,\dot{\vartheta}^2 + g_\varphi\,\dot{\varphi}^2 + g_t)_1^{1/2}}. \tag{7 a}$$

Die rechte Seite von Gl. (7) setzt sich aus einem periodischen, mit $P(t_1)$ multiplizierten, und aus einem „säkularen", linear mit der Zeit anwachsenden Teil zusammen.

Im folgenden werden wir uns auf den säkularen Anteil beschränken, da er allein Anlaß zu einer relativistischen Zeitdilatation gibt, die sich nicht wie beim periodischen Teil im Zeitmittel heraushebt.

IV. Spezialisierung auf eine Kreisbahn

Um die Verhältnisse an einem einfachen Beispiel zu studieren, legen wir jetzt die Annahme einer Kreisbahn des künstlichen Satelliten zugrunde. Die Überlegungen lassen sich unschwer auf elliptische Bahnen erweitern.

Wir wollen annehmen, daß der Satellit sich mit dem Neigungswinkel i gegen die Äquatorebene bewegt. Um das vierdimensionale Linienelement des Satelliten zu berechnen, benützen wir die Invarianz von ds in Beziehung auf räumliche Drehungen und berechnen ds im Bezugssystem, das die Bahnebene als Grundebene hat. Unter diesen Voraussetzungen wird:

$$\vartheta_1 = 90^0; \qquad \dot{r}_1 = \dot{\vartheta}_1 = 0; \qquad \dot{\varphi}_1 = \omega_1 = c\sqrt{\frac{a}{{r_1}^3}},$$

woraus sich ergibt:

$$g_r\,\dot{r}_1{}^2 + g_\vartheta\,\dot{\vartheta}_1{}^2 + g_\varphi\,\dot{\varphi}_1{}^2 + g_t = -c^2\left[1 - 3\frac{a}{r_1}\right]. \tag{9}$$

Für den Beobachter auf der Erde legen wir das äquatoriale Polarkoordinatensystem zugrunde. Dabei ist zu berücksichtigen, daß

$$\dot{r}_2 = \dot{\vartheta}_2 = 0; \qquad \dot{\varphi}_2 = \omega_2$$

ist, wo ω_2 die Winkelgeschwindigkeit der Erdumdrehung ist. Mit der Abkürzung $\beta = {r_2}^3\,{\omega_2}^2/c^2$ erhalten wir:

$$g_r\,\dot{r}_2^2 + g_\vartheta\,\dot{\vartheta}_2^2 + g_\varphi\,\dot{\varphi}_2^2 + g_t = -c^2\left[1 - 2\frac{a}{r_2} - \frac{\beta\sin^2\vartheta_2}{r_2}\right]. \tag{10}$$

Einsetzen von (9) und (10) in (7 a) und Beschränkung auf den säkularen Anteil ergibt:

$$\frac{\Delta t_2}{\Delta t_1} = \frac{\left[1 - \dfrac{3a}{r_1}\right]^{1/2}}{\left[1 - \dfrac{2a}{r_2} - \dfrac{\beta\sin^2\vartheta_2}{r_2}\right]^{1/2}}. \tag{11}$$

Entwickeln wir hier die rechte Seite bis zu Gliedern zweiter Ordnung in v/c, so erhalten wir:

$$\frac{\Delta t_2}{\Delta t_1} = 1 - \frac{3}{2}\frac{a}{r_1} + \frac{a}{r_2} + \frac{\beta\sin^2\vartheta_2}{2r_2}. \tag{12}$$

Setzen wir $\Delta t_2 - \Delta t_1 = \Delta t$ und $\Delta t_1 = t$, so schreibt sich Gl. (12):

$$\frac{\Delta t}{t} = -\frac{3}{2}\frac{a}{r_1} + \frac{a}{r_2} + \frac{\beta\sin^2\vartheta_2}{2r_2}. \tag{12 a}$$

Der letzte Term auf der rechten Seite von (12 a) beschreibt den Einfluß der relativ zum Satelliten erfolgenden Erdrotation auf die Zeitdilatation. Dieser Beitrag ist gegenüber den anderen Beiträgen von untergeordneter Bedeutung. Vernachlässigen wir der Einfachheit halber diesen Term, so zeigt sich das interessante Resultat, daß die Zeitdilatation für die durch die Bedingung

$$-\frac{3}{2}\frac{a}{r_1} + \frac{a}{r_2} = 0 \tag{13}$$

gegebene Höhe der Kreisbahn über der Erdoberfläche verschwindet. Aus (13) folgt dafür:

$$r_1 = \frac{3}{2}\,r_2. \tag{14}$$

Da der Erdradius $r_2 = 6400$ km beträgt, folgt für die Höhe der Kreisbahn $h = r_1 - r_2 = 3200$ km. Dieses Resultat ist deshalb bemerkenswert, weil ohne Berücksichtigung der allgemeinen Relativitätstheorie sich dies nicht ergeben hätte.

Wir wollen die Betrachtungen mit einem numerischen Beispiel beschließen, indem wir annehmen, daß der Beobachter auf der Erdoberfläche sich auf dem Nordpol befindet. In diesem Fall verschwindet das von der Erdrotation herrührende Glied. Weiter soll der Satellit in einer Höhe von 1650 km die Erde umkreisen. Damit ergibt sich:

$$\frac{\Delta t}{t} = \alpha\left(\frac{1}{r_2} - \frac{3}{2}\frac{1}{r_2}\right) = -1{,}3 \cdot 10^{-10}. \tag{15}$$

Im Laufe eines Jahres geht daher die auf dem Satelliten sich befindende Uhr gegenüber der auf der Erde befindlichen um $4{,}2 \cdot 10^{-3}$ sec nach. Um den skizzierten Effekt reproduzierbar zu machen, ist es erforderlich, über Uhren zu verfügen, die mindestens mit einer Genauigkeit von 10^{-11} gehen. Dieser Forderung genügen die eingangs erwähnten Atomuhren. Sie erlauben den vorausgesagten Effekt auf zwei Dezimalen genau zu bestimmen.

Auf den hier hingewiesenen Effekt begründet sich eine neue eindrucksvolle Möglichkeit zur Überprüfung der allgemeinen Relativitätstheorie.

Relativistische Raketenmechanik

Von

H. G. L. Krause[1], GfW

(*Eingelangt am 24. September 1955*)

Zusammenfassung. In dieser Arbeit wird die Mechanik der speziellen Relativitätstheorie auf Systeme mit zeitlich veränderlicher Ruhemasse (Raketen) erweitert. Untersucht werden der Impuls- und Energiesatz sowie das Gesetz der Massenabnahme einer beliebig beschleunigten Rakete im freien Raum ohne äußere Kräfte, und zwar im System des ruhenden Erdbeobachters und im System des mit der Rakete mitbewegten Astronauten. Sodann werden zwei Spezialfälle behandelt, nämlich die Bewegung einer Rakete mit konstanter Eigenbeschleunigung und die Bewegung einer Rakete mit konstantem Massendurchsatz (Schub).

Abstract. In this paper the mechanics of the Special Theory of Relativity are extended to systems with timely changeable rest masses (rockets). There will be examined the theorem of impulse and energy as well as the law of the decrease of the mass of a rocket with an optional acceleration in a free space without outward power, that is, in the system of the resting ground observer and in the system of the astronaut, moved with the rocket. Then two special cases are treated, namely the movement of a rocket with constant self-acceleration and the movement of a rocket with a constant amount of mass flow rate (thrust).

Résumé. Ce travail étend la mécanique de la relativité restreinte aux systèmes dont la masse de repos est variable dans le temps (fusées). Les théorèmes d'impulsion et d'énergie sont examinés ainsi que la réduction de masse d'une fusée subissant une accélération quelconque dans l'espace libre sans forces extérieures appliquées. Les théorèmes sont exprimés aussi bien en coordonnées géodesiques que dans celles liées à la fusée. Deux cas spéciaux sont ensuite traités: le mouvement d'une fusée avec accélération propre constante et son mouvement avec un flux massique (poussée) constante.

I. Ableitung der Beziehung zwischen Beschleunigung und Eigenbeschleunigung einer Rakete aus den Lorentz-Transformationen

Betrachtet man ein ruhendes Koordinatensystem $K\,[\mathfrak{r}(x, y, z); t]$ und ein gleichförmig bewegtes System $K'[\mathfrak{r}'(x', y', z'); t']$, das sich mit der konstanten Geschwindigkeit $\mathfrak{v}$ gegen das System K parallel bewegt (Systemgeschwindigkeit), so ist der Übergang von einem System zum anderen gegeben durch die allgemeine LORENTZ-Transformation [1]:

$$\mathfrak{r}' = \mathfrak{r} - \mathfrak{v}\left\{\frac{(\mathfrak{r}\,\mathfrak{v})}{v^2}\left(1 - \frac{1}{a}\right) + \frac{t}{a}\right\}; \qquad t' = \frac{t - \dfrac{(\mathfrak{r}\,\mathfrak{v})}{c^2}}{a} \tag{1}$$

[1] Stuttgart-Bad Cannstatt, Tölzerstraße 10/I, Bundesrepublik Deutschland.

oder umgekehrt

$$\mathfrak{r} = \mathfrak{r}' + \mathfrak{v}\left\{-\frac{(\mathfrak{r}'\,\mathfrak{v})}{v^2}\left(1-\frac{1}{\alpha}\right)+\frac{t'}{\alpha}\right\}; \qquad t = \frac{t'+\frac{(\mathfrak{r}'\,\mathfrak{v})}{c^2}}{\alpha} \tag{2}$$

mit den Abkürzungen (c = Lichtgeschwindigkeit)

$$\beta^2 = \frac{v^2}{c^2}, \qquad \alpha = \sqrt{1-\beta^2}, \qquad \beta = \sqrt{1-\alpha^2}.$$

Dabei ist $\mathfrak{r} = \mathfrak{r}' = 0$ für $t = t' = 0$. Hat ein Punkt die Geschwindigkeit $\mathfrak{w} = \dot{\mathfrak{r}}$ relativ zum System K und die Geschwindigkeit $\mathfrak{w}' = \dot{\mathfrak{r}}'$ relativ zum System K', so folgen durch zeitliche Differentiation der Gln. (1) und (2) die Beziehungen:

$$\mathfrak{w}' = \frac{d\mathfrak{r}'}{dt'} = \frac{d\mathfrak{r}'/dt}{dt'/dt} = \frac{\mathfrak{w}\,\alpha - \mathfrak{v}\left\{\frac{(\mathfrak{w}\,\mathfrak{v})}{v^2}(\alpha-1)+1\right\}}{1-\frac{(\mathfrak{w}\,\mathfrak{v})}{c^2}} \tag{3}$$

und

$$\mathfrak{w} = \frac{d\mathfrak{r}}{dt} = \frac{d\mathfrak{r}/dt'}{dt/dt'} = \frac{\mathfrak{w}'\,\alpha + \mathfrak{v}\left\{-\frac{(\mathfrak{w}'\,\mathfrak{v})}{v^2}(\alpha-1)+1\right\}}{1+\frac{(\mathfrak{w}'\,\mathfrak{v})}{c^2}} \tag{4}$$

als Grundlage der relativistischen Kinematik, wobei

$$\frac{dt'}{dt} = \frac{1}{\alpha}\left\{1-\frac{(\mathfrak{w}\,\mathfrak{v})}{c^2}\right\} \tag{5}$$

ist. Wenn $\mathfrak{w}\|\mathfrak{v}$, bzw. $\mathfrak{w}'\|\mathfrak{v}$ ist, dann lautet das Additionstheorem der Geschwindigkeiten

$$\mathfrak{w}' = \frac{\mathfrak{w}-\mathfrak{v}}{1-\frac{(\mathfrak{w}\,\mathfrak{v})}{c^2}}; \qquad |\mathfrak{w}'| = c\left[1-\frac{\left(1-\left|\frac{\mathfrak{w}}{c}\right|\right)\cdot\left(1+\left|\frac{\mathfrak{v}}{c}\right|\right)}{1-\frac{(\mathfrak{w}\,\mathfrak{v})}{c^2}}\right] \leqq c \tag{6}$$

beziehungsweise

$$\mathfrak{w} = \frac{\mathfrak{w}'+\mathfrak{v}}{1+\frac{(\mathfrak{w}'\,\mathfrak{v})}{c^2}}; \qquad |\mathfrak{w}| = c\left[1-\frac{\left(1-\left|\frac{\mathfrak{w}'}{c}\right|\right)\cdot\left(1-\left|\frac{\mathfrak{v}}{c}\right|\right)}{1+\frac{(\mathfrak{w}'\,\mathfrak{v})}{c^2}}\right] \leqq c. \tag{7}$$

Für die relativistische Dynamik benötigt man die Beschleunigungen, die sich durch zeitliche Differentiation der Gln. (3) und (4) ergeben:

$$b' = \frac{d\mathfrak{w}'}{dt'} = \frac{d\mathfrak{w}'/dt}{dt'/dt} = \alpha^2\frac{\dot{\mathfrak{w}}\left(1-\frac{(\mathfrak{w}\,\mathfrak{v})}{c^2}\right)+\frac{(\dot{\mathfrak{w}}\,\mathfrak{v})}{c^2}\left\{\mathfrak{w}-\frac{\mathfrak{v}}{1+\alpha}\right\}}{\left(1-\frac{(\mathfrak{w}\,\mathfrak{v})}{c^2}\right)^3} \tag{8}$$

beziehungsweise

$$b = \dot{w} = \frac{d\mathfrak{w}}{dt} = \frac{d\mathfrak{w}/dt'}{dt/dt'} = \alpha^2\frac{\dot{\mathfrak{w}}'\left(1+\frac{(\mathfrak{w}'\,\mathfrak{v})}{c^2}\right)-\frac{(\dot{\mathfrak{w}}'\,\mathfrak{v})}{c^2}\left\{\mathfrak{w}'+\frac{\mathfrak{v}}{1+\alpha}\right\}}{\left(1+\frac{(\mathfrak{w}'\,\mathfrak{v})}{c^2}\right)^3}. \tag{9}$$

Vol. 2 1956

Diese Gleichungen sollen nun auf die Bewegung einer schnellen Rakete angewendet werden. Im Zeitpunkt t habe die Rakete die Geschwindigkeit $\mathfrak{v}$ relativ zum System K des ruhenden Erdbeobachters (z. B. im Startort). In der Rakete sei jetzt der Anfangspunkt des mitbewegten Systems K' der Astronauten (Raumschiffbesatzung). Die Systemgeschwindigkeit, mit der sich das System K' gegenüber dem System K verschiebt, ist also gleich der Geschwindigkeit $\mathfrak{v}$ der Rakete im System K. Setzt man in die Gl. (3) $\mathfrak{w} = \mathfrak{v}$ ein, so erhält man $\mathfrak{w}' = 0$ (Transformation auf Ruhe). Im System K' der Astronauten ist also die Geschwindigkeit der Rakete $\mathfrak{w}' = 0$. Ferner folgt aus Gl. (5)

$$\frac{dt'}{dt} = \sqrt{1 - \frac{v^2}{c^2}} = \sqrt{1 - \beta^2} = a. \tag{10}$$

Die zum System K' zugehörige Zeit t' nennt man auch die Lokalzeit oder die Eigenzeit τ. Die Beschleunigung im Ruhesystem K' ergibt sich, wenn man in der Gl. (8) $\mathfrak{w} = \mathfrak{v}$ setzt, nämlich

$$b' = \dot{\mathfrak{w}}' = \frac{a\,\dot{\mathfrak{w}} + \dfrac{(\dot{\mathfrak{w}}\,\mathfrak{v})}{c^2} \cdot \dfrac{\mathfrak{v}}{1+a}}{a^3} = \frac{a\,\dot{\mathfrak{w}} + \dfrac{(\dot{\mathfrak{w}}\,\mathfrak{v})}{v^2}\,\mathfrak{v}\,(1-a)}{a^3}. \tag{11}$$

Ist $\dot{\mathfrak{w}} \| \mathfrak{v}$, so folgt daraus

$$b' = \dot{\mathfrak{w}}' = \frac{\dot{\mathfrak{w}}}{a^3} = \frac{\dot{\mathfrak{w}}}{(1-\beta^2)^{3/2}}; \tag{12}$$

hingegen ist für $\dot{\mathfrak{w}} \perp \mathfrak{v}$

$$b' = \dot{\mathfrak{w}}' = \frac{\dot{\mathfrak{w}}}{a^2} = \frac{\dot{\mathfrak{w}}}{1-\beta^2}. \tag{13}$$

Da das System der Astronauten mit der Rakete gekoppelt ist, so sind jetzt $\mathfrak{v}$ und $a = \sqrt{1 - v^2/c^2}$ Funktionen der Zeit t. Mithin wird jetzt mit $\mathfrak{w} = \mathfrak{v}$:

$$\frac{d}{dt}\left(\frac{\mathfrak{w}}{\sqrt{1 - v^2/c^2}}\right) = \frac{\left(1 - \dfrac{v^2}{c^2}\right)\dot{\mathfrak{w}} + \dfrac{(\mathfrak{v}\,\dot{\mathfrak{v}})}{c^2}\,\mathfrak{w}}{\left(1 - \dfrac{v^2}{c^2}\right)^{3/2}} = \frac{a^2\,\dot{\mathfrak{w}} + \dfrac{(\dot{\mathfrak{w}}\,\mathfrak{v})}{c^2}\,\mathfrak{v}}{a^3}. \tag{14}$$

Ist $\dot{\mathfrak{w}} \| \mathfrak{v}$, so gilt im Hinblick auf die Gln. (14) und (12) für ein beschleunigtes System:

$$\frac{d}{dt}\left(\frac{\mathfrak{w}}{\sqrt{1 - v^2/c^2}}\right) \equiv \frac{d}{dt}\left(\frac{\mathfrak{w}}{a}\right) = \frac{\dot{\mathfrak{w}}}{a^3} = b' \equiv \dot{\mathfrak{w}}'. \tag{15}$$

Hingegen folgt für $\dot{\mathfrak{w}} \perp \mathfrak{v}$ aus den Gln. (14) und (13):

$$\frac{d}{dt}\left(\frac{\mathfrak{w}}{\sqrt{1 - v^2/c^2}}\right) \equiv \frac{d}{dt}\left(\frac{\mathfrak{w}}{a}\right) = \frac{\dot{\mathfrak{w}}}{a} = a\,b' \equiv a\,\dot{\mathfrak{w}}'. \tag{16}$$

II. Der Schub und das Gesetz der Massenabnahme einer beliebig beschleunigten Rakete im freien Raum ohne äußere Kräfte

Im folgenden sollen die Daten der Rakete und der ausgestoßenen Gase im System K des ruhenden Erdbeobachters (z. B. am Startplatz) ohne Index und diejenigen im System K_0 des mit der Rakete mitbewegten Astronauten mit dem Index 0 gekennzeichnet werden, wie das in Tab. 1 geschehen ist.

Tabelle 1

	Im System K des ruhenden Erdbeobachters	Im System K_0 der mitbewegten Astronauten
Geschwindigkeit der Rakete	v	0
Jeweilige Masse der Rakete	$m = \dfrac{m_0}{\sqrt{1 - v^2/c^2}}$	m_0
Geschwindigkeit der ausgestoßenen Gase	$a = \dfrac{a_0 - v}{1 - \dfrac{a_0 v}{c^2}}$	a_0
Masse der ausgestoßenen Gase	$dm = \dfrac{dm_0^*}{\sqrt{1 - a^2/c^2}}$	$dm_0 = \dfrac{dm_0^*}{\sqrt{1 - a_0^2/c^2}}$
Zeitelement	$dt = \dfrac{dt_0}{\sqrt{1 - v^2/c^2}}$	dt_0
Beschleunigung der Rakete	$b = b_0 (1 - v^2/c^2)^{3/2}$	b_0
Schubkraft der Rakete	$\dfrac{d}{dt}(m v) = -a \dfrac{dm}{dt} = F$	$m_0 b_0 = -a_0 \dfrac{dm_0}{dt_0} = F_0$

Ist m_0 die Ruhemasse der Rakete und dm_0^* die Ruhemasse der ausgestoßenen Gase, dann ist die Masse der Rakete, bzw. der Gase im System K des Erdbeobachters:

$$m = \frac{m_0}{\sqrt{1 - v^2/c^2}}, \qquad \text{bzw.} \qquad dm = \frac{dm_0^*}{\sqrt{1 - a^2/c^2}}. \tag{17}$$

In diesem System lautet der Impulssatz

$$\frac{d}{dt}\left(\frac{m_0 \mathfrak{v}}{\sqrt{1 - v^2/c^2}}\right) = -\mathfrak{a} \frac{dm_0^*/dt}{\sqrt{1 - a^2/c^2}} \equiv \mathfrak{F} \tag{18}$$

oder wegen Gl. (17)

$$\frac{d}{dt}(m \mathfrak{v}) = -\mathfrak{a} \frac{dm}{dt} \equiv \mathfrak{F}. \tag{19}$$

Dabei ist $\mathfrak{F}$ die Schubkraft der Rakete im System des Erdbeobachters. Durch Anwendung des relativistischen Additionstheorems der Geschwindigkeiten hat man, wenn der Schub in Richtung der Geschwindigkeit $\mathfrak{v}$ wirkt $(\mathfrak{a} \| \mathfrak{v})$:

$$\mathfrak{a} = \frac{\mathfrak{a}_0 - \mathfrak{v}}{1 - \dfrac{(\mathfrak{a}_0 \mathfrak{v})}{c^2}}, \qquad \text{bzw.} \qquad \mathfrak{a}_0 = \frac{\mathfrak{a} + \mathfrak{v}}{1 + \dfrac{(\mathfrak{a} \mathfrak{v})}{c^2}}, \tag{20}$$

also

$$d(m \mathfrak{v}) = m\, d\mathfrak{v} + \mathfrak{v}\, dm = -\mathfrak{a}\, dm = -\frac{\mathfrak{a}_0 - \mathfrak{v}}{1 - \dfrac{(\mathfrak{a}_0 \mathfrak{v})}{c^2}}\, dm$$

oder

$$m\,dv = -(a+v)\,dm = -\left(\frac{a_0 - v}{1 - \frac{(a_0\,v)}{c^2}} + v\right) dm = -a_0 \frac{1 - \frac{v^2}{c^2}}{1 - \frac{(a_0\,v)}{c^2}}\,dm.$$

Somit wird

$$\frac{dm}{m} = -\frac{1 - \frac{(a_0\,v)}{c^2}}{a_0\,(1 - v^2/c^2)}\,dv. \tag{21}$$

Nun ist wegen Gl. (17)

$$\frac{dm}{m} = \frac{\sqrt{1 - v^2/c^2}}{m_0}\,d\left(\frac{m_0}{\sqrt{1 - v^2/c^2}}\right) = \frac{dm_0}{m_0} + \sqrt{1 - \frac{v^2}{c^2}}\,d\left(\frac{1}{\sqrt{1 - v^2/c^2}}\right) =$$

$$= \frac{dm_0}{m_0} + \frac{\frac{(v\,dv)}{c^2}}{1 - v^2/c^2} = \frac{dm_0}{m_0} + \frac{\frac{(a_0\,v)}{c^2}\,dv}{a_0\,(1 - v^2/c^2)}. \tag{22}$$

Setzt man die Gl. (21) in die Gl. (22) ein, so folgt sofort $(a_0 \| v)$

$$\frac{dm_0}{m_0} = -\frac{dv}{a_0\,(1 - v^2/c^2)}. \tag{23}$$

Für konstantes a_0 läßt sich diese Gleichung leicht integrieren. Ist M_0 die Ruhemasse der Rakete zur Zeit $t = 0$ $(v = 0)$, so ergibt sich

$$\ln\frac{m_0}{M_0} = -\frac{c}{a_0}\int_0^v \frac{\frac{1}{c}\,dv}{1 - \left(\frac{v}{c}\right)^2} = -\frac{c}{2\,a_0}\ln\frac{1 + v/c}{1 - v/c}$$

oder

$$\frac{m_0}{M_0} = \left[\frac{1 - \frac{v}{c}}{1 + \frac{v}{c}}\right]^{\frac{c}{2a_0}}, \tag{24}$$

beziehungsweise

$$\frac{v}{c} = \frac{1 - \left(\frac{m_0}{M_0}\right)^{\frac{2a_0}{c}}}{1 + \left(\frac{m_0}{M_0}\right)^{\frac{2a_0}{c}}}. \tag{25}$$

Die von J. ACKERET [2] (1946) gefundene Beziehung (24) läßt sich mittels der Relationen $\beta = v/c = \sqrt{1 - \alpha^2}$ oder $\alpha = \sqrt{1 - v^2/c^2} = \sqrt{1 - \beta^2}$ umformen in

$$\frac{m_0}{M_0} = \left[\frac{1 - \beta}{1 + \beta}\right]^{\frac{c}{2a_0}} = \left[\frac{\sqrt{1 - \beta^2}}{1 + \beta}\right]^{\frac{c}{a_0}} = \left[\frac{\alpha}{1 + \sqrt{1 - \alpha^2}}\right]^{\frac{c}{a_0}}. \tag{26}$$

Diese Formel hat bereits R. ESNAULT-PELTERIE [3] (1930) gefunden durch die relativistische Behandlung des Spezialfalles einer Rakete mit konstanter

Eigenbeschleunigung b_0 und er bemerkt dazu, daß diese Beziehung vom Bewegungsgesetz unabhängig ist.

Die relativistische Raketengrundgleichung (24) geht in der klassischen Physik ($v/c \to 0$) über in die bekannte Formel:

$$r \equiv \frac{M_0}{m_0} = e^{\frac{v}{a_0}} \quad \text{bzw.} \quad \ln r = \frac{v}{a_0},$$

da

$$\lim_{\frac{v}{c}\to 0} \ln r = \lim_{\frac{v}{c}\to 0} \frac{v}{a_0} \cdot \frac{\ln\left(1+\frac{v}{c}\right) - \ln\left(1-\frac{v}{c}\right)}{2\frac{v}{c}} = \lim_{\frac{v}{c}\to 0} \frac{v}{a_0} \frac{\frac{1}{1+v/c} + \frac{1}{1-v/c}}{2} = \frac{v}{a_0}$$

ist. Setzt man $x = v/c$ $(0 \leqq x \leqq 1)$ und $y = 1/r = m_0/M_0$ $(0 \leqq y \leqq 1)$, so ist nach Gl. (24):

$$y = \left[\frac{1-x}{1+x}\right]^{\frac{c}{2a_0}}, \qquad y' = -\frac{c}{a_0(1+x)^2}\left[\frac{1-x}{1+x}\right]^{\frac{c}{2a_0}-1},$$

$$y'' = \frac{2\frac{c}{a_0}}{(1+x)^4}\left[\frac{1-x}{1+x}\right]^{\frac{c}{2a_0}-2} \cdot \left\{\frac{c}{2a_0} - x\right\}.$$

Ein Wendepunkt ($y'' = 0$) tritt auf für

$$x_w = \frac{c}{2a_0} \qquad \text{und} \qquad y_w = \left[\frac{1-\frac{c}{2a_0}}{1+\frac{c}{2a_0}}\right]^{\frac{c}{2a_0}} = \left[\frac{1-x_w}{1+x_w}\right]^{x_w},$$

falls $a_0 > c/2$ ist. Im günstigsten Falle $a_0 = c$ (Photonen) wird $x_w = 1/2$ und $y_w = 1/\sqrt{3}$, das heißt der Wendepunkt tritt auf bei $v = c/2$ und $r = \sqrt{3}$.

Mittels der Beziehungen (20) folgen die Relationen

$$\left(1+\frac{(\mathfrak{a}\,\mathfrak{v})}{c^2}\right)\cdot\left(1-\frac{(\mathfrak{a}_0\,\mathfrak{v})}{c^2}\right) = 1-\frac{v^2}{c^2}; \qquad \left(1+\left|\frac{\mathfrak{v}}{\mathfrak{a}}\right|\right)\cdot\left(1-\left|\frac{\mathfrak{v}}{\mathfrak{a}_0}\right|\right) = 1-\frac{v^2}{c^2} \tag{27}$$

und

$$\frac{\sqrt{1-a_0^2/c^2}}{\sqrt{1-a^2/c^2}} = \frac{1-\frac{(\mathfrak{a}_0\,\mathfrak{v})}{c^2}}{\sqrt{1-v^2/c^2}} = \frac{\sqrt{1-v^2/c^2}}{1+\frac{(\mathfrak{a}\,\mathfrak{v})}{c^2}}. \tag{28}$$

Ein Vergleich von Gl. (21) und (23) zeigt, daß

$$\frac{dm}{m} = \left[1-\frac{(\mathfrak{a}_0\,\mathfrak{v})}{c^2}\right]\frac{dm_0}{m_0}; \tag{29}$$

also wegen Gl. (28) und (17)

$$\frac{dm}{dm_0} = \left[1-\frac{(\mathfrak{a}_0\,\mathfrak{v})}{c^2}\right]\frac{m}{m_0} = \frac{1-\frac{(\mathfrak{a}_0\,\mathfrak{v})}{c^2}}{\sqrt{1-v^2/c^2}} = \frac{\sqrt{1-a_0^2/c^2}}{\sqrt{1-a^2/c^2}} \tag{30}$$

und in Hinsicht auf Gl. (17)

$$dm_0 = \frac{dm_0^*}{\sqrt{1-a_0^2/c^2}}. \tag{31}$$

Das ist also die Masse der ausgestoßenen Gase im System K_0 der mit der Rakete mitfahrenden Astronauten. Die Schubkraft $\mathfrak{F}_0$ in diesem System soll nun abgeleitet werden. Nach Gl. (10) ist

$$dt_0 = dt\sqrt{1 - v^2/c^2} \tag{32}$$

und, falls die Beschleunigung $b = \dot{\mathfrak{v}} = \ddot{\mathfrak{r}}$ in Richtung der Geschwindigkeit $\mathfrak{v}$ wirkt, ist nach Gl. (15)

$$\frac{d}{dt}\left(\frac{\mathfrak{v}}{\sqrt{1 - v^2/c^2}}\right) = \frac{\dot{\mathfrak{v}}}{(1 - v^2/c^2)^{3/2}} = \frac{b}{(1 - v^2/c^2)^{3/2}} = b_0. \tag{33}$$

Unter Verwendung dieser beiden letzten Beziehungen gibt dann Gl. (18)

$$\mathfrak{F} = \frac{d}{dt}\left(\frac{m_0\,\mathfrak{v}}{\sqrt{1 - v^2/c^2}}\right) = \frac{m_0\,\dot{\mathfrak{v}}}{(1 - v^2/c^2)^{3/2}} + \frac{\mathfrak{v}}{\sqrt{1 - v^2/c^2}}\frac{dm_0}{dt} = m_0\,b_0 + \mathfrak{v}\frac{dm_0}{dt_0}. \tag{34}$$

Andererseits ist nach den Gln. (19), (30), (20) und (32):

$$\mathfrak{F} = -\mathfrak{a}\frac{dm}{dt} = -\mathfrak{a}\frac{1 - \dfrac{(\mathfrak{a}_0\,\mathfrak{v})}{c^2}}{\sqrt{1 - v^2/c^2}}\frac{dm_0}{dt} = -(\mathfrak{a}_0 - \mathfrak{v})\frac{dm_0}{dt_0} = -\mathfrak{a}_0\frac{dm_0}{dt_0} + \mathfrak{v}\frac{dm_0}{dt_0}. \tag{35}$$

Ein Vergleich der beiden Gln. (34) und (35) ergibt für die Schubkraft $\mathfrak{F}_0$ der Rakete im System der Astronauten (Raumschiffbesatzung)

$$\frac{m_0\,\dot{\mathfrak{v}}}{(1 - v^2/c^2)^{3/2}} = m_0\,b_0 = \mathfrak{F}_0 = -\mathfrak{a}_0\frac{dm_0}{dt_0} = -\mathfrak{a}_0\frac{dm_0{}^*/dt_0}{\sqrt{1 - a_0{}^2/c^2}}. \tag{36}$$

Ferner folgt aus den Gln. (35) und (36)

$$\mathfrak{F} = \frac{\mathfrak{a}_0 - \mathfrak{v}}{\mathfrak{a}_0}\,\mathfrak{F}_0 = \left(1 - \frac{v}{a_0}\right)\mathfrak{F}_0. \tag{37}$$

Ist somit $v = a_0$ erreicht, so wird $a = 0$ und ebenso auch $\mathfrak{F} = 0$. Vom technischen Standpunkt aus interessiert natürlich in erster Linie die primäre Schubkraft $\mathfrak{F}_0$ der Rakete im Ruhesystem K_0. Formt man Gl. (36) folgendermaßen um:

$$\frac{dm_0}{m_0} = -\frac{b_0}{a_0}\,dt_0 = -\frac{\dot{v}}{a_0\,(1 - v^2/c^2)^{3/2}}\,dt_0 = -\frac{dv}{a_0\,(1 - v^2/c^2)},$$

so hat man wieder Gl. (23). Aus den Gln. (36) und (37) folgen noch die Beziehungen

$$\mathfrak{F}_0 = m_0\,b_0 = \frac{m_0\,\dot{\mathfrak{v}}}{(1 - v^2/c^2)^{3/2}} = \frac{m\,\dot{\mathfrak{v}}}{1 - v^2/c^2} = \frac{m\,b}{1 - v^2/c^2}$$

und

$$\mathfrak{F} = \left(1 - \frac{v}{a_0}\right)\cdot\mathfrak{F}_0 = \frac{1 - \dfrac{v}{a_0}}{1 - v^2/c^2}\,m\,\dot{\mathfrak{v}} = \frac{m\,b}{1 + v/a}.$$

Das heißt

$$\mathfrak{F} < m\,\dot{\mathfrak{v}} < \mathfrak{F}_0.$$

Schließlich soll noch der Energiesatz abgeleitet werden. Es ist

$$E_0 = m_0\,c^2 \tag{38}$$

die Gesamtenergie der Rakete im System K_0 der Astronauten und

$$E = m\,c^2 = \frac{m_0\,c^2}{\sqrt{1 - v^2/c^2}} = \frac{E_0}{\sqrt{1 - v^2/c^2}} \tag{39}$$

diejenige im System K des Erdbeobachters. Aus den Gln. (30) und (32) ergibt sich

$$\frac{dm}{dt} = \left(1 - \frac{(\mathfrak{a}_0\,\mathfrak{v})}{c^2}\right)\frac{dm_0}{dt_0}, \tag{40}$$

also auch

$$\frac{dE}{dt} = \left(1 - \frac{(\mathfrak{a}_0\,\mathfrak{v})}{c^2}\right)\frac{dE_0}{dt_0}, \tag{41}$$

oder wegen Gl. (36) auch

$$\frac{dE}{dt} = \frac{dE_0}{dt_0} - (\mathfrak{a}_0\,\mathfrak{v})\,\frac{dm_0}{dt_0} = \frac{dE_0}{dt_0} + (\mathfrak{v}\,\mathfrak{F}_0). \tag{42}$$

Der Energiesatz läßt sich demnach schreiben:

$$(\mathfrak{v}\,\mathfrak{F}_0) = \frac{dE}{dt} - \frac{dE_0}{dt_0} = \frac{dE_{kin}}{dt} - \left(1 - \sqrt{1 - v^2/c^2}\right)\frac{dE_0}{dt_0}; \tag{43}$$

dabei ist

$$E_{kin} = E - E_0 = (m - m_0)\,c^2 = m\,c^2\left(1 - \sqrt{1 - v^2/c^2}\right) =$$
$$= m_0\,c^2\left(\frac{1}{\sqrt{1 - v^2/c^2}} - 1\right) = \frac{m_0\,v^2}{2}\left(1 + \frac{3}{4}\frac{v^2}{c^2} + \ldots\right) \tag{44}$$

die Bewegungsenergie. Der Energiesatz besagt daher, daß die von der Schubkraft in der Zeiteinheit geleistete Arbeit (Leistung) gleich ist der Energieänderung des Systems in der Zeiteinheit. Für Systeme mit zeitlich konstanter Ruhemasse folgt sofort der Energiesatz in der bekannten Form

$$(\mathfrak{v}\,\mathfrak{F}) = \frac{dE}{dt} = \frac{dE_{kin}}{dt}.$$

Der verallgemeinerte Energiesatz (43) läßt sich in Hinsicht auf Gl. (34) auch in folgender Gestalt schreiben:

$$(\mathfrak{v}\,\mathfrak{F}) = (\mathfrak{v}\,\mathfrak{F}_0) + v^2\frac{dm_0}{dt_0} = (\mathfrak{v}\,\mathfrak{F}_0) + \frac{v^2}{c^2}\frac{dE_0}{dt_0} =$$
$$= \frac{dE}{dt} - \left(1 - \frac{v^2}{c^2}\right)\frac{dE_0}{dt_0} = \frac{dE}{dt} - \sqrt{1 - v^2/c^2}\,\frac{dE_0}{dt};$$

das heißt schließlich

$$(\mathfrak{v}\,\mathfrak{F}) = \frac{dE}{dt} - \sqrt{1 - v^2/c^2}\,\frac{dE_0}{dt} = \frac{dE_{kin}}{dt} + \left(1 - \sqrt{1 - v^2/c^2}\right)\frac{dE_0}{dt}. \tag{45}$$

III. Bewegung und Massenverbrauch einer Rakete mit konstanter Eigenbeschleunigung

Dieser Fall ist zuerst, wenn auch nicht erschöpfend, von R. Esnault-Pelterie [3] behandelt worden. Ein kurzer Beitrag zu diesem Problem ist auch von W. L. Bade [4] geliefert worden. Für eine Rakete, die mit konstanter Eigenbeschleunigung b_0 fliegt, gilt unter Verwendung von Gl. (33)

$$\frac{d}{dt}\left(\frac{v}{\sqrt{1 - v^2/c^2}}\right) = \frac{\dot{v}}{(1 - v^2/c^2)^{3/2}} = b_0\ (\text{const.}); \tag{46}$$

also

$$v = b_0\,t\sqrt{1 - v^2/c^2} = a\,b_0\,t \qquad (\text{mit } v = 0 \text{ für } t = 0),$$

das heißt

$$\frac{1}{b_0\,t} = \sqrt{\frac{1}{v^2} - \frac{1}{c^2}}$$

und somit die Geschwindigkeit

$$v = \dot{x} = \frac{1}{\sqrt{\frac{1}{b_0^2 t^2} + \frac{1}{c^2}}} = c\frac{\frac{b_0}{c}t}{\sqrt{1+\left(\frac{b_0}{c}t\right)^2}} = b_0 t\left[1 - \frac{1}{2}\left(\frac{b_0}{c}t\right)^2 + \frac{1\cdot 3}{2\cdot 4}\left(\frac{b_0}{c}t\right)^4 \mp \ldots\right]. \tag{47}$$

Daher wird

$$\alpha = \sqrt{1-\frac{v^2}{c^2}} = \frac{v}{b_0 t} = \frac{1}{\sqrt{1+\left(\frac{b_0}{c}t\right)^2}} = 1 - \frac{1}{2}\left(\frac{b_0}{c}t\right)^2 + \frac{1\cdot 3}{2\cdot 4}\left(\frac{b_0}{c}t\right)^4 \mp \ldots \tag{48}$$

und die Beschleunigung

$$b = \dot{v} = \ddot{x} = b_0\alpha^3 = \frac{b_0}{\left[1+\left(\frac{b_0}{c}t\right)^2\right]^{3/2}} =$$

$$= b_0\left[1 - \frac{1\cdot 3}{1}\frac{1}{2}\left(\frac{b_0}{c}t\right)^2 + \frac{1\cdot 3\cdot 5}{1\cdot 2}\frac{1}{2^2}\left(\frac{b_0}{c}t\right)^4 \mp \ldots\right]. \tag{49}$$

Die Umkehrung von Gl. (47) ist nun

$$\frac{b_0}{c}t = \frac{v/c}{\alpha} = \frac{\beta}{\alpha} = \frac{\sqrt{1-\alpha^2}}{\alpha} = \frac{v/c}{\sqrt{1-v^2/c^2}}. \tag{50}$$

Durch Integration von Gl. (47) folgt für den Weg

$$x = \int_0^t v\,dt = \frac{c^2}{b_0}\int_0^t \frac{\frac{b_0}{c}t}{\sqrt{1+\left(\frac{b_0}{c}t\right)^2}}\frac{b_0}{c}dt = \frac{c^2}{b_0}\int_0^{\frac{b_0}{c}t}\frac{z\,dz}{\sqrt{1+z^2}} = \frac{c^2}{b_0}\sqrt{1+z^2}\Big|_0^{\frac{b_0}{c}t},$$

demnach

$$x = \frac{c^2}{b_0}\left[\sqrt{1+\left(\frac{b_0}{c}t\right)^2} - 1\right] = \frac{b_0}{2}t^2\left[1 - \frac{1}{4}\left(\frac{b_0}{c}t\right)^2 + \frac{1\cdot 3}{4\cdot 6}\left(\frac{b_0}{c}t\right)^4 \mp \ldots\right]. \tag{51}$$

Die Umkehr dieser Beziehung lautet

$$t = \frac{c}{b_0}\sqrt{\left(1+\frac{b_0 x}{c^2}\right)^2 - 1} = \sqrt{\frac{2x}{b_0} + \left(\frac{x}{c}\right)^2}. \tag{52}$$

Mißt man die Zeit nicht im System des ruhenden Erdbeobachters, sondern im System des mit der Rakete mitfahrenden Astronauten (Eigenzeit oder Lokalzeit t_0), so hat man nach den Gln. (32) und (48) folgenden Zusammenhang:

$$t_0 = \int_0^t \sqrt{1-v^2/c^2}\,dt =$$

$$= \frac{c}{b_0}\int_0^t \frac{\frac{b_0}{c}\,dt}{\sqrt{1+\left(\frac{b_0}{c}t\right)^2}} = \frac{c}{b_0}\int_0^{\frac{b_0}{c}t}\frac{dz}{\sqrt{1+z^2}} = \frac{c}{b_0}\ln\left(z+\sqrt{1+z^2}\right)\Big|_0^{\frac{b_0}{c}t},$$

also

$$t_0 = \frac{c}{b_0} \ln\left[\frac{b_0}{c} t + \sqrt{1 + \left(\frac{b_0}{c} t\right)^2}\right] = \frac{c}{b_0} \operatorname{Ar\,Sin}\left(\frac{b_0}{c} t\right) = \\ = t\left[1 - \frac{1}{2 \cdot 3}\left(\frac{b_0}{c} t\right)^2 + \frac{1 \cdot 3}{2 \cdot 4 \cdot 5}\left(\frac{b_0}{c} t\right)^4 \mp \ldots\right]. \tag{53}$$

Die Umkehrformel lautet

$$t = \frac{c}{b_0} \operatorname{Sin}\left(\frac{b_0}{c} t_0\right) = \frac{c}{2 b_0}\left\{e^{\frac{b_0}{c} t_0} - e^{-\frac{b_0}{c} t_0}\right\} = t_0\left[1 + \frac{1}{3!}\left(\frac{b_0}{c} t_0\right)^2 + \frac{1}{5!}\left(\frac{b_0}{c} t_0\right)^4 + \ldots\right]. \tag{54}$$

Setzt man diese Beziehung in die Gln. (47), (48), (49) und (51) ein, so erhält man Beschleunigung, Geschwindigkeit und Weg der Rakete als Funktion der Eigenzeit t_0 des Astronauten, nämlich

$$a = \frac{1}{\operatorname{Cos}\left(\frac{b_0}{c} t_0\right)} = 1 - \frac{1}{2!}\left(\frac{b_0}{c} t_0\right)^2 + \frac{5}{4!}\left(\frac{b_0}{c} t_0\right)^4 \mp \ldots \tag{55}$$

$$b = \ddot{x} = \frac{b_0}{\operatorname{Cos}^3\left(\frac{b_0}{c} t_0\right)} = b_0\left[1 - \frac{3}{2}\left(\frac{b_0}{c} t_0\right)^2 + \frac{11}{8}\left(\frac{b_0}{c} t_0\right)^4 \mp \ldots\right] \tag{56}$$

$$v = \dot{x} = c \operatorname{Tg}\left(\frac{b_0}{c} t_0\right) = b_0 t_0\left[1 - \frac{1}{3}\left(\frac{b_0}{c} t_0\right)^2 + \frac{2}{15}\left(\frac{b_0}{c} t_0\right)^4 \mp \ldots\right] \tag{57}$$

$$x = \frac{c^2}{b_0}\left[\operatorname{Cos}\left(\frac{b_0}{c} t_0\right) - 1\right] = \frac{b_0}{2} t_0^2\left[1 + \frac{1}{3 \cdot 4}\left(\frac{b_0}{c} t_0\right)^2 + \frac{1}{3 \cdot 4 \cdot 5 \cdot 6}\left(\frac{b_0}{c} t_0\right)^4 + \ldots\right]. \tag{58}$$

Zusammenfassend gelten also die Beziehungen der Tab. 2 für die Bewegung einer Rakete mit konstanter Eigenbeschleunigung b_0.

Eine Rakete, die mit konstanter Eigenbeschleunigung b_0 fliegt, braucht, um eine vorgegebene Entfernung X zu erreichen, eine Zeit

$$T = \sqrt{\frac{2X}{b_0}} \tag{59}$$

im System der klassischen Physik („Euklidische Zeit");

$$t = \frac{c}{b_0}\sqrt{\left(1 + \frac{b_0 X}{c^2}\right)^2 - 1} = \sqrt{\frac{2X}{b_0} + \left(\frac{X}{c}\right)^2} = T\sqrt{1 + \frac{1}{2}\left(\frac{b_0 X}{c^2}\right)} = \\ = T\left[1 + \frac{1}{2}\left(\frac{b_0 X}{2c^2}\right) - \frac{1}{2 \cdot 4}\left(\frac{b_0 X}{2c^2}\right)^2 + \frac{1 \cdot 3}{2 \cdot 4 \cdot 6}\left(\frac{b_0 X}{2c^2}\right)^3 \mp \ldots\right] \tag{60}$$

im System des ruhenden Erdbeobachters;

$$t_0 = \frac{c}{b_0} \operatorname{Ar\,Cos}\left(1 + \frac{b_0 X}{c^2}\right) = T\,\frac{\operatorname{Ar\,Sin}\sqrt{\left(1 + \frac{b_0 X}{c^2}\right)^2 - 1}}{\sqrt{2\frac{b_0 X}{c^2}}} = \\ = T\left[1 - \frac{1}{2 \cdot 3}\left(\frac{b_0 X}{2c^2}\right) + \frac{1 \cdot 3}{2 \cdot 4 \cdot 5}\left(\frac{b_0 X}{2c^2}\right)^2 - \frac{1 \cdot 3 \cdot 5}{2 \cdot 4 \cdot 6 \cdot 7}\left(\frac{b_0 X}{2c^2}\right)^3 \pm \ldots\right] \tag{61}$$

im System des mit der Rakete mitfahrenden Astronauten (Eigen- oder Lokalzeit). Es ist allgemein $t_0 < T < t$. Man erkennt daraus den gewaltigen Zeitgewinn durch das relativistische Gesetz.

Vol. 2 1956

Zur Vereinfachung der numerischen Rechnung empfiehlt sich, c/b_0 als Zeiteinheit, c als Geschwindigkeitseinheit und c^2/b_0 als Längeneinheit zu wählen. Alle Beziehungen lassen sich dann dimensionslos darstellen. Mit $c = 3 \cdot 10^{10}$ cm/s und $b_0 = g = 981$ cm/s^2 wird

$$\frac{c}{g} = \frac{3 \cdot 10^{10}}{981} = 3{,}06 \cdot 10^7 \text{ s} = 354{,}2 \text{ d} = 0{,}97 \text{ a (Jahre)},$$

$$\frac{c^2}{g} = \frac{9 \cdot 10^{20}}{981} = 9{,}18 \cdot 10^{17} \text{ cm} = 9{,}18 \cdot 10^{12} \text{ km} = 0{,}97 \cdot \text{l. y. (Lichtjahre)}$$

Der Schub F_0 im System des Astronauten ist nach Gl. (36)

$$m_0 b_0 = F_0 \equiv - a_0 \frac{dm_0}{dt_0}. \tag{62}$$

Daraus folgt sofort das Gesetz der Massenabnahme zu

$$\frac{dm_0}{m_0} = - \frac{b_0}{a_0} dt_0$$

oder integriert für konstante Ausströmungsgeschwindigkeit a_0

$$\int_{M_0}^{m_0} \frac{dm_0}{m_0} = - \frac{b_0}{a_0} \int_0^{t_0} dt_0, \qquad \ln \frac{m_0}{M_0} = - \frac{b_0}{a_0} t_0,$$

Tabelle 2

Beschleunigung $b = \ddot{x} = \dot{v}$	$b_0 \, [1 - v^2/c^2]^{3/2}$	$\dfrac{b_0}{\left(1 + \dfrac{b_0 x}{c^2}\right)^3}$
Geschwindigkeit $v = \dot{x}$	–	$c \dfrac{\sqrt{\left(1 + \dfrac{b_0 x}{c^2}\right)^2 - 1}}{1 + \dfrac{b_0 x}{c^2}}$
Weg x	$\dfrac{c^2}{b_0}\left[\dfrac{1}{\sqrt{1 - v^2/c^2}} - 1\right]$	–
Kontraktionsfaktor $\alpha = \dfrac{dt_0}{dt}$	$\sqrt{1 - v^2/c^2}$	$\dfrac{1}{1 + \dfrac{b_0 x}{c^2}}$
Zeit t	$\dfrac{c}{b_0}\left[\dfrac{v/c}{\sqrt{1 - v^2/c^2}}\right]$	$\dfrac{c}{b_0}\sqrt{\left(1 + \dfrac{b_0 x}{c^2}\right)^2 - 1}$
Eigenzeit t_0	$\dfrac{c}{b_0} \operatorname{Ar\,Tg}\left(\dfrac{v}{c}\right)$	$\dfrac{c}{b_0} \operatorname{Ar\,Cos}\left(1 + \dfrac{b_0 x}{c^2}\right)$
	$= \dfrac{c}{2 b_0} \ln \dfrac{1 + v/c}{1 - v/c}$	$= \dfrac{c}{b_0} \ln \left[1 + \dfrac{b_0 x}{c^2} + \sqrt{\left(1 + \dfrac{b_0 x}{c^2}\right)^2 - 1}\right]$

das heißt unter Benutzung der Tab. 2

$$\frac{m_0}{M_0} = e^{-\frac{b_0}{a_0} t_0} = \left[\frac{b_0}{c} t + \sqrt{1 + \left(\frac{b_0}{c} t\right)^2}\right]^{-\frac{c}{a_0}} =$$

$$= \left[1 + \frac{b_0 x}{c^2} + \sqrt{\left(1 + \frac{b_0 x}{c^2}\right)^2 - 1}\right]^{-\frac{c}{a_0}} = \left[\frac{1 + \frac{v}{c}}{1 - \frac{v}{c}}\right]^{-\frac{c}{2a_0}} \tag{63}$$

Die letzte dieser Beziehungen ist unabhängig von b_0, das heißt vom Bewegungsgesetz. Sie gilt, wie im vorherigen Abschnitt gezeigt wurde, allgemein für eine beliebig beschleunigte Rakete. Der Schub ist nun nach Gln. (62) und (63):

$$F_0 = m_0 b_0 = M_0 b_0 e^{-\frac{b_0}{a_0} t_0} = M_0 b_0 \left[\frac{b_0}{c} t + \sqrt{1 + \left(\frac{b_0}{c} t\right)^2}\right]^{-\frac{c}{a_0}} =$$

$$= M_0 b_0 \left[1 + \frac{b_0 x}{c^2} + \sqrt{\left(1 + \frac{b_0 x}{c^2}\right)^2 - 1}\right]^{-\frac{c}{a_0}} = M_0 b_0 \left[\frac{1 + \frac{v}{c}}{1 - \frac{v}{c}}\right]^{-\frac{c}{2a_0}} \tag{64}$$

Fortsetzung der Tabelle 2

$b_0 a^3$	$\frac{b_0}{\left[1 + \left(\frac{b_0}{c} t\right)^2\right]^{3/2}}$	$\frac{b_0}{\mathrm{Cos}^3\left(\frac{b_0}{c} t_0\right)}$
$c\sqrt{1 - a^2}$	$c \frac{\frac{b_0}{c} t}{\sqrt{1 + \left(\frac{b_0}{c} t\right)^2}}$	$c\,\mathrm{Tg}\left(\frac{b_0}{c} t_0\right)$
$\frac{c^2}{b_0}\left(\frac{1}{a} - 1\right)$	$\frac{c^2}{b_0}\left[\sqrt{1 + \left(\frac{b_0}{c} t\right)^2} - 1\right]$	$\frac{c^2}{b_0}\left[\mathrm{Cos}\left(\frac{b_0}{c} t_0\right) - 1\right]$
–	$\frac{1}{\sqrt{1 + \left(\frac{b_0}{c} t\right)^2}}$	$\frac{1}{\mathrm{Cos}\left(\frac{b_0}{c} t_0\right)}$
$\frac{c}{b_0}\sqrt{\frac{1}{a^2} - 1}$	–	$\frac{c}{b_0}\mathrm{Sin}\left(\frac{b_0}{c} t_0\right)$
$\frac{c}{b_0}\mathrm{Ar\,Cos}\left(\frac{1}{a}\right)$	$\frac{c}{b_0}\mathrm{Ar\,Sin}\left(\frac{b_0}{c} t\right)$	–
$= \frac{c}{b_0}\ln\left[\frac{1}{a} + \sqrt{\frac{1}{a^2} - 1}\right]$	$= \frac{c}{b_0}\ln\left[\frac{b_0}{c} t + \sqrt{1 + \left(\frac{b_0}{c} t\right)^2}\right]$	–

Durch Umkehrung von Gl. (63) findet man

$$v = c\,\frac{1-\left(\frac{m_0}{M_0}\right)^{\frac{2a_0}{c}}}{1+\left(\frac{m_0}{M_0}\right)^{\frac{2a_0}{c}}}, \quad \text{also} \quad \alpha = \sqrt{1-v^2/c^2} = \frac{2\left(\frac{m_0}{M_0}\right)^{\frac{a_0}{c}}}{1+\left(\frac{m_0}{M_0}\right)^{\frac{2a_0}{c}}}. \tag{65}$$

Damit folgt für den Weg

$$x = \frac{c^2}{b_0}\left(\frac{1}{\alpha}-1\right) = \frac{c^2}{b_0}\left[\frac{1+\left(\frac{m_0}{M_0}\right)^{\frac{2a_0}{c}}}{2\left(\frac{m_0}{M_0}\right)^{\frac{a_0}{c}}}-1\right] = \frac{c^2}{2\,b_0}\,\frac{\left[1-\left(\frac{m_0}{M_0}\right)^{\frac{a_0}{c}}\right]^2}{\left(\frac{m_0}{M_0}\right)^{\frac{a_0}{c}}} \tag{66}$$

und für die Zeit

$$t = \frac{c}{b_0}\left[\frac{v/c}{\alpha}\right] = \frac{c}{2\,b_0}\,\frac{1-\left(\frac{m_0}{M_0}\right)^{\frac{2a_0}{c}}}{\left(\frac{m_0}{M_0}\right)^{\frac{a_0}{c}}}. \tag{67}$$

Im Gegensatz dazu ist nach Gl. (63) die Eigen- oder Lokalzeit

$$t_0 = -\frac{a_0}{b_0}\ln\frac{m_0}{M_0}. \tag{68}$$

IV. Bewegung einer Rakete mit konstantem Massendurchsatz (Schub) im freien Raum ohne äußere Kräfte

In diesem Falle geht man wieder von der Bewegungsgleichung (36) der Rakete im System des mit der Rakete mitfahrenden Astronauten aus, nämlich

$$\frac{m_0\,\dot{v}}{(1-v^2/c^2)^{3/2}} = m_0\,b_0 = F_0 = -\,a_0\,\frac{dm_0}{dt_0}; \tag{69}$$

dabei ist jetzt der sekundliche Massendurchsatz

$$\mu_0 = -\,\frac{dm_0}{dt_0} = \text{const.} \tag{70}$$

Die Masse nimmt also linear mit der Zeit t_0 ab nach dem Gesetz

$$m_0 = M_0 - \mu_0\,t_0 = M_0\left(1-\frac{\mu_0}{M_0}\,t_0\right), \tag{71}$$

wobei M_0 die Anfangsruhemasse der Rakete zur Zeit $t_0 = 0$ ist. Nimmt man wieder die Ausströmungsgeschwindigkeit der Gase $a_0 = \text{const.}$ an, dann ist auch der Schub

$$F_0 = a_0\mu_0 = \text{const.} \tag{72}$$

Hingegen ist $F = F_0\,(1 - v/a_0) = \mu_0(a_0 - v)$ variabel. Die Eigenbeschleunigung nimmt jetzt nach folgendem Gesetz zu:

$$\frac{\dot{v}}{(1-v^2/c^2)^{3/2}} = b_0 = \frac{F_0}{m_0} = \frac{a_0\mu_0}{M_0-\mu_0 t_0} = a_0 \frac{\frac{\mu_0}{M_0}}{1-\frac{\mu_0}{M_0}t_0}. \tag{73}$$

Wegen $dt_0 = \sqrt{1-v^2/c^2}\cdot dt$ ist dann

$$\frac{dv}{1-v^2/c^2} = \frac{a_0\mu_0}{M_0-\mu_0 t_0}\,dt_0 = a_0 \frac{\frac{\mu_0}{M_0}}{1-\frac{\mu_0}{M_0}t_0}\,dt_0$$

oder integriert

$$c\int_0^v \frac{\frac{1}{c}dv}{1-v^2/c^2} = a_0 \int_0^{t_0} \frac{\frac{\mu_0}{M_0}\,dt_0}{1-\frac{\mu_0}{M_0}t_0}\,; \quad \frac{c}{2}\ln\frac{1+\frac{v}{c}}{1-\frac{v}{c}} = -a_0\ln\left(1-\frac{\mu_0}{M_0}t_0\right),$$

Vol. 2 1956

das heißt wegen Gl. (71)

$$\frac{m_0}{M_0} = 1-\frac{\mu_0}{M_0}t_0 = \left[\frac{1-\frac{v}{c}}{1+\frac{v}{c}}\right]^{\frac{c}{2a_0}}. \tag{74}$$

Damit ist die allgemeingültige Formel (24) nicht nur für den Spezialfall konstanter Eigenbeschleunigung (63), sondern auch für den Fall konstanten Schubes F_0 bewiesen.

Die Umkehrung von Gl. (74) lautet

$$v = c\,\frac{1-\left(\frac{m_0}{M_0}\right)^{\frac{2a_0}{c}}}{1+\left(\frac{m_0}{M_0}\right)^{\frac{2a_0}{c}}} = c\,\frac{1-\left(1-\frac{\mu_0}{M_0}t_0\right)^{\frac{2a_0}{c}}}{1+\left(1-\frac{\mu_0}{M_0}t_0\right)^{\frac{2a_0}{c}}}, \tag{75}$$

also

$$\alpha = \sqrt{1-v^2/c^2} = \frac{2\left(\frac{m_0}{M_0}\right)^{\frac{a_0}{c}}}{1+\left(\frac{m_0}{M_0}\right)^{\frac{2a_0}{c}}} = \frac{2\left(1-\frac{\mu_0}{M_0}t_0\right)^{\frac{a_0}{c}}}{1+\left(1-\frac{\mu_0}{M_0}t_0\right)^{\frac{2a_0}{c}}} = \frac{dt_0}{dt}. \tag{76}$$

Setzt man diesen Ausdruck in Gl. (73) ein, so folgt für die Beschleunigung

$$b = \dot{v} = b_0\alpha^3 = a_0\frac{\frac{\mu_0}{M_0}}{\frac{m_0}{M_0}}\left[\frac{2\left(\frac{m_0}{M_0}\right)^{\frac{a_0}{c}}}{1+\left(\frac{m_0}{M_0}\right)^{\frac{2a_0}{c}}}\right]^3 = a_0\frac{\frac{\mu_0}{M_0}}{1-\frac{\mu_0}{M_0}t_0}\left[\frac{2\left(1-\frac{\mu_0}{M_0}t_0\right)^{\frac{a_0}{c}}}{1+\left(1-\frac{\mu_0}{M_0}t_0\right)^{\frac{2a_0}{c}}}\right]^3. \tag{77}$$

Die Gl. 76) gestattet die Bestimmung der Zeit t als Funktion der Eigenzeit t_0, nämlich

$$t = \int_0^{t_0} \frac{dt_0}{a} = \int_0^{t_0} \frac{1 + \left(1 - \frac{\mu_0}{M_0} t_0\right)^{\frac{2a_0}{c}}}{2\left(1 - \frac{\mu_0}{M_0} t_0\right)^{\frac{a_0}{c}}} dt_0 =$$

$$= \frac{1}{2}\left[\int_0^{t_0} \frac{dt_0}{\left(1 - \frac{\mu_0}{M_0} t_0\right)^{\frac{a_0}{c}}} + \int_0^{t_0} \left(1 - \frac{\mu_0}{M_0} t_0\right)^{\frac{a_0}{c}} dt_0\right] =$$

$$= \frac{M_0}{2\mu_0}\left[\int_{1-\frac{\mu_0}{M_0} t_0}^{1} \frac{dz}{z^{\frac{a_0}{c}}} + \int_{1-\frac{\mu_0}{M_0} t_0}^{1} z^{\frac{a_0}{c}} dz\right] = \frac{M_0}{2\mu_0}\left[\frac{z^{1-\frac{a_0}{c}}}{1-\frac{a_0}{c}} + \frac{z^{1+\frac{a_0}{c}}}{1+\frac{a_0}{c}}\right]_{1-\frac{\mu_0}{M_0} t_0}^{1};$$

folglich wegen Gl. (74)

$$t = \frac{M_0}{2\mu_0}\left[\frac{1 - \left(\frac{m_0}{M_0}\right)^{1-\frac{a_0}{c}}}{1-\frac{a_0}{c}} + \frac{1 - \left(\frac{m_0}{M_0}\right)^{1+\frac{a_0}{c}}}{1+\frac{a_0}{c}}\right] =$$

$$= \frac{M_0}{2\mu_0}\left[\frac{1 - \left(1 - \frac{\mu_0}{M_0} t_0\right)^{1-\frac{a_0}{c}}}{1-\frac{a_0}{c}} + \frac{1 - \left(1 - \frac{\mu_0}{M_0} t_0\right)^{1+\frac{a_0}{c}}}{1+\frac{a_0}{c}}\right] = \tag{78}$$

$$= \frac{M_0}{2\mu_0}\left[\frac{1 - \left(\frac{1-v/c}{1+v/c}\right)^{\frac{1}{2}\left(\frac{c}{a_0}-1\right)}}{1-\frac{a_0}{c}} + \frac{1 - \left(\frac{1-v/c}{1+v/c}\right)^{\frac{1}{2}\left(\frac{c}{a_0}+1\right)}}{1+\frac{a_0}{c}}\right].$$

Der Weg läßt sich folgendermaßen bestimmen:

$$x = \int_0^t v\, dt = \int_0^{t_0} \frac{v}{a} dt_0 = \frac{c}{2} \int_0^{t_0} \frac{1 - \left(1 - \frac{\mu_0}{M_0} t_0\right)^{\frac{2a_0}{c}}}{\left(1 - \frac{\mu_0}{M_0} t_0\right)^{\frac{a_0}{c}}} dt_0 =$$

$$= \frac{c}{2}\left[\int_0^{t_0} \frac{dt_0}{\left(1 - \frac{\mu_0}{M_0} t_0\right)^{\frac{a_0}{c}}} - \int_0^{t_0} \left(1 - \frac{\mu_0}{M_0} t_0\right)^{\frac{a_0}{c}} dt_0\right] =$$

$$= \frac{c}{2}\frac{M_0}{\mu_0}\left[\int_{1-\frac{\mu_0}{M_0}t_0}^{1}\frac{dz}{z^{\frac{a_0}{c}}} - \int_{1-\frac{\mu_0}{M_0}t_0}^{1} z^{\frac{a_0}{c}}\,dz\right] = \frac{c}{2}\frac{M_0}{\mu_0}\left[\frac{z^{1-\frac{a_0}{c}}}{1-\frac{a_0}{c}} - \frac{z^{1+\frac{a_0}{c}}}{1+\frac{a_0}{c}}\right]_{1-\frac{\mu_0}{M_0}t_0}^{1};$$

folglich wegen Gl. (74)

$$x = \frac{c}{2}\frac{M_0}{\mu_0}\left[\frac{1-\left(\frac{m_0}{M_0}\right)^{1-\frac{a_0}{c}}}{1-\frac{a_0}{c}} - \frac{1-\left(\frac{m_0}{M_0}\right)^{1+\frac{a_0}{c}}}{1+\frac{a_0}{c}}\right] =$$

$$= \frac{c}{2}\frac{M_0}{\mu_0}\left[\frac{1-\left(1-\frac{\mu_0}{M_0}t_0\right)^{1-\frac{a_0}{c}}}{1-\frac{a_0}{c}} - \frac{1-\left(1-\frac{\mu_0}{M_0}t_0\right)^{1+\frac{a_0}{c}}}{1+\frac{a_0}{c}}\right] = \tag{79}$$

$$= \frac{c}{2}\frac{M_0}{\mu_0}\left[\frac{1-\left(\frac{1-v/c}{1+v/c}\right)^{\frac{1}{2}\left(\frac{c}{a_0}-1\right)}}{1-\frac{a_0}{c}} - \frac{1-\left(\frac{1-v/c}{1+v/c}\right)^{\frac{1}{2}\left(\frac{c}{a_0}+1\right)}}{1+\frac{a_0}{c}}\right].$$

In der klassischen Physik ($c \to \infty$, $\varepsilon \equiv a_0/c \to 0$) gehen die Formeln (76), (77) und (78) über in

$$\alpha = \sqrt{1-v^2/c^2} = 1, \qquad b = b_0 = a_0\frac{\frac{\mu_0}{M_0}}{1-\frac{\mu_0}{M_0}t_0}, \qquad t = t_0.$$

Bei den Gln. (75) und (79) muß man einen Grenzübergang mittels der Formel von BERNOULLI-DE L'HOSPITAL machen.

$$\frac{v}{a_0} = \lim_{\varepsilon\to 0}\frac{1-\left(1-\frac{\mu_0}{M_0}t_0\right)^{2\varepsilon}}{\varepsilon\left[1+\left(1-\frac{\mu_0}{M_0}t_0\right)^{2\varepsilon}\right]} = \frac{1}{2}\lim_{\varepsilon\to 0}\frac{1-\left(1-\frac{\mu_0}{M_0}t_0\right)^{2\varepsilon}}{\varepsilon} =$$

$$= \frac{1}{2}\lim_{\varepsilon\to 0}\left\{-2\left(1-\frac{\mu_0}{M_0}t_0\right)^{2\varepsilon}\ln\left(1-\frac{\mu_0}{M_0}t_0\right)\right\} = \tag{80}$$

$$= \ln\frac{1}{1-\frac{\mu_0}{M_0}t_0} = \ln\frac{M_0}{m_0}$$

und

$$\frac{x}{a_0} = \frac{M_0}{\mu_0} \lim_{\varepsilon \to 0} \frac{1}{2\varepsilon} \left[\frac{1 - \left(\frac{m_0}{M_0}\right)^{1-\varepsilon}}{1-\varepsilon} - \frac{1 - \left(\frac{m_0}{M_0}\right)^{1+\varepsilon}}{1+\varepsilon} \right] =$$

$$= \frac{M_0}{\mu_0} \lim_{\varepsilon \to 0} \frac{1}{1-\varepsilon^2} \left[1 - \frac{(1+\varepsilon)\left(\frac{m_0}{M_0}\right)^{1-\varepsilon} - (1-\varepsilon)\left(\frac{m_0}{M_0}\right)^{1+\varepsilon}}{2\varepsilon} \right] =$$

$$= \frac{M_0}{\mu_0} \lim_{\varepsilon \to 0} \left[1 - \frac{(1+\varepsilon)\left(\frac{m_0}{M_0}\right)^{1-\varepsilon} - (1-\varepsilon)\left(\frac{m_0}{M_0}\right)^{1+\varepsilon}}{2\varepsilon} \right] =$$

$$= \frac{M_0}{\mu_0} \lim_{\varepsilon \to 0} \left[1 - \frac{1}{2} \left\{ \left(\frac{m_0}{M_0}\right)^{1-\varepsilon} - (1+\varepsilon)\left(\frac{m_0}{M_0}\right)^{1-\varepsilon} \ln \frac{m_0}{M_0} + \right.\right.$$

$$\left.\left. + \left(\frac{m_0}{M_0}\right)^{1+\varepsilon} - (1-\varepsilon)\left(\frac{m_0}{M_0}\right)^{1+\varepsilon} \ln \frac{m_0}{M_0} \right\} \right] =$$

$$= \frac{M_0}{\mu_0} \left[1 - \frac{m_0}{M_0} \left(1 - \ln \frac{m_0}{M_0} \right) \right] = \frac{M_0}{\mu_0} \left[1 - \left(1 - \frac{\mu_0}{M_0} t_0 \right) \cdot \left\{ 1 - \ln \left(1 - \frac{\mu_0}{M_0} t_0 \right) \right\} \right] =$$

$$= \frac{M_0}{\mu_0} \left[\frac{\mu_0}{M_0} t_0 + \left(1 - \frac{\mu_0}{M_0} t_0 \right) \ln \left(1 - \frac{\mu_0}{M_0} t_0 \right) \right]. \tag{81}$$

Leider ist es nicht möglich, Beschleunigung, Geschwindigkeit und Weg auch durch die Zeit t auszudrücken, wie im Spezialfall konstanter Eigenbeschleunigung, da die Gl. (78) sich nicht nach t_0 auflösen läßt. Entwickelt man Gl. (78) in eine Potenzreihe

$$t = t_0 \left[1 + \left(\frac{a_0}{c}\right)^2 \frac{\left(\frac{\mu_0}{M_0} t_0\right)^2}{3!} + 3 \left(\frac{a_0}{c}\right)^2 \frac{\left(\frac{\mu_0}{M_0} t_0\right)^3}{4!} + \right.$$

$$\left. + \left(\frac{a_0}{c}\right)^2 \left\{ \left(\frac{a_0}{c}\right)^2 + 11 \right\} \frac{\left(\frac{\mu_0}{M_0} t_0\right)^4}{5!} + \dots \right], \tag{82}$$

dann lautet die Umkehrung

$$t_0 = t \left[1 - \left(\frac{a_0}{c}\right)^2 \frac{\left(\frac{\mu_0}{M_0} t\right)^2}{3!} - 3 \left(\frac{a_0}{c}\right)^2 \frac{\left(\frac{\mu_0}{M_0} t\right)^3}{4!} + \right.$$

$$\left. + \left(\frac{a_0}{c}\right)^2 \left\{ 9 \left(\frac{a_0}{c}\right)^2 - 11 \right\} \frac{\left(\frac{\mu_0}{M_0} t\right)^4}{5!} + \dots \right]. \tag{83}$$

Die mit dieser Reihe ermittelten Werte für t_0 werden nun in die Gln. (77), (75) und (79) eingesetzt, um Beschleunigung, Geschwindigkeit und Weg der Rakete in Abhängigkeit von t zu erhalten.

Alle Beziehungen lassen sich dimensionslos darstellen, wenn man M_0/μ_0 als Zeiteinheit, c als Geschwindigkeitseinheit und $c\,M_0/\mu_0$ als Längeneinheit wählt.

Literaturverzeichnis

1. E. Madelung, Die mathematischen Hilfsmittel des Physikers, S. 415. Berlin: Springer, 1950.
2. J. Ackeret, Zur Theorie der Raketen. Helvet. Physica Acta **19**, 103 (1946); On the Theory of Rockets. J. Brit. Interplan. Soc. **6**, 116 (1947).
3. R. Esnault-Pelterie, L'Astronautique, S. 229. Paris: A. Lahure, 1930. L'Astronautique, Complément, S. 89. Paris: A. Lahure, 1935.
4. W. L. Bade, Relativistic Rocket Theory. Amer. J. Physics **21**, 310 (1953).

Zur Verwendung von Kernenergie für Staustrahltriebwerke

Von

H. J. Kaeppeler[1], ARS, BIS, GfW

(Mit 3 Abbildungen)

(*Eingelangt am 7. Oktober 1955*)

Zusammenfassung. Die Aufheizung der Luft in Staustrahltriebwerken durch einen Lichtbogen an Stelle chemischer Heizung ist bereits verschiedentlich erwogen worden. Dabei wird es erforderlich sein, das Gewicht der Stromerzeugungsanlage, wobei die Energie aus Kernreaktionen gewonnen werden soll, möglichst klein zu halten. Es wird hier vorgeschlagen, eine direkte Stromerzeugung durch Auffang der beim β-Zerfall verschiedener Elemente entstehenden Elektronen in einer sogenannten β-Zerfallsbatterie, wie sie schon für Ionen-Strahltriebwerke erwogen wurde, zu verwenden. Eine Abschätzung der zu erwartenden Leistungsgewichte zeigt, daß entgegen dem Fall der Ionenstrahltriebwerke beim Staustrahltriebwerk den Elementen mit relativ kurzen Halbwertszeiten für den β-Zerfall Beachtung geschenkt werden soll.

Abstract. The heating of air in ram-jet power plants by means of gaseous discharges instead of chemical combustion has been suggested several times. In such cases, it will be necessary to keep the weights of the current generators using nuclear reactions as energy sources as low as possible. Here it is suggested to use a direct method of electrical current generation by collecting the electrons liberated in β-decay of various elements in a so-called β-decay battery, as has been considered for application in ion rockets. An estimate of weight to power ratios to be expected shows that, contrary to the case of ion rockets, elements with relatively short half-lives for the β-decay will be preferred in the case of ram-jet power plants.

Résumé. La possibilité de substituer un arc électrique à une réaction chimique pour chauffer le flux d'air d'un stato-réacteur a déjà été suggérée à plusieurs reprises. En supposant l'énergie nécessaire empruntée à une réaction nucléaire, cette solution exige que le poids du générateur de courant soit réduit au minimum. Il est proposé d'obtenir le courant par capture des électrons libérés par émission β de divers éléments dans une batterie dite "de désintégration β" analogue à celles qui ont été proposées pour les réacteurs à flux ionique.

Une estimation du rapport poids-puissance montre que, contrairement au cas des réacteurs à flux ionique, on est amené à prendre en considération des éléments dont la demi-période de désintégration est relativement courte.

Das mitunter erwogene Problem, chemische Heizung in Staustrahltriebwerken durch eine Lichtbogenheizung zu ersetzen, die ihre Energie aus Kernreaktionen bezieht [1], spitzt sich offenbar darauf zu, wieweit die einzusparenden Gewichte chemischer Treibstoffe durch die erforderlichen Gewichte der Kernreaktoranlage wieder verschlungen werden.

---

[1] Forschungsinstitut für Physik der Strahlantriebe, Stuttgart-Flughafen, Bundesrepublik Deutschland.

Eine erste Beurteilung läßt die sekundlich notwendige Wärmezufuhr Q im Triebwerk je Einheit des Fluggewichtes G zu.

Im stationären Horizontalflug ist der Schub P des Triebwerks bekanntlich gleich dem mit der Gleitzahl $\varepsilon = c_w/c_a$ multiplizierten Fluggewicht,

$$P = \varepsilon G. \tag{1}$$

Mit dem Wirkungsgrad $\eta = P\,v/Q$ des Triebwerkes (v = Horizontalfluggeschwindigkeit) folgt ohne weiteres die gesuchte Größe

$$Q/G = \varepsilon\, v/\eta \qquad \left[\frac{\text{mkg/sec}}{\text{kg}} = \text{m/sec}\right], \tag{2}$$

und kann daher mittels der bekannten Gesamtwirkungsgrade η der Staustrahltriebwerke leicht dargestellt werden.

Mittels der bekannten [2, 3] ersten Näherungsbeziehung des Staustrahlantriebes

$$\eta = \frac{v^2}{g\,c_p\,T_2\left[\sqrt{(T_3/T_2)}+1\right]}$$

ergibt sich beispielsweise

$$Q/G = \frac{\varepsilon\, g\, c_p\, T_2\left[\sqrt{(T_3/T_2)}+1\right]}{v}, \tag{2 a}$$

worin T_2 und T_3 die Stautemperaturen der Frischluft, bzw. der aufgeheizten Luft, g die Schwerebeschleunigung und c_p die spezifische Wärme der Luft bei konstantem Druck sind.

Der Wärmeaufwand je Fluggewichtseinheit ist daher nur wenig abhängig von der Flughöhe, wächst im allgemeinen mit der Fluggeschwindigkeit (T_2!) und wird stark durch die Gleitzahl des Flugzeuges bestimmt.

Aus Gl. (2) folgt beispielsweise bei $v = 1200$ m/sec mit $\varepsilon = 0{,}1$ und $\eta = 0{,}5$, daß $Q/G = 240$ m/sec $= 2{,}35$ kW/kg $= 3{,}2$ PS/kg ist. Bei $v = 300$ m/sec mit $\varepsilon = 0{,}05$ und $\eta = 0{,}1$ folgt $Q/G = 150$ m/sec $= 1{,}47$ kW/kg $= 2$ PS/kg. Mit $v = 0$ folgt $Q/G = \infty$.

Um vom Wärmeaufwand je Fluggewichtseinheit Q/G zum Leistungsgewicht der Triebwerksanlage G_T/Q zu kommen, kann man beispielsweise annehmen, daß das Gewicht der Triebwerksanlage etwa ein Drittel des gesamten Fluggewichts ausmachen kann, also $G_T = 0{,}3\,G$. Damit erhält man

$$G_T/Q = \frac{0{,}3\,v}{\varepsilon\, g\, c_p\, T_2\left[\sqrt{(T_3/T_2)}+1\right]} \tag{3}$$

für das unter der obigen Annahme erlaubte Leistungsgewicht der Triebwerksanlage.

Die Gln. (2) und (3) sind in Abb. 1 dargestellt, und zwar sind G/Q und G_T/Q aufgetragen als Funktion der MACH-Zahl. Für das obige Beispiel mit $v = 1200$ m/sec ergibt sich $G_T/Q = 0{,}128$ kg/kW und für das Beispiel mit $v = 300$ m/sec folgt $G_T/Q = 0{,}204$ kg/kW. Würde man erlauben, daß das Triebwerksgewicht etwa die Hälfte des Fluggewichtes ausmachen dürfte, so hätte man Leistungsgewichte von etwa 0,21 bzw. 0,34 kg/kW für die beiden genannten Beispiele.

Um derart kleine Leistungsgewichte zu erzielen, scheinen Wege der direkten Erzeugung von elektrischem Strom aus Kernreaktionen am ehesten Erfolg zu versprechen. Ein solcher Vorschlag zur Verwendung in Ionen-Strahltriebwerken wurde bereits von L. R. SHEPHERD und A. V. CLEAVER [4] gemacht. Ebenfalls verwendet diesen Vorschlag H. PRESTON-THOMAS [5] in seiner Betrachtung der verschiedenen Arten der elektrischen Strahltriebwerke.

Es wurde vorgeschlagen, in einer β-Zerfallsbatterie (s. Abb. 2) die von einem β-radioaktiven Material emittierte Strahlung aufzufangen und damit zwischen emittierendem Material und Kollektorplatten einen Potentialunterschied herzustellen. Wie bekannt, erklärt die einfachste Theorie des β-Zerfalls diesen Vorgang im Atomkern dadurch, daß ein Neutron in ein Proton und ein Elektron zerfällt und das Elektron abgestrahlt wird [6]. Auf die komplizierteren Theorien, wie z. B. die Mesonentheorie des β-Zerfalls, soll hier nicht eingegangen werden. Ebenso wird für die folgenden Betrachtungen eine Beschränkung auf den *einfachen* β-Zerfall gemacht. Durch diese Umwandlung von Neutronen in Protonen und Elektronen, wobei dann die Elektronen abgestrahlt werden, erfolgt eine positive Aufladung des emittierenden Materials. Die abgestrahlten β-Elektronen rufen durch den Einfang auf den Kollektorplatten eine negative Aufladung dieser Platten hervor. Dieser Ladungsunterschied ergibt dann bei einer Überbrückung einen Gleichstrom, der zur Speisung des Lichtbogens verwendet werden kann.

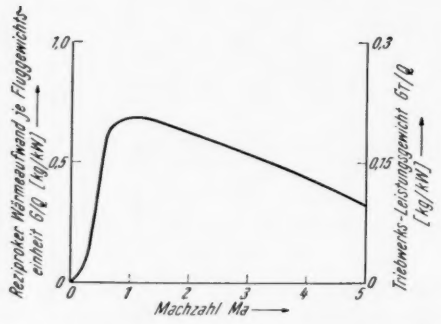

Abb. 1. Wärmeaufwand je Fluggewichtseinheit und Leistungsgewichte für Staustrahltriebwerke [s. Gln. (2) und (3)]

$$G/Q = (\eta/\varepsilon \cdot v) \qquad G_T = 0{,}3 \cdot G$$

Die β-Elektronen müssen über eine ausreichende Energie verfügen, um sich gegen das Potential zwischen den Platten bis zur Kollektorplatte bewegen zu können. Die bis dahin noch nicht verbrauchte Bewegungsenergie der Elektronen wird beim Aufprall in thermische Energie umgewandelt und heizt die Platten auf. Bekanntlich haben die β-Elektronen ein kontinuierliches Energie-Spektrum, das durch die maximale β-Energie nach oben begrenzt ist. Das Intensitätsmaximum dieses Spektrums liegt etwa bei ein Drittel der maximalen Energie. Man wird also wahrscheinlich den Abstand der Platten so wählen, daß die β-Elektronen mit der Energie aus dem Bereich der maximalen Intensität mit annähernd der Geschwindigkeit Null auf den Kollektorplatten auftreffen, um so möglichst die Erwärmung der Platten klein zu halten. Der Abstand zwischen emittierendem Material und Kollektorplatten bestimmt auch die Spannung des entstehenden Gleichstroms.

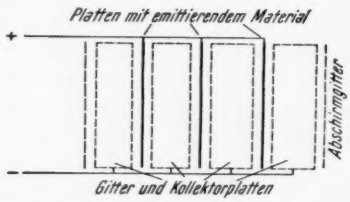

Abb. 2. Schema einer β-Zerfallsbatterie

Gleichzeitig wird es wichtig sein, dünne Schichten des emittierenden Materials auszubilden, um die Absorption der β-Elektronen in diesem Material möglichst zu reduzieren. Diese Absorption hat einen ungünstigen Einfluß auf den inneren Wirkungsgrad der β-Zerfallsbatterie, der im übrigen von PRESTON-THOMAS [5] zu etwa $\eta_i = 0{,}75$ angegeben wird.

Eine Abschirmung ist beim β-Zerfall in einer solchen Batterie fast nicht notwendig, da die Kollektorplatten ja die β-Strahlung auffangen. Man wird daher möglichst nur β-aktives Material verwenden, welches keine gleichzeitige α- oder

γ-Aktivität zeigt. Ein gewisser Betrag von γ-Strahlung jedoch wird immer infolge des β-Bremsspektrums vorhanden sein.

Eine wichtige Rolle bei der Auswahl des β-aktiven Materials spielt die Halbwertszeit des Zerfalls und die maximale β-Energie. So wurde z. B. für die Anwendung in Ionen-Strahltriebwerken eine möglichst große Halbwertszeit gefordert [5], um die Betriebsdauer der Batterie bis zur Erneuerung des radioaktiven Materials möglichst lang zu gestalten. Man denkt an eine Erneuerung der β-aktiven Platten in der Batterie etwa nach einem Viertel der Halbwertszeit.

Für die Anwendung der β-Zerfallsbatterie für Staustrahltriebwerke mit Lichtbogenheizung, wie sie hier vorgeschlagen wird, gelten jedoch etwas andere Gesichtspunkte. Man wird für diesen Zweck Elemente mit kürzeren Halbwertszeiten für den β-Zerfall wählen, um so in kurzer Zeit relativ große Leistungen zur Verfügung zu haben.

Im folgenden soll nun eine Abschätzung der zu erwartenden Leistungsgewichte für solche β-Zerfallsbatterien durchgeführt werden. Wie bekannt, wird der radioaktive Zerfall eines Elementes beschrieben durch die Differentialgleichung

$$dN/dt = -\alpha N, \qquad \alpha = \ln 2/\tau,$$

mit der Lösung

$$N = N_0 e^{-\ln 2\,(t/\tau)}. \tag{4}$$

Vol. 2 1956

N ist die jeweilige Zahl der Teilchen (z. B. pro Volumseinheit), N_0 die Zahl der vorhandenen (nichtzerfallenen) Atome zur Zeit $t_0 = 0$, $\alpha = \ln 2/\tau$ die Reaktionsgeschwindigkeit [sec^{-1}] und τ die Halbwertszeit. Entsprechend der Zahl der erfolgten Reaktionen $N_0 - N = N_0\,(1 - e^{-\alpha t})$ ergibt sich die Zahl der im Zeitelement dt erfolgenden Reaktionen $= \alpha N_0 e^{-\alpha t}$ [$\mathrm{m}^{-3}\,\mathrm{sec}^{-1}$], (5)

und damit die von einer Masse m pro Sekunde abgegebene Energie, das heißt die jeweilige Leistung der β-Zerfallsbatterie, zu

$$Q = \eta_i E\, m(N_0/\varrho)\,(\ln 2/\tau)\, e^{-\ln 2\,(t/\tau)}, \tag{6}$$

wobei η_i der innere Wirkungsgrad, E die pro Reaktion freiwerdende Energie und ϱ die Dichte der zerfallenden Substanz ist. Es interessiert nun insbesondere die kleinste Leistung der Batterie während der Betriebsdauer, also diejenige für $t = \tau/4$. Führt man ferner noch die Loschmidtsche Zahl L und das Molekulargewicht M des Stoffes ein, so erhält man für das Leistungsgewicht einer β-Zerfallsbatterie aus Gl. (6)

$$G_B/Q = (5\sqrt[4]{2}/\ln 2)\,\frac{M\tau}{E L \eta_i}, \tag{7}$$

wobei angenommen wurde, daß das Gewicht der gesamten Batterie etwa fünfmal so groß wie das erforderliche Gewicht des β-aktiven Materials ist. Dies scheint zunächst als plausibler Wert gelten zu können. Man kann nun in Ermanglung konkreter Zahlenangaben annehmen, daß $G_T \approx 2\,G_B$ ist, und erhält somit die einfache Relation

$$G_T/Q = (7{,}72 \times 10^{-6}/\eta_i)\,\frac{M\ [\mathrm{kg/kmol}]\,\tau\,[\mathrm{d}]}{E\ [\mathrm{MeV}]}, \qquad [\mathrm{kg/kW}] \tag{8}$$

für das Leistungsgewicht der gesamten β-Zerfallsbatterie-Lichtbogenanlage. Dieses Leistungsgewicht G_T/Q steigt also linear mit dem Molekulargewicht der aktiven Substanz und ebenso linear mit der Halbwertszeit des Zerfalls. Das Leistungsgewicht ist umgekehrt proportional der maximalen β-Energie E. Wie bekannt, ist hier wegen der Erfüllung des Energiesatzes nicht die mittlere, sondern die maximale β-Energie zu setzen [7].

In Abb. 3 ist nun Gl. (8) für das Leistungsgewicht G_T/Q dargestellt, und zwar ist G_T/Q aufgetragen über der Halbwertszeit τ mit Werten von $M/\eta_i E$ als Parameter. Als Punkte eingetragen sind die Substanzen Phosphor ^{32}P, Eisen ^{59}Fe, Kupfer ^{67}Cu und Yttrium ^{91}Y, wobei hier der von PRESTON-THOMAS [5] angegebene Wert von $\eta_i = 0{,}75$ verwendet wurde. Die Daten für diese Elemente wurden dem Buch von RIEZLER [7] entnommen. Interessant sind die außerordentlich niederen Leistungsgewichte, insbesondere von ^{32}P mit $G_T/Q = 2{,}8 \times 10^{-3}$ kg/kW und ^{91}Y mit $G_T/Q = 3{,}5 \times 10^{-2}$ kg/kW. Dies würde bedeuten, daß, wenn die Annahme über das Gesamtgewicht der Anlage, das hier gleich dem zehnfachen des Gewichts der radioaktiven Substanz geschätzt wurde, sich als nicht zutreffend erwiese, noch genügend Spielraum für zusätzliche Gewichte zur Verfügung stünde. Eingezeichnet in Abb. 3 sind ferner die Leistungsgewichte des Kolbenflugmotors, eines Nickelakkumulators, und einer Uranreaktor-Turbogeneratoranlage nach konservativen Gewichtsschätzungen [5].

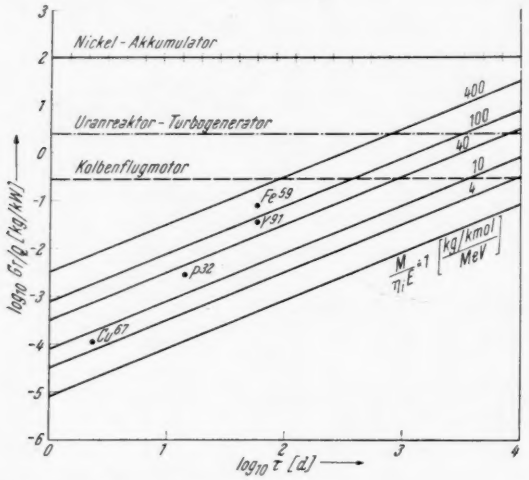

Abb. 3. Näherungsweise ermittelte Leistungsgewichte von β-Zerfallsbatterien [s. Gl. (8)]

Den vorgelegten näherungsweisen Überlegungen entsprechend, denen selbstverständlich noch eingehende Untersuchungen folgen müßten, dürfte die Verwendung von β-Zerfallsbatterien als Energiequelle für die Lichtbogenheizung in Staustrahltriebwerken unter Umständen von einigem Interesse sein.

Der Verfasser möchte an dieser Stelle dem Leiter des Forschungsinstitutes für Physik der Strahlantriebe, Herrn Dr. E. SÄNGER, für wertvolle Hinweise sowie für die Durchsicht der Arbeit seinen aufrichtigen Dank aussprechen.

Literaturverzeichnis

1. E. SÄNGER, Wege des Strahlfluges. Mitt. Forsch.-Inst. Physik d. Strahlantriebe, Nr. 3. München: R. Oldenbourg, 1955.
2. E. SÄNGER und I. BREDT, Über einen Lorinantrieb für Strahljäger. Forschungsbericht UM 3509. Berlin: ZWB, 1943; N.A.C.A. Techn. Mem. 1106, 1947.
3. E. SÄNGER, Schweiz. Arch. angew. Wiss. **16**, 341, 369 (1951).
4. L. R. SHEPHERD and A. V. CLEAVER, J. Brit. Interplan. Soc. **7**, 184, 234 (1948); **8**, 23, 59 (1949).
5. H. PRESTON-THOMAS, J. Brit. Interplan. Soc. **11**, 173 (1952).
6. W. HEISENBERG, Theorie des Atomkerns. Göttingen: Max-Planck-Institut, 1951.
7. W. RIEZLER, Einführung in die Kernphysik, 5. Aufl. München: R. Oldenbourg, 1953.

Statement

It is widely known that during the International Geophysical Year (1 July 1957 — 31 December 1958) the United States will launch a number of earth satellite vehicles as part of its contribution to the overall program of the IGY. It has been announced that full details of the satellite vehicles — their instrumentation, radio transmission equipment, and anticipated orbits will be released to the public.

Because of the significance of the earth satellite program in the evolution of the rocket powered guided missile to eventual manned space flight, the IAF has arranged with the U.S. National Committee for the IGY of the National Academy of Sciences to receive all pertinent details as released. Commencing with the next issue, *Astronautica Acta* will publish regularly technical and administrative details of this program, either in complete or summarized form.

The offer of the IAF to collaborate with the U.S. Earth Satellite Project has been accepted in connection with the optical satellite-tracking program. Details of this collaboration are being discussed with Member Societies of the IAF.

Frederick C. Durant, III
President

Buchbesprechungen — Book Reviews — Comptes rendus

Aerodynamik der reinen Unterschall-Strömung. Von F. Dubs. (Flugtechnische Reihe: Band I.) Mit 178 Textabb., 225 S. Basel und Stuttgart: Verlag Birkhäuser. 1954. sfr. 22.—, DM 22.—.

Im vorliegenden Buche werden die Grundlagen der reinen Unterschall-Aerodynamik dem Leser in einfacher, aber korrekter Form zugänglich gemacht. Der Verfasser, der als Hauptlehrer an der mechanisch-technischen Abteilung der Gewerbeschule der Stadt Zürich tätig ist, setzt zum Verständnis seiner Ausführungen nur geringe mathematische Kenntnisse voraus. Er erläutert die Strömungsvorgänge vor allem an Hand vieler gut gewählter Abbildungen. Einige Formeln, die entsprechend der Wichtigkeit mehr oder weniger hervorgehoben sind, ergänzen den Text.

Nach einem einleitenden Abschnitt über die Atmosphäre, der unter anderem auch die in der Flugtechnik häufig gebrauchten Werte der CINA-Normalatmosphäre enthält, behandelt der Verfasser die Strömungsgesetze, die Strömungsformen und Strömungsbilder. Der Unterschied zwischen laminarer und turbulenter Strömung wird dabei richtig, wenn auch etwas kurz erklärt. Weitere Kapitel befassen sich mit der Grenzschicht, den Mitteln zur Verhinderung der Strömungsablösungen und den verschiedenen Arten von Windkanälen. Besonders ausführlich sind die anschließenden Abschnitte über die Tragflügeltheorie, die Profilform und Polare und die auftretenden Widerstände gehalten. Die Wirkung der Pfeilung der Flügel auf den induzierten Widerstand, wie auch die Einflüsse der Staffelung und Schränkung der Flügel bei Mehrdeckern auf Auftrieb und Widerstand werden diskutiert. Auch die Ausführungen über die Besonderheiten der Laminarprofile nehmen einen breiten Raum ein. Der Abschnitt über die Profilsystematik verdient es, ebenso beachtet zu werden wie derjenige über die Auftriebssteigerung durch Klappen.

Das systematisch aufgebaute Buch schließt mit einem Literatur-, Namen- und Sachverzeichnis ab. — Abschließend darf man wohl sagen, daß es wünschenswert wäre, wenn in nächster Zeit ein Werk im selben Rahmen über das Gebiet der Flugmechanik erscheinen würde.

A. Burgdorfer, Zürich.

Frontier to Space. Von E. Burgess. Mit einem Vorwort von Sir H. S. Jones. Mit 104 Textabb., XVI, 174 S. London: Chapman & Hall Ltd. 1955. 21 s.

Dieses neue Werk des Verfassers des bekannten Buches „Rocket Propulsion" befaßt sich mit der Erforschung der hohen Atmosphäre mittels Raketen. Es beschreibt in fesselnder Weise die Entwicklung der letzten zehn Jahre, zum Teil an Hand der bedeutenderen amerikanischen Raketenaufstiege. Das Buch ist auch deshalb aktuell, weil es — kurz vor dem Start künstlicher Satelliten in die Ionosphäre und Exosphäre — auf jene Forschungsmethoden verweist, die statt der nur kurze Zeit im Flug befindlichen Rakete dem verhältnismäßig langlebigen Satelliten vorbehalten sind.

Der Leser wird in wichtige Probleme der kosmischen Physik eingeführt und mit den bisherigen Ergebnissen der Forschung mit Raketen vertraut gemacht. Vom radiotechnischen Teil abgesehen genügen zum Verständnis solide Grundkenntnisse aus Physik und Chemie. Spezialliteratur ist nach jedem Kapitel angegeben. Besonders eingehend werden die Beobachtungen der Solarstrahlung in den verschiedenen Wellenlängenbereichen und ihr Zusammenhang mit irdischen Erscheinungen behandelt. Der Einbau der benutzten Meß- und Fernmeldegeräte wird in Abbildungen und photographischen Tafeln beschrieben. Das Schlußkapitel hat die Errichtung künstlicher Satelliten der Erde und des Mars zum Inhalt. Burgess' Werk, eine sehr erfreuliche Neuerscheinung der raketentechnischen und geophysikalischen Literatur, wurde soeben auch in deutscher Übersetzung unter dem Titel „Raketen in der Ionosphärenforschung" bei der Deutschen Radar-Verlagsgesellschaft m. b. H., Garmisch-Partenkirchen, veröffentlicht.

F. Hecht, Wien.

Herausgeber, Eigentümer und Verleger: Springer-Verlag, Wien I, Mölkerbastei 5. — Für den Inhalt verantwortlich: Prof. Dr. Friedrich Hecht, Wien VIII, Alserstraße 69. — Druck: Berger & Schwarz, Zwettl, N.-Ö.

A Calculus of Variations Solution of Goddard's Problem

By

G. Leitmann[1], BIS

(With 2 Figures)

(*Received October 24, 1955*)

Abstract. The problem of optimum thrust programming is investigated for a rocket to achieve a given altitude with given velocity and pay load and with minimum fuel expenditure. The rocket model is that considered by R. H. GODDARD in his paper "A Method of Reaching Extreme Altitudes". A solution is given by means of the Calculus of Variations.

Zusammenfassung. Das Problem der Berechnung der günstigsten Größe des Schubes einer Rakete wird untersucht, um eine gegebene Höhe mit gegebener Geschwindigkeit und Nutzlast und minimalem Brennstoffverbrauch zu erreichen. Das Raketenmodell ist dasjenige, das R. H. GODDARD in seiner Arbeit "A Method of Reaching Extreme Altitudes" behandelt hat. Eine Lösung wird mittels der Variationsrechnung abgeleitet.

Résumé. Le problème d'un programme d'une poussée optimum se pose pour qu'une fusée puisse réaliser une altitude donnée avec une vitesse donnée, une charge payante donnée et une dépense minimum de combustible. Le modèle de fusée est celui considéré par R. H. GODDARD dans son article "A Method of Reaching Extreme Altitudes". La solution est obtenue par le calcul de variations.

Vol. 2 1956

I. Introduction

In 1919, the American rocket pioneer R. H. GODDARD published his classical paper "A Method of Reaching Extreme Altitudes". In so doing, he was the first scientist to bring to public attention the problem of sending a rocket to high altitude in the most economical and hence practical way. GODDARD stated the basic problem, recognized it as a problem in the Calculus of Variations, and gave an approximate solution. In this note, we present a Calculus of Variations solution of GODDARD's problem.

II. Problem

The problem, posed by GODDARD, can be stated as follows: What is the velocity as a function of time of a rocket required to transport a given pay load to a specified altitude and velocity so that the initial rocket mass be a minimum?

In order to solve this problem, GODDARD considered an idealized rocket, greatly simplified, yet incorporating what he considered the important char-

[1] Aeroballistic Analysis Branch, U.S. Naval Ordnance Test Station, China Lake/Calif., USA.

acteristics of a real rocket. Fig. 1 shows the idealized rocket envisioned by GODDARD.

The idealized rocket is a right, circular cone. The pay load, M_1, is at the tip. Case, K, which surrounds propellant, P, is supposed to drop away continuously (having zero velocity with respect to the remaining rocket) as the propellant burns. It is also assumed that mass is expelled from the rocket with a constant velocity, c, with respect to the rocket.

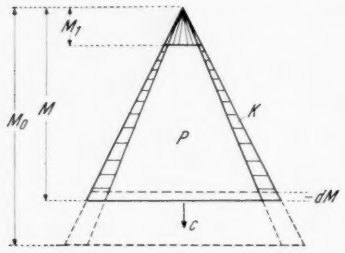

Fig. 1

GODDARD inferred the existence of a minimum initial mass (i.e. minimum propellant) to raise a given pay load to specified height from the following plausible argument. "If, at any intermediate altitude, the velocity of ascent be very great, the air resistance (depending on the square of the velocity) will also be great. On the other hand, if the velocity of ascent be very small, force will be required to overcome gravity for a long period of time. In both cases the mass necessary to be expelled will be excessively large. Evidently, then, the velocity of ascent must have a special value at each point in space."

GODDARD went on to state that the determination of the necessary velocity-time function presents a new and unsolved problem in the Calculus of Variations. Consequently, he abandoned a rigorous approach and constructed an approximate solution. For a discussion of this approximate solution and numerical work, we refer the reader to the basic reference [1]. Suffice it to say that the fundamental assumption made by GODDARD consisted in assuming aerodynamic drag, gravity, and acceleration constant over a large number of short portions of the trajectory.

In what follows, we shall derive the relations necessary for the existence of a minimum initial rocket mass by the more rigorous methods of the Calculus of Variations.

III. Solution

At the outset, we define some quantities used throughout this paper.

M = rocket (total) mass at time t
s = height
D = aerodynamic drag
g = acceleration of gravity
k = constant fraction of dM, consisting of casing, K, expelled with zero velocity relative to rocket
c = velocity of expelled mass relative to rocket

Dot $(\cdot)$ will stand for differentiation with respect to time.

The classical equation of motion of the rocket in vertical ascent, neglecting the earth's rotation, is

$$\dot{M}\, c\,(1-k) + M(\ddot{s} + g) + D = 0. \tag{1.1}$$

After all fuel has been expended, the motion will be governed by

$$M_1(\ddot{s} + g) + D = 0 \tag{1.2}$$

where

M_1 = burnt mass (pay load).

For a specified altitude, S, and velocity $\dot{S}$, eq. (1.2) has a solution

$$\dot{s} = \varphi(s). \tag{1.3}$$

If burn-out occurs at sufficiently high altitude, where drag is negligible, eq. (1.3) becomes

$$\dot{s} = \sqrt{2\,g(S-s) + \dot{S}^2}$$

with the additional restriction that gravitational acceleration, g, is considered constant. For moderately high altitudes, i.e. 100 miles, this assumption yields a value within 5% of the actual value of g. For the sake of simplicity, we shall assume a constant g throughout this paper. It should be pointed out that a solution could be obtained with variable g, albeit at the expense of simplicity.

In general, aerodynamic drag is written in the following form

$$D = \tfrac{1}{2}\,\varrho\,A\,C_D\,\dot{s}^2 \tag{1.4}$$

where

ϱ = air density
C_D = drag coefficient
A = reference area (usually the greatest cross-sectional area) of the missile.

Air density, ϱ, is a function of altitude, s. Drag coefficient, C_D, is expressible as a function of MACH and REYNOLDS numbers and hence is well approximated by a function of altitude, s, and velocity, $\dot{s}$. For a body whose shape remains constant, such as our idealized rocket, cross-sectional area, A, may be expressed as

$$A = a\,M^{2/3} \tag{1.5}$$

where the proportionality number, a, is given by

$$a = \pi\,[\tfrac{1}{3}\pi\,\varrho_R \cot\theta]^{-2/3} \tag{1.6}$$

and

ϱ_R = rocket density
θ = semi-vertex angle of cone.

For constant rocket density, ϱ_R, the proportionality number, a, is indeed constant.

We shall now proceed with the solution, treating the problem as one of MAYER type [2].

In view of our assumptions, we may write

$$D = \tfrac{1}{2}\,\varrho\,a\,M^{2/3}\,C_D\,\dot{s}^2 = M^{2/3}\,\mathfrak{D}(s,\dot{s}) \tag{1.7}$$

so that eq. (1.1) becomes

$$\dot{M}c\,(1-k) + M(\ddot{s}+g) + M^{2/3}\,\mathfrak{D}(s,\dot{s}) = 0. \tag{1.8}$$

If we let

$$\dot{s} \equiv v \tag{1.9}$$

we may write eqs. (1.8) and (1.9) as

$$\Phi_1 \equiv \dot{M}\,c\,(1-k) + M(\dot{v}+g) + M^{2/3}\,\mathfrak{D}(s,\dot{s}) = 0 \tag{1.10}$$

$$\Phi_2 \equiv \dot{s} - v = 0. \tag{1.11}$$

For the purpose of studying the properties of the optimum path, we form $\delta\Phi_1$, and $\delta\Phi_2$; these variations correspond to "neighboring" paths. If "neighboring" paths are to satisfy the equation of motion,

$$\begin{aligned} \delta\Phi_1 &= 0 \\ \delta\Phi_2 &= 0. \end{aligned} \tag{1.12}$$

At this time, LAGRANGIAN multipliers, $\lambda_1(t)$ and $\lambda_2(t)$, are introduced and $\sum_i \lambda_i \, \delta\Phi_i$ is formed. In view of (1.12), this may be written

$$\left[\lambda_1 M^{2/3} \frac{\partial \mathfrak{D}}{\partial s} - \dot{\lambda}_2\right] \delta s + \frac{d}{dt}(\lambda_2 \, \delta s) +$$

$$+ \left[\lambda_1 M^{2/3} \frac{\partial \mathfrak{D}}{\partial v} - \lambda_1 \dot{M} - \dot{\lambda}_1 M - \lambda_2\right] \delta v + \frac{d}{dt}(\lambda_1 M \, \delta v) + \tag{1.13}$$

$$+ \left[\lambda_1(\dot{v} + g) + \tfrac{2}{3} \lambda_1 \mathfrak{D} M^{-1/3} - \dot{\lambda}_1 c (1 - k)\right] \delta M + \frac{d}{dt}[\lambda_1 c (1 - k) \, \delta M] = 0.$$

We shall assume that the velocity, $\dot{s} \equiv v$, is continuous throughout burning. However, we shall admit the possibility of discontinuities in $\dot{s}$ at the beginning and end of powered flight. A discontinuity in $\dot{s}$ is equivalent to an instantaneous change in the value of the velocity; ideally, this is brought about by an impulsive boost. Consequently, we note the following definitions.

At $t = 0$	$s = 0$ $\dot{s} \equiv v = 0$ $M = M_0$ $\lambda_i = \lambda_{i0}$	before initial boost
At $t = 0^+$	$s = 0$ $\dot{s} \equiv v = \dot{s}^0 = v^0$ $M = M^0$ $\lambda_i = \lambda_i{}^0$	after initial boost
At $t = t_1^-$	$s = s'$ $\dot{s} \equiv v = \dot{s}' = v'$ $M = M'$ $\lambda_i = \lambda_i{}'$	before final boost
At $t = t_1$ (end of burning)	$s = s_1$ $\dot{s} \equiv v = \dot{s}_1 = v_1$ $M = M_1$ $\lambda_i = \lambda_{i1}$	after final boost.

Conditions at $t = t_1$ correspond to those at the out-set of coasting flight. Integrating eq. (1.13) between $t = 0^+$ and $t = t_1^-$, i.e. between boosts, yields

$$c (1 - k) [\lambda_1{}^0 \, \delta M^0 - \lambda_1{}' \, \delta M'] = \lambda_2{}' \, \delta s' - \lambda_2{}^0 \, \delta s_0 + \lambda_1{}' M' \, \delta v' - \lambda_1{}^0 M^0 \, \delta v^0 +$$

$$+ \int_{0^+}^{t_1^-} \left\{ \left[\lambda_1 M^{2/3} \frac{\partial \mathfrak{D}}{\partial s} - \dot{\lambda}_2\right] \delta s + \right.$$

$$+ \left[\lambda_1 M^{2/3} \frac{\partial \mathfrak{D}}{\partial v} - \lambda_1 \dot{M} - \dot{\lambda}_1 M - \lambda_2\right] \delta v + \tag{1.14}$$

$$\left. + \left[\lambda_1(\dot{v} + g) + \tfrac{2}{3} \lambda_1 \mathfrak{D} M^{-1/3} - \dot{\lambda}_1 c (1 - k)\right] \delta M \right\} dt.$$

The LAGRANGIAN multipliers are as yet arbitrary. In order to express δM_0 as a function of δs and δv only, we impose the condition

$$\lambda_1(\dot{v}+g)+\tfrac{2}{3}\lambda_1 \mathfrak{D} M^{-1/3}-\dot{\lambda}_1 c(1-k)=0. \tag{1.15}$$

Since δs and δv are arbitrary, their coefficients must vanish separately, i.e.

$$\begin{aligned}\lambda_1 M^{2/3}\frac{\partial \mathfrak{D}}{\partial s}-\dot{\lambda}_2&=0\\ \lambda_1 M^{2/3}\frac{\partial \mathfrak{D}}{\partial v}-\lambda_1\dot{M}-\dot{\lambda}_1 M-\lambda_2&=0.\end{aligned} \tag{1.16}$$

Eqs. (1.8), (1.15), and (1.16) can be regarded as a set of four differential equations in the dependent variables λ_1, λ_2, M, and s. It is desired to eliminate λ_1, λ_2, and M. In so doing, there arises the useful relationship

$$\lambda_2=\lambda_1 M^{2/3}\left[\frac{\partial \mathfrak{D}}{\partial v}+\frac{\mathfrak{D}}{3c(1-k)}\right]. \tag{1.17}$$

Finally, the elimination of λ_1, λ_2, and M results in the EULER-LAGRANGE equation

$$\begin{aligned}\frac{\partial \mathfrak{D}}{\partial s}&=\frac{\partial^2 \mathfrak{D}}{\partial s\,\partial v}v+\frac{\partial^2 \mathfrak{D}}{\partial v^2}\dot{v}+\\ &+\frac{1}{3c(1-k)}\left[\frac{\partial \mathfrak{D}}{\partial s}v+(2\dot{v}+g)\frac{\partial \mathfrak{D}}{\partial v}+\frac{1}{3c(1-k)}(\dot{v}+g)\mathfrak{D}\right].\end{aligned} \tag{1.18}$$

The EULER-LAGRANGE equation must be satisfied throughout powered flight with the exception of beginning and end boosts, if any.

If a discontinuous velocity must be permitted at $t=0$ and $t=t_1$, the impulsive boost relations are

$$\begin{aligned}M_0&=M^0 e^{\frac{v^0}{c(1-k)}}\\ M_1&=M' e^{\frac{v'-v_1}{c(1-k)}}.\end{aligned} \tag{1.19}$$

In view of eqs. (1.15) and (1.16), eq. (1.14) becomes

$$c(1-k)\left[\lambda_1^{\,0}\delta M^0-\lambda_1'\delta M'\right]=\lambda_2'\delta s'-\lambda_2^{\,0}\delta s_0+\lambda_1' M'\delta v'-\lambda_1^{\,0}M^0\delta v^0. \tag{1.20}$$

We note the following boundary relations,

$$\begin{aligned}&\left.\begin{aligned}\delta s(0)&=\delta s_0=0\\ \delta M(t_1)&=\delta M_1=0\end{aligned}\right\}\quad s(0)\text{ and }M(t_1)\text{ being specified}\\ &\delta v(t_1)=\delta v_1=\frac{\partial \varphi}{\partial s_1}\delta s_1,\qquad\text{in view of (1.3) at } t=t_1\\ &\delta s(t_1^-)=\delta s'=\delta s_1=\delta s(t_1),\quad\text{displacement being continuous.}\end{aligned} \tag{1.21}$$

A necessary condition for the existence of a minimum initial mass, M_0, is

$$\delta M_0=0. \tag{1.22}$$

Consideration of eqs. (1.17), (1.19), (1.21), and (1.22), reduces eq. (1.20) to

$$\left[\frac{\partial \mathfrak{D}}{\partial v}+\frac{\mathfrak{D}}{3c(1-k)}\right]_{t=t_1-}=-\left[M_1 e^{\frac{\varphi(s_1)-v'}{c(1-k)}}\right]^{1/3}\frac{\partial \varphi}{\partial s_1}. \tag{1.23}$$

Eqs. (1.3) and (1.8) then permit us to write eq. (1.23) as

$$\varphi(s_1)\left[\frac{\partial \mathfrak{D}}{\partial v}+\frac{\mathfrak{D}}{3c(1-k)}\right]_{t=t_1-}=\left[M_1 e^{\frac{\varphi(s_1)-v'}{c(1-k)}}\right]^{1/3}[g+M_1^{-1/3}\mathfrak{D}_1]. \tag{1.24}$$

Eqs. (1.24) and (1.3) at $t = t_1$, must both be satisfied. If $\dot{s} \equiv v$ is continuous at $t = t_1$, no boost is required at the end of powered flight and eq. (1.24) becomes

$$\varphi(s_1)\left[\frac{\partial \mathfrak{D}}{\partial v} + \frac{\mathfrak{D}}{3\,c\,(1-k)}\right]_{t=t_1} = M_1^{1/3}\,g + \mathfrak{D}_1. \tag{1.25}$$

The EULER-LAGRANGE equation, eq. (1.18), is a second order differential equation in $s(t)$ subject to initial conditions $s(0^+) = 0$ and $\dot{s}(0^+) = v^0$. Initial velocity, v^0, is not specified but is nonetheless determined by the requirement that eq. (1.24) [or (1.25)] be satisfied.

IV. Particular Case

In order to obtain a solution to the optimum problem, it is necessary to specify the form of the drag function $\mathfrak{D}(s, \dot{s})$. The quadratic drag law, i.e. $C_D =$ constant, is often assumed and we shall use it here to proceed with a solution. We remember that

$$\mathfrak{D}(s, \dot{s}) = \tfrac{1}{2}\varrho\, a\, C_D\, \dot{s}^2. \tag{2.1}$$

A good approximation to the function $\varrho = \varrho(s)$ is

$$\varrho = \varrho_0\, e^{-\alpha s} \tag{2.2}$$

where ϱ_0 is the air density at sea level and α is a constant. Thus we write

$$\mathfrak{D}(s, \dot{s}) = R\, e^{-\alpha s}\, \dot{s}^2 \tag{2.3}$$

where

$$R \equiv \tfrac{1}{2}\varrho_0\, a\, C_D. \tag{2.4}$$

The integration of the EULER-LAGRANGE eq. (1.18) is fairly straightforward. Let us define

$$\begin{aligned} V &\equiv \frac{\dot{s}}{3\,c\,(1-k)} = \frac{v}{3\,c\,(1-k)} \\ \beta &\equiv \frac{g}{9\,\alpha\,c^2\,(1-k)^2} \\ \gamma &\equiv [(1-\beta)^2 + 8\,\beta]^{1/2}. \end{aligned} \tag{2.5}$$

Eq. (1.18) may then be written as

$$\frac{\ddot{s}}{g} = \frac{V\,[V^2 + (1-\beta)\,V - 2\,\beta]}{\beta\,[V^2 + 4\,V + 2]}. \tag{2.6}$$

Integrating eq. (2.6) for $s(V)$ and $t(V)$ gives

$$\begin{aligned} \alpha\, s = V - V^0 + \frac{\gamma}{2}\ln\frac{2\,V + (1-\beta) - \gamma}{2\,V + (1-\beta) + \gamma}\cdot\frac{2\,V^0 + (1-\beta) + \gamma}{2\,V^0 + (1-\beta) - \gamma} + \\ + \frac{3+\beta}{2}\ln\frac{V^2 + (1-\beta)\,V - 2\,\beta}{V^{02} + (1-\beta)\,V^0 - 2\,\beta} \end{aligned} \tag{2.7}$$

and

$$\begin{aligned} \frac{g}{3\,c\,(1-k)}\,t = \ln\frac{V^0}{V} + \frac{\gamma}{2}\ln\frac{2\,V + (1-\beta) - \gamma}{2\,V + (1-\beta) + \gamma}\cdot\frac{2\,V^0 + (1-\beta) + \gamma}{2\,V^0 + (1-\beta) - \gamma} + \\ + \frac{1+\beta}{2}\ln\frac{V^2 + (1-\beta)\,V - 2\,\beta}{V^{02} + (1-\beta)\,V^0 - 2\,\beta}. \end{aligned} \tag{2.8}$$

Eqs. (2.6), (2.7) and (2.8) lead to the relations

$$\dot{s} = \dot{s}(t) \quad \text{from eq. (2.8)} \tag{2.9}$$

and hence

$$s = s(t) \quad \text{from eq. (2.7) with (2.9)} \tag{2.10}$$

$$\ddot{s} = \ddot{s}(t) \quad \text{from eq. (2.6) with (2.9).} \tag{2.11}$$

For the quadratic drag law, the solution of the free-flight equation, eq. (1.2), is given by

$$V_1^2 = \left(\frac{\dot{S}}{3c(1-k)}\right)^2 e^{2\beta\frac{Rc^2}{M_1 g}(\xi_1-\xi_2)} - 2\beta e^{2\beta\frac{Rc^2}{M_1 g}\xi_1}\int_{\xi_1}^{\xi_2} e^{-\left(2\beta\frac{Rc^2}{M_1 g}\xi\right)}\frac{d\xi}{\xi} \tag{2.12}$$

where

$$\xi_1 = e^{-as_1}, \qquad \xi_2 = e^{-aS}$$

and

$$\int e^{-b\xi}\frac{d\xi}{\xi} = \ln|\xi| - \frac{b\xi}{1\cdot 1!} + \frac{(b\xi)^2}{2\cdot 2!} - \cdots \tag{2.13}$$

Of course, if S is specified as the actual summit altitude, $\dot{S} = 0$. If drag is neglected in free flight, eq. (2.12) may be replaced by

$$\dot{s}_1 = [\dot{S}^2 + 2g(S - s_1)]^{1/2}. \tag{2.14}$$

The boundary relation, eq. (1.24), becomes

$$R\left[2 + \frac{v'}{3c(1-k)}\right]v_1 v' e^{-as_1} = \left[M_1 e^{\frac{v_1 - v'}{c(1-k)}}\right]^{1/3}[g + M_1^{-1/3} R e^{-as_1} v_1^2]. \tag{2.15}$$

The alternate boundary relation, eq. (1.25), is

$$R\left[1 + \frac{v_1}{3c(1-k)}\right]v_1^2 e^{-as_1} = M_1^{1/3} g. \tag{2.16}$$

In solving for position, s, and velocity, $\dot{s}$, at the end of powered flight, three cases may arise. These are illustrated in Fig. 2.

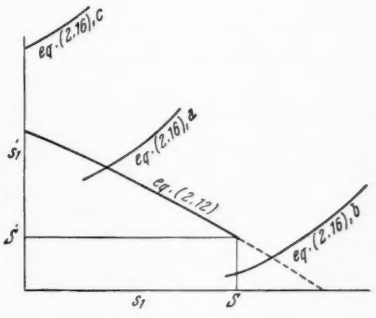

Fig. 2

a) Eqs. (2.12) and (2.16) possess a point of intersection. In that case, they can be solved for s_1 and $\dot{s}_1$.

b) Eqs. (2.12) and (2.16) have no point of intersection; however, eqs. (2.12) and (2.15) can both be satisfied for $s_1 = S$ and $\dot{s}_1 = \dot{S}$ (i.e. no free flight before the specified end conditions). This can occur if $v' \leqslant \dot{S}$. In that case, we substitute $s_1 = S$ and $v_1 = \dot{S}$ in eq. (2.15) and solve for v'.

c) Finally, if eqs. (2.12) and (2.16) have no common solution and $v' > \dot{S}$ [from eq. (2.15)], the requirements of the calculus of variations cannot be met. No minimum exists in the assumed sense. However, it can be shown that all-boost, i.e. instantaneous expenditure of all fuel to reach $v_1 = v^0$ yields a minimum initial mass. This latter case may occur for very low drag-to-weight ratio. In the limiting case of zero drag, it is well known that all-boost is the optimum condition.

It is our aim to find $M(t)$ and the minimum required mass, M_0. We may do so by integrating eq. (1.8). The change of variable

$$M^{1/3} \equiv m \tag{2.17}$$

allows us to write eq. (1.8) as a linear equation

$$3\,c\,(1-k)\,\dot{m} + (\ddot{s}+g)\,m + \mathfrak{D} = 0. \tag{2.18}$$

This equation may be easily integrated.

$$m\,e^{\frac{\dot{s}+gt}{3c(1-k)}}\Bigg|_{t_1}^{t} = -\int_{t_1}^{t} \frac{\mathfrak{D}}{3\,c\,(1-k)}\,e^{\frac{\dot{s}+gt}{3c(1-k)}}\,dt. \tag{2.19}$$

Resubstituting for M and employing relation (2.5) allows us to write eq. (2.19) as

$$M^{1/3}\,e^{\left[V+\frac{gt}{3c(1-k)}\right]} = M_1^{1/3}\,e^{\left[V_1+\frac{gt_1}{3c(1-k)}\right]} + R\int_{V}^{V_1}\frac{\dot{s}^2}{\ddot{s}}\,e^{\left[V+\frac{gt}{3c(1-k)}-as\right]}dV\,. \tag{2.20}$$

In view of eqs. (2.6), (2.7), and (2.8), we may complete the integration. This leads to

$$M(t) = \left\{\frac{9\,R\,c^2\,(1-k)^2}{g}\,\beta\,V^0\,e^{V^0}\,[V^{02}+(1-\beta)\,V^0-2\,\beta]\cdot\right.$$
$$\cdot\left[\frac{V+2}{V^2+(1-\beta)\,V-2\,\beta}-\frac{V_1+2}{V_1^2+(1-\beta)\,V_1-2\,\beta}\right]+$$
$$\left.+\,M_1^{1/3}\,e^{\left[V_1+\frac{gt_1}{3c(1-k)}\right]}\right\}^3 e^{-3\left[V+\frac{gt}{3c(1-k)}\right]}. \tag{2.21}$$

For case b, eq. (2.21) holds with M_1 replaced by M' and V_1 by V'. Of course, $t_1 = t_1^-$.

Once we have found s_1 and v_1 (or s_1 and v'), we may solve eq. (2.7) for V^0 and (2.8) for t_1. Payload M_1 is specified and M' (for case b) is determined by

$$M' = M_1\,e^{3(V_1-V')}. \tag{2.22}$$

Finally, M^0 is given by (2.21) with $t = 0$ and $V = V^0$. The initial mass, M_0 is then found by

$$M_0 = M^0\,e^{3V^0}. \tag{2.23}$$

For case c, M_0 is simply

$$M_0 = M_1\,e^{3V_1} \tag{2.24}$$

where V_1 is determined by eq. (2.12) for $s_1 = 0$.

Note

The optimum thrust programming problem for rockets of constant cross-section has been discussed by TSIEN and EVANS [3] and by LAWDEN [4].

Acknowledgment

The author wishes to thank Dr. L. E. WARD for critically reviewing this note.

References

1. R. H. GODDARD, A Method of Reaching Extreme Altitudes. Smithsonian Inst. Publ., Misc. Collect. **71**, No. 2 (1919).
2. A. MAYER, Über das allgemeinste Problem der Variationsrechnung. Leipzig: Akademie der Wissenschaften, 1879.
3. H. S. TSIEN and R. C. EVANS, J. Amer. Rocket Soc. **21**, 99 (1951).
4. D. F. LAWDEN, Quart. J. Mech. **7**, 488 (1954).

The Satelloid[1]

By

Krafft A. Ehricke[2], ARS

(With 21 Figures)

Abstract. A theoretical analysis is presented of a powered, orbiting vehicle, which is designated as satelloid in distinction from the (non-powered) satellite. The operational altitude of this vehicle lies above that of an aerodynamic rocket glider and below that of a satellite, in the region between 350,000 and 450,000 ft (110 to 140 km) or higher, based on presently available atmospheric data.

The satelloid can be useful for a variety of purposes; for instance for an extended and global exploration of the chemopause and the lower ionosphere (300,000 — 400,000 ft) which are too low for a satellite, but which are of importance for the descent of glider vehicles from space. Other applications discussed are the use as intermediate step toward manned space flight in the form of a test and crew-training vehicle and finally as a scout vehicle for the exploration of extraterrestrial atmospheres and possibly as a means for radar-mapping of the Venusian surface which is hidden from optical observation by a completely opaque atmosphere. The analysis considers the flight mechanics of the circular and the subcircular velocity satelloid, its free molecule flow aerodynamic qualities and aspects of aerodynamic heating. The main results are discussed and the operational conditions of a given satelloid are presented. In an Appendix, upper and outer atmospheric data are discussed.

Zusammenfassung. Ein angetriebenes, die Erde umlaufendes Gerät — bezeichnet als Satelloid zum Unterschied vom (nicht angetriebenen) Satelliten — wird analysiert. Die Operationshöhe dieses Gerätes liegt über der des aerodynamischen Raketengleiters, aber unterhalb der eines Satelliten, in einem Bereich zwischen 350,000 und 400,000 ft (110 bis 140 km) oder darüber, basierend auf gegenwärtig verfügbaren atmosphärischen Daten.

Der Satelloid kann verschiedenen Zwecken dienen; zum Beispiel einer ausführlichen Erforschung der Chemopause und der unteren Ionosphäre (300,000 bis 400,000 ft) auf globaler Basis. Diese Regionen sind zu niedrig für einen Satelliten, aber sie sind für den Abstieg von Gleitgeräten aus dem Weltraum von Bedeutung. Andere diskutierte Anwendungsmöglichkeiten sind die Benutzung dieses Gerätes als eine Zwischenstufe in der Entwicklung bemannten Raumfluges, als Versuchs- und Trainings-Geräte für Flugpersonal, und schließlich als eine Sonde für die Erforschung außerirdischer Atmosphären, möglicherweise auch für die Kartographierung der Venusoberfläche, die sich infolge der undurchsichtigen Atmosphäre optischer Beobachtung entzieht. Die Untersuchung bezieht sich auf die Flugmechanik des Satelloiden mit zirkulärer und unterzirkulärer Geschwindigkeit, seine aerodynamischen Eigenschaften im Gebiet

---

[1] This paper was presented at the Sixth I.A.F. Congress at Copenhagen, August 3, 1955.

[2] Design Specialist, Guided Missile Group, Convair, A Division of General Dynamics Corporation, San Diego/Calif., USA. The author wishes to state that the opinions and results presented in this paper are his own and not necessarily those of Convair.

Vol. 2 1956

der gaskinetischen Strömung und seine aerodynamische Erwärmung. Die Hauptergebnisse werden diskutiert und die Operationsbedingungen für einen gegebenen Satelloiden dargestellt. Ein Anhang bringt die Daten der äußeren Atmosphäre.

Résumé. L'auteur présente l'analyse théorique d'un véhicule orbitant propulsé dénommé "satelloide" pour le distinguer des "satellites" non propulsés. L'altitude opérationnelle de cet engin est supérieure à celle d'une fusée planeur et inférieure à celle d'un satellite. Suivant les données atmosphériques dont on dispose actuellement elle serait comprise entre 350 000 et 450 000 pieds (110 à 140 kms).

L'utilisation du satelloide répond à des objectifs variés, en particulier l'exploration étendue de la chemopause et de l'ionosphère inférieure (300 000 à 400 000 pieds) dont l'altitude est trop basse pour un satellite et la connaissance importante pour le retour en planeur des véhicules de l'espace. D'autres applications prévues font du satelloide un véhicule d'essai et d'entraînement des équipages pour le vol spatial, un éclaireur pour l'exploration des atmosphères extra-terrestres et, le cas échéant, pour la cartographie par radar de la surface de Vénus, laquelle se dérobe à l'observation optique par une atmosphère opaque. L'analyse comprend la mécanique du vol du satelloide en orbite circulaire ou sub-circulaire, les qualités aérodynamiques pour l'écoulement en atmosphère raréfiée avec libre parcours moyen important et le problème correspondant de l'échauffement cinétique. Les résultats principaux sont discutés ainsi que les problèmes opérationnels. Les données actuelles pour l'atmosphère supérieure et extérieure sont passées en revue dans l'appendice.

Nomenclature

A Cross-section
A_t Throat area of rocket motor
a Accommodation coefficient
C_D Drag coefficient
C_{D_s} Drag coefficient at specular reflection
C_F Thrust coefficient: $C_F = F/A_t p_c$
C_L Lift coefficient
C_{L_s} Lift coefficient at specular reflection
c_i Most probable thermal velocity of the impinging molecules (normally the same as c_m)
c_m Most probable thermal velocity of the molecules
c_r Most probable thermal velocity of the re-emitted molecules
D Drag
E_i Energy of the impinging molecules
E_R Rotational energy of molecules
E_r Energy of the re-emitted molecules
E_t Translational energy of molecules
E_w Energy of molecules having wall temperature
$erf(x)$ Error function of x:

$$erf(x) = \frac{2}{\sqrt{\pi}} \int_0^a e^{-x^2} dx$$

F Thrust
F_{sp} Specific thrust (lb thrust per lb propellant per sec)
f Fraction of total mass of molecules, which is reflected diffusely
g Gravitational acceleration
g_{app} Apparent gravitational constant:

$$g_{app} = g\left[1 - \left(\frac{v}{v_c}\right)^2\right]$$

g_{00} Surface value of gravitational acceleration
k_D Drag parameter $= q\, C_D$
k BOLTZMANN constant ($5{,}66 \cdot 10^{-24}$ ft-lb/°R molecule)
M Molecular weight lb/lb-mole
m Mass
m Mass of the individual molecule (slugs/molecule)
m' Mass of the individual oxygen atom
m'' Mass of the individual nitrogen molecule
N Number of air molecules per cubic foot
N_A AVOGADRO number $= 3.73 \times 10^{26}$ molecules/lb mole
n Number of air molecules striking the surface per ft² per sec
n Axial load factor (g_{00})
n_b Axial load factor at burn-out
n_c Centrifugal factor
n_0 Initial axial load factor
n' Number of monatomic oxygen striking the surface per ft² per second

n''	Number of diatomic nitrogen striking the surface per ft² per second
n^*	Number of lb moles of air striking the surface per ft² per second
n'^*	Number of lb moles of monatomic oxygen striking the surface per second
p_c	Combustion chamber pressure
p_i	Pressure produced by stream of impinging molecules
p_r	Pressure produced by stream of re-emitted molecules
q	Dynamic pressure
R	Universal gas constant (1,544 ft-lb/lb-mole ^{0}R)
R_i	Incident radiation energy
R_r	Re-emitted radiation energy
r	Radial distance from center of the earth
S	Lifting surface area (vehicle plan form area)
s	Ratio of flight speed to most probable thermal velocity of the molecules: $s = v/c_m$
T_i	Temperature of the impinging molecular stream
T_r	Temperature of the re-emitted molecular stream
t	Time
t_b	Total burning time
t_r	Period of revolution
v	Velocity
v_c	Circular velocity
W	Weight
W_{app}	Apparent weight $= mg_{app}$
W_b	Burn-out weight (empty weight plus residual fluids)
W_p	Propellant weight
$\dot{W}_{sp}$	Specific propellant consumption: $\dot{W}_{sp} = 1/F_{sp}$
W'	Weight of monatomic oxygen striking the surface (lb)
$\dot{w}$	Propellant consumption per second
y	Altitude
X_c	Range equal to circumference of the earth (1 circumnavigation)
X_{tot}	Total range covered during satelloid operation
α	Angle of attack
β	Exponent in density altitude relation
β	Wedge angle
ε	Emissivity
γ	Gravitational parameter $= gr^2$
ψ	Energy distribution factor
ϱ	Density
σ	Density ratio (ϱ/ϱ_{00})
σ	STEPHAN-BOLTZMANN constant [$3.74 \cdot 10^{-10}$ ft-lb/ft² sec (^{0}R)⁴]
θ	Trajectory angle (angles between velocity and local horizon)

List of Content

I. Introduction

In space flight, the main interest will always pertain to the exploration of celestial bodies, their atmospheres, if any, and their surfaces. This process quite naturally begins with the earth, looking at it as a celestial body; and before man can venture out into space, he first must develop "coastal" shipping and navigation, which is important not only for securing the safety of his return, but also for enabling him to operate near other "islands" in space. In other words, a period of satellitory operation must precede the astronautical or interorbital phase in the development of manned space flight.

This satellitory period, which is roughly equivalent to the phase 1 (leading to a manned satellite rocket plane) and phase 2 (leading to a permanent space station) described in Ref. [1] must logically start out with the exploration of the physical and chemical conditions of the natural environment at different altitudes or distances from the surface. Based on the resulting information, suitable technical systems and operational, as well as navigational methods, can then be developed for the return from space and for operations near celestial bodies.

The attack can be and partly already has been carried forward along several lines; by means of hypersonic airplanes close to the earth, of high-altitude rockets and by means of instrumental satellites. High altitude rockets are capable only of vertical explorations, while "circumferential" explorations and longer stay times at given altitudes must be carried out by means of vehicles like the rocket plane and the satellite.

The establishment of satellites requires a certain minimum altitude in order to remain outside the relevant atmosphere for a certain length of time, depending on the purpose of the orbital system. For the desired orbital lifetime, the initial altitude of the satellite is a function of body shape (drag coefficient C_D) and of the ratio of weight to cross-sectional area, W/A. From the well-known equations of non-powered motion under the effect of small drag and with consideration of the conversion of potential to kinetic energy, as the satellite spirals closer to the surface, the orbital lifetime of a spherical body of given specifications has been computed and is plotted in Fig. 1. It can be seen that for a lifetime of only a few days, the initial altitude must be above 180 km (100 n. mi.) while below 162 (90 n. mi.) the lifetime is less than one revolution (less than about $1-\frac{1}{2}$ hours)[1]. For a lifetime of about 1 year the required initial altitude is approximately 325 km (180 n. mi.). Therefore, it can be seen that the operational range of satellites extends from roughly 180 km on upward.

At lower altitudes rocket airplanes can be employed. It is well known [2], [3] that for minimum propellant expenses, such a rocket powered airplane must be driven to high speed quickly with a subsequent unpowered glide path to cover the desired range. The equilibrium altitude of such a hypersonic glider depends, for a given flight speed, upon the lift parameter [4] defined as the ratio of lift coefficient over lifting area load where the lifting area load is the ratio of weight to lifting area of the glider. For technically realistic values of the lift parameter between 0.003 and 0.015 ft^2/lb and a velocity as high as 24,000 ft/sec (about 7.2 km/sec), the glide altitude lies between 240,000 and 290,000 ft (70 to 90 km). A higher velocity is certainly not required, even at modest lift-to-drag ratios,

[1] It is realized that the orbital lifetime varies considerably with the weight to cross-sectional area ratio, however, even much higher values of weight to area would not increase materially the orbital lifetime below about 160 km.

in order to fly half around the globe, the greatest distance required to reach any point on earth from a given launching site.

Thus, roughly between 90 and 180 km (300,000 and 600,000 ft or 50 and 100 n. mi., respectively), there is a region too high for glide vehicles, because of very unfavorable aerodynamic conditions, and too low for satellites, because the atmosphere is not yet sufficiently rarified to permit an adequate orbital lifetime. Still, since one period of revolution is about 5,200 seconds at these altitudes, the phrase "adequate orbital lifetime" implies a duration of many thousands of seconds. It is therefore the integral effect of deceleration due to drag, times its duration which cuts down local stay times. The numerical value of the deceleration proper can be quite small and still cause the satellite orbit to deteriorate comparatively rapidly. Therefore, initial satellite orbits must lie beyond about 180 km [1].

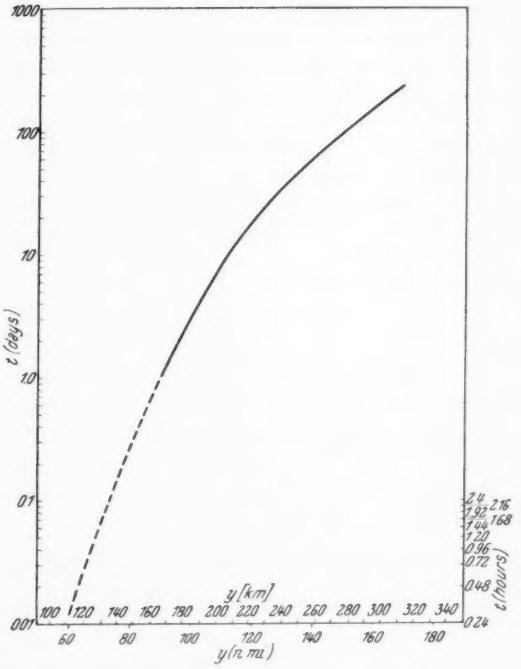

Fig. 1. Satellite orbital life time. Shape: sphere; drag coefficient: 2.2 (based on A); area load: $W/A = 80$ lb/ft^2; A = maximal cross section area of sphere; W = weight of sphere

Because the deceleration is small in the region above 90 km (300,000 ft) only a correspondingly minute thrust force is required to balance the drag force and prevent a decay of the orbit into a spiral of descent.

A vehicle flying at these altitudes would then have to operate under small, but continuous power. High flight speed and low drag make it possible to maintain this thrust power over a significant number of revolutions. The vehicle can follow a circular orbit around the earth at circular velocity, like a satellite. However, motion under power represents a significant difference from a satellite. Therefore, the designation satelloid is suggested for such a system.

Because of the well-known limitations in chemical rocket propulsion energy, the satelloid cannot stay in its orbit for the same length of time as desirable for satellites (at least several weeks or a few months). However, the satelloid is not "competing" with the satellite, but rather amending it on merits of its own. The satelloid can easily operate for a period of 5, 10, 20 or more revolutions at altitudes at which the satellite could not exist for one or two revolutions. If non-chemical propulsion systems are considered, the superiority of the satelloid at these altitudes is increased even further.

[1] These numbers, as well as Fig. 1 are based on atmospheric data discussed in the appendix.

From the above considerations as well as from the discussions presented in the subsequent section, it appears that the satelloid (manned or possibly remote controlled) has some interesting possibilities in the development of space flight. A theoretical analysis of some aspects, pertaining to the circular orbit satelloid, is presented in this paper, with the intention of following up with additional flight mechanical studies (elliptical orbit satelloid) and with applications in a subsequent presentation.

Two operational aspects are explored: the circular-velocity satelloid and the subcircular-velocity satelloid. In view of the low drag, hence, low thrust of the circular-velocity type, any subcircular operation suffers from the fact that a rapidly increasing apparent weight (due to loss of centrifugal relief) must be supported by an adequate lifting force. In the flight region of the satelloid, that is, in the free molecule flow region, this adequate aerodynamic lift cannot be obtained, unless very large surfaces and specular reflection of the impinging molecules (cf. next section) can be realized. If the lift has to be produced by means of thrust (lifting thrust component), then the power requirements, hence the propellant consumption per revolution, will greatly exceed that of the circular-velocity satelloid.

II. Purpose of the Satelloid

The above outlined characteristics of the satelloid and its position between airplane and space craft suggest a number of useful applications in the development of manned space flight as well as in the exploration of other celestial bodies, once interplanetary flight is established. Three applications will be discussed subsequently:

1. Atmospheric research.

2. Development of orbital passenger vehicle.

3. Exploration of extra-terrestrial atmospheres and radar mapping of the Venusian surface.

1. Atmospheric Research

The satelloid is the vehicle to conduct an extended and global survey of the chemopause and the lower ionosphere (300,000 to 500,000 ft or above), a region which cannot be covered adequately by either rocket plane or satellite, as discussed before. This region is the "gate to the atmosphere", where aerodynamic forces are beginning to act on incoming vehicles. Its importance for re-entry from space, therefore, requires a thorough knowledge of relevant atmospheric conditions during all seasons and at all latitudes. Hypersonic rocket airplanes could enter this region temporarily by following a skip path flight technique similarly to the one proposed originally by SÄNGER and BREDT for long-range rocket bombers, [3], but then their stay time would be comparatively short, and their altitude would vary. For a systematic exploration of individual strata in this altitude region along great circle paths during a number of revolutions, a satelloid would be required. Among the interesting research subjects are information on density, temperature, composition, and degree of ionization of the atmosphere, variation of these characteristics with latitude, season and solar activity and the exploration of upper atmosphere dynamics, winds, gust and electrical currents.

2. *Development of Orbital Passenger Vehicle*

As a test and crew-training craft for the development of orbital passenger vehicles, the satelloid can play an important role as a stepping stone toward manned space flight. This function has several aspects pertaining to engineering, human integration and operation.

From the engineering point of view the problems of satelloid aerodynamics are probably most important. This is the aerodynamics of a vehicle moving at circular or near-circular velocity in the region of free molecule flow or possibly between free molecule flow and slip flow [7]. The problems pertain mainly to the interaction between vehicle surface and gas molecules at the high flight speeds involved. On the basis of presently available knowledge it appears that the molecules will be reflected diffusely (in all directions) from the wall, rather than specularly. It is not known whether the diffuse reflection will be essentially elastic or inelastic, that is, whether little or much energy exchange takes place between impinging molecules and vehicle surface. This depends on the duration of adsorption of the molecules by the wall and probably the reflection will, to a large extent, be inelastic. The type of reflection (specular or diffuse) greatly affects the aerodynamic coefficients, especially the drag coefficient, and the mode of diffuse reflection (elastic or inelastic) means a great difference in surface temperature. Specular reflection is preferable, yielding a lower drag coefficient and a higher lift coefficient, but the technique of providing smooth surfaces must be developed considerably beyond the present status if specular reflection is to be achieved. In the case of diffuse reflection, elastic recoil is preferable, transferring theoretically none of the impact energy into the surface, thus yielding lower wall temperatures. This again will call for utmost smoothness of the wall to eliminate as much as possible interstices in which the impinging molecules can be trapped. The impact energy of the particles is high enough to dissociate oxygen molecules and, to a lesser extent, nitrogen (depending on the molecular velocity distribution), provided the adsorption time is long enough to permit excitation of the vibrational modes of the molecule. Conversely, the violent impact of gas molecules might knock molecules out of the surface. This possibility of mechanical erosion of the vehicle's skin may frustrate attempts toward diffuse-elastic or perhaps specular reflection, even if extremely smooth surfaces can be provided initially. This adds the technical requirement for extreme surface hardness to that for great smoothness. Whatever happens to the surface (and this will also be a function of the surface inclination with respect to flight direction) will greatly affect its temperature history (hence its weight) and the aerodynamic qualities of the vehicle, and it is of great importance for the design of orbital passenger vehicles to find this out in detail under actual flight conditions.

In regard to human integration and adaptation to space flight it is of interest to note that the apparent weight of the crew can be regulated, depending on the flight velocity. The apparent weight varies proportional to $(1 - v^2/v_c^2)$, being zero at circular velocity v_c. Different weight conditions can be simulated for various durations.

The satelloid can also serve as a test vehicle for novel propulsion systems of low thrust capacity, such as the ion propulsion system, since the required vacuum conditions can be approached sufficiently at altitudes around 140 to 150 km (460,000 to 490,000 ft).

From the operations point of view, the development of a technique of re-entry into the denser atmosphere is of special importance. Re-entry from space is an intricate maneuver and not as straightforward as an analysis under the usual

simplifying assumptions indicates. These assumptions include, for instance, correct re-entry path (i.e., correct perigee height of the return ellipse), no density variation with latitude (in the case of non-equatorial return orbits), no winds or gust, no effect of frictional heating on the aerodynamic characteristics of the vehicle (due to distortions or configurational changes caused by thermal stress or by more or less controlled melting of exposed portions of the vehicle). Such effects are likely to introduce considerable dynamic problems through vehicle oscillations about its three axes, and flight path oscillations. They not only cause severe control problems, but also call for safety factors which unduly increase the vehicle weight. Flight operation and vehicle stability and control are therefore areas in which the satelloid can do considerable development work. Usually a "dead stick" (i.e., non-powered) re-entry is considered. The vehicle is assumed to immediately cut into the atmosphere deep enough to have an adequate aerodynamic force available for stability and attitude control. The vehicle first goes into a negative angle of attack to slow down from elliptic to circular velocity, when returning from a satellite, and thereafter takes a positive attitude. This is, of course, possible, using aerodynamic force and comparatively large angles of attack (higher than for conventional airplanes). Nevertheless it is a dangerous maneuver, leading the vehicle at very high speed into a region of very large density gradients with altitude. Therefore, even comparatively small errors in the perigee height of the return ellipse must result in a large variation in dynamic pressure, producing aerodynamic forces and frictional heating gradients of greatly differing magnitude.

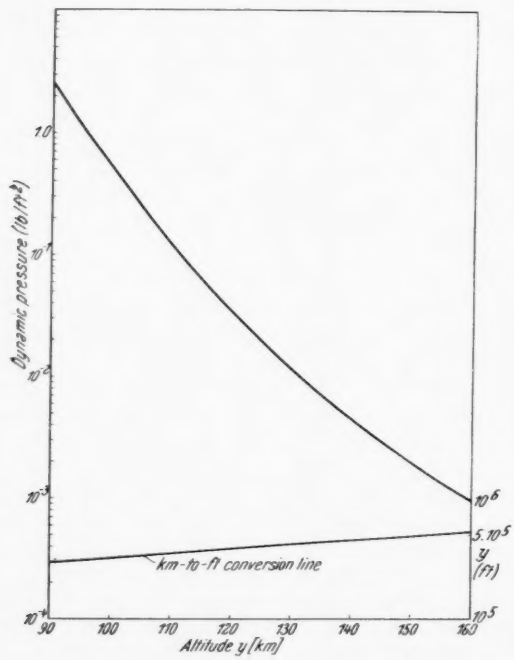

Fig. 2. Dynamic pressure as function of altitude

If the perigee height is placed at a higher, safer altitude of 80 to 100 km (260,000 to 325,000 ft), the dynamic pressure is too low (cf. Fig. 2) to produce adequate aerodynamic forces and the vehicle must be controlled and stabilized by means of an attitude control. Of the various possibilities of attitude control by means of gyros, flywheels, or small jets, the latter method appears to be most attractive in the present case, because it yields rapid response to control commands. In this type of re-entry maneuver then, the vehicle is not regarded as an airplane immediately after it has ceased to be a space ship. An intermediate, satelloidal phase is introduced, defined by the conditions that the vehicle is attitude-controlled, independently of aerodynamic forces, while using the air drag and as much lift as possible to slow itself down and maintain maximum altitude all the time. This maneuver has a number of practical advantages. The

slow-down process can start greater altitude, compensating for the lower density by assuming steeper attitude angles than would aerodynamically be feasible. A flat, surf-board type body as suggested in Ref. [1], for example, would, under these conditions, produce about the highest drag possible, a drag which at the same time would have to be classified as drag due to lift. Thereby highest flight altitude and lowest heat transfer rate into the skin are maintained. Jet attitude control in the initial phase also avoids the complications due to non-linearity with angles of attack of the aerodynamic control forces. Furthermore, the normal force curve slope is very small at the high velocities under consideration. As far as the lift is concerned, this effect is at least partly compensated for by the large bottom area (or lifting area) of the vehicle. However, for control purposes the small normal force curve slope would result in a certain "sluggishness" in contrast to the rapidly responding jet control. To minimize this effect, aerodynamic control would require large control surfaces which must be deflected rapidly (heavy actuators) and which are inclined considerably with respect to the flow, resulting in intense aerodynamic heating. All these requirements, which would add a great deal to the overall vehicle weight, are not needed to the same extent in the subsequent phase of aerodynamic descent, and therefore are replaced preferably by the less weighty attitude control system.

The re-entry maneuver can thus be visualized, first as a transition from purely inertial, attitude-controlled (space) flight, to largely inertial, but partly aerodynamic, attitude-controlled (satelloidal) flight, and finally, when velocity and altitude are sufficiently low, but of course still hypersonic, conversion to purely aerodynamic flight (aerodynamic descent). The intermediate phase provides a "cushion" between re-entry and aerodynamic descent, increasing the safety and reliability of return from space. For the exploration of this phase, and transition to aerodynamic descent, the satelloid can be quite useful, because it operates with jet attitude control in the relevant altitude range and ultimately must descend aerodynamically.

3. Extra-Terrestrial Activities

In interplanetary research the satelloid can investigate the dynamics of upper extra-terrestrial atmospheres, preparing for landings on the respective planet by establishing the conditions for correct re-entry, satelloidal, and aerodynamic descent maneuvers.

The exploration of Venus offers another interesting application for a satelloid vehicle. Optical surface observation is not possible, due to the well-known opacity of the atmosphere. A fairly detailed radar mapping requires a closer approach to the planet than the interorbital (space) ships, turned into Venusian satellites, could afford. By use of a satelloid, cruising at 400,000 ft or less above the surface, a rather accurate exploration of the Venusian topography (if any)[1] appears feasible. This information is needed should a landing on Venus ever be attempted.

III. Flight Performance

This section derives the basic equations governing the flight performance of the satelloid for circular orbits, at both, circular and sub-circular velocity, so that thrust requirement, propellant consumption, mass ratio, flight time, and the effect of altitude, aerodynamic coefficients, and of the angle of attack can be

[1] Dr. F. WHIPPLE recently forwarded the interesting theory that the surface of Venus is covered entirely by water.

assessed. Especially for the latter case it is not possible in free molecule flow to give a general relationship between drag and angle of attack. Therefore, three different analytical expressions have been used to bracket the region of probable values.

1. Circular-Velocity Satelloid

At circular velocity no aerodynamic lift is required. The vehicle preferably maintains zero angle of attack. The deceleration due to drag, in g-units, follows from

$$-n = -\frac{\dot{v}}{g_{00}} = \frac{D}{W} = q\,C_D\frac{S}{W}. \tag{1}$$

The thrust is equal to the drag, $F = -n(t)\cdot W(t)$. Therefore, the propellant consumption during the cruise is given by

$$-\dot{w} = \frac{F}{F_{sp}} = -\frac{n}{F_{sp}}W = q\,C_D\frac{F}{F_{sp}}. \tag{2}$$

If t_b designates the total burning time, the propellant weight consumed during this period is

$$W_p = \frac{q\,C_D\,S}{F_{sp}}t_b. \tag{3}$$

Adding the burn-out weight W_b — which includes residual fluids — to the propellant weight, yields the initial weight W_0 of the vehicle. In view of the glide descent through the denser atmosphere after termination of the powered cruise, the lifting area S will be determined by the desired area load during glide, W_b/S. The initial area load is then W_0/S; and by inserting the corresponding values into Eq. (1), the initial and final value of the axial load factor n is obtained. The required loading factor (propellant weight to initial weight of the satelloid) follows from

$$\Lambda = \frac{W_p}{W_0} = \frac{q\,C_D}{F_{sp}}\frac{S}{W_0}t_b = n_0\frac{t_b}{F_{sp}}. \tag{4}$$

Finally, the mass ratio is found from the relations

$$\frac{m_0}{m_b} = \frac{1}{1-\Lambda} = \frac{F_{sp}}{F_{sp}-n_0 t_b} = \exp\left[\frac{(n_0+n_1)\,t_b}{2\,F_{sp}}\right]. \tag{5}$$

The last expression on the right hand side results from the classical mass ratio equation, using n which is a linear function of time, if velocity and attitude are held constant.

2. The Subcircular-Velocity Satelloid

If the ratio of flight velocity to local circular velocity v/v_c is less than one, the vehicle must have a positive angle of attack, in order to produce the necessary lift for supporting the apparent weight of the body, that is, the weight fraction not supported by the centrifugal effect due to path curvature parallel to the earth's surface,

$$W_{app} = W\left[1-\left(\frac{v}{v_c}\right)^2\right] = L_{tot} = q\,C_L\,S + F\sin\alpha, \tag{6}$$

where the total lift is the sum of aerodynamic lift and lift due to thrust, assuming a rocket engine installation in the rear of the satelloid. The thrust in flight direction is then

$$F\cos\alpha = -n\,W. \tag{7}$$

Solving for F and substituting Eq. (1) for n, one obtains

$$F \sin \alpha = q\, C_D\, S \tan \alpha. \tag{8}$$

Inserting this expression into Eq. (6) yields the required dynamic pressure for the particular subcircular velocity

$$q(y) = \frac{W}{S\, D_D} \left[\frac{1 - \left(\frac{v}{v_c}\right)^2}{\frac{C_L}{C_D} + \tan \alpha} \right]. \tag{9}$$

The altitude follows from the density ratio

$$\sigma = \frac{W}{S\, C_D} \frac{2}{\varrho_{00} v^2} \left[\frac{1 - \left(\frac{v}{v_c}\right)^2}{\frac{C_L}{C_D} + \tan \alpha} \right]. \tag{10}$$

The propellant consumption per unit time is again given by Eq. (2), where C_D is now a function of the angle of attack and therefore will be larger than in the case of circular velocity. Eqs. (3) through (5) are likewise valid without change.

If the lifting surface, but not the thrust axis, are inclined with respect to the flight direction (e.g. at positive attitude angle between body axis and wing plane) and if thereby sufficient lift is provided, then the lift due to thrust can be zero and $\tan \alpha$ disappears in Eqs. (9) and (10).

Generally, the thrust required for the subcircular velocity satelloid is

$$F = \sqrt{(W_{app} - q\, C_L\, S)^2 + (q\, C_D\, S)^2}.^1 \tag{11}$$

3. Effect of Variable Weight on the Flight Path of a Subcircular-Velocity Satelloid

a) Discussion of Variables

For the circular-velocity satelloid, a change in weight has no effect on thrust and/or flight altitude, because the weight is compensated by the centrifugal effect and therefore does not enter the flight mechanical equations as a variable.

The same independence of a change in weight has been assumed tacitly in deriving the equations for the subcircular-velocity satelloid. This is not strictly correct, however, because the apparent weight and its compensating variables, aerodynamic lift and lift due to thrust, enter the flight path equations as function of time. Consequently, the above equations are approximations only.

The initial apparent weight is a function of the flight velocity which in turn, together with the altitude, determines the vehicle thrust and the angle of attack, $W_{app}\,(F, v, y, \alpha)$. Consequently, since W_{app} varies, due to the consumption of propellant, anyone of these parameters, or a combination thereof, must vary also. A systematic evaluation of these variations leads to the following cases:

1. *v and α constant.*
   y and F vary; y increases, F decreases.
2. *v and y constant.*
   α and F vary; both decrease.

[1] For a representative empty weight (glide weight) of 10,000 lb (4.5 tons) of a small satelloid with a wing load for the return glide of 20 lb/ft^2.

Vol. 2 1956

3. *v and F constant.*

α should stay constant, to keep v constant in view of the requirement $F =$ constant; but then γ increases, causing v to go up. Consequently α must be increased so that increased drag due to lift and decreased $F \cos \alpha$ keep v constant at the resulting increase in γ which then becomes a function of the increase in α. Guidancewise this would be a very complicated method of flight.

4. *γ and α constant.*

F must decrease to keep γ constant in view of the requirement $\alpha =$ constant. Decreasing thrust leads to decreasing velocity, unless the drag can be reduced. Thus γ cannot be held constant and, aside from configurational changes during flight, the above conditions cannot be fulfilled.

5. *γ and F constant.*

α must decrease, to compensate for the decreasing weight which otherwise would cause γ to go up; but with α also the drag due to lift decreases, whence v must increase. It is not possible to say beforehand whether these two simultaneous changes will permit of keeping γ constant. In any case, this would likewise be a rather complicated method of operation.

6. *α and F constant.*

v and γ vary; both increase. This case appears not particularly attractive for a research vehicle, because velocity and altitude, rather than angle of attack and altitude should be kept constant. As a transient condition this case may have practical significance when approaching, after the powered ascent, the correct flight conditions in velocity and altitude in a form of vernier maneuver.

This leaves essentially the cases 1, 2, and 6 for further investigation. The second case, in which velocity and altitude are held constant, resembles most closely that of the circular-velocity satelloid. However, the first case is somewhat simpler, because it does not involve a change in the aerodynamic coefficients due to changing angle of attack. The effect of changing angle of attack on the aerodynamic coefficients cannot be assessed accurately at the present time, because of insufficient knowledge of the accomodation coefficient per se and of the effect on the accomodation coefficient of the resulting change in skin temperature due to changing angle of attack.

b) Constant Velocity, Constant Angle of Attack

$v =$ constant, hence $\dot{v} = 0$; $F_{sp} =$ constant; $\alpha =$ constant, hence, $\gamma = \gamma(t)$ and $F = F(t)$; because of $\gamma = \gamma(t)$, the flight path angle with respect to the local horizon, θ, as well as $\dot{\theta}$ must be different from zero.

The basic equations governing the flight path are

$$m \dot{v} = 0 = F \cos \alpha - D - g\, m \sin \theta \tag{12}$$

$$m v \dot{\theta} = F \sin \alpha + L - g_{app}\, m \cos \theta \tag{13}$$

where

$$g_{app} = g_{00} \left[1 - \left(\frac{v}{v_c} \right)^2 \right]. \tag{14}$$

From Eq. (12)

$$F = \frac{D}{\cos \alpha} + \frac{g\, m \sin \theta}{\cos \alpha}. \tag{15}$$

Inserting Eq. (15) in (13),

$$\left.\begin{aligned} m\,v\,\dot{\theta} &= q\,S\,C_D \tan\alpha + g\,m \sin\theta \tan\alpha + q\,S\,C_L - g_{app}\,m\cos\theta \\ m\,v\,\dot{\theta} &= m\,[g\sin\theta\tan\alpha - g_{app}\cos\theta] + q\,S\,[C_L + C_D\tan\alpha] \end{aligned}\right\}. \tag{16}$$

Solving this equation for the dynamic pressure yields

$$q = \frac{M\,v\,\dot{\theta} + m\,(g_{app}\cos\theta - g\sin\theta\tan\alpha)}{S(C_L + C_D\tan\alpha)}. \tag{17}$$

It also holds that

$$q = \sigma\,\varrho_{00}\,v^2/2 \tag{18}$$

whence

$$\sigma = \frac{2\,m}{S\,\varrho_{00}\,v^2}\left(\frac{v\,\dot{\theta} + g_{app}\cos\theta - g\sin\theta\tan\alpha}{C_L + C_D\tan\alpha}\right)$$

or

$$\sigma = \frac{2}{g_{00}\,\varrho_{00}\,v^2}\frac{W}{S}\left(\frac{v\,\dot{\theta} + g_{app}\cos\theta - g\sin\theta\tan\alpha}{C_L + C_D\tan\alpha}\right). \tag{19}$$

Vol. 2 1956

This equation gives the change in altitude as function of the weight, at constant angle of attack. For $\theta = 0$ and $\dot{\theta} = 0$, only g_{app} remains in the numerator inside the bracket and Eq. (19) reduces to Eq. (10).

The propellant weight is given by

$$W_p = \frac{1}{F_{sp}}\int_0^t F\,dt \tag{20}$$

$$F = \frac{D}{\cos\alpha}\,\frac{v^2\,S\,C_D}{2\cos\alpha}\,\varrho \tag{21}$$

so that

$$W_p = \frac{v^2\,S\,C_D}{2\,F_{sp}\cos\alpha}\int_0^t \varrho(t)\,dt. \tag{22}$$

The instantaneous weight is

$$W = W_0 - W_p(t) = W_0 - \frac{v^2\,S\,C_D}{2\,F_{sp}\cos\alpha}\int_0^t \varrho(t)\,dt. \tag{23}$$

This equation takes the change in altitude into account.

Inserting Eq. (23) in Eq. (10), substituting ϱ/ϱ_∞ for σ and solving for ϱ, yields

$$\varrho(t) = \frac{2\left(1 - \left(\frac{v}{v_c}\right)^2\right)W_0}{v^2\,S\,(C_L + C_D\tan\alpha)} - \frac{C_D\left(1 - \left(\frac{v}{v_c}\right)^2\right)}{F_{sp}\cos\alpha\,(C_L + C_D\tan\alpha)}\int_0^t \varrho(t)\,dt. \tag{24}$$

Differentiation of (24) with respect to time yields

$$\frac{d\varrho}{dt} = -\frac{C_D\left(1 - \left(\frac{v}{v_c}\right)^2\right)}{F_{sp}\cos\alpha\,(C_L + C_D\tan\alpha)}\,\varrho(t) \tag{25}$$

which can be written in the form

$$\frac{d\varrho}{\varrho} = -\frac{C_D\left(1-\left(\frac{v}{v_c}\right)^2\right)}{F_{sp}\cos\alpha\,(C_L + C_D\tan\alpha)}\,dt \tag{26}$$

and, upon integration, yields the density at the time t,

$$\varrho_t = \varrho_{t=0}\exp\left[-\frac{C_D\,t\left(1-\left(\frac{v}{v_c}\right)^2\right)}{F_{sp}\cos\alpha\,(C_L + C_D\tan\alpha)}\right]. \tag{27}$$

Therewith the thrust as function of time becomes, using Eq. (21)

$$F(t) = q_{t=0}\frac{S\,C_D}{\cos\alpha}\exp\left[-\frac{C_D\,t\left(1-\left(\frac{v}{v_c}\right)^2\right)}{F_{sp}\cos\alpha\,(C_L + C_D\tan\alpha)}\right]. \tag{28}$$

The propellant consumption at the time t is, referring to Eq. (22),

$$W_p(t) = \frac{V^2\,S\,C_D}{2\,F_{sp}\cos\alpha}\left[\varrho_{t=0}\left(-\frac{F_{sp}\cos\alpha\,(C_L + C_D\tan\alpha)}{C_D\left(1-\left(\frac{v}{v_c}\right)^2\right)}\right)\cdot\right.$$
$$\left.\cdot\exp\left[-\frac{C_D\,t\left(1-\left(\frac{v}{v_c}\right)^2\right)}{F_{sp}\cos\alpha\,(C_L + C_D\tan\alpha)}\right]\right]_0^t.$$

Simplifying, it follows finally,

$$W_p(t) = q_{t=0}\,S\frac{C_L + C_D\tan\alpha}{1-\left(\frac{v}{v_c}\right)^2}\left[1-\exp\left[-\frac{C_D\,t\left(1-\left(\frac{v}{v_c}\right)^2\right)}{F_{sp}\cos\alpha\,(C_L + C_D\tan\alpha)}\right]\right]. \tag{29}$$

The propellant consumption per revolution is obtained from Eq. (29) by substituting for t the period of revolution,

$$t_r = \frac{X_0}{v}. \tag{30}$$

Using again the first equation (16) and assuming θ and $\dot{\theta}$ to be very small, one can write

$$g_{app}\,m_0 = W_{0,app} = q_{t=0}\,S\,(C_L + C_D\tan\alpha) = W_0\,(1-(v/v_c)^2). \tag{31}$$

Solving for W_0, inserting in Eq. (29), and solving for the mass ratio W_0/W_b, one obtains finally

$$\frac{W_0}{W_b} = \exp\left[\frac{C_D\,X_{tot}}{v\,F_{sp}\cos\alpha}\cdot\frac{1-\left(\frac{v}{v_c}\right)^2}{C_L + C_D\tan\alpha}\right]. \tag{32}$$

Where X_{tot} designates the whole range, rather than just one circumnavigation X_c.

For the purpose of computing the altitude variation during flight, let the density at altitude be expressed by

$$\varrho = \varrho_r\,e^{-\beta\Delta y} \tag{33}$$

where ϱ_r is the reference density at a reference altitude y_r and $\Delta y = y - y_r$. Taking ϱ as ϱ_t in Eq. (33), using Eq. (27) and solving for $\beta \Delta y$, one can write

$$\beta \Delta y = \frac{C_D t \left(1 - \left(\frac{v}{v_c}\right)^2\right)}{F_{sp} \cos \alpha \, (C_L + C_D \tan \alpha)} - \ln \frac{\varrho_{t=0}}{\varrho_r} \tag{34}$$

at $t = 0$,

$$y_0 - \dot{y}_r = \Delta y_0 = -\frac{1}{\beta} \ln \frac{\varrho_{t=0}}{\varrho_r}. \tag{35}$$

At $t = t_b$, where t_b is the total time of sustained flight,

$$y_b - y_r = \Delta y_b = \frac{C_D t_b \left(1 - \left(\frac{v}{v_c}\right)^2\right)}{\beta F_{sp} \cos \alpha \, (C_L + C_D \tan \alpha)} - \frac{1}{\beta} \ln \frac{\varrho_{t=0}}{\varrho_r}, \tag{36}$$

hence the altitude difference between beginning and termination of the satelloid operation becomes simply

$$\Delta y_b - \Delta y_0 = y_b - y_0 = \frac{C_D t_b \left(1 - \left(\frac{v}{v_c}\right)^2\right)}{\beta F_{sp} \cos \alpha \, (C_L + C_D \tan \alpha)} = \frac{1}{\beta} \ln \frac{W_0}{W_b}. \tag{37}$$

The mean climb angle follows then from

$$\sin \bar{\theta} = \frac{y_b - y_0}{X_{tot}} = -\frac{y_b - y_0}{v t_b}. \tag{38}$$

This last relationship indicates that X_{tot} is not the horizontal range, but the slant range due to the inclination of the flight path by an angle θ. The true horizontal range is therefore $X_{tot} \cos \bar{\theta}$. However, the difference is small because of the small value of the trajectory angle.

That the change in altitude is indeed quite small, is illustrated by the following example:

Assume the satelloid begins to operate at an initial altitude of $y_i = 113$ km (370,000 ft) and has the comparatively high mass ratio of $W_0/W_b = 4$ ($\ln 4 = 1.387$). The difference between initial and final altitude at burnout follows then from Eq. (37) to be

$$y_b - y_0 = \frac{1.387}{\beta}.$$

As shown in the Appendix, the value of β for this case is approximately 1/9.1 (in km units), so that $y_b - y_0 = 12.6$ km or 41,400 ft. The increase in altitude is about 11 per cent of the initial altitude, or about 0.000 33 of the circumference of the earth. Since a satelloid with this mass ratio would complete many revolutions, it follows that the mean climb angle $\bar{\theta}$ is very small. Even if the whole altitude increment would be covered in one revolution, the mean climb angle would be only 1′08″. The density change, however, would not be negligible in this case (about 50%).

c) Constant Velocity, Constant Altitude

v = constant, hence $\dot{v} = 0$; F_{sp} = constant; α = variable, hence, $F = F(t)$; because of y = constant, the flight path angle θ must be zero.

Vol. 2 1956

The basic flight path equations become now

$$0 = D + F \cos \alpha \tag{39}$$

$$0 = F \sin \alpha + L - m g_{app} \tag{40}$$

where $m g_{app} = W_{app}$, the instantaneous apparent weight of the vehicle.

Since the interesting range of α during the cruise comprises relatively small angles of attack (for reasons of drag and aerodynamic heating of the wind side), one may tentatively simplify the subsequent analysis, by putting $\cos \alpha \approx 1$ and $\sin \alpha \approx \alpha$, whence the basic equations become

$$F - D = 0 \tag{41}$$

$$F \alpha + L - W_{app} = 0. \tag{42}$$

Since α is variable, L and D must be expressed in terms of α. The physics of free molecule flow does not lead to analytic expressions for the drag as the sum of form drag C_{D_0} and drag due to lift $C_{D_L}(\alpha)$ (cf. section III), but rather requires separate consideration of each surface element as it changes its angle with respect to the oncoming molecular stream. However, after having calculated the drag coefficient as function of α for a given shape and flight velocity, it is possible to formally express the resulting curves in a form corresponding to $C_D = C_{D_0} + C_{D_L}(\alpha)$, or, between certain limits of α, in the form of $C_D = a\,\alpha$.

Subsequently, an analysis of the angle of attack variation will be made for the following three types of changes of the drag coefficient with the angle of attack:

$$C_{D_{tot}} = C_{D_0} + C_{D_L} \alpha^2 \tag{43}$$

$$C_{D_{tot}} = C_{D_0} + C_{D_L} \alpha \tag{44}$$

$$C_{D_{tot}} = a\,\alpha. \tag{45}$$

The lift coefficient is in all cases determined as function of the angle of attack by

$$C_L = \frac{dC_L}{d\alpha} \alpha = C_L' \alpha. \tag{46}$$

The analytical technique is the same in all cases: First an expression for $F(t)$ is obtained and thereafter an equation for $\alpha(t)$, from which then the difference in thrust, $F = F_0 - F(t)$ and in angle of attack, $\alpha = \alpha_0 - \alpha(t)$, respectively, can be determined as function of the difference in apparent weight, ΔW_{app}, due to the decrease in propellant weight.

1. $C_{D_{tot}} = C_{D_0} + C_{D_L} \alpha^2$

Inserting Eq. (43) in Eq. (41), and Eq. (46) in (42), one obtains a transformation of the basic equations into

$$F - q S C_{D_0} - q S C_{D_L} \alpha^2 = 0 \tag{47}$$

$$\alpha(F - C_L' q S) - W_{app} = 0. \tag{48}$$

From Eq. (48)

$$\alpha = \frac{W_{app}}{F + C_L' q S}. \tag{49}$$

Inserted in Eq. (47)

$$F - q S C_{D_0} - q S C_{D_L} \frac{W_{app}^2}{(F + C_L' q S)^2} = 0. \tag{50}$$

Re-arranging Eq. (50) in power terms of the thrust yields a cubic equation for the basic relation (47), containing only F and W_{app} as variable,

$$F^3 + F^2\,[q\,S\,(2\,C_L' - C_{D_0})] + F\,[q^2\,S^2(C_L'^2 - 2\,C_L'\,C_{D_0})] - q^3\,S^3\,C_L'^2\,C_{D_0} - q\,S\,C_{D_L}\,W_{app} = 0. \tag{51}$$

This equation gives the instantaneous thrust requirement at the time t and the instantaneous apparent weight. The difference between initial thrust and thrust at any time t or at burn-out time t_b is found from Eq. (51) by substituting the corresponding difference in apparent weight ΔW_{app} for the term W_{app} in the equation. This difference, of course, represents the propellant consumption during the time period.

$$\Delta W_{app} = W_p(t)\left[1 - \left(\frac{v}{v_c}\right)^2\right]. \tag{52}$$

In order to obtain the variation in angle of attack, one starts from Eq. (47), solving for α,

$$\alpha^2 = \frac{F}{q\,S\,C_{D_L}} - \frac{C_{D_0}}{C_{D_L}}. \tag{53}$$

From the second of the basic equations (64), one finds for the thrust

$$F = \frac{W_{app}}{\alpha} - C_L'\,q\,S. \tag{54}$$

Inserting Eq. (54) in (53) yields

$$\alpha^2 = \frac{W_{app}}{\alpha\,q\,S\,C_{D_L}} - \frac{C_L'}{C_{D_L}} - \frac{C_{D_0}}{C_{D_L}}$$

or, the cubic equation in α,

$$\alpha^3 + \alpha\left(\frac{C_L'}{C_{D_L}} + \frac{C_{D_0}}{C_{D_L}}\right) - \frac{W_{app}}{q\,S\,C_{D_L}} = 0 \tag{55}$$

which has the solution

$$\alpha = \left[\frac{W_{app}}{2\,q\,S\,C_{D_L}} + \frac{\sqrt{27\,C_{D_L}\,W_{app}^2 + 4\,q^2\,S^2(C_{D_0} + C_L')^3}}{6\,q\,S\,C_{D_L}\sqrt{3\,C_{D_L}}}\right]^{1/3} + \left[\frac{W_{app}}{2\,q\,S\,C_{D_L}} - \frac{\sqrt{27\,C_{D_L}\,W_{app}^2 + 4\,q^2\,S^2(C_{D_0} + C_L')^3}}{6\,q\,S\,C_{D_L}\sqrt{3\,C_{D_L}}}\right]^{1/3}. \tag{56}$$

The change in angle of attack $\Delta\alpha = \alpha - \alpha_0(t)$ is then again found from Eq. (56) by replacing W_{app} by ΔW_{app} for the time interval under consideration.

With Eq. (56) the variation of α can only be determined for the whole period of sustained flight. For any value in between it would be necessary to know the variation in propellant consumption with time. This variation is a function of thrust and follows from

$$dW = -\dot{w}_{sp}\,F\,dt. \tag{57}$$

Using Eq. (47), one can replace F by the angle of attack

$$dW = -\dot{w}_{sp}\,q\,S(C_{D_0} + C_{D_L}\,\alpha^2)\,dt. \tag{58}$$

In order to determine the change in angle of attack for a given time of operation, say, per revolution, it is necessary to obtain α not as function of W_{app}, but as function of time. Dividing Eq. (58) by $d\alpha$,

$$\frac{dW}{d\alpha} = -W_{sp}\,q\,S(C_{D_0} + C_{D_L}\,\alpha^2)\,\frac{dt}{d\alpha} \tag{59}$$

Vol. 2 1956

differentiating Eq. (55) with respect to a, replacing W_{app} by $n_c W$,

$$\frac{dW}{da} = \left(3a^2 + \frac{C_{D_0} C_L'}{C_{D_L}}\right) \frac{q S C_{D_L}}{n_c} \tag{60}$$

and combining Eqs. (59) and (60), yields ultimately

$$dt = -\frac{3}{n_c \dot{W}_{sp}} \cdot \frac{a^2 + \dfrac{C_{D_0} + C_L'}{3 C_{D_L}}}{a^2 + \dfrac{C_{D_0}}{C_{D_L}}} . \tag{61}$$

Integration over a period of revolution, t_r,

$$t_r = \frac{3}{n_c \dot{W}_{sp}} \int_{a_{tr}}^{a_0} \left(1 + \frac{\dfrac{C_L' + 2 C_{D_0}}{3 C_{D_L}}}{a^2 + \dfrac{C_{D_0}}{C_{D_L}}}\right) da. \tag{62}$$

Integrated and solved for a_{tr},

$$\begin{aligned} \frac{3\sqrt{C_{D_0} C_{D_L}}}{C_L' - 2 C_{D_0}} a_{tr} + \tan^{-1}\left(a_{tr}\sqrt{\frac{C_{D_L}}{C_{D_0}}}\right) &= \frac{3 a_0 \sqrt{C_{D_0} C_{D_L}}}{C_L' - 2 C_{D_0}} \\ &+ \tan^{-1}\left(a_0\sqrt{\frac{C_{D_L}}{C_{D_0}}}\right) - \frac{t_r n_c \dot{W}_{sp}\sqrt{C_{D_0} C_{D_L}}}{C_L' - 2 C_{D_0}} . \end{aligned} \tag{63}$$

This equation must be solved by trial and error. Conversely, for a given range of angle of attack, from a_0 to a_1, the cruising time follows from

$$t = \frac{3}{n_c \dot{W}_{sp}} \left[a_0 - a_1 + \frac{C_L' - 2 C_{D_0}}{3\sqrt{C_{D_0} C_{D_L}}} \left[\tan^{-1}\left(a_0\sqrt{\frac{C_{D_L}}{C_{D_0}}}\right) - \tan^{-1}\left(a_1\sqrt{\frac{C_{D_L}}{C_{D_0}}}\right) \right] \right] . \tag{64}$$

2. $C_{D_{tot}} = C_{D_0} + C_{D_L} a$

In a manner analogous to the previous case, one obtains presently

$$F(t) = -\frac{1}{2}(C_L' q S - C_{D_0} q S) + \sqrt{\frac{1}{4}(C_L' q S - C_{D_0} q S) + q^2 S^2 C_{D_0} C_L' + q S C_{D_L} W_{app}} \tag{65}$$

$$a(t) = -\frac{1}{2}\left(\frac{C_L'}{C_{D_L}} + \frac{C_{D_0}}{C_{D_L}}\right) + \sqrt{\frac{1}{4}\left(\frac{C_D'}{C_{D_L}} + \frac{C_{D_0}}{C_{D_L}}\right)^2 + \frac{W_{app}}{q S C_{D_L}}} \tag{66}$$

$$\frac{2 C_{D_L}}{C_L' - C_{D_0}} a_{tr} + \ln\left(a_{tr} + \frac{C_{D_0}}{C_{D_L}}\right) = \frac{2 C_{D_L}}{C_L' - C_{D_0}} a_0 + \ln\left(a_0 + \frac{C_{D_0}}{C_{D_L}}\right) - \frac{n_c \dot{W}_{sp} C_{D_L}}{C_L' - C_{D_0}} \tag{67}$$

$$t = \frac{2}{n_c \dot{W}_{sp}} \left[a_0 - a_1 + \frac{C_L' - C_{D_0}}{2 C_{D_L}} \ln \frac{a_0 + \dfrac{C_{D_0}}{C_{D_L}}}{a_1 + \dfrac{C_{D_0}}{C_{D_L}}} \right] . \tag{68}$$

3. $C_{D_{tot}} = a\,\alpha$

In this case the corresponding relations assume the form

$$F(t) = -\frac{1}{2} C_L' q S + \sqrt{\frac{1}{4} C_L' q^2 S^2 + q S a W_{app}} \tag{69}$$

$$\alpha(t) = -\frac{1}{2}\frac{C_L'}{a} + \sqrt{\frac{1}{4}\left(\frac{C_L'}{a}\right)^2 + \frac{W_{app}}{q S a}} \tag{70}$$

$$2 d_{tr} + \frac{C_L'}{a} \ln \alpha_{tr} = 2 \alpha_0 + \frac{C_L'}{a} \ln \alpha_0 - n_c \dot{W}_{sp} t_r \tag{71}$$

$$t = \frac{1}{n_c \dot{W}_{sp}} \left[2 (\alpha_0 - \alpha_1) + \frac{C_L'}{a} \ln \frac{\alpha_0}{\alpha_1} \right]. \tag{72}$$

d) Angle of Attack and Thrust Constant

As the vehicle loses propellant weight, $(F/m) \sin \alpha$ increases and the vehicle gains altitude. This causes a decrease in drag due to lower density. However, this results in an increase of $F \cos \alpha - D$, producing an increase in velocity which counteracts the trend toward decreasing drag. The decrease in density can be found as follows: The basic flight path equations are now written in the form

$$\dot{v} = \frac{F}{m} \cos \alpha - \frac{D}{m} - g \sin \theta \tag{73}$$

$$0 = F \sin \alpha - L - g_{app}\, m \cos \theta - m v \dot{\theta}. \tag{74}$$

Again, one may assume that θ and $\dot{\theta}$ are small and can be neglected. Solving Eq. (74) for the density, one obtains

$$\varrho(t) = 2 \frac{W_{app} - F \sin \alpha}{C_L S v^2}. \tag{75}$$

The initial conditions are $t_0 = 0$, $W = W_0$, $v = v_0$, and the final conditions $t = t_b$, $W = W_0 - W_p$, $v = v_b$. Thus, using Eq. (75), the change in density during the flight period of the satelloid can finally be expressed by means of the following convenient parameters,

$$\varrho_0 - \varrho_b = 2 \frac{W_0}{C_L S} \left\{ \frac{1 - \left(\frac{v_0}{v_c}\right)^2 - \frac{F}{W_0} \sin \alpha}{{v_0}^2} - \frac{1 - \Lambda\left[1 - \left(\frac{v_b}{v_c}\right)^2\right] - \left(\frac{v_b}{v_c}\right)^2 - \frac{F}{W_0} \sin \alpha}{{v_b}^2} \right\} \tag{76}$$

and, if $v_b = v_c$,

$$\varrho_0 - \varrho_b = 2 \frac{W_0}{C_L S} \left[\frac{1 - \left(\frac{v_0}{v_c}\right)^2 - \frac{F}{W_0} \sin \alpha}{{v_0}^2} + \frac{\frac{F}{W_0} \sin \alpha}{{v_b}^2} \right]. \tag{77}$$

Assuming a constant drag value and disregarding $g \sin \theta$, Eq. (73) can be integrated to obtain the burn-out velocity,

$$v_b = v_0 + \frac{F \cos \alpha - D}{\dot{m}} \ln \left(\frac{m_0}{m_b} \right). \tag{78}$$

The drag variation will be approximately linear, at least for moderate changes in velocity. Therefore, D can be replaced by the arithmetic mean value between initial and final condition, $D = (D_0 - D_b)/2$. Assuming constant C_D,

$$\overline{D} = \frac{C_D S}{4} (\varrho_0 v_0^2 + \varrho_b v_b^2). \tag{79}$$

Among other parameters, the decrease in density is a function of initial and final velocity. The velocity increase, given by Eq. (78) is a function of mass ratio and mean drag. The drag, however, follows from the change in density and velocity, as shown by Eq. (79). The Eq. (77) through (79) are therefore a set of simultaneous equations which must be solved iteratively.

The relations presented in Section III,3 permit a detailed analysis of the dynamics of continuously propelled vehicles at subcircular velocity.

4. Comparison of Thrust Requirements at Various Velocities

The period of operation of a satelloid depends in the first place on the propellant consumption and therefore on the thrust requirement. Obviously, the thrust requirement decreases with decreasing density or increasing altitude. However, the thrust requirement is also greatly affected by the flight velocity, especially when the amount of aerodynamic lift available is much less than the increase in apparent weight due to reduction in velocity, so that the difference must be made up by lift due to thrust.

Consider two satelloids of equal weight and lifting surface operating at two different velocities v' and v''. With these velocities are associated the respective apparent weights, dynamic pressures and drag coefficients as well as lift coefficient. From Eq. (11) the two corresponding thrust requirements can be found immediately,

$$\frac{F''}{F'} = \sqrt{\frac{(W_{app}'' - q'' C_L'' S)^2 + (q'' C_D'' S)^2}{(W_{app}' - q' C_L' S)^2 + (q' C_D' S)^2}}. \tag{80}$$

When the deviation from circular velocity exceeds about 10 per cent, the apparent weight becomes very large compared to the lift obtainable in the case of diffuse reflection, so that the lift can be omitted in the first approximation. Furthermore, the dynamic pressure q'' can be expressed in terms of q' as $q'(v''/v')^2$ assuming, both vehicles fly at the same altitude so that the density is the same; Eq. (80) can then be written in the simplified form

$$\frac{F''}{F'} = \sqrt{\frac{(W_{app}'')^2 + \left(q' \left(\frac{v''}{v'}\right)^2 C_D'' S\right)}{(W_{app}')^2 - (q' C_D' S)^2}}. \tag{81}$$

If a subcircular-velocity satelloid is compared with a circular-velocity satelloid, the equations can be written in the form:
with aerodynamic lift considered,

$$\frac{F}{F_c} = \sqrt{\frac{\left[W\left(1 - \left(\frac{v}{v_c}\right)^2 - q_c \left(\frac{v}{v_c}\right)^2 C_L S\right]^2}{(q_c C_{D_c} S)^2} + \left(\frac{v}{v_c}\right)^4 \left(\frac{C_D}{C_{D_c}}\right)^2} \tag{82}$$

and with aerodynamic lift neglected,

$$\frac{F}{F_c} = \sqrt{\frac{W^2\left[1 - \left(\frac{v}{v_c}\right)^2\right]^2}{(q_c C_{D_c} S)^2} + \left(\frac{v}{v_c}\right)^4 \left(\frac{C_D}{C_{D_c}}\right)^2} \tag{83}$$

where the subscript c indicates the values pertaining to the circular-velocity satelloid.

IV. Aspects of Satelloid Aerodynamics

Because of the before-mentioned operational requirements, the aerodynamics of the satelloid is essentially the aerodynamics of free molecule flow. In this case the aerodynamic coefficients are greatly affected by the physics of interaction between the molecules and the wall of the moving body (cf. Ref. [5] to [13]). Theory distinguishes between three basic types of interaction:

1. Specular reflection.
2. Diffuse elastic reflection.
3. Diffuse inelastic reflection.

Specular reflection implies that the molecules are reflected from the wall at an angle which is equal to the angle of incidence (optical reflection). Their momentum normal to the wall is exactly reversed and their tangential momentum change is zero, i.e. no tangential momentum is transferred to the wall and the shear force on the wall is therefore zero. For these reasons the drag in the case of specular reflection is small and the lift is comparatively large. However, as has been mentioned already by SÄNGER [6], earlier studies indicated that specular reflection begins at angles of attack at which the surface roughness height, projected on the molecular beam must be smaller than DE BROGLIE's wavelength of the beam and he concludes that this fact limits the possibility of specular reflection to very small angles of attack (a few minutes only). This is probably true for metallic surfaces, but improvements may be possible by the development of suitable coatings. Defining a reflection coefficient f such that the fraction f of the impinging molecules is reflected diffusely and $(1 - f)$ specularly, it has been found that, although f was close to 1.0 in many tests conducted (cf. Ref. [9]), there were some instances, such as air molecules impinging on fresh shellac, where f was only 0.79 or air on oil ($f = 0.895$) and air on glass ($f = 0.89$ to 1.0). These examples indicate that the development of an advanced technique of surface finishing might be feasible, with a significant fraction of the impinging molecules reflected specularly. Here lies a very interesting and potentially quite important field of research on the nature of solid surfaces and their interaction with impinging molecular beams.

Under the assumption of more conventional metallic surfaces, almost completely diffuse reflection must be assumed. This situation has been compared to the bouncing of a tennis ball on a cobblestone pavement. Strictly, this comparison applies to the diffuse elastic reflection only where the time of contact between molecule and wall is so short that no exchange of energy can take place, for instance, a few collisions between molecule and wall molecules only, while the molecule is trapped in one of the interstices of the wall (Ref. [14]). If the adsorption of the molecule lasts for a large number of collisions (ten to thousand or more) then energy is exchanged between molecule and wall. The high-speed molecule will transfer energy to the wall, and the reflection becomes inelastic. In the case of diffuse elastic reflection the impulse normal to the wall is reversed like in the specular case, but in a completely random direction. All tangential momentum is transferred to the wall so that the shear force ("friction drag") becomes very high. Fore these reasons the drag is much higher and the lift much smaller for diffuse elastic reflection than in the specular case.

The same is essentially true for the diffuse inelastic reflection. The tangential momentum is transferred to the wall. The normal momentum is not completely reversed, but is used partly to excite the wall molecules and the higher degrees of freedom of the air molecules so that diffusivity in this case does not only refer to the direction but also to the translational magnitude of the recoil momentum

Vol. 2 1956

with which the molecule leaves the wall. With increasing adsorption time, first the translational, then the rotational, and finally the vibrational degrees of freedom of the impinging molecule are affected. If the energy of impact (flight speed) is large enough and the adsorption time sufficient, then the vibrational degrees of freedom of diatomic molecules can be excited to such an extent that dissociation results. A vehicle moving at circular speed at satelloid altitudes contains an energy of about 7.6 kcal/gm. The dissociation energies of hydrogen, nitrogen and oxygen are, respectively, in kcal/gm, 51.6, 8 and 3.65. A circular velocity satelloid therefore would be marginal for dissociating nitrogen and could more likely dissociate oxygen. However, most of the oxygen at these altitudes appears to be dissociated permanently due to local environmental conditions, as indicated by spectra from aurorae and the night sky. Monatomic oxygen is produced photochemically by ultraviolet radiation. A certain amount of variation in the monatomic oxygen concentration takes place between day and night, due to the partial recombination to molecular oxygen in the absence of sunlight. The effect of dissociation or even of ionization on the free molecule aerodynamic coefficients can therefore be neglected in the first approximation, from energy considerations alone[1]. In addition, a sufficiently long adsorption time for accomodation of the vibrational excitations is necessary. One may therefore consider only translational and rotational accomodation. Greater refinements apparently rest with additional ground experimental and, above all, flight test data in the free molecule flow region in the correct speed range. A descending instrumental satellite could be extremely useful in providing authoritative data in this respect.

The degree to which the gas molecules are energetically accomodated to the wall is expressed by the accomodation coefficient, e.g. [11]

$$a = \frac{E_i - E_r}{E_i - E_w} \tag{84}$$

where E_i is the energy of the impinging stream, E_r the energy of the re-emitted molecules, and E_w the average energy of the gas molecules at a temperature equal to the wall temperature.

For the translational and rotational accomodation coefficients, a wide variety of values has been given in the literature (cf. Ref. [14] through [20] which were obtained from Ref. [21]). Latest values (Ref. [19]) indicate that most likely the accomodation coefficient lies between 0.87 and 0.97. However, these measurements have been made at molecular speed ratios below those of interest in this paper. Therefore, it is not possible at the present time to determine a "likely" accomodation coefficient and calculations will be restricted to the two boundary cases of $a = 0$ (elastic reflection; no energy exchange with the wall) and $a = 1$ (completely inelastic reflection).

Taking the possibility of specular reflection into account, the accomodation coefficient can be written in the following form, using temperatures instead of energies,

$$a = f\frac{T_0 - T_r}{T_0 - T_w} \tag{85}$$

[1] This conclusion does not apply to continuum flow, firstly, because no ambient oxygen is in dissociated state at lower altitudes. Secondly, because the molecules behind the shock or in the boundary layer experience a vastly greater number of collisions.

where T_0 is the stagnation temperature of the impinging stream of the static temperature T_i and T_r is the temperature of the re-emitted stream. Assuming completely diffuse reflection, $f = 1$, it follows that $a = 0$ for completely elastic reflection (kinetic energy of impinging and re-emitted stream is the same, hence their thermal temperatures T_i and T_r are also the same) and $a = 1$ for completely inelastic reflection, in which case $T_r = T_w$.

The aerodynamic coefficients are found by proper use of the following fundamental equations, defining the impact pressure, the recoil pressure and the shear stress, which have been derived in several places in the literature on free molecule flow aerodynamics (cited in [5] to [13]).

Pressure produced by the impinging molecules, in terms of the dynamic pressure $q = (\varrho/2)\, v^2$,

$$\frac{p_i}{q} = \frac{\sin a}{S\sqrt{\pi}}\, e^{-s^2 \sin^2 a} + \left(\frac{1}{2\,S^2} + \sin^2 a\right)[1 + erf\,(s \sin a)]. \tag{86}$$

Pressure produced by the re-emitted molecules

$$\frac{p_r}{q} = \frac{1}{2\,S^2}\,\frac{C_r}{C_i}\, e^{-s^2 \sin^2 a} + \frac{\sqrt{\pi}}{2}\,\frac{\sin a}{2}\,\frac{C_r}{C_i}\,[1 + erf\,(s \sin a)]. \tag{87}$$

Shear stress produced by the transfer of tangential momentum from the gas to the wall

$$\frac{\tau}{q} = \frac{\cos a}{S\sqrt{\pi}}\, e^{-s^2 \sin^2 a} + \sin a \cos a\,[1 + erf\,(s \sin a)]. \tag{88}$$

For the shear stress it is not necessary to distinguish between shear stress from the impinging and from the re-emitted molecules, because at diffuse reflection there exists no preferred direction of re-emission and therefore $\tau_r = 0$, whence $\tau = \tau_i$. In the case of specular reflection no tangential momentum at all is transferred to the wall and therefore $\tau = 0$.

For diffuse reflection in general, the coefficients of drag and of lift of a flat plate at angle of attack a are found from the relations

$$C_D = \frac{D}{q\,s} = \left[\frac{\Delta\, p_i(a)}{q} - \frac{\Delta\, p_r(a)}{q}\right]\sin a + \frac{\Sigma\,\tau(a)}{q}\cos a \tag{89}$$

and

$$C_L = \frac{L}{q\,s} = \left[\frac{\Delta\, p_i(a)}{q} - \frac{\Delta\, p_r(a)}{q}\right]\cos a - \frac{\Sigma\,\tau(a)}{q}\sin a. \tag{90}$$

Here $\Delta\, p_i(a)$ represents the difference between the pressure produced by the impinging molecules on the wind side and on the lee side, respectively,

$$\Delta\, p_i(a) = p_i(a) - p_i(-a). \tag{91}$$

Likewise, $\Delta\, p_r(a)$ is the difference between the pressures caused by the re-emitted molecules on the wind side and on the lee side,

$$-\Delta\, p_r(-a) = p_r(a) - p_r(-a). \tag{92}$$

Since $\tau_r = 0$, the sum of all shear forces $\Sigma\tau = \Sigma\tau_i$ is

$$\Sigma\tau(a) = \tau(a) - \tau(-a). \tag{93}$$

Developing Eqs. (89) and (90) with the use of Eq. (86) through (88) one obtains for the flat plate the expressions

$$C_D = \frac{2}{S\sqrt{\pi}}\, e^{-s^2 \sin^2 a} + \frac{\sqrt{\pi}\sin^2 a}{S}\,\frac{C_r}{C_i} + 2 \sin a\left(1 + \frac{1}{2\,S^2}\right) erf\,(s \sin a) \tag{94}$$

Vol. 2 1956

and

$$C_L = \frac{\sqrt{\pi}\,\sin\alpha\cos\alpha}{S}\,\frac{C_r}{C_i} + \frac{\cos\alpha}{S^2}\,erf\,(s\sin\alpha). \tag{95}$$

For diffuse elastic reflection,

$$\frac{c_r}{c_i} = \frac{\sqrt{2\,g\,\frac{R}{M}\,T_r}}{\sqrt{2\,g\,\frac{R}{M}\,T_i}} = \sqrt{\frac{T_r}{T_i}} = 1 \tag{96}$$

and for completely inelastic reflection,

$$\frac{c_r}{c_i} = \sqrt{\frac{T_w}{T_i}}. \tag{97}$$

In the latter case it is necessary to determine the wall temperature, before the aerodynamic coefficients can be determined.

For flight speeds which are high enough so that $s\sin\alpha = c_m$, the pressure on the lee side of the body is zero, hence, $p_i(-\alpha) = 0$, $p_r(-\alpha) = 0$, $\tau(-\alpha) = 0$. At the velocities under consideration here this is certainly the case for the base of the satelloid body and in some cases also for the lee side of its wings at angle of attack.

If a single wedge with half angle β is considered at an angle of attack α, one finds the same relations as given in Eqs. (91) through (93), except that α is replaced by $\sigma = \alpha + \beta$ and $-\sigma = \alpha - \beta$. If the wedge drag coefficient is to be referred to the planform area rather than to the slant area, the above pressure and shear force terms must be divided by $\cos\alpha$.

In the case of specular reflection it has been stated before that $p_r = p_i$ and $\tau = 0$, so that

$$q\,C_{Ds} = [2\,p_i(\alpha) - 2\,p_i(-\alpha)]\sin\alpha \tag{98}$$

$$q\,C_{Ls} = [2\,p_i(\alpha) - 2\,p_i(-\alpha)]\cos\alpha \tag{99}$$

yielding

$$C_{Ds} = \frac{4}{S\sqrt{\pi}}\sin^2\alpha\,e^{-s^2\sin^2\alpha} + \left(\frac{2\sin\alpha}{S^2} + 4\sin^3\alpha\right) erf\,(s\sin\alpha) \tag{100}$$

$$C_{Ls} = \frac{4}{S\sqrt{\pi}}\sin\alpha\cos\alpha\,e^{-s^2\sin^2\alpha} + \left(\frac{2\cos\alpha}{S^2}\right) + 4\sin^2\alpha\cos\alpha\Big) erf\,(s\sin\alpha). \tag{101}$$

Differentiation of the diffuse and the specular expressions for the lift coefficient with respect to the angle of attack yields the equations for the lift-curve slope,

$$\frac{dC_L}{d\alpha} = \frac{\sqrt{\pi}}{S}\,\frac{c_r}{c_i}\,(\cos^2\alpha - \sin^2\alpha) + \frac{2\cos^2\alpha}{S\sqrt{\pi}}\,e^{-s^2\sin^2\alpha} - \frac{\sin\alpha}{S^2}\,erf\,(s\sin\alpha) \tag{102}$$

for diffuse reflection, and

$$\frac{dC_{Ls}}{d\alpha} = \frac{4}{S\sqrt{\pi}}\,e^{-s^2\sin^2\alpha}\,(2\cos^2\alpha - \sin^2\alpha) + (8\sin\alpha\cos\alpha - 4\sin^3\alpha)\,erf\,(s\sin\alpha) \tag{103}$$

for specular reflection. For $\alpha \to 0$, these equations become, respectively,

$$\left.\frac{dC_L}{d\alpha}\right|_{\alpha=0} = \frac{\sqrt{\pi}}{S}\,\frac{c_r}{c_i} + \frac{2}{S\sqrt{\pi}} \tag{104}$$

$$\left.\frac{dC_{Ls}}{d\alpha}\right|_{\alpha=0} = \frac{8}{S\sqrt{\pi}}. \tag{105}$$

Eqs. (104) and (105) are also found in Ref. [10].

V. Skin Temperature of the Satelloid

In computing the skin temperature of the satelloid in free molecule flow, essentially the method of Ref. [21] has been followed, using more recent atmospheric data. It also has been assumed that no heat is conducted into the interior of the vehicle and that no heat is removed by means of internal cooling or other methods of artificial cooling.

The basic energy balance equation yields

$$E_i - R_i = E_r - R_r \tag{106}$$

where E_i is the energy transferred to the wall by the impinging molecules and R_i is the incident radiation energy. The subscript r designates the re-emitted energies. The wall temperature is obtained under steady state conditions, as shown in Ref. [21], for a monatomic gas where — neglecting vibrational excitations — all impinging energy is translational energy of the molecules, $E_i = E_t$,

$$a E_t - \frac{3}{2} a n k T_w + \varepsilon J_0 - \varepsilon \sigma T_w^4 = 0. \tag{107}$$

Vol. 2 1956

It can be seen that for the accomodation coefficient $a = 0$, the wall temperature is determined only by the radiation equilibrium. Therefore, in subsequent calculations, only the case of $a = 1$ will be assumed, which is conservative, since it results in the highest wall temperatures (however, the increase in wall temperature between $a = 0.7$ and 1.0 is not very large). Under these conditions the wall temperature equation for a monatomic gas is

$$E_t - \frac{3}{2} n k T_w + \varepsilon J_0 - \varepsilon \sigma T_w^4 = 0. \tag{108}$$

For a diatomic gas the incident molecular energy E_i is assumed to be divided into translational and rotational energy, according to $E_i = E_t - n E_r$. The equation is ($a = 1$),

$$E_t + n k T_i - \frac{5}{2} n k T_w + \varepsilon J_0 - \varepsilon \sigma T_w^4 = 0. \tag{109}$$

For a mixture of monatomic (superscript ′) and diatomic (″) gas, the equation can be written in the form

$$E_t' + E_t'' + n'' k T_i - (n' + n'') \frac{3}{2} k T_w + \varepsilon J_0 - \varepsilon \sigma T_w^4 = 0. \tag{110}$$

The equations of definition will be given below.

The number of air molecules, n, striking the surface per square foot and second is given by

$$n = \frac{N C M}{2\pi} \{e^{-s^2 \sin^2 \delta} + \sqrt{\pi}\, s \sin \delta \,[1 + erf\,(s \sin \delta)]\}. \tag{111}$$

N being the number of air molecules per unit volume,

$$N = \frac{N_A g \varrho}{M} \tag{112}$$

where N_A is the AVOGADRO number ("LOSCHMIDTsche Zahl") of $2.73 \cdot 10^{26}$ molecules per lb-mole, $g\,\varrho$ is the local density in lb/ft^3 and M is the molecular weight in lb/lb-mole; c_m is the most probable velocity of the molecules in the gas at rest,

$$c_m = \sqrt{2 g \frac{R}{M} T}, \tag{113}$$

T being the local absolute temperature. The translational energy of the molecules striking the wind side of the wall is given by

$$E_t = n\left(\frac{M V^2}{2} + \psi k T\right) \tag{114}$$

where, [21],

$$\psi = 1 + \frac{1 + \frac{1}{3} s \sin\delta \,[1 + erf\,(s \sin\delta)]\, e^{s^2 \sin^2\delta}}{1 + \sqrt{\pi}\, s \sin\delta \,[1 + erf\,(s \sin\delta)]\, e^{s^2 \sin^2\delta}}\,. \tag{115}$$

For $v = 0 = s$ (vehicle at rest), $\psi = 2$, thus yielding the well-known relation $E_t = 2\,n\,k\,T$ for the translational kinetic energy of a static gas crossing a reference plane. For v very large ($s \sin\delta > 1.6$), ψ becomes $5/2$.

In the atmosphere used here (cf. Appendix), the composition is assumed to consist of N_2 and O_2 up to 110 km. In this case the computation of E_t is straightforward, using the molecular weight $M = 28.95 \approx 29$ and, for the mass of the individual molecule

$$m = \frac{M}{g\,N_A} \approx 3.3 \cdot 10^{-27} \text{ slugs/molecule.} \tag{116}$$

At 130 km and above, the atmosphere is considered to consist of N_2 and monatomic oxygen. In this case

$$E_t' = n'\left(\frac{m'}{2} v^2 + \psi k T\right) \tag{117}$$

$$E_t'' = n''\left(\frac{m''}{2} v^2 + \psi k T\right) \tag{118}$$

$$n' + n'' = n \tag{119}$$

where n' and n'' represent the number of particles of monatomic oxygen and diatomic nitrogen, respectively, striking the surface per square foot and second. The total number of particles, n, is computed according to Eq. (111) using $M = 24$ as new molecular weight. With all oxygen dissociated, the weight percentage of oxygen and nitrogen shifts from about 0.23 and 0.77 to 0.375 and 0.625, respectively.

The number of monatomic oxygen particles, n', follows then from

$$n' = n'^* N_A \text{ oxygen atoms/ft}^2\,\text{sec} \tag{120}$$

where

$$n'^* = \frac{W'}{M'}\,(M' = 16) \text{ lb-mole/ft}^2\,\text{sec} \tag{121}$$

is the number of pound-moles of monatomic oxygen striking the surface, and

$$W' = 0.375\, n'\, M\, (M = 24) \text{ lb/ft}^2\,\text{sec} \tag{122}$$

is the weight of the monatomic oxygen striking the surface, and

$$n^* = \frac{n}{N_A} \text{ lb-mole/ft}^2\,\text{sec} \tag{123}$$

is the number of pound-moles of *air* striking the surface (the weight of air striking the surface would be $W = n^*\,M$; $M = 24$); n is computed according to Eq. (111), using $M = 24$. In the same manner the number of nitrogen molecules striking the surface, per square foot and second, n'', is obtained, using 0.625 instead 0.375.

VI. Numerical Analysis

In this section some of the previously derived relationships are evaluated. The operational aspects of the satelloid system are discussed numerically.

Based on the atmospheric data given in the Appendix, the dynamic pressure at circular velocity is shown in Fig. 2 as function of altitude. In Fig. 3 the dynamic pressure is presented as function of velocity for a number of altitudes. A comparison of the two graphs shows that, within the velocity limits under consideration, the effect of altitude on the dynamic pressure is considerably greater than the effect of velocity.

The molecular-speed ratio, $s = v_c/c_m$, for the circular-velocity satelloid is presented in Fig. 4 as function of altitude, using Eq. (113) for calculating c_m. In accordance with the assumption made in the Appendix, two molecular weights have been assumed for two different altitude regions, with a transition curve between these regions (dashed line). Actually, since the increase in the degree of dissociation will be gradual, the curve more probably will follow the dotted line. The speed ratio s, which is roughly the molecular flow equivalent of the MACH number used in continuum flow, varies considerably with altitude and reaches quite large values in the lower altitude region.

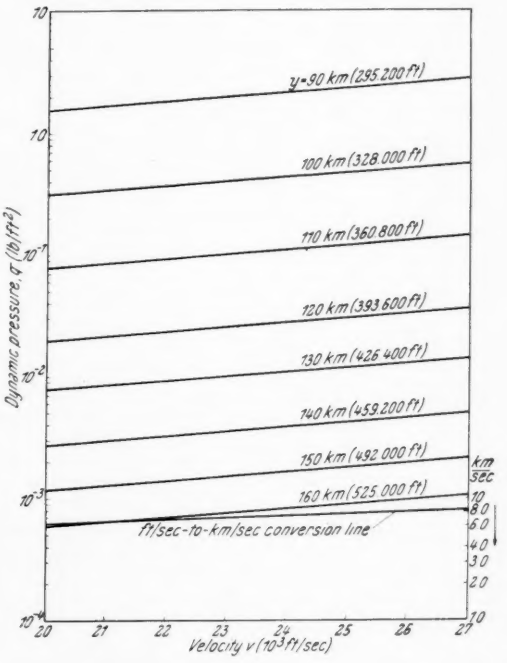

Fig. 3. Variation of dynamic pressure with velocity for different altitudes.

$1\ \mathrm{lb/ft^2} = 4.725 \cdot 10^{-4}$ atm (= 760 mm Hg)

Using Eqs. (95) and (101), the lift coefficient for a flat plate is plotted in Fig. 5 as function of the angle of attack, for different speed ratios as parameter. Fig. 6 is an evaluation of Eqs. (94) and (100) for the diffuse and the specular case, showing the variation of the drag coefficient with angle of attack for different values of s. A comparison between Figs. 5 and 6 clearly indicates the advantages of having specular reflection, if this condition could be realized. The lift curve slope for diffuse reflection is practically constant at all relevant speeds, while, for specular reflection, the slope increases with the angle of attack. The specular lift coefficient varies very little with velocity in the relevant range. For diffuse reflection the lift coefficient becomes zero as the velocity approaches infinity. Eq. (95) shows immediately that C_L must become zero for this boundary case, while for specular reflection,

$$(C_{Ls})_{s\to\infty} = 4 \sin^2 a \cos a. \tag{124}$$

This is twice the value which is obtained for the hypersonic boundary case in continuum flow. This latter case corresponds to inelastic NEWTONian flow, because of adsorption of the impinging molecules in the boundary layer. Eq. (124), therefore, gives the lift coefficient for the case of elastic NEWTONian flow at infinite speed. For the diffuse drag coefficient one obtains in this case

$$(C_D)_{s\to\infty} = 2\sin\alpha \tag{125}$$

while in the specular case

$$(C_{Ds})_{s\to\infty} = 4\sin^3\alpha. \tag{126}$$

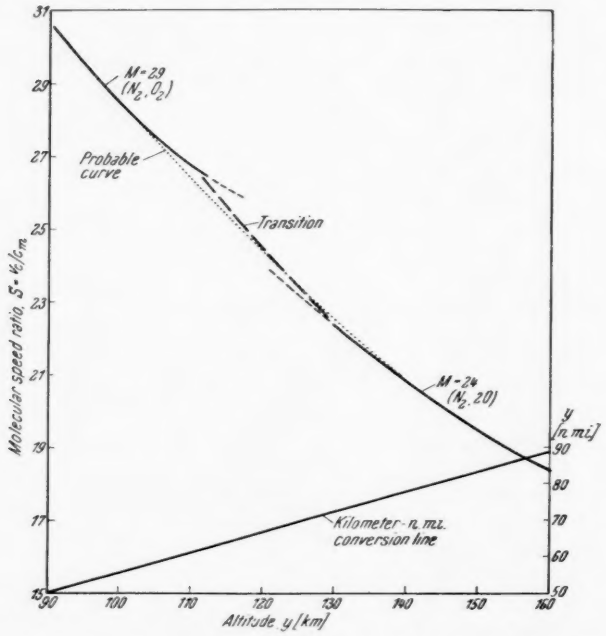

Fig. 4. Molecular-speed ratio of circular-velocity satelloid as function of altitude. M = molecular weight; v_c = circular velocity = $f(y)$; c_m = most probable velocity of molecules = $f(T, M)$

The drag factor, $q\,C_D$, for the circular-velocity case, is plotted in Fig. 7 as function of the drag coefficient, using the altitude as parameter.

Based on the dynamic pressure, Fig. 8 gives the propellant consumption at circular velocity in pounds per second per square foot of reference area (lifting area), according to Eq. (2), for a number of specific thrust values, plotted against altitude. C_D was taken as 0.1 to simplify the use of this graph for other C_D values, since the propellant consumption is directly proportional to the drag coefficient. In a more general graph, Fig. 9, the propellant consumption per square foot and second is plotted against C_D/F_{sp} for a number of interesting altitudes. The arrows attached to each curve indicate whether the upper of the lower abscissa should be used.

Considering that the profile of the satelloid is probably wedge-shaped, the wedge half-angle being 10 to 20 degrees, it follows from Fig. 6 that the drag coefficient is of the order of 0.35 to 0.70. For the case of $C_D = 0.7$, the propellant consumption per square foot and *revolution* is plotted as function of altitude in

Fig. 10 for a variety of specific thrust values. A specific thrust of 250 lb sec/lb can be realized without difficulties, for instance on the basis of oxygen-gasoline combustion. Assuming this specific thrust, the propellant consumption drops

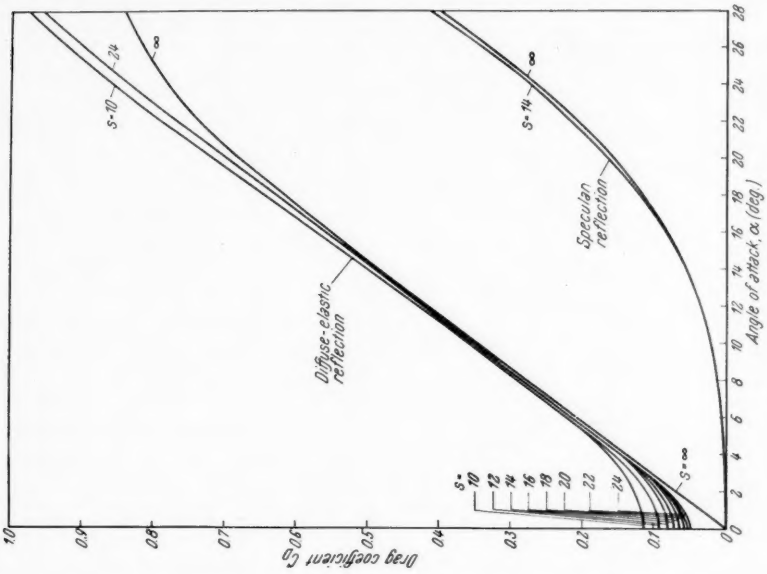

Fig. 6. Comparison of drag coefficients of a flat plate in free molecule flow

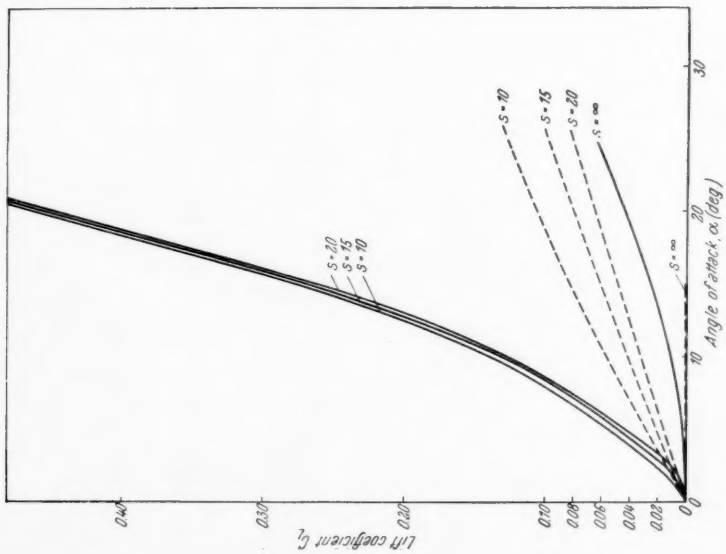

Fig. 5. Comparison of lift coefficients of a flat plate in free molecule flow. ——— specular reflection, — — — — diffuse elastic reflection

below 1 lb/ft²rev. above approximately 115 km (380,000 ft). At higher altitudes the specific thrust is no longer quite so important, unless very long stay times are considered.

With the preceding information, and the theoretical relations presented in section III,1, basic data for the circular-velocity satelloid have been computed

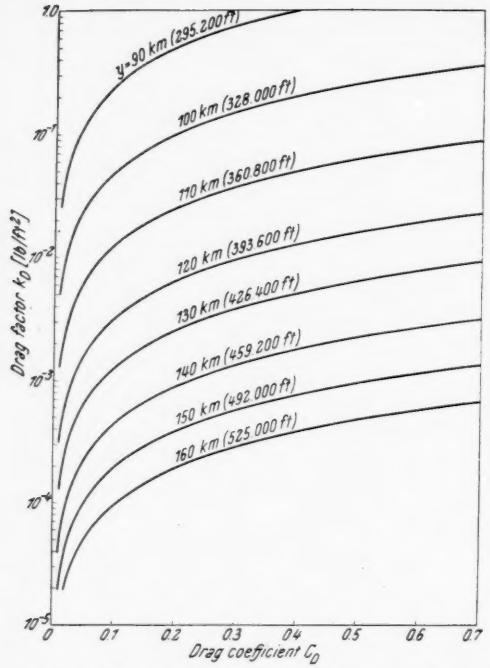

Fig. 7. Variation of drag factor k_D with drag coefficient for circular-velocity satelloid. $k_D = q\,C_D$, $q = \varrho/2\,v^2$

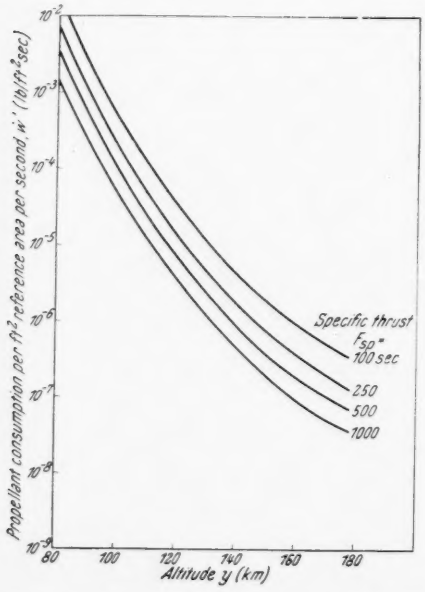

Fig. 8. Variation of propellant consumption with altitude for different values of the specific thrust. 1 lb/ft² sec = 4.725 kg/m² sec. Assumptions: 1. Circular-velocity satelloid, 2. $C_D = 0.1$

for a specific example, as function of altitude. The results are plotted in Figs. 11 and 12. For the burn-out weight, a value of 10,000 lb has been assumed. The value for the wing area (500 ft²) was based on the premise that for the eventual glide descent to the surface a low wing loading of not more than 20 lb/ft² would be desirable. Fig. 12 shows that, beyond 115 km altitude, the satelloid data for one revolution are practically constant, that is, the mass ratio required for one revolution is very close to unity. Above 115 km, the propellant consumption per revolution falls below 20 lb assuming that oxygen and gasoline are used as propellants, the propellant mean weight-volume ratio is about 8.3 lb/gallon (about 0.9 kg/liter). This then means that the propellant consumption at 115 km altitude is about 2.8 gallons per revolution, or 11.2 liters per revolution; in other words, about 8,200 n.mi. per gallon, or 3,570 km per liter of propellant.

The thrust is equal to the burn-out weight of the vehicle multiplied by the burn-out load factor n_b shown in Fig. 12. In the above example, the value of the thrust is 10 lb (4.5 kg). In such very small engines, a fine thrust regulation, as would be required for maintaining constant flight conditions, appears well feasible.

Fig. 13, based on the example, shows the orbital lifetime and the number of revolutions which the satelloid can complete per 1,000 lb propellant expense at a specific thrust of 250 lb sec/lb. At 115 km the satelloid completes about 3 revolutions, corresponding to a stay time of close to 4 hours. The stay time per unit propellant weight

consumed increases rapidly with altitude. At 127 km the stay time is 24 hours or 18 revolutions at constant altitude. A stay time per 1,000 lb propellant of one week requires an altitude of 147.5 km (484,000 ft).

The feasibility of a subcircular velocity satelloid has been studied by comparing the ratio of thrust F in the subcircular case with the thrust F_c at circular velocity (Fig. 14) assuming diffuse reflection in determining the aerodynamic lift coefficient. It is found that the required thrust increases rapidly as the velocity becomes subcircular. For example, under the conditions specified in Fig. 14, a decrease

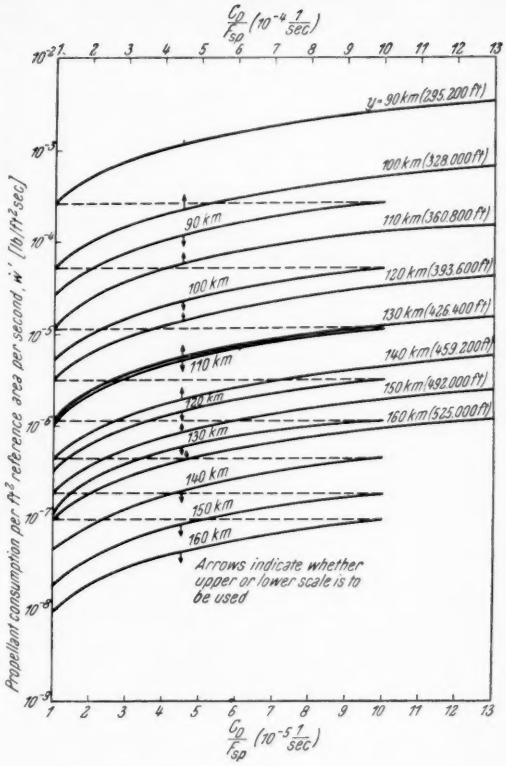

Fig. 9. Propellant consumption per ft² of reference area per second as function of drag coefficient and specific thrust for different altitudes. Circular-velocity satelloid

of the velocity to 0.933 v_c, causes the thrust, hence the propellant consumption, to go up by a factor of 10. This is, of course, caused by the low aerodynamic lift so that practically all the increase in apparent weight must be compensated by lift due to thrust. In view of the very strong increase in thrust required, the lifting thrust cannot be produced simply by increasing the angle of attack, as in the case of conventional rocket vehicles. The overall thrust output must be increased considerably. It should be noted that the curve in

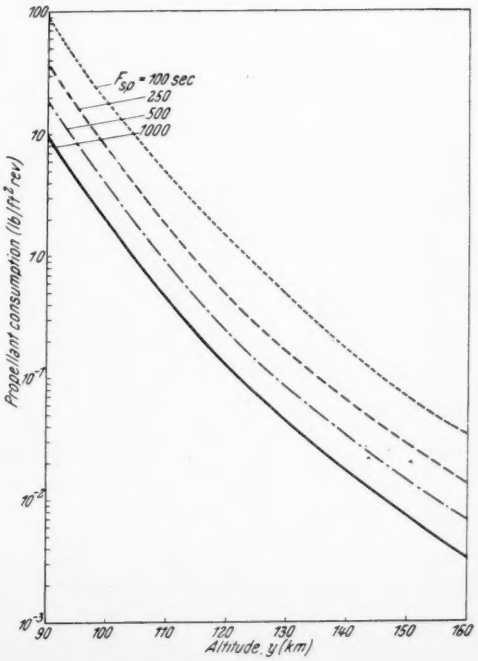

Fig. 10. Satelloid-propellant consumption per unit lifting area per revolution. $C_D = 0.7$; v = circular

Vol. 2 1956

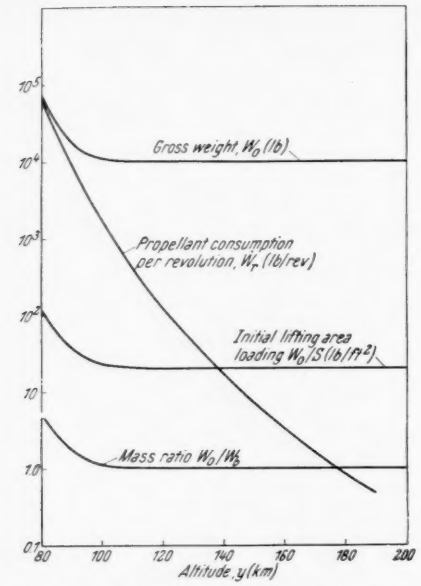

Fig. 11. Variation of satelloid vehicle data for one revolution. $F_{sp} = 250$ sec; $W_b = 10{,}000$ lb; $S = 500$ ft²; $C_D = 0.35$ (diffuse reflection); v = circular

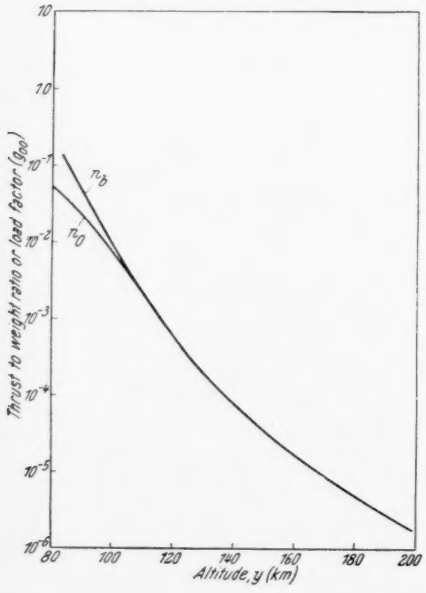

Fig. 12. Variation of initial and final thrust-to-weight ratio, or load factor, with altitude. n_0 = initial load factor; n_b = burn-out load factor; $F_{sp} = 250$ sec; $W_b = 10{,}000$ lb; $S = 500$ ft²; $C_D = 0{,}35$ (diffuse reflection); v = circular; period: 1 revolution

Fig. 14 has been computed under the simplifying assumption of a constant drag coefficient. At angle of attack the drag coefficient would become larger also, causing a further boost in thrust requirement.

It may be mentioned at this point that tentative calculations of subcircular thrust requirements for the case of specular reflection result in an even greater ratio of F/F_c. However, this is mainly due to the fact that at small inclinations (wedge half-angle) and specular reflection, the drag is nearly zero, hence that the thrust is also vanishingly small in the circular-velocity case.

Consequently, independent of the type of molecular reflection, a decrease of the operational velocity

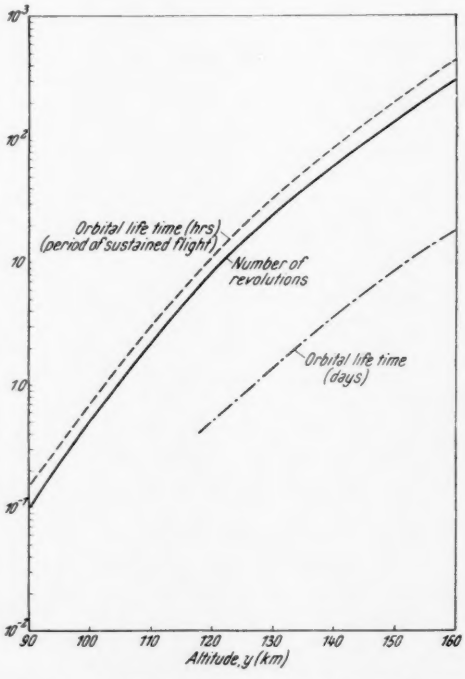

Fig. 13. Satelloid orbital data based on 1000 lb propellant consumption.

$W_b = 10{,}000$ lb; $W_0 = 11{,}000$ lb; $S = 500$ ft²; $C_D = 0.35$; $F_{sp} = 250$ sec

of the satelloid below circular velocity is accompanied by a considerable increase in thrust requirement and propellant consumption. This statement is valid only for the free molecule flow conditions under consideration here. The ratio F/F_c will doubtlessly improve as one goes to lower altitude, out of the free molecule flow region, where one can obtain a higher lift force. However, since the higher lift force would, to a large extent, be due to an increase in dynamic pressure, the drag would also go up so that, even at increased glide number, the decrease in F/F_c would essentially be due to a higher F_c. Furthermore, aerodynamic heating will in this case reduce the practical range of subcircular velocities to much lower values than considered in Fig. 14. The case of departure from free molecule flow conditions has not been considered in the present paper. However, it is felt that its study would be of interest. The theoretical analyses presented in section III,3 would apply.

An interesting corollary with respect to the results gained from Fig. 14 is that a circular-velocity satelloid must have a thrust reserve of 200 to 300 percent, in order to be able to return to correct flight conditions, should the velocity temporarily drop below circular. However, this is not a difficult proposition in view of the very small regular thrust.

For temperature calculations of the satelloid surface in free molecule flow, Fig. 15 shows the number of molecules striking the lifting (wind) side surface per square foot and second for different values of

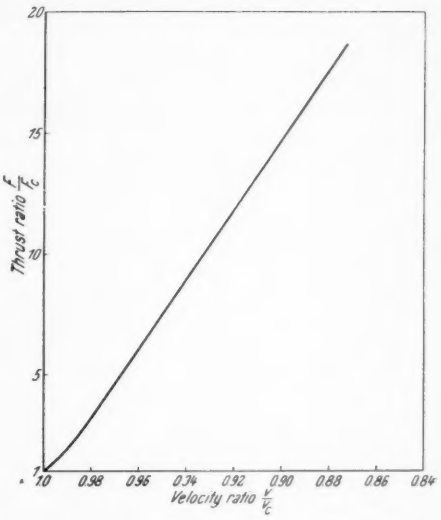

Fig. 14. Comparison of thrust requirement for circular-velocity satelloid and for the subcircular-velocity satelloid. Small deviation from circular velocity. Drag based on diffuse reflection, $C_D = 0.1$. Lift neglected. Vehicle weight $W = 10{,}000$ lb; lifting area $S = 500$ ft²; altitude $y = 90$ km $= 295{,}000$ ft; dynamic pressure $q_c = 2{,}68$ lb/ft²

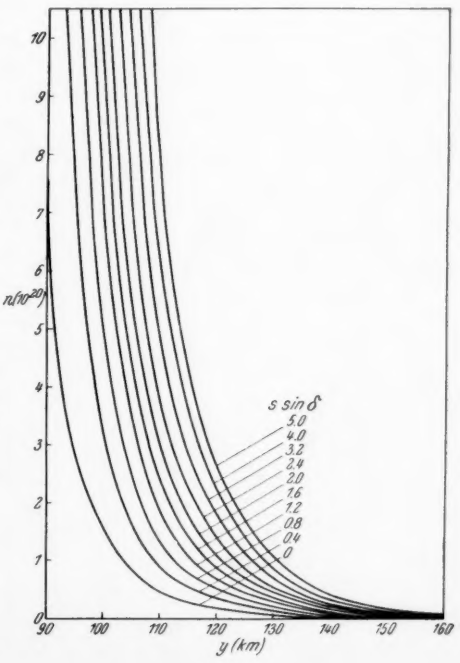

Fig. 15. Number of molecules striking the lifting surface per square foot/second. 90 to 110 km: N_2, O_2 atmosphere; 130 to 160 km: N_2, O atmosphere; 110 to 130 km: faired in

$s \sin \delta$, δ being the wedge half-angle β or the sum of wedge half-angle and angle of attack $\beta + \alpha$. The skin temperatures — assuming no heat conduction into the interior of the vehicle — are shown in Fig. 16, for the two cases of presence and absence of solar radiation. These two cases roughly correspond to flight on the daylight side and the night side, respectively, of the earth. The effect of solar radiation is small at 90 and 100 km altitude. Above 130 km the difference becomes appreciable. However, already above 110 km (360,000 ft), the temperatures cease to be critical or even severe from a technical point of view, if one takes into account that periodic change between sunlight and the earth's shadow and the damping effect of the vehicle's heat capacity actually would reduce the extremes shown in Fig. 16 considerably. Moreover, during the eventual aerodynamic descent, much higher temperatures will anyway be encountered which determine the layout of the heat protection system. Consequently, for the satelloid operation proper, if it takes place above 110 to 115 km, there will be a comfortable margin in heat protection, even if one considers extended orbital lifetimes.

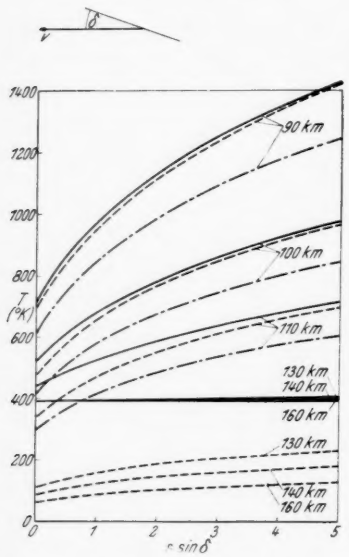

Fig. 16. Skin temperature of satelloid (wind-side surface). $s = v/c_m$; c_m = most probable molecular velocity of gas at rest; $c_m = \sqrt{2\,g\,(R/M)\,T}$. ——— $v = 26{,}000$ ft/sec, with solar radiation, — — — $v = 26{,}000$ ft/sec, without solar radiation, — · — · — $v = 20{,}000$ ft/sec, without solar radiation

VII. Summary and Conclusions

The theoretical analysis of a powered, orbiting vehicle, called satelloid, is presented. The analysis comprises the flight mechanics of the circular and subcircular-velocity satelloid in a circular orbit under continuous propulsion, the aerodynamics of the satelloid in free molecule flow, and the skin temperature of the satelloid. A discussion of the upper atmosphere data and selection of the data used in this paper is presented in an Appendix.

The results of the study indicate that a circular-velocity satelloid requires little propellant per revolution at altitudes roughly of 115 km or above ($\geqslant$ 380,000 ft). At drag coefficients, referred to the lifting area, between 0.35 and 0,7 and a specific thrust of 250 lb sec/lb, the propellant consumption at 120 km lies between 0.25 and 0.5 pounds per square foot lifting area per revolution. A satelloid of 10,000 lb burn-out weight and 500 ft^2 lifting area has a stay time of 0.5 days per 1,000 lb propellant expense (250 lb sec/lb specific thrust) at an altitude of 120 km, completing 8.5 revolutions with respect to inertial space during this period. At 147.5 km altitude the stay time is 1 week per 1,000 lb propellants, or 115 revolutions. A (non-powered) satellite would not last one revolution at this altitude.

An evaluation of aerodynamic heating shows that comparatively low skin temperatures can be expected if the satelloid stays above 110 km and does not have too steeply inclined surfaces ($\leqslant 15^0$) with respect to the free flow.

The continuous-propulsion, circular-orbit satelloid in free molecule flow should have circular velocity and should operate at an altitude of about 110 km or higher in the terrestrial atmosphere.

Appendix

Several years ago, GRIMMINGER [23] conducted a thorough theoretical analysis of the physical properties of the terrestrial atmosphere extending to an altitude of 5,500 miles (or about 8,900 km). Meanwhile, experimental data on pressure, density, and temperature have become available from high-altitude research, [24], [25].

In Figs. 17 and 18 are compared the atmospheric temperatures and the molecular weights on which the temperature data are based. Ref. [25] shows a great difference in temperature above 90 km, depending on whether constant molecular weight (no dissociation), or a somewhat arbitrary variation in molecular weight is assumed. Ref. [24] finds likewise a decrease in temperature by comparing an N_2, O atmosphere ($M = 24$) with an N_2, O_2 atmosphere ($M = 29$) above 110 km. Although [23] assumes a similar change in molecular weight (Fig. 18) as the two beforementioned references in two altitude regions (80—120 km) like [25], thereafter like [24] its temperatures do not agree, but rather are the same as those found in [25], assuming a molecular weight of $M = 28.966$, i.e. no dissociation. This discrepancy is due to a difference in pressure and density which is shown in Figs. 19 and 20. It can be seen that above 60 km the values of [23] are consistently higher.

Since there is little difference between the values given in [24] and [25], those of the Naval Research Laboratory [24] have been adopted in this paper, because this reference gives the temperature at altitude for a specific air composition, rather than for a somewhat arbitrary variation of

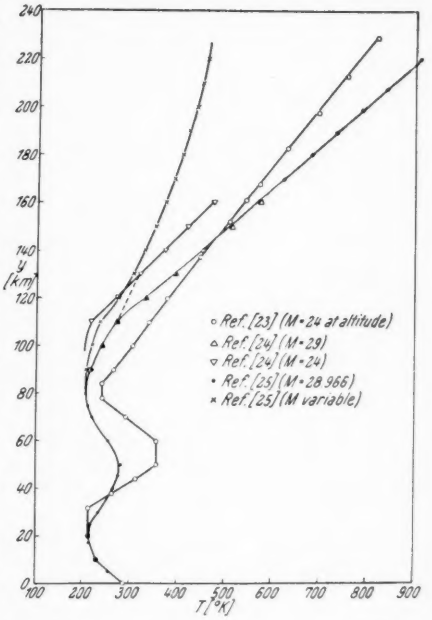

Fig. 17. Comparison of temperature variation with altitude

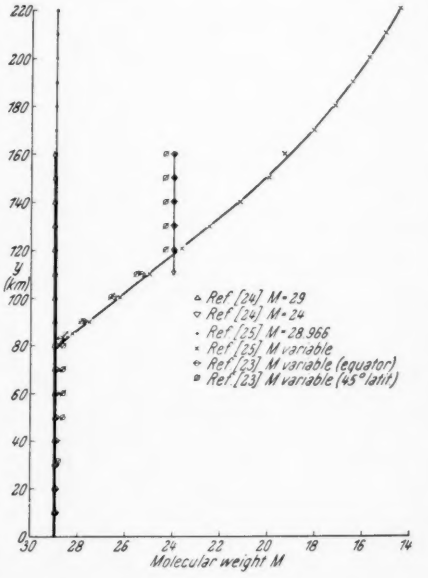

Fig. 18. Comparison of assumptions as to variation of the molecular weight with altitude

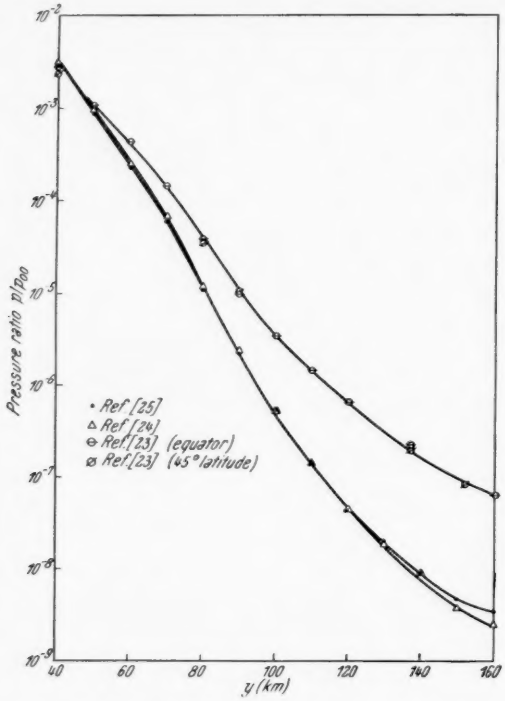

Fig. 19. Comparison of atmospheric pressures

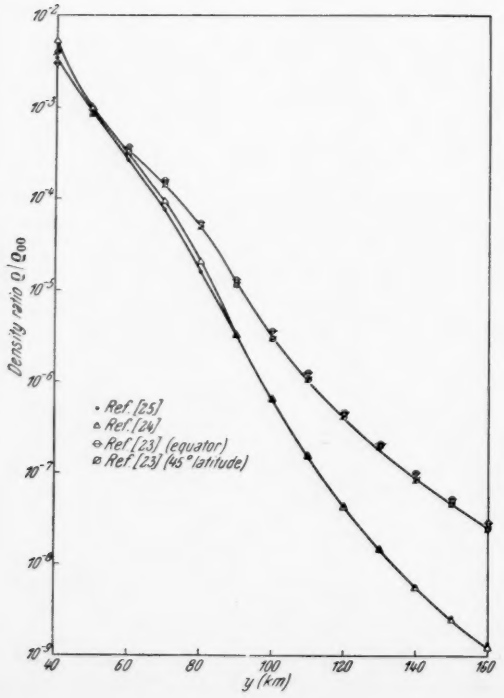

Fig. 20. Comparison of atmospheric densities

the molecular weight with altitude. Knowledge of a specific air composition must be assumed for the aerothermodynamic computations, as was outlined in section 5. A short transition line (dashed line in Fig. 17) has been used for connecting the temperature data for $M = 29$ with those for $M = 24$. This line deviates from the one given in Fig. 7 of Ref. [24]. The reason for this was the desire to keep, for the purpose of this paper, the interpolation range small, thereby avoiding the necessity of determining the air composition from molecular weights between 29 and 24. This is not difficult to do, if the computation is based on the assumption of oxygen dissociation only, but it represents an additional complexity which does not contribute particularly to the purpose of this paper. In view of the limited accuracy of these data, and because of the indiscriminate global use here, in spite of the fact that they have been measured only at the latitude of White Sands in New Mexico, U.S.A., this arbitrary simplification was regarded as permissible and within the general limits of accuracy of numerical evaluations.

Fig. 21 compares the molecular mean free path as given in [24] and [25]. The values are in fairly good agreement, although in the case of [25]

Table I

Interval Δy km	Interval Δy 10^3 ft	$\varrho(r)/\varrho_r$	β 1/km	β 1/ft
70— 84	230—276	$10^{-4}-10^{-5}$	1/5.65	1/18,500
84— 97	276—318	$10^{-5}-10^{-6}$	1/5.65	1/18,500
97—113	318—370	$10^{-6}-10^{-7}$	1/6.95	1/21,500
113—134	370—430	$10^{-7}-10^{-8}$	1/9.1	1/29,800
134—169	430—539	$10^{-8}-10^{-9}$	1/8.7	1/28,500

they are based on varying molecular weight, rather than on molecular nitrogen and monatomic oxygen like in [24].

In analyzing the density data of [24], adopted for the purposes of this paper, one finds for the relation, used in sub-section III,3 b

$$\varrho(r) = \varrho_r e^{-\beta \Delta y} \qquad (33)$$

the values for β (table I), in conjunction with the following altitude intervals.

Since, as pointed out in subsection III,3 b, the altitude variations are small when taking the change in satelloid weight during the period of subcircular flight into account, they are in most cases well within one of the altitude intervals given in the above table. The value $\varrho(r)$ is then found easily, by taking the density at the beginning of the respective interval as reference density, ϱ_r, and using the corresponding value of β.

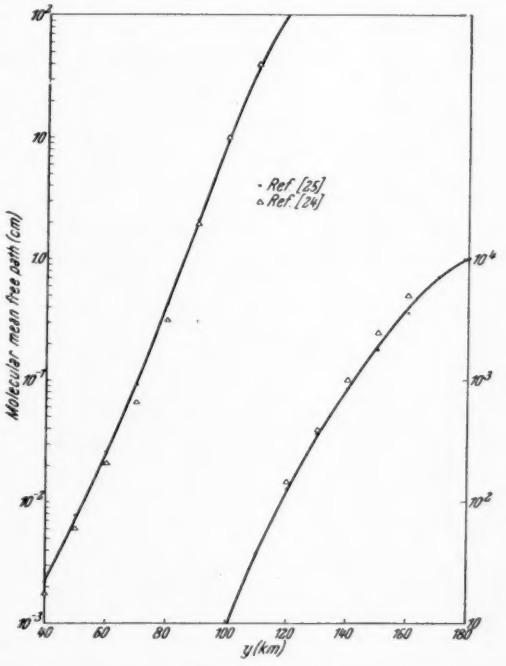

Fig. 21. Comparison of molecular mean free paths

References

1. K. A. Ehricke, Analysis of Orbital Systems, in: Bericht über den V. Internationalen Astronautischen Kongreß (Report on the V. International Astronautical Congress). Wien-Innsbruck: Springer, 1954, F. Hecht, ed., and an excellent detailed analysis by A. V. Cleaver, A Programme for Achieving Interplanetary Flight, J. Brit Interplan. Soc. **13** (1954).
2. E. Sänger, Raketenflugtechnik. Munich and Berlin: R. Oldenbourg, 1933.
3. E. Sänger and Irene Bredt, A Rocket Drive for Long Range Bombers. Dtsch. Luftfahrt-Forsch., UM 3538, August 1944; Transl. by M. Hammermesh, Radio Research Laboratory; Reproduced by R. Cornag, 990 Cheltenham Road, Santa Barbara, California.
4. K. A. Ehricke, On the Descent of Winged Orbital Vehicles. Astronaut. Acta **1**, 137 (1955).

5. A. F. ZAHM, Superaerodynamics. J. Franklin Inst. **217**, 153 (1934).
6. E. SÄNGER, The Gas Kinetics of Very High Flight Speeds. ZWB Forschungsbericht Nr. 972, May 1938, and N.A.C.A. Techn. Mem. 1270, May, 1950.
7. H.-S. TSIEN, Superaerodynamics, Mechanics of Rarified Gases. J. Aeronaut. Sci. **13**, 653 (1946).
8. M. HEINEMAN, Theory of Drag in Highly Rarified Gases. Commun. Pure Appl. Math. **1**, 259 (1948).
9. R. M. SNOW, Aerodynamics of Ultra-High Altitude Missiles. Applied Physics Laboratory, The Johns Hopkins University, Silver Springs, Md., Rep. CM—498, Sept. 20, 1948.
10. H. ASHLEY, Applications of the Theory of Free Molecule Flow to Aeronautics. J. Aeronaut. Sci. **16**, 95 (1949).
11. J. R. STALDER, G. GOODWIN, and M. O. CREAGER, A Comparison of Theory and Experiment for High-Speed Free Molecule Flow. N.A.C.A. Techn. Note 2244, 1950.
12. J. R. STALDER and V. J. ZURICH, Theoretical Aerodynamic Characteristics of Bodies in a Free-Molecule-Flow Field. N.A.C.A. Techn. Note 2423, July 1951.
13. L. B. LOEB, Kinetic Theory of Gases, 2nd ed. New York: McGraw-Hill Book Co., Inc., 1934.
14. B. G. DICKENS, The Effect of Accommodation on Heat Conduction Through Gases. Proc. Roy. Soc. London, Ser. A, **143** (1934).
15. J. K. ROBERTS, The Exchange of Energy Between Gas Atoms and Solid Surfaces. Proc. Roy. Soc. London, Ser. A, **129** (1930).
16. J. K. ROBERTS, The Exchange of Energy Between Gas Atoms and Solid Surfaces. II — The Temperature Variation of the Accommodation Coefficient of Helium. Proc. Roy. Soc. London, Ser. A, **135** (1932).
17. W. H. KEESOM and G. SCHMIDT, Researches on Heat Conduction of Rarified Gases. I — The Thermal Accommodation Coefficient of Helium, Neon, Hydrogen and Nitrogen on Glass at 0° C. Physica **3** (1936).
18. W. H. KEESOM and G. SCHMIDT, Researches on Heat Conduction by Rarified Gases. III — The Thermal Accommodation Coefficients of Helium, Neon, and Hydrogen at 12—20° K. Physica **4** (1937).
19. M. L. WIEDMANN and P. R. TRUMPLER, Thermal Accommodation Coefficients. Trans. Amer. Soc. Mech. Engrs. **68**, 57 (1946).
20. I. AMDUR, Pressure Dependence of Accommodation Coefficients. J. Chem. Physics **14**, 339 (1946).
21. J. R. STALDER and D. JUKOFF, Heat Transfer to Bodies Traveling at High Speed in the Upper Atmosphere. N.A.C.A. Techn. Note No. 1682, August 1948.
22. E. JAHNKE and F. EMDE, Tables of Functions, 4th ed. New York: Dover Publications, 1945.
23. G. GRIMMINGER, Analysis of Temperature, Pressure and Density of the Atmosphere Extending to Extreme Altitudes. The Rand Corporation, Santa Monica, California, Nov. 1948.
24. R. J. HAVENS, R. T. KOLL, and H. E. LAGOW, The Pressure, Density and Temperature of the Earth's Atmosphere to 160 Kilometers. J. Geophysic. Res. **57**, 59 (1952).
25. The Rocket Panel, Harvard College Observatory, Cambridge, Mass., Pressures, Densities and Temperatures in the Upper Atmosphere. Physic. Rev. **88**, 1027 (1952).

The Visibility of an Earth Satellite[1]

By

R. Tousey[2]

(With 4 Figures)

Abstract. The conditions for naked eye and telescopic visual observation of a white 21-inch diameter earth satellite are calculated using known values of the sky brightness, solar illumination, and visual thresholds of the eye. It is shown that the optimum position in the sky is at about zenith angle 70° in the azimuth opposite the sun. If between zenith angle 0° and 35° and at 200 miles altitude, this satellite will first be visible through 7 × 50 binoculars when the sun is 2° below the horizon, and will be visible to the naked eye for solar depression angles greater than 9°, so long as it is illuminated by sunlight. To see the satellite easily, and to detect it with high probability, 7 × 50 binoculars should be used at all times and observations not attempted unless the sun is 5 or more degrees below the horizon.

Zusammenfassung. Die Bedingungen, unter denen ein weißer Erdsatellit von 21 Zoll (53 cm) Durchmesser mit dem bloßen Auge und dem Teleskop visuell beobachtet werden kann, werden berechnet, wobei bekannte Werte für die Himmelshelligkeit, die Sonnenbeleuchtungsintensität und die Sehschwellen des Auges benützt werden. Es wird gezeigt, daß dafür die beste Stellung am Himmel ungefähr bei einem Zenitwinkel von 70° in dem der Sonne entgegengesetzten Azimut liegt. Wenn sich der Satellit in einem Zenitwinkel zwischen 0° und 35° in einer Höhe von 200 Meilen (320 km) befindet, kann er erst mit dem 7 × 50-Binokular wahrgenommen werden, wenn die Sonne 2° unter dem Horizont steht. Für das bloße Auge wird er bei einem Sonnendepressionswinkel über 9° sichtbar, solange er vom Sonnenlicht beleuchtet wird. Soll der Satellit mit großer Wahrscheinlichkeit entdeckt und leicht beobachtet werden, so muß jederzeit ein 7 × 50-Binokular benützt und die Beobachtung nicht früher versucht werden, als bis die Sonne 5° oder tiefer unter dem Horizont steht.

Résumé. A partir de valeurs connues pour la brilliance du ciel, l'illumination solaire et le seuil d'acuitè visuelle, les conditions requises pour une observation directe ou par télescope d'un satellite de 21 pouces de diamètre et de couleur blanche peuvent être calculées. La meilleure position dans le ciel est à 70° du zenith dans un plan azimutal opposé au soleil. S'il se trouve entre 0° et 35° du zenith à 200 miles d'altitude un tel satellite devient observable avec des jumelles 7 × 50 quand le soleil est 2° en dessous de l'horizon. Quand le soleil est plus de 9° sous l'horizon et tant qu'il l'éclaire, le satellite sera visible à l'oeuil nu. Pour être certain de le détecter et de l'observer des jumelles de 7 × 50 devraient être utilisées en toutes circonstances et les observations faites avec le soleil au moins 5° sous l'horizon.

---

[1] This paper was presented at the Sixth I.A.F. Congress at Copenhagen, August 4, 1955.

[2] U.S. Naval Research Laboratory, Washington 25, D.C., USA.

Introduction

The conditions under which an earth satellite can be seen are calculated. The satellite is assumed to be a sphere of 21 in. diameter, travelling in an orbit in the plane of the equator, and at altitudes varying from 200 to 800 miles. Illumination is provided by the sun. The calculation follows the lines of the papers "The Visibility of Stars in the Daylight Sky" by TOUSEY and HULBURT [1], and "The Visibility of Stars and Planets during Twilight" by TOUSEY and KOOMEN [2].

The calculation comprises the following steps:

1. Computation of the visual stellar magnitude of the satellite as a function of: (a) distance to the satellite, (b) elevation angle of the satellite, (c) phase of the satellite, and (d) altitude of the sun.

2. Comparison of the magnitude of the satellite with the threshold magnitude visible with the naked eye against the sky brightness for the case in question.

3. Consideration of the telescopic magnification necessary to see the satellite, and the angular field over which the satellite will be visible for a single fixation of the eye.

The steps in the calculation and the results are presented in the form of tables, applying to the most important cases.

It is concluded that if one knows exactly where and when to look, the satellite, when nearly directly overhead and at 200 miles altitude, will first be visible through 7×50 binoculars when the sun is 2^0 below the horizon, and will be visible to the naked eye for solar depression angles greater than 9^0 so long as it is illuminated by sunlight. To see the satellite easily, however, and to be sure of observing it when its position is not known exactly, it is suggested that 7×50 binoculars be used at all times, and that observation of the satellite not be attempted until the sun is 5 degrees below the horizon.

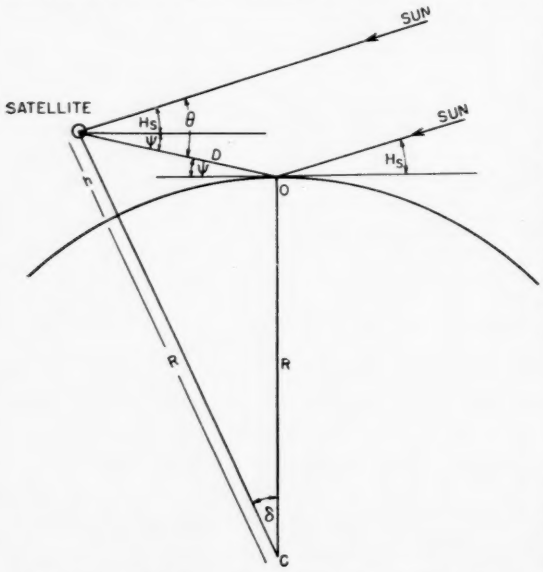

Fig. 1. The geometry of observing the satellite. The observer is at O

Stellar Magnitude of the Satellite

The geometry involved in the illumination of the satellite is shown in Fig. 1. The observer is located at O. The satellite, at an altitude h above the earth, is distant D from O, and is directly above a point separated from O by angle δ, measured at C, the center of the earth. The altitude angle of the satellite is ψ, and of the sun, H_s. The phase angle, θ, is given by $\psi + H_s$. For a given value of h, and of the earth's radius R, D and ψ are functions of the single parameter δ, and can be calculated trigonometrically.

The satellite is assumed to have a perfectly diffusing surface of 100 percent reflectance. This limit can only be approximated, but the error from this source

will be small compared to other uncertain factors. Though 100 percent reflectance cannot be attained with ordinary paint, something approaching and perhaps exceeding it can be realized with fluorescent paint, which converts some of the ultraviolet radiation into visible light.

A spherical satellite with a perfectly diffusing surface obeying LAMBERT's law, when illuminated in the "full" phase, will reflect in the direction of the observer 2/3 as much light as would a flat satellite of the same angular subtense. Taking 12,700 f. c. as the illumination due to the sun outside the atmosphere as given by JOHNSON [3], the luminous intensity of the satellite in the direction of the observer is

$$I = \frac{12{,}700}{\pi} \cdot \frac{2}{3} \cdot \pi R^2, \tag{1}$$

where R is its radius and its reflectance is 100 percent.

The illumination at the observer on the earth will be given by

$$E = 12{,}700 \cdot \frac{2}{3} \cdot \frac{R^2}{D^2} \cdot e^{-0.117 \csc \psi}, \tag{2}$$

where D is the distance to the satellite and ψ is its elevation angle. The exponential term allows for atmospheric attenuation; the value of the attenuation coefficient 0.117 applies to a very clear sky, an elevation of 10,000 feet, and about 3 mm of ozone.

In general the satellite will not be observed in full phase, but at a phase angle θ, defined as the angle between the direction to the sun and the line of sight. The factor describing the dependence of luminous intensity on phase angle for a perfectly diffusing sphere was given by RUSSELL [4] as

$$\frac{1}{\pi} [\sin \theta + (\pi - \theta) \cos \theta].$$

This factor is unity for $\theta = 0^0$, $1/\pi$ for $\theta = 90^0$ and 0 for $\theta = 180^0$. Hence the complete expression for E is

$$E = 12{,}700 \cdot \frac{2}{3} \cdot \frac{[\sin \theta + (\pi - \theta) \cos \theta]}{\pi} \cdot \frac{R^2}{D^2} \cdot e^{-0.117 \csc \psi}.$$

For a satellite of diameter 21 in. this becomes

$$E = 2.335 \cdot 10^{-4} \cdot \frac{[\sin \theta + (\pi - \theta) \cos \theta]}{\pi} \cdot e^{-0.117 \csc \psi} \tag{3}$$

where D is in statute miles.

It is convenient to introduce the quantity stellar magnitude in working with a satellite, since its appearance will be like a star and it will be compared with them. It is not necessary to do this, since all the photometric data for both the satellite and the visual sensitivities of the eye are given in ordinary photometric units. However, it has the advantage of presenting the results in more familiar terms.

The stellar magnitude, m, of the satellite can easily be derived from (3) by making use of the definition of m,

$$m = -2.5 \log E + m_0, \tag{4}$$

where m_0 is a constant. The constant m_0 can be determined by substitution of the data for the sun, $m = -26.72$, $E = 12{,}700$ f. c., and its value is -16.45.

Substituting into (4) the expression (3) for E we have for the magnitude, m, of the satellite,

$$m = 5 \log D + F(\theta) + 0.1268 \csc \psi - 7.37 \tag{5}$$

where $F(\theta) = -2.5 \log [\sin \theta + (\pi - \theta) \cos \theta]/\pi$.

The Limiting Magnitude Visible to the Eye

The limit of stellar magnitude visible to the naked eye depends on the brightness of the sky surrounding the star. The problem has been investigated in the laboratory by KNOLL, TOUSEY and HULBURT [5], and by BLACKWELL [6], who set up point sources of light in fields of brightness ranging from the daylight sky to zero. The illumination at the eye produced by the point source when just visible was determined as a function of the luminance of the surround. TOUSEY and HULBURT [1] have shown that the data from these two investigations are in agreement. The threshold illumination values, derived from BLACKWELL, were converted to threshold visual magnitude, m_{thr}, by eq. (4). The resulting data are given in Table I.

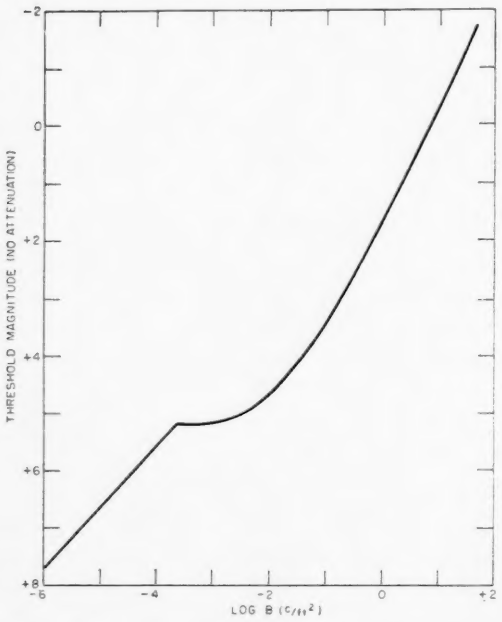

Fig. 2. The limiting magnitude of stars visible to the naked eye against a sky of luminance B

Table I

log B (c/ft²)	m_{thr}
2.5	−3.43
1.5	−1.27
0.5	+0.75
−0.5	2.62
−1.5	4.10
−2.5	5.05
−3.5	5.17
−4.5	6.07
−5.5	7.12

These values differ from those used by TOUSEY and KOOMEN [2] in that the value of the solar illumination used in determining the constant m_0 in eq. (4) was 12,700 f. c. rather than 10,000 f. c.

The threshold data apply to the case where the observer knows exactly where the point source of light is located. In BLACKWELL's [6] work, the data were presented for the case where the observer had a 50 percent probability of seeing the object. In preparing Table I the thresholds were raised by a factor of 2 so as to apply to about 98 percent probability of seeing, or almost continuous vision of the point source.

The data apply only to a point source. BLACKWELL found this to be one whose angular subtense at the eye was less than 0.6 minute. The satellite, even when viewed with a 100 power telescope, fulfills this condition, since its subtense at 200 miles is 0.006 minute. Although the data were obtained for a point source and sky that were white, they apply sufficiently accurately to a blue sky.

The threshold of visual magnitude data are plotted against the logarithm of the luminance of the field in Fig. 2. The sharp bend in the curve occurs at the luminance level where the eye shifts from cone to rod vision. At high brightnesses, cone vision is employed, the point source is seen best if the observer looks directly at it, and little or no dark adaptations is required. At low

brightnesses rod vision is employed, prolonged dark adaptation is required for best vision, and the point source must be seen by peripheral vision; in fact, if the observer looks directly at the source it will disappear.

The visual threshold data upon which Fig. 2 is based apply to the case where the observer knows exactly where the object is located. In actual search for a satellite this would not be the case. The threshold depends strongly on the angle between the direction of vision and the satellite. The nature of the dependence varies with the brightness of the sky. The few data available on this subject are shown in Fig. 3. Curve A is from TOUSEY and HULBURT [1] and was obtained with a background of 360 c/ft^2 brightness. The other three curves are from BLACKWELL [7]; the three brightnesses correspond to a dim daylight sky, the sky at civil twilight, $H_s = -6^0$, and the sky at nautical twilight, $H_s = -12^0$, which is just at the limit of cone vision. BLACKWELL's data are preferred to Curve A.

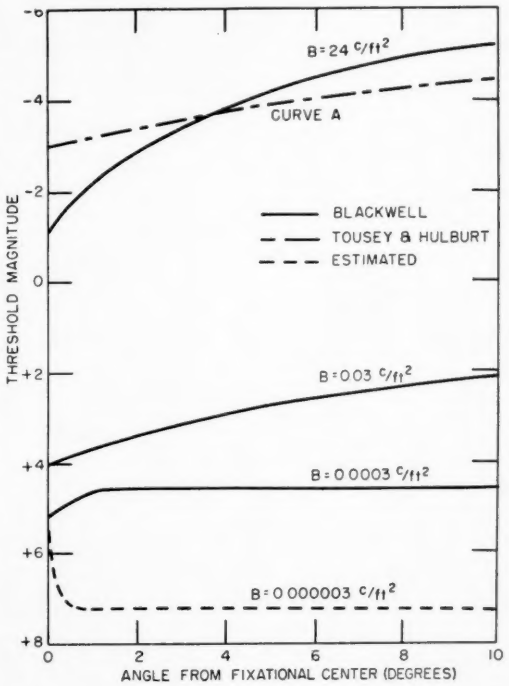

Fig. 3. The limiting magnitude of stars visible to the naked eye as a function of the angle between the star and the point in the sky at which the observer is looking, for several values of the luminance of the sky

It can be seen that the threshold rises extremely rapidly with angle in the retinal periphery when the background brightness is high. An angle of 1^0, according to BLACKWELL, produces nearly a magnitude change in threshold, while 5^0 causes more than 3 magnitudes change. At lower brightnesses, however, the change with angle is less rapid. At $B = 0.03$ c/ft^2, 5^0 is accompanied by a magnitude change of 1.3. At $B = 0.0003$ c/ft^2, the entire change takes place within the central 2^0, and is 0.75 magnitude. When the background brightness is reduced a little further and rod vision is required, a curve of the nature of the dotted curve holds, and the threshold is lowest if averted vision is used.

Telescopes

Stars which are invisible to the naked eye can, of course, be seen through telescopes. This is true in the daytime as well as at night. The action of a telescope at night is simply to collect more light from the star and image it on the retina of the eye; if the magnification is sufficient to cause all the light collected by the objective to pass through the eye pupil, the gain will be proportional to the square of the diameter of the objective.

The theory for daytime is more complicated and was given by TOUSEY and HULBURT [1]. They distinguished two cases. In the first, the eye pupil is filled by the exit pupil of the telescope. In this case the sky brightness is not changed, but the light flux from the star is increased by M^2, where M is the magnifying power of the telescope. In the second case the eye pupil is not filled. Here the light flux from the star is increased by the ratio of the area of the objective lens to that of the eye pupil; the sky is reduced in brightness by the ratio of the area of the exit pupil to the eye pupil. The reduction of background brightness changes the threshold in accordance with Fig. 2. The overall result in this second case is that the gain is not as great as M^2, because the threshold does not change as rapidly as the first power of the background brightness. An approximate equation was given by TOUSEY and HULBURT, but an exact solution would have to be made for each particular case.

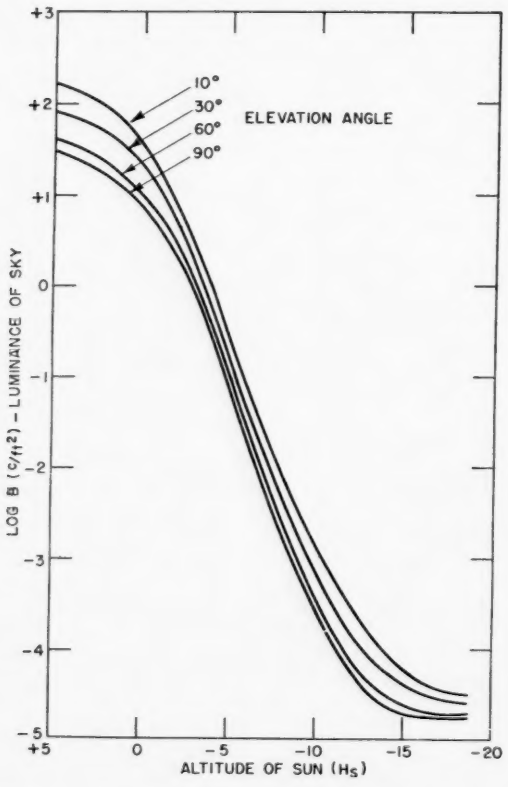

Fig. 4. The luminance of the twilight sky as a function of the altitude of the sun, for points in the sky in the azimuth opposite the sun

To simplify matters, the telescopes will be assumed to have sufficiently large objectives so that the eye pupil is filled and the gain will be taken as proportional to M^2. In terms of magnitude, the gain is given by

$$\Delta m = 5 \log M.$$

The small light loss due to the optics of the telescope can be neglected.

When using a telescope the curves of Fig. 3 apply to the apparent field as seen in the eyepiece. To convert them to the true field, i.e., the field angle in the sky between the star and the direction of vision, it is necessary to divide by M. Thus the area of true field in the sky over which a star can be seen at a single fixation of the eye is smaller by M^2 than the corresponding area of the apparent field.

Sky Brightness

Luminance values for the sky were taken from the work of KOOMEN, LOCK, PACKER, SCOLNIK, TOUSEY and HULBURT [8]. In Fig. 4, the luminance of the sky is plotted against the elevation angle of the sun. Curves are presented for the zenith, and for points in the sky at an azimuth of 180^0 to the sun and at elevation angles of 10, 30, and 60^0. It can be seen that the sky overhead changes

brightness very rapidly during dawn, and that the increase of brightness toward the horizon is only of the order of 30 percent from zenith to a point 30^0 away.

The brightness data of Fig. 4 are for an altitude of 10,000 ft and a very clear sky. At sea level the brightnesses are higher by a factor of 1.5, owing to the greater amount of air overhead.

The Visibility of the Satellite

All the data are now at hand from which to calculate the visibility of the satellite. The process was simply to determine the sky brightness from Fig. 4, the threshold magnitude for this brightness from Fig. 2, and to compare the threshold magnitude with the computed magnitude of the satellite. The calculation was made for the following cases:

I. Satellite at 200 miles altitude, sun at 0^0 elevation; satellite viewed at elevation angles from zenith to horizon, at an azimuth of 180^0 to the sun.

II. Satellite at 200 miles altitude, seen at zenith, for solar elevation angles from $+ 5^0$ to $- 15^0$.

III. Satellite at 200 miles altitude, seen at 65^0 elevation, for solar elevation angles from $+ 5^0$ to $- 15^0$.

IV. Satellite at altitudes 200, 400 and 800 miles, viewed at zenith, for solar elevation angles from $+ 5^0$ to $- 33^0$.

In Tables II – V are presented the results, together with certain steps in the calculation. The principal quantities to be examined are the magnitude of the satellite, m, and the difference Δm between m and the threshold magnitude, m_{th}, just visible to the naked eye. If positive, Δm tells how much too faint the satellite is to be seen with the naked eye; if negative, it is a measure of the ease with which the satellite can be seen with the naked eye.

The quantity M is the telescopic magnification necessary to make the satellite just visible to the naked eye. This, however, is not enough magnification to be really useful. M' is the magnification necessary to make the satellite fairly easy to see. It is taken to be 2.4 magnitudes brighter than threshold, or to produce in the retinal image of the satellite 10 times more flux than the threshold value. This includes, then, the necessary "safety factor".

Finally there is given angle Φ, the diameter of the true field over which the satellite can be seen with magnification M'. The angle in the apparent field is $\Phi \cdot M'$. The values of Φ are very rough; they were determined by reading $\Phi \cdot M'$ from BLACKWELL's curves of Fig. 3, interpolating and extrapolating.

From $H_s = 5^0$ through $- 3^0$ the entire field of the telescope will probably be larger than the field over which the satellite can be seen at a given fixation of the eye. This can be seen from the tables for, within this range of H_s, $\Phi \cdot M'$ is less than 60^0, which is taken to be the apparent field of a good telescope. For H_s from $- 6^0$ to $- 15^0$, however, the eye can see the satellite at a single fixation if it appears anywhere within the field of the telescope. In this case the values of Φ are computed on the assumption that the true field of the telescope is $60^0/M'$, which is just about the maximum attained in practice.

Symbols in Tables II – IV

δ = angle in degrees between the observer and the point on the earth's surface directly below the satellite.
ψ = elevation angle of the satellite.
$F(\theta)$ = phase function of the satellite.
θ = phase angle of the satellite.
D = distance in miles from the observer to the satellite.

m = stellar magnitude of the satellite as seen by the observer.
m_{thr} = threshold magnitude visible to the naked eye for a sky brightness B.
B = sky luminance near the satellite, c/ft^2.
m = number of magnitudes the satellite is below the naked eye threshold.
M = telescopic magnification to bring the satellite up to threshold.
M' = telescopic magnification to make the satellite easily visible.
Φ = angular diameter in the sky of the region over which the satellite can be seen at magnification M, for a single fixation of the eye.

Table II. *Visibility of a 21-in. spherical satellite, of 100 percent diffuse reflectance, at 200 miles altitude viewed at sunrise or sunset* (h = 200 mi, $H_s = 0^0$)

δ	θ	$F(\theta)$	D	m	log B	m_{thr}	$m = m - m_{thr}$	M	M'
0	90	1.24	200	5.51	0.90	0.00	5.51	12.5	40
1	70.0	0.74	213	5.14	0.98	−0.15	5.29	11.5	36
2	53.7	0.43	245	5.17	1.10	−0.40	5.57	13	41
3	41.8	0.26	291	5.40	1.20	−0.60	6.00	16	50
4	33.2	0.17	347	5.73	1.30	−0.80	6.53	20	63
6	22.2	0.08	469	6.41	1.40	−1.05	7.46	31	99
8	15.4	0.04	600	7.04	1.50	−1.25	8.29	45	>100
10	10.7	0.02	734	7.66	1.55	−1.35	9.01	63	>100
12	7.2	0.01	871	8.35	1.60	−1.45	9.80	91	>100
14	4.35	0.00	1008	9.32	1.60	−1.45	10.77	>100	>100
16	1.95	0.00	1146	11.66	1.60	−1.45	13.11	>100	>100

Table III. *Visibility of a 21-in. spherical satellite, of 100 percent diffuse reflectance, at 200 miles altitude, viewed at zenith* (h = 200 mi, $\psi = 90^0$)

H_s	θ	$F(\theta)$	m	log B	m_{thr}	$m = m - m_{thr}$	M	M'	Φ
5	95	1.40	5.66	1.49	−1.25	6.91	24	76	5′
3	93	1.33	5.59	1.32	−0.90	6.49	20	63	6′
0	90	1.24	5.50	0.90	−0.05	5.55	13	41	15′
−3	87	1.16	5.42	0.00	1.75	3.67	5.7	17	1.2^0
−6	84	1.07	5.33	−1.66	4.3	1.05	1.6	5.1	12^0
−9	81	0.99	5.25	−3.13	5.2	0.05	1	3.2	19^0
−12	78	0.92	5.18	−4.12	5.7	−0.50	<1	2.5	24^0
−15	75	0.85	5.11	−4.70	6.3	−1.17	<1	1.9	31^0
−18	72	0.79	5.05	−4.82	6.4	−1.35	sunset at $H_s = -17^0\,51'$		

Table IV. *Visibility of a 21-in. spherical satellite of 100 percent diffuse reflectance, at 200 miles altitude, viewed at 65^0 elevation angle* (h = 200 mi, $\psi = 65^0$)

H_s	θ	$F(\theta)$	m	log B	m_{thr}	$\Delta m = m - m_{thr}$	M	M'	Φ
5	70	0.735	5.23	1.55	−1.35	6.58	21	66	5′
3	68	0.693	5.18	1.45	−1.20	6.38	19	60	6′
0	65	0.632	5.12	1.00	−0.20	5.32	12	37	15′
− 3	62	0.575	5.07	0.07	1.60	3.47	4.9	15	1.3^0
− 6	59	0.521	5.01	−1.55	4.15	0.86	1.5	4.7	13^0
− 9	56	0.469	4.96	−3.00	5.15	−0.19	<1	2.9	21^0
−12	53	0.421	4.91	−4.10	5.65	−0.74	<1	2.2	27^0
−15	50	0.375	4.88	−4.60	6.20	−1.32	<1	1.7	35^0

Table V. *Visibility of 21-in. spherical satellite of 100 percent diffuse reflectance, viewed at zenith for 200, 400, and 800 miles altitude*

H_s \ h	m			M'			200	400	800
	200	400	800	200	400	800			
5	6.91	8.41	9.92	76	>100	>100	5′		
3	6.49	7.99	9.50	63	>100	>100	6′		
0	5.55	7.05	8.56	41	81	>100	15′	7′	
− 3	3.67	5.17	6.68	17	34	69	1.2°	36′	18′
− 6	1.05	2.55	4.06	5.1	10	20	12°	6°	3°
− 9	0.05	1.55	3.06	3.2	6.4	13	19°	10°	5°
−12	−0.50	1.00	2.51	2.5	5	10	24°	12°	6°
−15	−1.17	0.33	1.84	1.9	3.7	7.4	32°	16°	8°
−18	−1.35	0.15	1.65	1.7	3.4	6.7	35°	18°	9°
−24	—	0.15	1.65	—	3.4	6.7	—	18°	9°
−33	—	—	1.65	—	—	6.7	—	—	9°

Discussion and Conclusions

1. Optimum Area in the Sky

The region in the sky over which the satellite can be seen most easily is from zenith to an elevation angle of about 55° in the azimuth opposite the sun. This can be seen from Δm in Table II. The best position is near 70° elevation, where Δm is about 0.2 less than at zenith. The presence of this minimum in Δm is due to the increasingly favorable phase of the satellite when viewed farther from the sun, together with the fact that the distance to the satellite and the sky brightness change slowly near the zenith.

Δm increases rapidly as the satellite becomes low in the sky, due to increasing distance and attenuation, and on the side of the zenith toward the sun the phase factor also becomes unfavorable. Therefore, observation of the satellite at low elevation angles or on the side of the zenith toward the sun will be more difficult.

For deviations from zenith in the azimuth at right angles to the sun the satellite will become less easy to see, but a considerable deviation is permissible. In this case, the distance and attenuation both increase but the phase factor and the sky brightness stay approximately constant. At 70° elevation angle in the azimuth perpendicular to the sun Δm will have increased relative to the zenith by about 0.1, and at 55° elevation by approximately 0.4. Thus, considerable leeway in the direction of observation is permissible.

2. Permissible Altitude of the Sun

Table III shows that good viewing conditions are at hand, for a zenith satellite, when the sun is from about 5° to 17° below the horizon. Obviously, the optimum condition for seeing the satellite will be when the sun is so low as just to illuminate the satellite with its full intensity, for the sky will then be the darkest possible. For a satellite at 200 miles altitude and viewed at zenith, this occurs when the sun is about 17° below the horizon. Actually, sunset occurs at 200 miles for $H_s = 17° 51'$, but the solar illumination on the satellite will be greatly reduced under these conditions by the long light path through the lower atmosphere. For $H_s \cong 17°$, however, the illumination will still be close to 12,700 f.c.

Although it is possible to see the satellite before sunset a high power telescope is required and the real field over which it can be seen at a single fixation is extremely small; hence the probability of a single observer seeing it is practically zero. For example, at $H_s = 0^0$, this real field is 15′; since the satellite travels at an angular speed of 4^0/minute measured at the center of the earth, assuming a circular orbit and 90 minute period, if at 200 miles it will have an angular speed of $4/3\ ^0$/sec measured at the observer. Therefore, it will cross this field within which the eye will detect it in 3/16 second. The entire real field of the telescope would, of course, be somewhat larger than 15′, perhaps of the order of 1^0 for 41 power magnification, but this would be of no help since the satellite would cross the entire field before the eye had time to search the field at all.

Table IV applies when the satellite is viewed at an elevation angle of 65^0, which is near the optimum angle indicated by Table II. A comparison of Tables III and IV shows that the gain at 65^0, as against the zenith, remains approximately the same for all values of H_s, and is only about 0.2 magnitude, as was seen from Table II to be the case for $H_s = 0^0$. Therefore, the zenith case is sufficiently close and is the only one that need be considered in detail.

3. The Practical Conditions for Observing the Satellite

For a satellite at 200 miles, it appears from Table III that satisfactory conditions of observation can be had by using a low power telescope or binocular. The standard 7×50 binocular with a field of view of 7^0, is probably the best compromise if a single stock instrument is to be used. The satellite should be easily visible with the binocular when the sun is more than 5^0 below the horizon. A number of observers each with a binocular would be required to cover the region of the sky through which the object might pass. Each binocular should be fixed in position, and oriented carefully so as not to overlap the field of the adjacent binoculars more than necessary to insure complete coverage of the sky. Each binocular should be equipped with right angle prisms over the objectives so as to permit its use in a normal horizontal position.

Since the satellite can be seen with a 7×50 binocular for H_s from -5^0 to -17^0 and since the sun sets, or rises, on the equator, at a rate of approximately $1/4^0$ per minute, the available time during which a satellite can cross the sky and be easily observed at 200 miles is about three-quarters of an hour. Obviously, the probability of detecting the satellite increases the closer the end of the sunset period, or start of the sunrise period is approached.

Because the satellite is about fifth magnitude under these viewing conditions, there will probably be several stars in the field of view of about the same brightness, and possibly some that are brighter. The presence of stars in the field of view will be of aid in detecting the satellite by providing reference points which are practically stationary, and which keep the observer's eyes in proper focus. Motion of the satellite through a field containing a few stars should be more conspicuous than through an empty field.

The satellite will cross the field of the 7×50 binocular in 5 seconds, if it is at 200 miles altitude. Therefore, a sharp watch must be maintained. It may be advantageous, for solar positions farther below the horizon, to reduce the power of the binocular and so increase its field of view. For H_s below -15^0 only a magnification of 2 is needed. This will increase the time during which the satellite will be crossing the field of view.

4. The Effect of Different Altitudes

For altitudes greater than 200 miles the satellite becomes increasingly difficult to see because of the reduction in brightness due to the inverse square law of distance. Compensating this, however, is the fact that the sky will be darker, since the satellite will be sunlit for a longer period after sunset. Also, the higher the satellite, the slower it will appear to move, and the longer it will take to cross the field of a binocular; at 800 miles the time for a 7^0 field would be 21 seconds.

In Table V the visibility conditions are compared for altitudes of 200, 400, and 800 miles. Assuming the use of 7×50 binoculars, the range of H_s over which the satellite can be seen easily is -5^0 to -17^0 for 200 miles, -9^0 to -24^0 for 400 miles, and -17^0 to -33^0 for 800 miles. The lower limit is determined by sunset at the satellite, or a little before this. Thus the length of the period available for observing is not greatly different from 200 to 800 miles, though it is actually a little shorter at 200 miles. Of course, the satellite will be more difficult to see the higher it is, and this is brought out in Table V by Δm or M'. However, it can be seen easily with 7×50 binoculars up to 800 miles.

5. Use of a Polarizer

The sky light at right angles to the sun is very strongly polarized near sunset. The maximum polarization occurs with $H_s = -3^0$, as reported by KOOMEN et al. [8]; then the stronger component is 16 times as intense as the weaker.

Use can be made of a polarizer to increase, somewhat, the visibility of the satellite. The polarizer reduces the light from the satellite to about 35 percent, since it is nearly unpolarized, but reduces the sky brightness to about 6 percent, when $H_s = -3^0$. This appears to result in a gain of 6 times or 2 magnitudes. However, this gain is partly offset by the lack of linear relationship between threshold illumination and sky brightness. A complete calculation is possible. Suffice it to say, however, that the gain in Δm is of the order of one magnitude for H_s from $+5$ to -3^0; when H_s becomes less than -3^0 the gain is rapidly lost and, indeed, use of a polarizer soon becomes a disadvantage because the sky light rapidly becomes less polarized as astronomical twilight is approached.

6. Effect of Hazy Skies

The computations presented here were based upon the assumption that the sky is very clear. If the sky is hazy, the brightness of the sky is considerably increased and so is the attenuation of the light from the satellite. It is important, therefore, that observing stations be located as high as practicable in the mountains, where the sky is apt to be free from haze, and where it is less bright due to the lower atmospheric pressure. Absence of thin high cirrus clouds is also important; frequently such clouds cannot be seen from sea level during the daytime, but show near sunset, or from an airplane.

The effect of haze on sky brightness is greatest when the sun is well above the horizon, because the haze usually lies within 5000 to 10,000 feet of the ground. Near sunset it is not illuminated intensely, since the sunlight is strongly attenuated over the slant path through the haze layer itself, and after sunset it is not illuminated by direct sunlight at all. Therefore, low-lying haze is somewhat less serious when observations are to be made after sunset, than during the day.

7. Need for Further Study

This paper is to be considered only as a first step in the determination of the visibility of a satellite. Several points require further study. These are the reflection characteristics of the satellite, visual thresholds as a function of the angle between the object and the point where one is looking, the effect of telescopes in case the eye pupil is not filled, and the importance of haze.

The study of visibility can best be made in the laboratory where the optical conditions can be simulated quite exactly. The satellite should be painted exactly as in flight. In case fluorescent paint is used, it may be important to irradiate the satellite with ultraviolet as well as visible light. This can be done with an open carbon arc source, which has a spectrum that is sufficiently similar to that of the sun. The sky background is most easily introduced by reflection. The satellite can be made to appear exactly as it would in actual flight by viewing it through lenses. Motion across the field can be introduced with rotating prisms, and observations made through binoculars or telescopes.

References

1. R. TOUSEY and E. O. HULBURT, J. Opt. Soc. Amer. **38**, 886 (1948).
2. R. TOUSEY and M. J. KOOMEN, J. Opt. Soc. Amer. **43**, 177 (1953).
3. F. S. JOHNSON, J. Meteorol. **11**, 431 (1954).
4. H. N. RUSSELL, Astrophysic. J. **43**, 173 (1916).
5. H. A. KNOLL, R. TOUSEY, and E. O. HULBURT, J. Opt. Soc. Amer. **36**, 480 (1946).
6. H. R. BLACKWELL, J. Opt. Soc. Amer. **36**, 624 (1946).
7. H. R. BLACKWELL, Communicated to the 32nd Meeting of the Armed Forces — NRC Vision Committee, 1953.
8. M. J. KOOMEN, C. LOCK, D. M. PACKER, R. SCOLNIK, R. TOUSEY, and E. O. HULBURT, J. Opt. Soc. Amer. **42**, 353 (1952).

Buchbesprechungen — Book Reviews — Comptes rendus

Thermodynamische Zustandsgrößen und Stoffwerte für Luft bei Dissoziationsgleichgewicht. Von H. J. KAEPPELER und H. G. L. KRAUSE. (Mitteilungen aus dem Forschungsinstitut für Physik der Strahlantriebe e. V.: Heft 1.) Mit Textabb., 40 S. München: R. Oldenbourg. 1954. DM 18.—.

Die thermodynamischen Zustandsgrößen und Stoffwerte von Luft bei Berücksichtigung der Dissoziation spielen eine Rolle bei der Berechnung der Hauterwärmung von Flugkörpern und sind weiters wichtig für die rechnerische Verfolgung der Strömungsverhältnisse in Strahltriebwerken. Auch bei der Ausbreitung von Detonationswellen sowie bei elektrischen Entladungen in Luft kommen diese Größen in Betracht. Die den Autoren bekannt gewordenen Arbeiten auf diesem Gebiete von BETHE, BURCKHARDT, HÖCKER, FINKELNBURG, KRIEGER und WHITE sowie MEACKER werden erwähnt und näher besprochen. Die angenommenen Zusammensetzungen der Luft weichen bei diesen Autoren voneinander ab. Auch die angewandten Rechenmethoden und die berücksichtigten Reaktionen sind verschieden. Zum Vergleich dieser Abweichungen sind die Partialdrücke dreier Arbeiten (von BURCKHARDT, HÖCKER und KRIEGER-WHITE) in übersichtlicher Weise graphisch dargestellt. Auf Grund der Werte von KRIEGER und WHITE für die Zusammensetzung, Enthalpie und Entropie für Luft bei Dissoziationsgleichgewicht, die den Verfassern als die geeignetsten erschienen, werden dann die Stoffwerte für Luft berechnet. Die Methode zur Berechnung dieser Werte wird dabei angegeben. Die Quasifreiheitsgrade, spezifische Wärme, Viskosität, Wärmeleitfähigkeit und PRANDTL-Zahl von Luft bei Dissoziationsgleichgewicht werden als Funktionen der Temperatur bei konstantem Druck (für 0,01, 0,1 und 1 Atm.) für den Temperaturbereich von 500° K bis 800° K bestimmt. Nach Angabe muß im Dissoziationsbereich bis 6000° K mit einem Fehler von etwa ± 3% gerechnet werden, und darüber hinaus mit einem etwas größeren Fehler. Dieser Fehler beruht allein auf der Ungenauigkeit in der numerischen Differentiation der KRIEGER-WHITEschen Werte. Der durch die Ungenauigkeit der gaskinetischen Stoßquerschnitte verursachte Fehler kann nicht angegeben werden, da keine Vergleichsdaten dieser Fehler zur Verfügung stehen. Die vorliegenden Daten können nach Ansicht der Verfasser für sehr genaue Rechnungen nur bis 5000° K gebraucht werden. Darüber hinaus treten Ionisationseffekte auf, insbesondere der NO-Ionisation, die bei der Rechnung nicht berücksichtigt sind. Für die Durchführung einer sehr genauen Berechnung der Stoffwerte müßte eine weitaus genauere Ermittlung der thermodynamischen Zustandswerte vorliegen als die Ausgangsergebnisse von KRIEGER und WHITE, worauf die Autoren ihre Rechnungsarbeit basiert haben, und es müßte dabei auch der Einfluß der Thermodiffusion in Betracht gezogen werden.

Die vorliegende Arbeit mit den vorzüglichen graphischen Darstellungen gibt einen sehr guten Überblick und ist eine wertvolle Ergänzung der Literatur auf diesem Gebiete. Das Heft kann jedem Interessenten, der sich schnell orientieren will, warm empfohlen werden. Das ausgedehnte Literaturverzeichnis am Schluß wird dabei gute Dienste leisten.

J. M. J. KOOY, Breda

Über die Wirtschaftlichkeit von Wasserdampfraketen als Horizontal-Starthilfen. Von H. H. KÖLLE. (Mitteilungen aus dem Forschungsinstitut für Physik der Strahlantriebe e. V.: Heft 2.) Mit Textabb., 76 S. München: R. Oldenbourg. 1955. DM 24.—.

Der verkehrsmäßige Einsatz zukünftiger Staustrahlflugzeuge wird auf wirtschaftlich arbeitende Starthilfen angewiesen sein. Die heutigen Erfahrungen mit den treib-

stoffverbrauchs-intensiven chemischen sowie Feststoff-Raketen lassen erkennen, daß sich hiermit ungünstige Relationen gegenüber den allgemeinen Flugkosten nach erfolgtem Start des Staustrahlers ergeben müssen. Starthilfen, die auf den außerordentlich verkehrsintensiven Weltflughäfen Verwendung finden sollen, müssen als erste Forderung zudem eine unüberbietbare Betriebssicherheit gewähren können, was leider den eingangs erwähnten Raketen noch nicht nachgerühmt werden kann.

H. KÖLLE unterzieht in der vorliegenden Studie verschiedene Starthilfesysteme einem eingehenden Vergleich. Nach kurzer, prinzipieller Behandlung der Mechanik des Startvorganges werden Leistungen und Gewichte chemischer Raketentriebwerke sowie von Heißwasserraketen diskutiert. Leider kommen letztere in der Behandlung ihrer inneren Mechanik etwas zu kurz, auch vermißt man bereits zu Anfang erläuternde Betriebsschemata dieses immerhin nicht allzu konventionellen Raketenantriebes. Solche Schemata würden auch die Abschnitte über Startwagen sowie Betrieb von Startvorrichtungen und Anlagen auf Basis der Heißwasserrakete wesentlich auflockern können. Sehr weitgehende Betrachtungen widmet der Verfasser sodann den Wirtschaftlichkeitsvergleichen der betrachteten Startsysteme. Hieraus ergibt sich, daß die Heißwasserrakete sowohl wirtschaftlich als auch in Beziehung auf Betriebssicherheit als Starthilfe für Staustrahlflugzeuge den übrigen Konstruktionen sehr weit überlegen ist. Der technische Aufwand am Boden ist hierbei allerdings größer als bei anderen Starthilfen, doch wird auch da bestimmt der Sicherheitsfaktor ausschlaggebend sein.

Die Rechnungsgenauigkeiten bewegen sich im Rahmen der Ansprüche, wie sie für allgemeine Vorprojektstudien gemacht werden können. Hierin dürfte aber gerade der besondere Wert dieser Arbeit liegen, indem es KÖLLE gut gelingt, mit geringstem Papieraufwand einem Projektbearbeiter jene Hinweise und Daten zu vermitteln, die dieser für grundlegende Vorstudien benötigt.

J. STEMMER, Baden/Schweiz

Index mathematischer Tafelwerke und Tabellen aus allen Gebieten der Naturwissenschaften. Bearbeitet von K. SCHÜTTE. 143 S. München: R. Oldenbourg. 1955. Geb. DM 14.50.

Das vorliegende Werk bringt in 16 Kapiteln mit über 130 Unterabschnitten und mehr als 1200 Titeln eine chronologisch gereihte Zusammenstellung aller wichtigen Tafel- und Tabellenwerke, die etwa seit dem Anfang des 20. Jahrhunderts erschienen sind. Neuerscheinungen sind bis Anfang 1955 berücksichtigt. Vorwort und Überschriften sind deutsch und englisch abgefaßt. Aufgenommen sind folgende Gebiete: Numerisches und praktisches Rechnen (einschließlich Rechenmaschinen); Logarithmen der natürlichen Zahlen, der Kreisfunktionen und ihre Numeri; elementare, aus einfachen Funktionen abgeleitete Funktionen; Zins- und Rententafeln; Fakultäten, Exponential- und Hyperbelfunktionen; elliptische Funktionen und ihre Integrale; Kugelfunktionen, BESSELsche und verwandte Funktionen; Integraltafeln und weitere höhere Funktionen; Tafeln zur Lösung von Gleichungen und Differentialgleichungen. Den rein mathematischen folgen Tafeln für: Physik und Chemie (einschließlich technischer Wissenschaften); Astronomie und Astrophysik; Geodäsie und Geophysik; nautische und aeronautische Ortsbestimmung; Meteorologie; Astronautik; schließlich Tafeln für Maße, Gewichte, Währungen und Formelsammlungen. Die Titel russischer Werke sind ins Deutsche übersetzt. Autorenregister und Institutsverzeichnis schließen den Band ab, der für den Benützer aus vielen Fachrichtungen, nicht zuletzt der Astronautik, wegen seiner Ausführlichkeit und Aktualität ein sehr wichtiges Orientierungsmittel darstellt, worin die aufgewendete, jahrelange Mühe des bekannten Verfassers ihren Lohn finden wird. F. HECHT, Wien

Herausgeber, Eigentümer und Verleger: Springer-Verlag, Wien I, Mölkerbastei 5. — Für den Inhalt verantwortlich: Prof. Dr. Friedrich Hecht, Wien VIII, Alserstraße 69. — Druck: Berger & Schwarz, Zwettl, N.-Ö.

The U. S. Satellite Vehicle Program

An announcement was made at the White House in Washington on 29 July 1955 that the United States has "definite plans for the launching of small satellites" during the International Geophysical Year 1957—58. The text of this announcement, prepared by the National Academy of Sciences and the National Science Foundation of the United States, was approved by President EISENHOWER. It was stated that technical advice and assistance would be made available by the Department of Defense, including the "facilities for launching the satellite", i.e. the launching vehicles. The project, code-named VANGUARD, was turned over, in this connection, to the U. S. Navy for management and coordination, with financial support coming from the National Science Foundation.

Historically, this satellite announcement grew out of a resolution passed in 1954 by the Comité Spécial de l'Année Géophysique Internationale (CSAGI), a group that had been designated by the International Council of Scientific Unions of the U.N. to coordinate and direct the over-all international geophysical undertaking, including, naturally, the U.S. sponsored satellite endeavor. It is through the CSAGI that each nation's efforts are tied in to the whole international scientific picture.

In the United States, the National Academy of Sciences' National Research Council (which represents the U.S. in the I.C.S.U. and which had been given the responsibility for all American scientific programs in the I.G.Y.) and the National Science Foundation are both cooperating on the satellite project. In a letter from the chairman of the U.S. National Committee for the I.G.Y. (established by the Academy), the CSAGI was officially informed of American satellite planning, thereby assuring liaison with the international organizing scientific body. At the same time, the National Science Foundation has been charged with the coordination and administration of all government appropriations for the I.G.Y. in support of the world geophysical program.

Since the time of the American declaration of satellite support for the I.G.Y., Russia has indicated that she, too, may launch Earth-circling vehicles during the same period, although to date no specific program has been made known to the CSAGI by her national scientific representatives. A Soviet commission has been created, however, to study the satellite idea, and official announcements may be expected at any time.

Since the plans to launch satellite vehicles were released last summer, details of the launching missile have been slowly appearing. At the present time it is expected that 12 small, instrumented satellites will be launched from the U.S. Air Force Missile Test Center at Patrick Air Force Base, in Florida. The orbit will be inclined about 40 degrees, and rocket-launched satellites will be fired off in a southeasterly direction, taking advantage of the Earth's revolution for extra boost. The orbit chosen will allow observations to be made in both northern and southern hemispheres by most of the nations participating in the I.G.Y., since the satellite's latitude range will be about 40^0 on both sides of equator.

As the Earth rotates once in 24 hours, the 95 minute orbiting satellite will make between 15 and 16 complete turns. But the satellite's orbit will be elliptical rather than circular[1], so that somewhat more than 1/16th of a revolution will be made by Earth during each satellite revolution. Perturbations and characteristics of the elliptical path considered, the satellite will have a displacement, in terms of the Earth, of more then 25 degrees for each revolution. Therefore, assuming the satellite is launched from Florida, after one complete revolution it will turn up 25 or more degrees west, after two trips, 50 or more degrees, and so on. The satellite, incidently, will travel at about 18,000 miles per hour, and will have an estimated lifetime of one hour if the perigee dips to 100 miles, 15 days if it gets no lower than 200, and perhaps a year if its nearest approach to Earth is no less than 300 miles.

The Vanguard missile has a three stage configuration, with an all-up length of about 72 feet, and a maximum diameter of only 45 inches. The first stage is said to resemble the Viking, is 45 feet long, and provides 27,000 pounds of thrust on a gasoline-ethyl alcohol-silicone oil mixture and liquid oxygen rocket engine (modified by General Electric from a HERMES model). The second stage may be similar to the AEROBEE-HI rocket, is being developed by the Aerojet-General Corporation, and operates in a nitric acid-unsymmetrical dimethyl-hydrazine propellant combination. The third stage is a solid propellant rocket, and is unguided. Contracts have been awarded to the Alleghany Ballistic Laboratory and the Grand Central Rocket Company for its development.

The Vanguard three-stage missile has no fins, relies on an inertial reference guidance system located in the second stage. Roll control is assured by tangential jets, while pitch and yaw control are achieved by gimballing the rocket engine. A gyroscope controls the direction of the thrust vector, which has an angular deflection of about five degrees on either side of the missile's centerline.

Vanguard Satellite Characteristics

Missile length, 3 stages	72 feet
Missile diameter, maximum	45 inches
Fineness ratio	19 : 1
Payload, i.e. the satellite, weight	$20-21\frac{1}{2}$ pounds
Maximum range, 3rd stage	1500 miles
Maximum altitude, 3rd stage	300 miles
Maximum velocity, 3rd stage	18,000 miles per hour
Time to orbit	10 minutes
Guidance system (1st and 2nd stages are guided, 3rd is spin stabilized only)	inertial reference
Engine thrust, 1st stage	27,000 pounds
Propellants, 1st stage	ethyl alcohol-gasoline-silicone oil/liquid oxygen
Firing time, 1st stage	131 seconds
Feed system, 1st stage	turbopump
Propellants, 2nd stage	nitric acid/unsymmetrical dimethyl-hydrazine
Feed system, 2nd stage	helium gas pressure
Propellants, 3rd stage	solid
Airframe and overall contractor	Glenn L. Martin Co.
Second stage contractor	Aerojet-General Corp.

[1] Its perigee will probably be 200 miles, apogee up to 800, or even out as far as 1400 miles, without destroying the conceived usefulness of the satellite.

Third stage contractor	Alleghany Ballistic Laboratory Grand Central Rocket Co.
First stage engine contractor	General Electric Co.
Percent orbital velocity given by each stage (approximate)[1]: First	15
Second	32
Third	50
Launching site	Patrick Air Force Base, Fla.
Initial heading	28–35° south of east
First stage burnout altitude	36 miles
Angle of ascent at this point	45°
Second stage burnout altitude[2]	140 miles

The satellites will be both radio and optically tracked. A system of radio triangulation, called MINITRACK, will be employed, and it is expected that the complexity of the ground stations will be such that the satellite need carry merely a small, compact radio transmitter (consisting of an 108 megacycle continuous-wave oscillator). A number of Minitrack stations will be set up so that the satellite position can be accurately determined. Some data accumulated in the satellite will be telemetered through Minitrack facilities upon signal from the surface, and other data will pass through a pulse-width FM modulation of a radio frequency carrier in the 216 to 235 megacycle telemetering band. Aside from the telemetering transmitter and instruments to make primary observations, it is assumed that there will be available instrumentation to ascertain the satellite's space orientation, a power supply, devices to actuate measuring equipment, a control receiver, and so forth.

Signals from the satellite's radio transmitter are expected to reach from 1000 to possibly 3000 miles, the exact distance being determined by the satellite's altitude. The following table was prepared by the U.S. National Committee for the I.G.Y. earlier this year:

Altitude of Satellite (miles)	Radio Detection Range, approx. (miles)
200	1200
400	1700
600	2000
800	2300

Plans have proceeded rapidly to set up a series of optical tracking stations across those sections of the Earth where the I.G.Y. satellites will be visible. The satellites will be observable at dawn and at dusk, when the Sun's rays will still provide illumination, but when the contrast between sky and vehicle brightness is such as to enhance its visibility. When in the Earth's shadow, it has been proposed to use mammouth searchlights to illuminate the satellites for optical tracking purposes. Whether or not a satellite will be easily seen by binoculars will depend on position, sight angle, altitude, background luminosity, and atmospheric conditions. The satellite will have a zenith angular motion of

[1] They do not add up to 100%. The difference is provided by the Earth's rotation.

[2] Ascent tilts toward horizontal even further. From here it coasts to 300 mile altitude, and roughly 700 miles along its horizontal trajectory, following which the 3rd stage is separated and fires satellite into orbit.

approximately a degree each second, a speed that will complicate attempts at precise tracking. At the present time, only rapid, large aperture (48 inches) SCHMIDT cameras could efficiently handle such elusive objects.

The Smithsonian Astrophysical Observatory, Cambridge, Mass., has been designated by the National Academy of Sciences to administer the satellite optical tracking program, and it is planned that the observing network will include both professional and amateur observers and observing facilities. Collaborating agencies for the latter are the International Astronautical Federation, the Astronomical League, the American Association of Variable Star Observers, and the Western Amateur Astronomers. Professionally, at least a dozen specially designed tracking telescopes will be set up around the Earth for extremely accurate tracking and timing of the small satellite vehicles. Observations will be reported to area captains, data will be furnished to computing facilities, and the exact satellite orbit will then be determined.

Available space will be extremely limited in the small satellites that will be launched during the International Geophysical Year, and only a few of many desired measurements will initially be made. Among the geophysical, astronomical and other measurements that could be aided by a satellite vehicle are the following:

Radiative energy output of Sun, over all wavelenghts

Study of solar flares, other activities, and relationship to Earth's weather

Connection between solar radiation, cosmic rays, Earth's magnetic field, and magnetic storms

Ultraviolet and X-radiation studies; total solar corpuscular radiations

Sunspot studies

Study of ionosphere, aurora, airglow, general meteorology

Temperature, pressure, extreme altitude wind studies

Albedo determination

Outer atmosphere's density (observations of effect of air drag on satellite orbit)

Composition of Earth's crust (observations of non-uniform distribution of mass in the crust by noting variations in orbit), and figure for oblateness

Structure and composition of the atmosphere

Accurate measurements of intercontinental distances

Observations of the STÖRMER current ring

Determination of percent of Earth covered by clouds

Electron density measurements above the F layer

Observations of atomic, ionic, molecular masses in ambiant air

Measurements of pressure inside and outside of satellite

Measurements of temperature inside and outside of satellite

Observation of effect of meteoric impacts on satellite hull

Determination of density of hydrogen atoms, ions in space; investigation of interplanetary dust, gas. Size, distribution of particles

Intensity, and variations in intensity, of extra-terrestrial energy impingements on Earth's atmosphere

Frederick I. Ordway, III[1]
Member
Editorial Board
Astronautica Acta

April 1956

---

[1] General Astronautics Corp., Oyster Bay, N.Y., USA.

Stationary Trajectories for a High-Altitude Rocket with Drop-Away Booster[1]

By

G. Leitmann[2], BIS

(*Received February 4, 1956*)

Abstract. In this paper a solution to the problem of optimum thrust programming is deduced for a rocket which is required to reach given altitude with given pay load (rather than given burnt mass) and minimum fuel expenditure; i.e. the effect of rocket dead-weight is taken into account. In particular, the case of a rocket with disposable booster is considered and the necessary conditions for a minimum initial mass are found.

Zusammenfassung. Eine Lösung für den optimalen Schub einer Rakete, die eine gegebene Höhe mit gegebener Nutzlast (eher als mit gegebener Masse nach Brennschluß) und mit minimalem Brennstoffverbrauch zu erreichen hat, ist abgeleitet; das heißt der Einfluß des Leergewichtes der Rakete ist in Erwägung gezogen. Insbesondere wird der Fall einer Rakete mit abwerfbarer Zusatzrakete behandelt, und die nötigen Bedingungen für eine minimale Anfangsmasse werden abgeleitet.

Résumé. L'article présente une solution au problème de la distribution optimum de poussée en vue d'atteindre une altitude donnée avec une charge utile spécifiée, la consommation totale de combustible étant rendue minimum. La masse en fin de combustion n'étant pas imposée le calcul tient compte du poids mort de la fusée. Le cas de fusées d'appoint éjectables est considéré et les conditions obtenues sous lesquelles la masse initiale totale est minimum.

Introduction

The problem of optimum thrust programming for high altitude rockets, i.e. the problem of reaching a specified altitude with a given final mass and with minimum initial mass, has been treated previously, e.g. see Ref. [1]—[5]. A requirement of the optimal solution is the attainment of an initial velocity by impulsive boosting, i.e. by expending instantaneously a portion of propellant. This ideal requirement can be approached, in the practical case, by giving the rocket the required initial velocity by means of a high performance booster.

In the cases previously discussed, the mass at burn-out (which includes the expended motor as well as the payload) was treated as a known quantity. Furthermore, the booster was considered as part of the rocket, i.e. the effect of dropping away the booster at the end of the boost was not taken into account.

---

[1] This is an informal report and is transmitted for information only. It is not an official report of the Naval Ordnance Test Station and must not be used as a basis for action.

[2] Aeroballistic Analysis Branch, U.S. Naval Ordnance Test Station, China Lake, Calif., USA.

In this paper we shall investigate the optimum problem for which the actual payload (rather than the burnt mass) is given and for which the booster drops away at the end of boost.

I. Formulation of the Problem

Let M be the mass of the rocket configuration and s the altitude at time t. Denote differentiation with respect to time t by dot. It is assumed that the aerodynamic drag, D, is a function of s and $\dot{s}$ only and is a known function for the given configuration. The effective gas velocity, c, and the acceleration of gravity, g, are taken as constant.

At the onset of powered flight, $t = 0$, $s = 0$, $\dot{s} = 0$, and $M = M_0$. After impulsive boosting but before drop-away of booster, $t = 0$ and $s = 0$ still, but $\dot{s} = v^{0-}$ and $M = M^{0-}$; after drop-away of (expended) booster, $\dot{s} = v^{0+}$ and $M = M^{0+}$. It is assumed the expended booster drops away instantaneously and with zero velocity relative to the main rocket. At burn-out, $t = t_1$, $s = s_1$, $\dot{s} = v_1$, and $M = M_1$. The actual payload is denoted by M_l.

If the ratio of expended rocket motor mass to propellant mass is denoted by r, and of expended booster mass to propellant mass by r_b, where r and r_b are given, and if M_p and M_{bp} denote the rocket propellant and booster propellant mass, respectively, then

$$\begin{aligned} M_0 &= M_l + (1 + r)\, M_p + (1 + r_b)\, M_{bp} \\ M^{0-} &= M_l + (1 + r)\, M_p + r_b\, M_{bp} \\ M^{0+} &= M_l + (1 + r)\, M_p \\ M_1 &= M_l + r\, M_p. \end{aligned} \tag{1.1}$$

The problem then is: Given M_l, r, r_b, c, g, and $D(s, \dot{s})$, what if the function $s(t)$ in order that M_0 be minimum? Auxiliary conditions are $S(0) = 0$, and s_1, v_1, and M_1 are so related that the required altitude, S, is reached.

II. Solution

The classical equation of motion for vertical flight, neglecting the effects of the earth's rotation, is

$$c\,\dot{M} + (\ddot{s} + g)\, M + D\,(s, \dot{s}) = 0. \tag{2.1}$$

During free flight eq. (2.1) applies with $\dot{M} = 0$. The solution of the free flight equation for a required summit altitude, S, may be written as

$$\dot{s} = \varphi(s, M_1) \tag{2.2}$$

which becomes, at $t = t_1$,

$$v_1 = \varphi(s_1, M_1). \tag{2.3}$$

We shall obtain the necessary conditions for a stationary M_0 by the method of MAYER, Ref. [7].

Letting $\dot{s} \equiv v$, eq. (2.1) can be written as

$$\begin{aligned} \Phi_1 &= c\,\dot{M} + (\dot{v} + g)\, M + D(s, v) = 0 \\ \Phi_2 &= \dot{s} - v = 0 \end{aligned} \tag{2.4}$$

where $s = s(t)$ is the optimal function.

From eq. (2.4),

$$\begin{aligned} \delta\Phi_1 &= c\,\delta\dot{M} + (\dot{v} + g)\,\delta M + M\,\delta\dot{v} + \frac{\partial D}{\partial s}\,\delta s + \frac{\partial D}{\partial v}\,\delta v = 0 \\ \delta\Phi_2 &= \delta\dot{s} - \delta v = 0 \end{aligned} \tag{2.5}$$

We now introduce Lagrangian multipliers $\lambda_1(t)$ and $\lambda_2(t)$, and form $\Sigma\lambda_i\,\delta\Phi_i$. Assuming the validity of interchanging differentiation, we get in view of eq. (2.5)

$$\cdot\left[\lambda_1\frac{\partial D}{\partial s}-\dot\lambda_2\right]\delta s+\frac{d}{dt}(\lambda_2\,\delta s)$$
$$+\left[\lambda_1\frac{\partial D}{\partial v}-\lambda_2-\lambda_1\dot M-\dot\lambda_1 M\right]\delta v+\frac{d}{dt}(\lambda_1 M\,\delta v) \tag{2.6}$$
$$+[\lambda_1(\dot v+g)-\dot\lambda_1 c]\,\delta M+\frac{d}{dt}(\lambda_1 c\,\delta M)=0.$$

We integrate eq. (2.6) from the instant after the booster drops away to burnout, i.e.

$$\lambda_{11}c\,\delta M_1-\lambda_1^{0+}c\,\delta M^{0+}=\lambda_2^{0+}\delta s^{0+}-\lambda_{21}\delta s_1+\lambda_1^{0+}M^{0+}\delta v^{0+}-\lambda_{11}M_1\delta v_1$$
$$-\int_0^{t_1}\left\{\left[\lambda_1\frac{\partial D}{\partial s}-\dot\lambda_2\right]\delta s+\left[\lambda_1\frac{\partial D}{\partial v}\lambda_2-\lambda_1\dot M-\dot\lambda_1 M\right]\delta v+[\lambda_1(\dot v+g)-\dot\lambda_1 c]\,\delta M\right\}dt. \tag{2.7}$$

We desire to express δM_0, and hence δM^{0+}, as a function of δs only. Consequently, we impose on the undetermined multipliers λ_1 and λ_2 the conditions

$$\lambda_1(\dot v+g)-\dot\lambda_1 c=0.$$
$$\lambda_1\frac{\partial D}{\partial v}-\lambda_2-\lambda_1\dot M-\dot\lambda_1 M=0 \tag{2.8}$$

In view of the arbitrariness of δs, eq. (2.7) yields

$$\lambda_1\frac{\partial D}{\partial s}-\dot\lambda_2=0 \tag{2.9}$$

and

$$\lambda_{11}c\,\delta M_1-\lambda_1^{0+}c\,\delta M^{0+}=\lambda_2^{0+}\delta s^{0+}-\lambda_{21}\delta s_1+\lambda_1^{0+}M^{0+}\delta v^{0+}-\lambda_{11}M_1\delta v_1. \tag{2.10}$$

The impulsive boost relation at $t=0$ is

$$M_0=M^{0-}e^{\frac{v^{0-}}{c}}. \tag{2.11}$$

Since $s=0$ and the booster drops away with zero velocity relative to the main rocket

$$\delta s^{0+}=0$$
$$v^{0-}=v^{0+}\equiv v^0. \tag{2.12}$$

Furthermore, in view of eq. (2.3),

$$\delta v_1=\frac{\partial\varphi}{\partial s_1}\delta s_1+\frac{\partial\varphi}{\partial M_1}\delta M_1. \tag{2.13}$$

For a stationary M_0,

$$\delta M_0=0. \tag{2.14}$$

Invoking definitions (1.1), we get then

$$c\,\delta M^{0+}=\{r_b e^{\frac{v^0}{c}}[r_b(e^{\frac{v^0}{c}}-1)-1]^{-1}-1\}M^{0+}\delta v^0 \tag{2.15}$$

$$c\,\delta M_1=r\frac{1+r_b}{1+r}M^{0+}[r_b(e^{\frac{v^0}{c}}-1)-1]^{-1}\delta v^0. \tag{2.16}$$

Vol. 2 1956

We now substitute eqs. (2.13), (2.15), and (2.16) in eq. (2.10) and note that δs_1 and δv^0 are independent variations so that their coefficients vanish separately. Eq. (2.8) yields upon integration

$$\lambda_{11} = \lambda_1{}^{0+} e^{\frac{v_1 + g t_1 - v^*}{c}}. \tag{2.17}$$

Also, eqs. (2.1) and (2.8), give at $t = t_1$

$$\lambda_{11}\left[\frac{\partial D}{\partial v} + \frac{D}{c}\right]_{t_1} = \lambda_{21}. \tag{2.18}$$

Thus, finally eq. (2.10) leads to

$$v_1\left[\frac{\partial D}{\partial v} + \frac{D}{c}\right]_{t_1} = M_1 g + D_1 \tag{2.19}$$

and

$$r(1 + r_b)\left(1 + \frac{M_1}{c}\frac{\partial \varphi}{\partial M_1}\right) e^{\frac{v_1 + g t_1}{c}} - r_b(1 + r)\, e^{\frac{2 v^*}{c}} = 0. \tag{2.20}$$

Eliminating λ_1 and λ_2 between eqs. (2.1), (2.8) and (2.9) yields the EULER-LAGRANGE equation

$$\varepsilon \equiv \frac{\partial^2 D}{\partial v\, \partial s} v + \frac{\partial^2 D}{\partial v^2}\dot{v} + \frac{1}{c}\left[\frac{\partial D}{\partial s} v + (2\dot{v} + g)\frac{\partial D}{\partial v} + \frac{1}{c}(\dot{v} + g) D\right] - \frac{\partial D}{\partial s} = 0. \tag{2.21}$$

The initial mass M_0 will then have a stationary value when the linear second-order differential equation, eq. (2.21), in $s(t)$ is satisfied during powered flight, and when conditions (2.19) and (2.20) are met.

III. First Integral

The EULER-LAGRANGE equation, eq. (2.21), possesses a first integral

$$I = M g + D - v\left(\frac{\partial D}{\partial v} + \frac{D}{c}\right) = 0. \tag{3.1}$$

This can be verified by differentiating I, i.e.

$$\begin{aligned} \dot{I} = \dot{M} g + v\frac{\partial D}{\partial s} + \dot{v}\frac{\partial D}{\partial v} - \dot{v}\left(\frac{\partial D}{\partial v} + \frac{D}{c}\right) \\ - v\left(\frac{\partial^2 D}{\partial s\, \partial v} v + \frac{\partial^2 D}{\partial v^2}\dot{v} + \frac{v}{c}\frac{\partial D}{\partial s} + \frac{\dot{v}}{c}\frac{\partial D}{\partial v}\right). \end{aligned} \tag{3.2}$$

Invoking eqs. (2.1) and (2.21) allows us to rewrite eq. (3.2) as

$$\dot{I} = -v\left(\varepsilon + I\frac{\dot{v} + g}{v c}\right). \tag{3.3}$$

If $I = 0$,

$$\dot{I} = -v\varepsilon = 0. \tag{3.4}$$

However, if I is indeed a first integral of ε,

$$I - I_1 = -\int_{t_1}^{t} v\varepsilon\, dt = 0. \tag{3.5}$$

But by eq. (2.19), $I_1 = 0$, i.e. $I = 0$, so that relation (3.4) is satisfied.

Solution may now proceed in the following manner. The EULER-LAGRANGE equation may be integrated (e.g. see Ref. [1, 2, 5] and [6]) to give

$$s_1 = s_1(v^0, v_1)$$
$$t_1 = t_1(v^0, v_1). \tag{3.6}$$

Eq. (3.6) may be solved for $v^0(s_1, v_1)$ and $t_1(s_1, v_1)$ and these are then substituted in eq. (2.20). Eqs. (2.3), (2.19), and (2.20) may then be solved for s_1, v_1, and M_1. Knowledge of M_1 immediately gives M_p. Eqs. (1.1) and (2.11) then yield M_{bp}, i.e.

$$M_{bp} = [r_b\,(e^{\frac{v^0}{c}} - 1) - 1]^{-1}\,(1 - e^{\frac{v^0}{c}})\,M^{0+}. \tag{3.7}$$

Furthermore, throughout powered flight, M is determined by eq. (3.1).

IV. Note

Integration of the equation of motion, eq. (2.1), gives

$$M^{0+}\,e^{\frac{v^0}{c}} - M_1\,e^{\frac{v_1 + g t_1}{c}} = \int_0^{t_1} \frac{D}{c}\,e^{\frac{v + g t}{c}}\,dt. \tag{4.1}$$

Eq. (4.1) must be satisfied by the solution of the optimum problem. One can easily show that it is.

One form of eq. (3.6) is

$$\left[\left(\frac{\partial D}{\partial v} + \frac{D}{c}\right)v - D\right]_{t=0} e^{\frac{v^0}{c}} - \left[\left(\frac{\partial D}{\partial v} + \frac{D}{c}\right)v - D\right]_{t=t_1} e^{\frac{v_1 + \int_0^{s_1} \frac{ds}{v}}{c}} = \frac{g}{c}\int_0^{s_1} D\,e^{\frac{v + g\int_0^{s} \frac{ds}{v}}{c}} \frac{ds}{v}. \tag{4.2}$$

However substituting eq. (3.2) at $t = 0$ and $t = t_1$ and $t = \int_0^{s} ds/v$ into eq. (4.2) reduces it immediately to eq. (4.1).

In order that there exist a stationary value of M_0, eq. (2.20) must be satisfied. This cannot occur for all values of r and r_b. In particular, if $r = 0$, eq. (2.20) can only be satisfied if $r_b = 0$ also.

However, $r = 0$ is a rather special case, since then $M_1 = M_t$ and the solution is greatly simplified.

It is of interest to note that for $r = r_b \neq 0$, eq. (2.20) reduces to the simple relation

$$v^0 = \frac{1}{2}\,g\,T \tag{4.3}$$

where $T = \int_{s_1}^{s} ds/v$ time of free flight.

V. Non-Drop-Away-Booster

We consider now the optimum problem for which the booster is taken as part of the main rocket and for which the payload rather than the burnt mass is given. This problem is of practical interest for the following reason. If the burnt mass is specified, the mass of the expended motor is then also given. However, the mass of the expended motor is not really known until the amount of propellant

Vol. 2 1956

necessary to attain the desired altitude is known. That latter quantity, however, is dependent on the burnt mass.

The optimum solution for the case of the non-drop-away booster is obtained in a fashion completely analogous to that used in the problem of the drop-away booster. Now we have

$$\begin{gathered} M_0 = (1 + r_b)\, M_{bp} + (1 + r)\, M_p + M_l \\ M^{0+} = M^{0-} = M^0 = r_b\, M_{bp} + (1 + r)\, M_p + M_l \\ M_1 = r_b\, M_{bp} + r\, M_p + M_l. \end{gathered} \tag{5.1}$$

Proceeding as before, we arrive at the same EULER-LAGRANGE equation $\varepsilon = 0$, eq. (2.21). However, eq. (2.10) leads to

$$\lambda_{11} \frac{r_b - r}{r + 1} M^0 \left(1 + \frac{\partial \varphi}{\partial M_1} \frac{M_1}{c}\right) \delta v^0 + \left(\lambda_{11} M_1 \frac{\partial \varphi}{\partial s_1} + \lambda_{21}\right) \delta s_1 = 0. \tag{5.2}$$

Thus,

$$\begin{gathered} \lambda_{11} \frac{r_b - r}{r + 1} M^0 \left(1 + \frac{\partial \varphi}{\partial M_1} \frac{M_1}{c}\right) = 0 \\ \lambda_{11} M_1 \frac{\partial \varphi}{\partial s_1} + \lambda_{21} = 0\,. \end{gathered} \tag{5.3}$$

For $r \neq r_b$, eq. (5.3) leads to

$$1 + \frac{\partial \varphi}{\partial M_1} \frac{M_1}{c} = 0. \tag{5.4}$$

Since $\partial\varphi/\partial M_1$ is a continuous function of r and r_b, eq. (5.4) applies also when $r_b \to r$. Eq. (5.3) again leads to eq. (2.19). In short, all equations, except eq. (2.20), are as in the case of the drop-away booster. Eq. (2.20) is replaced by eq. (5.4).

Solution proceeds as follows. From eq. (5.4) M_1 is obtained as a function of s_1. This is substituted for M_1 in eq. (2.19) and (2.3). These equations are now solved for s_1 and v_1. Eq. (3.6) may now be used to obtain v^0 and t_1, and eq. (5.4) yields M_1. M_p and M_{bp} are then found as before.

The solution of the problem discussed above reduces to that given in Ref. [1—3, 5] when $r = r_b = 0$, for in that case eq. (5.4) does not arise and $M_1 = M_l$.

Acknowledgment

The author wishes to thank M. L. LUTHER for reviewing this note.

References

1. H. S. TSIEN and R. C. EVANS, Optimum Thrust Programming for a Sounding Rocket. J. Amer. Rocket Soc. **21**, 99 (1951).
2. D. F. LAWDEN, Stationary Rocket Trajectories. Quart. J. Mech. **7**, 488 (1954).
3. G. LEITMANN, The Problem of Optimum Thrust Programming. Nav. Ordn. Test Station, Techn. Note 5038-11, 1955.
4. G. LEITMANN, A Calculus of Variations Solution of GODDARD's Problem. Astronaut. Acta **2**, 55 (1956).
5. L. E. WARD, A Calculus of Variations Problem in Thrust Programming. Nav. Ordn. Test Station, Techn. Note 3502-2, 1955.
6. G. LEITMANN, Integration of the EULER-LAGRANGE Equation and Numerical Example for Optimum Thrust Programming. Nav. Ordn. Test Station, Techn. Note 5038-10, 1955.
7. A. MAYER, Über das allgemeinste Problem der Variationsrechnung. Ber. Verh. sächs. Akad. Wiss. Leipzig, math.-physische Kl., 1878.

Studies of a Minimum Orbital Unmanned Satellite of the Earth (MOUSE)

Part II. Orbits and Lifetimes of Minimum Satellites[1]

By

S. F. Singer[2], ARS

(With 16 Figures)

(*Received April 3, 1956*)

Abstract. The purpose of this paper is two-fold:

(1) To describe the (elliptical) orbit of an artificial satellite in terms of the launching conditions (i.e. at "burnout"); in particular, to give perigee (minimum) and apogee (maximum) altitudes of the ellipse as a function of launching altitudes and of errors in launching velocity and angle. Criteria are then developed for controlling the launching conditions.

(2) To investigate the subsequent behavior of the orbit under the influence of the drag of the upper atmosphere. The "lifetime" of the satellite depends on its area and mass, and is related to the upper atmosphere densities; hence these densities can be determined from measured changes of the orbit by methods discussed in detail. Both circular and elliptic orbits are investigated using appropriate approximation methods. The appendices take up: (a) some features of orbit theory; (b) upper atmosphere densities; (c) critical examination of approximation methods.

Zusammenfassung. Der Zweck dieser Veröffentlichung ist ein zweifacher:

1. Die (elliptische) Bahn eines künstlichen Satelliten mit Ausdrücken der Startbedingungen (das heißt bei „Brennschluß") zu beschreiben, im besonderen Perigäum-(Minimum-) und Apogäum-(Maximum-)Höhen der Ellipse als Funktion der Starthöhen und der Fehler der Startgeschwindigkeit und des Startwinkels anzugeben; Kriterien für die Kontrolle der Startbedingungen werden entwickelt.

2. Das nachfolgende Verhalten der Bahn unter dem Einfluß des Widerstandes der hohen Atmosphäre zu untersuchen. Die „Lebensdauer" des Satelliten hängt von seiner Oberfläche und Masse ab und steht in Beziehung zu den Dichten der hohen Atmosphäre. Daher können diese Dichten aus Messungen der Bahnveränderungen nach genau erörterten Verfahren abgeleitet werden. Sowohl Kreis- als auch Ellipsenbahn werden unter Benützung geeigneter Annäherungsmethoden untersucht. Im Anhang werden (a) einige Besonderheiten der Kreisbahntheorie, (b) Annahmen über die Dichte der oberen Atmosphäre, (c) eine kritische Prüfung der Annäherungsmethoden gebracht.

Résumé. L'objet de cet article est double:

(1) Il décrit l'orbite (elliptique) d'un satellite artificiel en fonction des conditions en fin de propulsion; en particulier les altitudes du périgée et de l'apogée en fonction des altitudes de lancement et des erreurs sur la vitesse et l'angle en fin de lancement.

Vol. 2 1956

---

[1] Presented at the Ninth Annual Meeting of the American Rocket Society, New York, N. Y., December 1954.

[2] Associate Professor, Department of Physics, University of Maryland, College Park, Md., USA.

Des critères peuvent alors être développés pour le contrôle des conditions de lancement.

(2) Il étudie le comportement subséquent de l'orbite sous l'influence de la traînée dans la haute atmosphère. La vie du satellite dépend de sa masse et de sa surface; elle est en relation avec la densité de la haute atmosphère. Ces densités peuvent par conséquent être déterminées en mesurant les variations de l'orbite par des méthodes discutées en détail. Les méthodes d'approximation appropriées aux orbites circulaires et elliptiques sont examinées. Les appendices traitent a) de quelques caractéristiques de la théorie des orbites, b) des densités dans la haute atmosphère, c) d'une recherche critique des méthodes d'approximation.

List of Symbols

r = distance of satellite from center of the earth
a = semimajor axis of orbit ellipse
Φ = polar angle of orbit ellipse (measured from perigee) (geocentric angle)
ε = eccentricity of orbit ellipse
R_A = apogee distance
R_P = perigee distance
R_L = distance of launching point from center of the earth
R_E = (mean earth's radius) $6.37 \cdot 10^6$ meter
h = altitude above sea-level
h_A = apogee altitude
h_P = perigee altitude
h_L = altitude of launching point
G = (NEWTON's gravitational constant) $6.67 \cdot 10^{-11}$ nt -m^2 -kg^{-2}
M_E = (mass of the earth) $5.98 \cdot 10^{24}$ kg
m = mass of the satellite
T = kinetic energy of satellite
V = potential energy of satellite
n = mean motion (ang. vel.) rad/sec
E_T = total specific energy, E_{TC} for circular orbit, $E_{T(ell)}$ for elliptic orbit, in joules/kg
g_0 = gravitational acceleration at sea-level 9.8 m/sec^2
g_h = gravitational acceleration at altitude h
v_L = launching velocity
v_A = velocity at apogee
v_P = velocity at perigee
Δv = magnitude error in the launching velocity
$\Delta \theta$ = angular error (in the vertical plane) in the launching velocity
A = projected area of satellite
C_D = drag coefficient
ϱ = atmospheric density kg/m^3
F_D = drag force
y_L = v_L/v_C
y_P = v_P/v_C
Δt_{12} = time to descend from altitude h_1 to h_2
t_L = lifetime, time to descend to sea-level
J = orbital angular momentum of satellite

Some Conversion Factors

Density 1 Kg/m^3 = $1.94 \cdot 10^{-3}$ slug/ft^3
Force 1 newton = 0.225 lb
Length 1 Km = .6215 miles = 3280 ft
Area 1 m^2 = 10.76 ft^2 = 1550 in^2
Energy 1 joule = 0.738 ft-lb

Introduction

Before discussing its orbit, it is clearly important to specify first the utility of an artificial satellite, to discuss the applications to which it is to be put, and to solve some of the technical problems of its instrumentation, including power supply and means of orientation [1]. For a satellite like the MOUSE, whose main application is geophysical and astrophysical research, many features of the orbit are of minor importance, e.g. the exact altitude and shape. It is only desirable to keep it above the ionosphere for a sufficiently long period of time so that it can carry out its observations.

But some important questions must be asked. How accurately do we have to place the satellite in its orbit? What is the effect of launching errors on the lifetime? How important is the choice of launching altitude, and the satellite's size and weight? These and other questions must be answered to decide, e.g. on the degree of precision, and therefore on the weight of the guidance system in the rocket stages, and thus allow the designer to achieve an optimum balance of the propulsion and control requirements. For this purpose we will present the results of our calculations in the form of graphs wherever possible.

(1) We will first derive the perigee and apogee altitudes as a function of launching errors.

(2) We will then calculate the lifetime as a function of perigee and apogee altitudes.

Satellite Orbit

At the instant of burn-out of the last propulsion stage the satellite is "launched" in its orbit. In the inverse-square law central-force field of the earth's gravitation the orbit is given by the well-known equation for an ellipse [2]:

$$r = a\,(1 - \varepsilon^2)\,(1 + \varepsilon \cos \Phi)^{-1}. \tag{1}$$

For our purposes it is more convenient to introduce the altitudes of apogee and perigee of the ellipse, h_A and h_P:

$$\begin{aligned} h_A &= R_A - R_E \\ h_P &= R_P - R_E. \end{aligned} \tag{2}$$

In Equation (1), both ε and a can be expressed in terms of R_A and R_P:

$$\begin{aligned} \varepsilon &= \frac{R_A - R_P}{R_A + R_P} \\ a &= \frac{R_A + R_P}{2}. \end{aligned} \tag{3}$$

(These relationships can be seen most clearly by inspecting Fig. 1.) We easily derive

$$\begin{aligned} R_A &= a\,(1 + \varepsilon), \\ R_P &= a\,(1 - \varepsilon), \end{aligned} \tag{4}$$

and

$$r = \frac{2\,R_A\,R_P}{(R_A + R_P) + (R_A - R_P)\cos \Phi}. \tag{5}$$

It is sometimes useful to give the expression for geocentric angle

$$\cos \Phi = \frac{2\,R_A\,R_P/r - R_A - R_P}{R_A - R_P}.$$

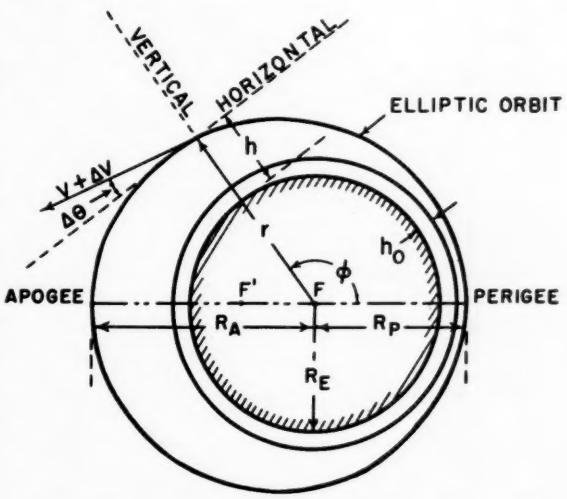

Fig. 1. Elliptic orbit of satellite showing notation. Equation of orbit: $r = \frac{a\,(1 - \varepsilon^2)}{1 + \varepsilon \cos \Phi}$; $\varepsilon = \left(\frac{R_A - R_P}{R_A + R_P}\right)$; $a = \frac{R_A + R_P}{2}$. R_E = Mean radius of earth; R_P = Perigee distance; R_A = Apogee distance; h = altitude; h_0 = critical drag altitude; F, F' = Foci of elliptic orbit

It is useful also to take the KEPLERian expression for the period T of an elliptical orbit and express it in terms of R_A and R_P:

$$T = \frac{2\pi a^{3/2}}{(G M_E)^{1/2}} = 2\pi (G M_E)^{-1/2} \left(\frac{R_A + R_P}{2} \right)^{3/2}. \tag{6}$$

T is shown for various values of h_P and h_A in Fig. 2.

Effect of Launching Errors

The simplest orbit is the circular one. At any altitude h the gravitational force (weight) is $m\, g_h$, and this is balanced by the centrifugal force $\frac{m\, v^2}{r}$, so that

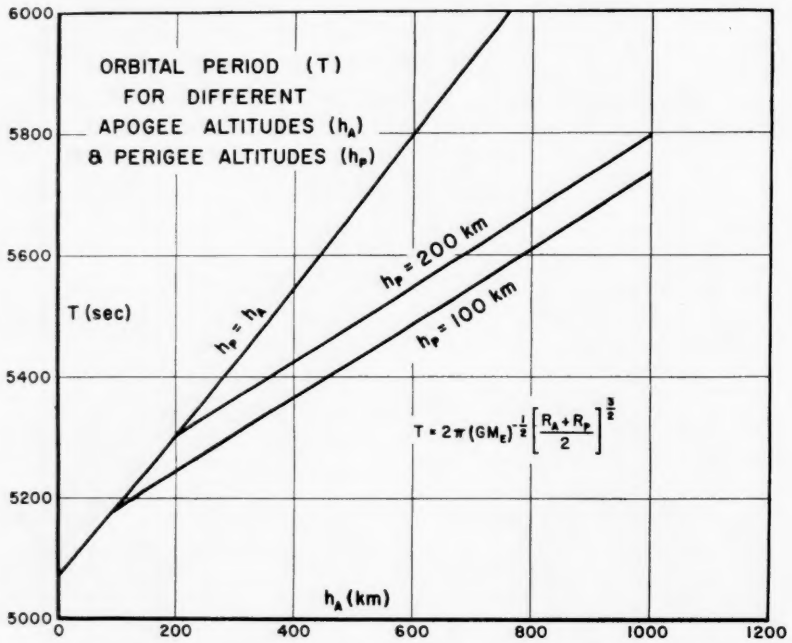

Fig. 2. Orbital period for circular orbit ($h_P = h_A$) and for elliptic orbits

$$\frac{G M_E m}{r^2} = m\, g_h = \frac{m\, v_C^2}{r}; \tag{7}$$

Now g_h varies with altitude according to the inverse-square law:

$$g_h = g_0 \left(\frac{R_E}{R_E + h} \right)^2 \text{ (see Fig. 3).}$$

Therefore, the circular velocity is given by

$$v_C = \left[g_0 \frac{R_E^2}{R_E + h} \right]^{1/2} \quad \text{(see Fig. 4).} \tag{8}$$

Now in general it is quite impossible to achieve a mathematically perfect circular orbit; we always have a launching velocity v_L which is slightly different from v_C by an amount Δv; $v_L = v_C + \Delta v$; and we have an angular error (in the plane of the orbit) $\Delta \theta$ (see Fig. 1).

Problem

The problem we want to solve is the following:

Given the launching altitude h_L, and the launching errors Δv and $\Delta \theta$, we want to find the perigee and apogee altitudes of the resulting orbit.

Solution

We simply use only the principles of (a) conservation of angular momentum, and (b) conservation of energy (see Appendix I).

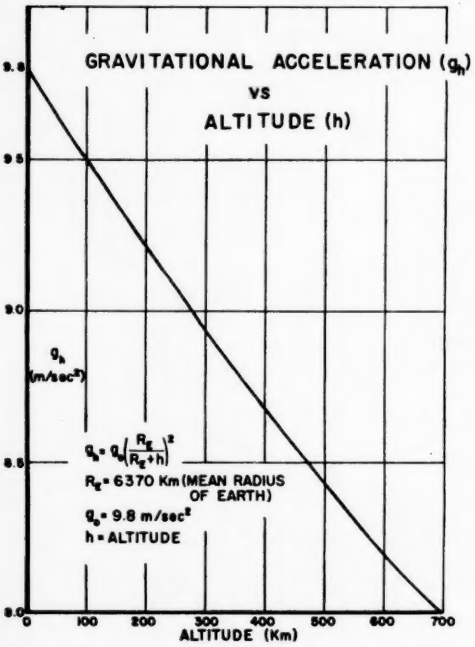

Fig. 3. Decrease of gravitational acceleration (and force) with altitude above sea-level

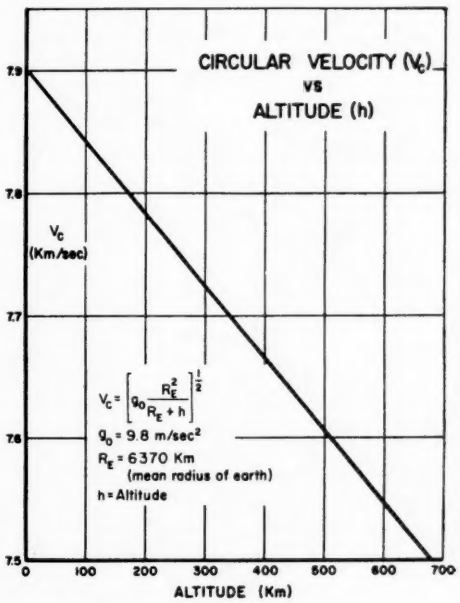

Fig. 4. Satellite velocity in a circular orbit as function of orbit altitude

From (a)
$$(v_L \cos \Delta\theta)\, R_L = v_A\, R_A = v_P\, R_P \tag{9}$$

From (b)
$$G M_E \left(\frac{1}{R_L} - \frac{1}{R_P}\right) = \frac{1}{2}\,(v_L{}^2 - v_P{}^2),$$
$$\therefore\ v_P{}^2 = 2 G M_E \left(\frac{1}{R_P} - \frac{1}{R_L}\right) + v_L{}^2. \tag{10}$$

It is most convenient to solve (9) for $\cos \Delta\theta$ and use (10):

$$\cos \Delta\theta = \frac{R_P}{R_L v_L} \cdot v_P = \frac{R_P}{R_L v_L}\left[v_L{}^2 + 2 G M_E \left(\frac{1}{R_P} - \frac{1}{R_L}\right)\right]^{1/2} =$$
$$= \frac{R_P}{R_L}\left[1 + 2\frac{G M_E}{v_L{}^2}\left(\frac{1}{R_P} - \frac{1}{R_L}\right)\right]^{1/2}. \tag{11}$$

We now define $y_L \equiv \frac{v_L}{v_C}$; because of (7):

$$v_C^2 = \frac{G M_E}{r}, \qquad \therefore y_L^2 = \frac{v_L^2 R_L}{G M_E},$$

and substituting we arrive at:

$$\cos \Delta\theta = \frac{R_P}{R_L}\left[1 + 2\frac{1}{y_L^2}\left(\frac{R_L - R_P}{R_P}\right)\right]^{1/2}. \tag{12}$$

For a nearly circular orbit, $(R_L - R_P)$ is small, and we can write

$$\cos \Delta\theta \sim \frac{R_P}{R_L}\left[1 + \frac{1}{y_L^2}\left(\frac{R_L - R_P}{R_P}\right)\right]. \tag{13}$$

Note that a circular orbit, i.e. $R_L = R_P$, implies $\Delta\theta = 0$.

Presentation of Results

After a number of not altogether successful attempts I arrived at the presentation shown in Figs. 5 and 6. The problem was to make the results of the

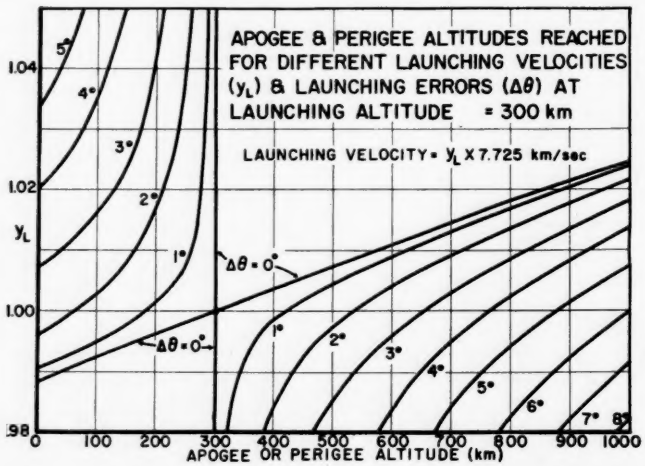

Fig. 5. Graphical representation which allows rapid determination of perigee and apogee altitudes of orbit, given the launching speed (in terms of the circular speed) and the (vertical) angular error $\Delta\theta$ (see Fig. 1). Note that $\Delta\theta = 0$ makes the launch point either perigee (for $y_L < 1$) or apogee (for $y_L > 1$)

preceeding section useful to a design engineer who wants to see at one glance what effect combinations of launching errors have on the perigee and apogee altitude. I decided to use the launching altitude R_L as a fixed parameter[1]; Fig. 5 is for $h_L = 300$ km (187 mi) and Fig. 6 is for $h_L = 600$ km (375 mi). The launching (burn-out) velocity is expressed as y_L, i.e. in terms of the circular velocity corresponding to R_L.

[1] J. JENSEN at the ARS Meeting, Chicago, November 1955, has used a presentation applicable to a range of R_L, if $R_L \sim R_E$.

Examples

(a) If one fixes h_L at 300 km, and takes the launching velocity as 1% higher than circular, and $\Delta\theta = 1^0$ (either up or down), then from Fig. 5: $y_L = 1.01$ intersects the two $\Delta\theta = 1^0$ lines at abscissa values of 260 km and 625 km. These are the resulting perigee and apogee altitudes.

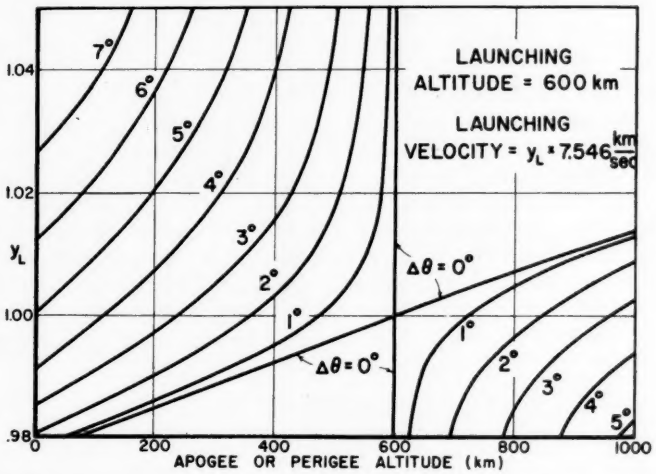

Fig. 6. Same as Fig. 5 but for a launching altitude 600 km above sea-level

(b) If one wishes to keep h_P above 200 km, then $\Delta\theta$ can be $\sim 1^0$. If $\Delta\theta = 2^0$, then we must raise y_L to 1.02, but this results in an apogee altitude of 960 km which may be undesirable.

Conclusion

The advantages of a higher launch altitude are clearly seen in Fig. 6; much larger errors are then allowed. This satellite orbit, however, requires more propulsion, the ascent control problem may be much more difficult, and because of the increased altitude the tracking and radiotelemetering problems for the satellite become more difficult. The results presented here are a convenient aid in arriving at a compromise solution.

It is apparent that it is not necessary or even desirable to try to attain a circular orbit velocity by fuel cutoff; complete burn-out allows larger angular errors in the velocity vector.

Lifetime in Circular Orbit

Introduction

Various authors [3] have considered the effects of air drag at high altitudes in great detail, but no discussion of the lifetime of a satellite vehicle seems to exist in the literature[1]. This may be because designers generally considered quite elaborate satellites or space stations, and placed them high enough to be above

[1] N. V. PETERSEN has obtained results similar to those presented here by somewhat different methods: ARS Preprint 276-55 (Nov 1955); J. Amer. Rocket Soc. **26**, 341 (1956).

any atmospheric effects. When we are faced, however, with the limited means of rocket propulsion presently at our disposal, we must reorient our thinking towards a minimum, unmanned satellite. If properly instrumented, this object can be extremely useful for various geophysical and astrophysical investigations [1]. It would be valuable even if the observations extended over a few hours or days. We will define here "lifetime" as due to atmospheric effects only. In reality, and particularly for longer periods, the effective or useful life may be limited by meteor hits, cosmic ray bombardment or deterioration of components of the satellite instrumentation.

The drag of the atmosphere will change the characteristics of the orbit gradually. We will be interested in deriving the variation of perigee and apogee altitude as a function of time. In this calculation we will neglect all *astronomical perturbations* and consider the earth a perfect sphere. Our justification is the following: For short lifetimes one can generally neglect astronomical perturbations anyway. For very long lifetimes we will consider them (Part III of this series) but neglect the drag. For intermediate cases it would be best to work out particular examples on high-speed computers. But by treating separately drag and astronomical perturbations we preserve a physical insight into the resulting orbit changes, and are able to give better qualitative arguments if, e.g., our picture of upper atmosphere densities changes.

Drag Loss

We will consider a (nearly) spherical satellite of (average) projected area A. A squat cylinder would do equally well. We will consider the drag coefficient C_D appropriate to the molecular flow region as ~ 2. Any errors in A or C_D are completely absorbed by the uncertainty in the atmospheric density ϱ. $\varrho(h)$ is plotted vs h in Fig. 7; its derivation is discussed critically in Appendix II.

The drag force is given by

$$F_D = \frac{1}{2} C_D A v^2 \varrho(h). \tag{14}$$

To appreciate the effect of this drag force on the satellite's orbit, I would like to point out first a fallacy by means of a numerical example: For the case of the MOUSE at e.g. 210 km:

$$A = 0.1\ \mathrm{m}^2, \qquad V = 7{,}780\ \mathrm{m/sec}, \qquad \varrho = 10^{-10}\ \mathrm{kg/m}^3, \qquad m = 20\ \mathrm{kg}$$

$$\therefore F_D = 4 \cdot 10^{-4}\ \text{newtons}$$

The drag deceleration $= F_D/m = 3 \cdot 10^{-5}\ \mathrm{m/sec}^2$.

Multiplying the deceleration by the orbital period at 210 km (5310 sec) one would gain the impression that the satellite loses $1.6 \cdot 10^{-1}$ m/sec in velocity. But this is not correct; in fact the satellite speeds up. What happens is that it loses altitude; this recovery of potential energy overcomes the drag loss and even increases the kinetic energy of the satellite, so that its velocity becomes almost equal (but never quite) to the circular velocity corresponding to the lower altitude. Fig. 4 shows how v_C increases with lower altitude.

Perturbation Calculation

In order to avoid errors we use straightaway a method of energy balance to describe the shrinking orbit.

(a) We first express the total energy (potential with respect to sea-level + kinetic) of the satellite per unit mass of satellite: the total "specific" energy E_{TC} (in a circular orbit), measured in joules/kg:

$$\text{Potential Energy } V: \quad -m\left(\frac{G M_E}{R_E + h} - \frac{G M_E}{R_E}\right) = \frac{m G M_E}{R_E}\left(\frac{h}{R_E + h}\right)$$

$$\text{Kinetic Energy } T: \quad \frac{1}{2} m v_C^2 = \frac{1}{2} m \frac{G M_E}{R_E + h} \quad \text{from (7)}$$

$$\therefore \; E_{TC} = \frac{G M_E}{R_E}\left(\frac{h}{R_E + h} + \frac{1}{2}\frac{R_E}{R_E + h}\right). \tag{15}$$

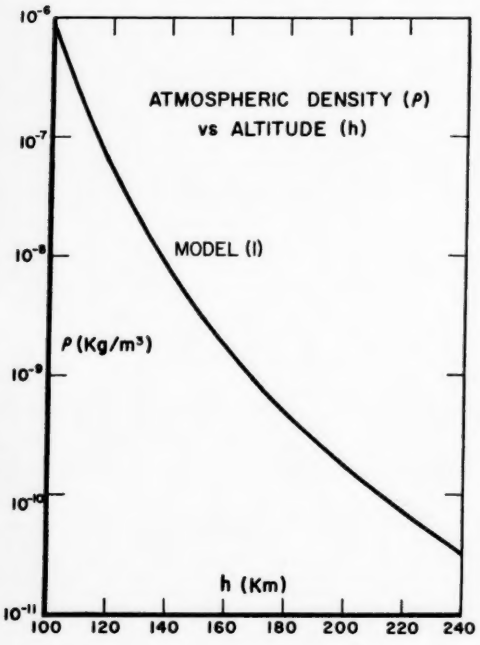

Fig. 7. Density of earth's atmosphere according to Model (1) of Appendix II

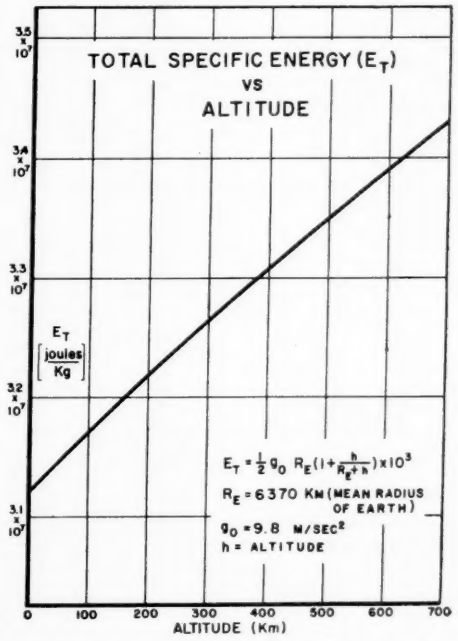

Fig. 8. Energy (kinetic, plus potential referred to sea-level) per unit mass of satellite increases slowly with altitude near sea-level

We can also express (15) as

$$E_T = \frac{1}{2} g_0 R_E \left(1 + \frac{h}{R_E + h}\right) \qquad \text{(see Fig. 8)}^1 \tag{16}$$

(b) Next we express the energy loss per orbit, and using (8)

$$\begin{aligned}(-\Delta E) = F_D \cdot 2\pi r &= \left[\frac{1}{2} C_D A v_C^2 \varrho(h)\right] \cdot 2\pi(R_E + h) \\ &= \pi C_D A (g_0 R_E^2) \varrho(h).\end{aligned} \tag{17}$$

We see therefore that the energy loss per unit projected area depends on h through $\varrho(h)$ only; namely

$$(-\Delta E/A) = 2.5 \cdot 10^{15} \varrho \text{ joule/m}^2. \tag{18}$$

[1] It can be seen that in going from $h = 0$ to $h = \infty$, the total energy increases by a factor of two, first linearly with h, then more slowly.

Note that here is the only place where C_D is used, and that it appears in combination with ϱ. Any slight error in C_D is thus absorbed by the much larger uncertainty in ϱ.

(c) The determination of the change in orbit, and of lifetime is now a very simple process. We use Fig. 7, or an analytical expression for $\varrho(h)$, evaluate $(-\Delta E)$ from (17) and divide by m to reduce it to the specific energy loss per orbit revolution. We then apply this loss $(-\Delta E_T)$ on the plot of Fig. 8 to determine the new altitude after one orbit. (In practice it may be more convenient to take a larger number of orbit revolutions, and use average values of ϱ.)

(d) Note that in our perturbation method we assume that both the energy loss, and therefore altitude loss, are so small that we can use a mean value for h and completely neglect this altitude loss *during* one orbit revolution. Our method breaks down in the very dense atmosphere near sea-level where the energy loss is large, and the altitude decreases rapidly. There we can no longer average over one orbit, but we must apply a step-by-step numerical calculation.

(e) We can express our procedure (c) analytically: By differentiating (16) we have:

$$\Delta E_T = \frac{1}{2} g_0 \left(\frac{R_E}{R_E + h}\right)^2 \Delta h;$$

$$\therefore \quad \Delta h/\text{per orbit} = \Delta E_T \left[\frac{1}{2} g_0 \left(\frac{R_E}{R_E + h}\right)^2\right]^{-1}$$

Expressing $\Delta E_T = \Delta E/m$, and using (17), we end up with

$$\Delta h/\text{orbit} = 2\pi C_D \cdot \left(\frac{A}{m}\right) \cdot (R_E + h)^2 \cdot \varrho(h). \tag{19}$$

In order to study h as a function of time, we remember the dependence of the orbital period on altitude given by (6); then

$$\begin{aligned} \frac{\Delta h}{\Delta t} &= C_D (G M_E)^{1/2} \cdot \left(\frac{A}{m}\right) \cdot (R_E + h)^{1/2} \varrho(h) \\ &= 4 \cdot 10^7 \left(\frac{A}{m}\right) \cdot (R_E + h)^{1/2} \varrho(h). \end{aligned} \tag{20}$$

To obtain the time required to descend from altitude h_1 to h_2, we integrate

$$\Delta t_{12} = 2.5 \cdot 10^{-8} \left(\frac{m}{A}\right) \int_{h_2}^{h_1} \frac{dh}{(R_E + h)^{1/2} \varrho(h)}. \tag{21}$$

Lifetime

We define "lifetime" t_L as the time required to descend from an initial altitude to sea-level. Fig. 9 shows plots of t_L for different satellites[1]; (a) a densely packed one corresponding to a MOUSE or similar instrumented satellite, (b) a large, light-weight "balloon" satellite designed for visibility rather than for carrying instrumentation.

[1] Here we have used upper air densities which are rather similar to Model (4), Appendix II. Fig. 16 gives universal lifetime curves for various density models and any m/A.

Measurement of Air Density

Equation (19) or (20) and Fig. 9 show clearly how observations of changes of the orbit can be used to deduce the density of the upper atmosphere. We see also how the sensitivity of the determination can be improved by suitably designing A/m.

In actual practice it may be easier to determine the change in orbital period, and deduce Δh from Equation (6), rather than to measure Δh directly.

It would appear that the method described here is the only one known at present for measuring densities in the very high atmosphere[1].

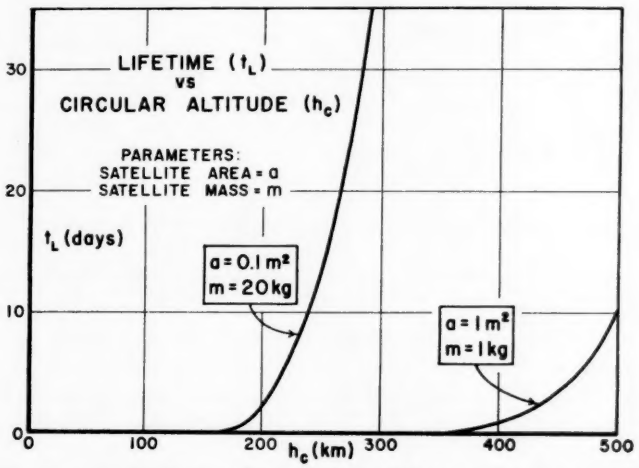

Fig. 9. Lifetime for two spherical satellites of widely differing density. Atmospheric density models (1) and (4) have been used for this graph

Lifetime in Elliptic Orbit

Introduction

As pointed out earlier, the satellite orbit will in general be an ellipse, whose eccentricity (or "elongation") depends on the magnitude of the launching errors. Clearly then, since the altitude now varies considerably over the orbit, we can no longer use the perturbation method applied above to circular orbits. Instead we now introduce a new method based on an impulse approximation. We assume (and this holds quite well for very elongated ellipses) (a) that all of the

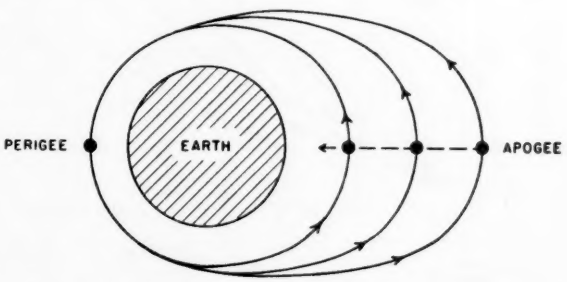

Fig. 10. Schematic diagram showing the change in an elliptic orbit using the impulse approximation of the present paper (i.e. perigee held fixed; the validity of this assumption is investigated in Appendix III)

[1] In a highly elliptical orbit one measures essentially the density of the perigee region only. This is apparent from Figs. 12 and 13 and the accompanying text discussion.

drag loss can be concentrated at the perigee point, and (b) that the perigee remains fixed. We imagine therefore all of the drag is compressed into an

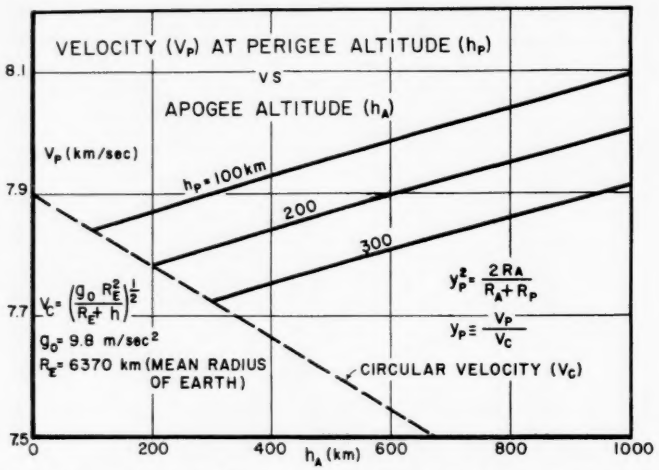

Fig. 11. This graph can be used also to estimate the change in apogee altitude due to a decrease (or increase) in perigee velocity

"impulse" which lasts for such a short time that it changes only the velocity, but not the position of the satellite.

Reduction of v_P, the velocity at perigee, without change in h_P leads to a decrease in the apogee altitude. This is shown graphically in Fig. 10, and can

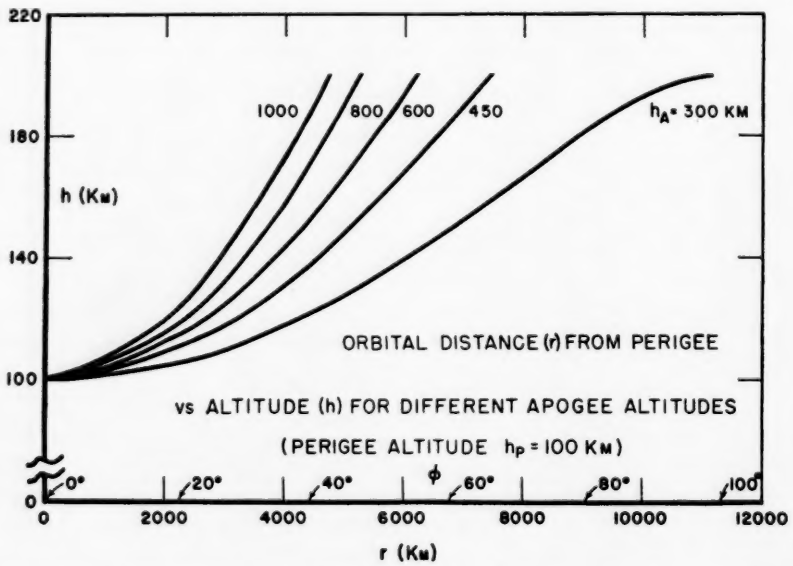

Fig. 12. The satellite altitude along its elliptic path as a function of path length from the perigee point. The graph illustrates how sharply the satellite dips into the dense atmosphere if the apogee altitude is large

be calculated most conveniently from Equations (9) to (13), remembering that $\Delta\theta = 0$ at the perigee and apogee. The results of this calculation are presented in Fig. 11.

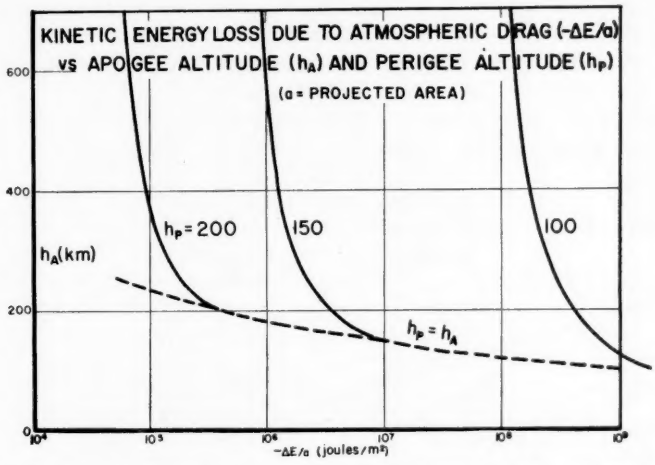

Fig. 13. Energy loss (per unit projected area of satellite) in one orbit; calculated by using the data of Figs. 7 and 12

Impulse Approximation Calculation

We proceed as follows:

1. Find energy loss due to atmospheric drag per orbit.

2. Calculate the new energy, apply impulse approximation discussed above, and find new value for h_A.

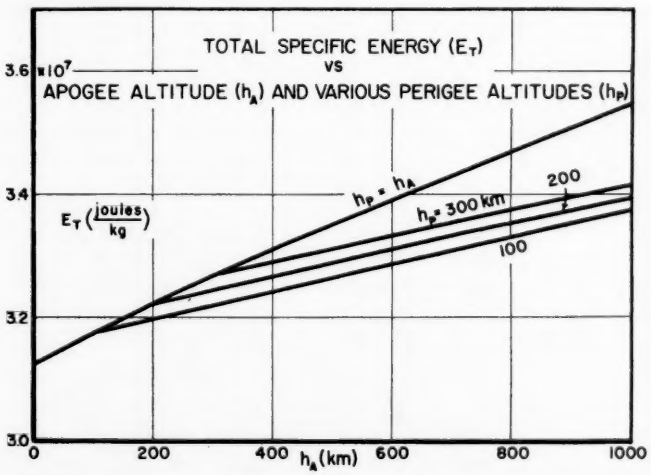

Fig. 14. Energy (kinetic and potential) per unit mass of satellite for elliptic and circular orbits

3. Repeat this procedure until $h_A \sim h_P$. The impulse approximation then breaks down and we return to the circular case.

(a) We first construct the satellite orbit trajectory in the vicinity of the perigee, in the manner shown in Fig. 12. (For the sake of definiteness I have chosen h_P values of 100, 150 and 200 km.) These "dip curves" show how quickly the satellite dips into and leaves the dense atmosphere around the perigee. (We recall that the atmosphere falls off exponentially with increasing altitude.)

(b) We now calculate the energy loss for all the dip curves by integrating (numerically) the drag force (14) over the trajectory. The results are shown in Fig. 13. Note that ΔE does not depend too strongly on h_A (for large values of h_A), but breaks away sharply when h_A becomes $\sim 2\,h_P$. This consideration establishes roughly the region of application of our approximation method.

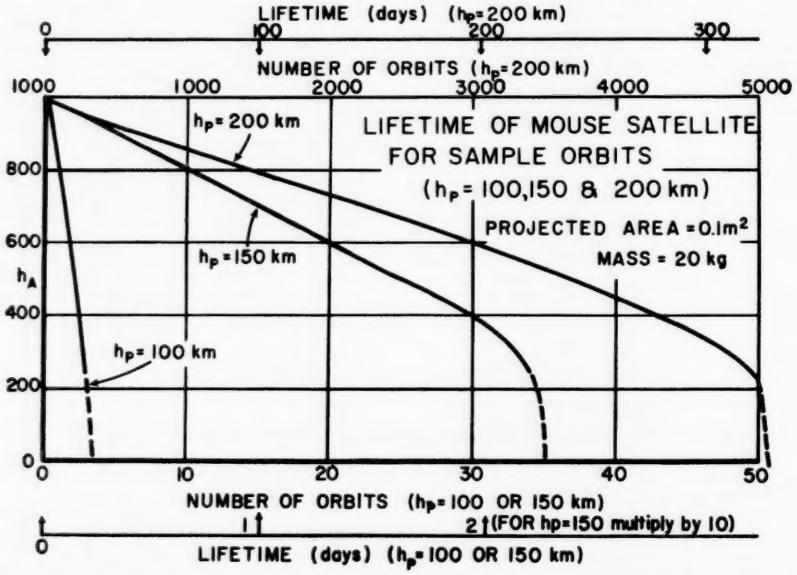

Fig. 15. Lifetime of MOUSE satellite in elliptic orbits with different perigee altitudes. Atmospheric density models (1) and (4), and the impulse approximation have been used to calculate the decrease in apogee altitude as a function of time. (For $h_P = 100$ km use lower scales; for $h_P = 150$ km use lower scales but multiply by 10; for $h_P = 200$ km use upper scales)

(c) As in the circular orbit case, we multiply by (A/m), and apply the resultant ΔE_T to Fig. 14, which shows the total specific energy as a function of h_A and h_P. Here we remember to keep h_P fixed, and slide down, e.g. the $h_P = 100$ km line to find our new value of h_A. $E_{T(ell)}$ is easily calculated using the same method which led to Equation (15), but using $\frac{1}{2} m v_P^2$ rather than $\frac{1}{2} m v_C^2$ for the kinetic energy.

Defining

$$y_P^2 = \frac{v_P^2}{v_C^2} = \frac{2\,R_A}{R_A + R_P} = \frac{2\,(R_E + h_A)}{2\,R_E + h_A + h_P}, \tag{22}$$

$$E_{T(ell)} = \frac{G\,M_E}{R_E}\left[\frac{h_P}{R_E + h_P} + \frac{1}{2}\,\frac{R_E}{R_E + h_P}\,y_P^2\right] = g_0\,\frac{R_E}{R_E + h_P}\left[h_P + \frac{1}{2}\,R_E\,y_P^2\right]. \tag{23}$$

(d) We have calculated (and plotted in Fig. 15) the variation of h_A with number of orbits (and with time) for the three values of h_P: 100, 150 and 200 km, and for a particular A/m. In Fig. 15 we note again how sensitive the lifetime is to the perigee altitude; t_L increases by over a factor 1000 in going from $h_P = 100$ km to 200 km.

Analytical Method

From the general energy relation in an ellipse [Equation (33) of Appendix I]

$$\frac{1}{2} v^2 = G M_E \left(\frac{1}{r} - \frac{1}{2a} \right).$$

We derive by differentiation, and since $T/m = \frac{1}{2} v^2$

$$\Delta a = \frac{2 a^2}{G M_E} \frac{\Delta T}{m}. \tag{24}$$

Assuming no appreciable change in h_P [1]

$$\Delta h_A/\text{orbit} = 2(\Delta a) = \frac{(R_A + R_P)^2}{2 G M_E m} C_D A v_P^2 \cdot \int \varrho \, ds$$
$$\sim \frac{1}{4 \cdot 10^{14}} [(R_A + R_P) v_P]^2 \cdot \left(\frac{A}{m} \right) \cdot \int \varrho \, ds. \tag{25}$$

It is apparent that the slope is again proportional to A/m.
Again we can use Equation (6) to derive

$$\frac{\Delta h_A}{\Delta t} = \frac{C_D}{\pi} (G M_E)^{1/2} \frac{R_A}{\left(\frac{R_A + R_P}{2} \right)^{1/2} R_P} \cdot \left(\frac{A}{m} \right) \cdot \int \varrho \, ds$$
$$\sim 5 \cdot 10^3 \cdot \frac{A}{m} \cdot \int \varrho \, ds. \tag{26}$$

(Here we assume R_A and R_P not much greater than R_E.)

Discussion

Fig. 15 shows the apogee altitude decreasing rather uniformly until a near-circular orbit is attained. This feature is, of course, a result of our approximation. What actually happens is that the perigee altitude decreases also, although much less rapidly than h_A. As pointed out earlier the effect becomes important when $h_A \sim 2 h_P$. But even small decreases of h_P affect the lifetime considerably (see Fig. 15)[1]. We conclude, therefore, that our method holds well when $h_A \gg h_P$ since the greatest portion of the satellite lifetime is spent in h_A decreasing down to $2 h_P$, and the subsequent shortening of the remaining life can be sometimes neglected, e.g. in Fig. 15, for $h_P = 200$ km, it takes 280 days for h_A to decrease from 1000 km to 400 km, with the remaining life only about 50 days, but probably somewhat less according to the reasoning given above. We must, therefore, regard our approximate methods as convenient but rough guides when appropriately used, but we must resort to detailed numerical orbit integrations when real accuracy is mandatory[2].

[1] See Appendix III where we derive the change in h_P.

[2] Note added in proof: Such integrations have been performed by G. E. Fosdick and M. H. Hewitt (Glenn L. Martin Co. Engng. Rep. No. 8262, June 1956). Their results are in close agreement with the results of this paper.

Appendix I:
Basic Relations about Orbits

We start with the equations of motion in polar coordinates

$$m(\ddot{r} - r\dot{\Phi}^2) = f(r) \tag{27}$$

$$m(r\ddot{\Phi} + 2\dot{r}\dot{\Phi}) = f(\theta). \tag{28}$$

We will neglect the atmospheric drag but introduce it later as a perturbation. We, therefore, set $f(\Phi) = 0$, and arrive at a pure central-force law; this is the NEWTONian gravitational law:

$$f(r) = -G M_E m r^{-2}. \tag{29}$$

Equations (27) and (28) are of second order. However, (28) can be written as $m/r\, d/dt\,(r^2\dot{\Phi}) = 0$ and integrated to $m r^2\dot{\Phi} = J = \text{Constant}$, i.e. the angular momentum is constant. (30)

Solution of the equations of motion leads to the familiar KEPLERian ellipse provided the initial conditions are such as to give a bound orbit. These conditions are satisfied if the kinetic energy T of the satellite is less than its potential energy.

The energy integral can be set up as

$$T + V = W = \text{constant}.$$

Where $T = \frac{1}{2} m v^2$

$$\text{and } V = -\int_{\infty}^{r} f(r)\, dr = -\frac{G M_E m}{r}.$$

In order for the orbit to be bound, i.e. elliptic or circular:

$|T|$ must be less than $|V|$; therefore W is negative.

This can be seen from the expression for the eccentricity ε of the conic section (which is the orbit)

$$\varepsilon = \left(\frac{2 W J^2}{G^2 M_E{}^2 m^3} + 1\right)^{1/2} \qquad \text{or} \qquad W = \frac{G^2 M_E{}^2 m^3}{2 J^2}(\varepsilon^2 - 1). \tag{31}$$

For a circular orbit:

$$\varepsilon = 0, \qquad \therefore W = -\frac{G^2 M_E{}^2 m^3}{2 J^2}.$$

For an elliptic orbit:

$$0 < \varepsilon < 1, \qquad \therefore W < W_{ell} < 0.$$

We want to state in detail some important properties of orbits. A body having zero velocity at infinity and falling towards the earth acquires kinetic energy at the expense of potential energy

$$\frac{1}{2} m v^2 = G M_E m \left(\frac{1}{r} - \frac{1}{\infty}\right) \tag{32}$$

where $v = \left(\frac{2 G M_E}{r}\right)^{1/2}$ is now the "escape velocity" since the body follows a parabolic orbit: $W = 0$, as can be seen from (32).

For an elliptic orbit the kinetic energy is less, and corresponds to a fall from an initial circle of radius $2a$ [2] where a is the semi-major axis, so that

$$\frac{1}{2} m v^2 = G M_E m \left(\frac{1}{r} - \frac{1}{2a}\right). \tag{33}$$

Since the body's potential energy is $\frac{-G M_E m}{r}$, its total energy

$$W_{ell} = -\frac{G M_E}{2a} m \tag{34}$$

is seen to depend only on a. It has been shown that the orbital period depends also only on a [see Equation (6)]. Conversely, when the speed at any point r of the orbit is given, W is determined, and therefore, a. The launching conditions R_L and v_L therefore determine $R_A + R_P$, since from Equation (33)

$$\begin{gathered} \frac{1}{2} {v_L}^2 = G M_E \left(\frac{1}{R_L} - \frac{1}{R_A + R_P} \right) \\ \therefore\ R_A + R_P = \left(\frac{1}{R_L} - \frac{{v_L}^2}{2 G m_E} \right)^{-1} = R_L \left(1 - \frac{{y_L}^2}{2} \right)^{-1}, \end{gathered} \tag{35}$$

using

$${y_L}^2 \equiv \frac{{v_L}^2}{{v_C}^2} = \frac{{v_L}^2 R_L}{G M_E}.$$

Note that the $\Delta\theta$ does not enter; only ${v_L}^2$. It is immediately obvious that the eccentricity does depend on $\Delta\theta$, being a minimum for $\Delta\theta = 0^0$ and a maximum (i.e. $\varepsilon = 1$) for $\Delta\theta = 90^0$. Using (31) and by suitable substitutions we derive ε in terms of the launching conditions y_L and $\Delta\theta$:

$$\varepsilon = \left[1 - 2 {y_L}^2 \left(1 - \frac{{y_L}^2}{2} \right) \cos^2 \Delta\theta \right]^{1/2}. \tag{36}$$

Since

$$\varepsilon = \frac{R_A - R_P}{R_A + R_P}, \tag{37}$$

we have now derived our ellipse in terms of the familiar R_A and R_P as functions of y_L, $\cos\Delta\theta$, and R_L.

We can finally express the orbit equation

$$r = a (1 - \varepsilon^2) (1 + \varepsilon \cos\theta)^{-1}$$

as

$$(R_E + h) = R_L {y_L}^2 \cos^2 \Delta\theta \, (1 + \varepsilon \cos\theta)^{-1}. \tag{38}$$

Appendix II:
Upper Air Densities

Values for upper air densities up to 220 km have been given based on rocket measurements[1]. Beyond this altitude all density values are deduced indirectly or arrived at by calculating particular atmospheric models. To get good density values one needs to know the atmospheric constitution and the temperature. It is generally agreed now that O_2 dissociates around the 100 km level and that at 150 km it is present only in its atomic form. Somewhere near this altitude diffusive equilibrium sets in between O and N_2 so that one can neglect the contribution of N_2 to atmospheric density beyond 400 km.

[1] There is some uncertainty about the rocket data beyond even 100 km. Recent measurements by H. FRIEDMAN, Annal. Geophys. **11**, 174 (1955), based on the absorption of solar X-rays give quite reliable density values in the 110–130 km region which are only 1/3 of the Rocket Panel densities.

Vol. 2 1956

The temperature in the upper layers is arrived at from a great variety of considerations: optical observation of night glow and aurorae, radio measurements of scale heights, and computations of the escape of helium from the exosphere. It is thought that the temperature at the base of the exosphere is 500 °K, or even 1000 °K, and may rise to even higher values during solar flares. Above 300—400 km the temperature probably does not increase much further and may gradually approach to that of interplanetary space.

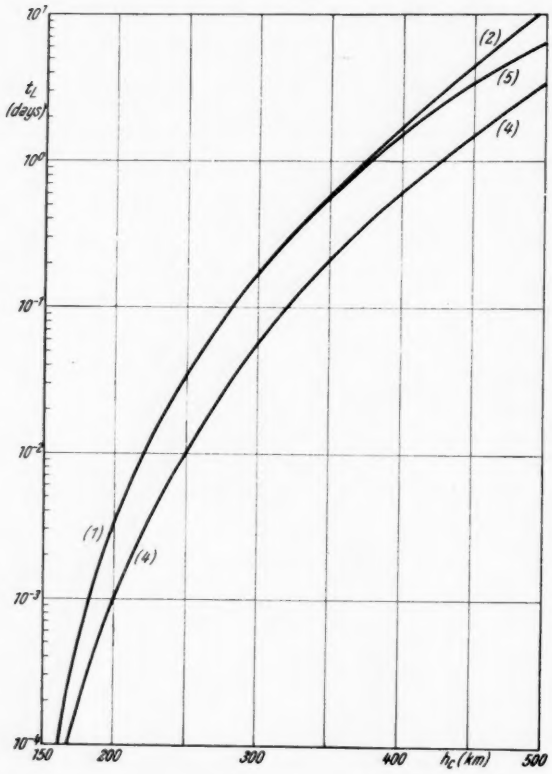

Fig. 16. Universal lifetime curves for circular satellite orbits. The lifetime shown is for a mass-area ratio of 1 kg/m²; to use these curves for any other satellite one simply multiplies t_L by the appropriate value of m/A expressed in kg/m²

The different curves refer to various atmospheric density models (see Appendix II). By observing the change in orbital altitude as a function of time one can measure the atmospheric density. The graph also allows one to select an optimum value of m/A for the test body to obtain the desired sensitivity and accuracy for a density measurement at the desired altitude

There is evidently a great deal of uncertainty in these extrapolations, and it may be hoped that observation of the satellite's orbit will settle not only values of density but, at the same time, many other interrelated problems about the structure of the upper atmosphere. No final conclusion is possible at the present time; only a compilation of values is given, together with references.

Using Equation (21) we have plotted universal lifetime curves for density models (1 and 2), (4), (1 and 5) (Fig. 16). t_L is shown for $m/A = 1$ kg/m²; to use these curves for any other satellite mass and area, one should simply multiply the value of t_L in Fig. 16 by the new m/A.

Compilation of Upper Atmosphere Densities

Model	Altitude (Km) 100	150	200	250	300	400	500
(1)	$8\cdot10^{-7}$	$3.5\cdot10^{-9}$	$1.7\cdot10^{-10}$				
(2)			$1.7\cdot10^{-10}$	$2.6\cdot10^{-11}$	$8\cdot10^{-12}$	$1\cdot10^{-12}$	$1.7\cdot10^{-13}$
(3)			$1.7\cdot10^{-10}$	$2.6\cdot10^{-11}$	$7.5\cdot10^{-12}$	$1.3\cdot10^{-12}$	$4.6\cdot10^{-13}$
(4)		$9.6\cdot10^{-9}$	$6.4\cdot10^{-10}$	$8\cdot10^{-11}$	$2\cdot10^{-11}$	$2.8\cdot10^{-12}$	$6.7\cdot10^{-13}$
(5)			$1.5\cdot10^{-10}$		$7.6\cdot10^{-12}$	$1.2\cdot10^{-12}$	$4.2\cdot10^{-13}$
(6)	$7\cdot10^{-7}$	10^{-9}	$9\cdot10^{-11}$	$2.6\cdot10^{-11}$	$8\cdot10^{-12}$	$1.3\cdot10^{-12}$	$4.6\cdot10^{-13}$

All Values in Kg/m^3

(1) Rocket Panel, Physic. Rev. **88**, 1027 (1952).
(2) D. R. BATES (isothermal above 250 km), in "Rocket Exploration of the Upper Atmosphere", p. 350. London: Pergamon Press Ltd., 1954.
(3) D. R. BATES (isothermal above 400 km), ibid.
(4) S. K. MITRA, "The Upper Atmosphere", p. 582. Calcutta: The Royal Asiatic Society of Bengal, 1952.
(5) M. NICOLET, in "The Earth as a Planet", p. 654. Chicago: University of Chicago Press, 1954.
(6) Present analysis: Based on and extrapolated from FRIEDMAN's data, isothermal above 400 km.

Appendix III:

Analytical Method for Deriving Change in Perigee Altitude

In calculating lifetime in an elliptical orbit we have assumed no change in h_P. For a near-circular orbit we can derive Δh_P by perturbation methods.

From Ref. [2], p. 405, we obtain the effect of a tangential perturbation acceleration T on the orbit parameters a and ε:

$$\frac{da}{dt} = \frac{2\sqrt{1+\varepsilon^2-2\varepsilon\cos\Phi}}{n\sqrt{1-\varepsilon^2}}\,T \tag{39}$$

$$\frac{d\varepsilon}{dt} = \frac{2\sqrt{1-\varepsilon^2}\,(\varepsilon-\cos\Phi)}{n\,a\sqrt{1+\varepsilon^2-2\varepsilon\cos\Phi}}\,T. \tag{40}$$

Since

$$\left.\begin{aligned} \Delta a &= \frac{1}{2}(\Delta R_A + \Delta R_P) \\ \text{and}\quad \Delta(\varepsilon a) &= \varepsilon\Delta a + a\Delta\varepsilon = \frac{1}{2}(\Delta R_A - \Delta R_P) \end{aligned}\right\} \text{from (3)}$$

we get

$$\Delta R_P = \Delta a - \Delta(\varepsilon a) = (1-\varepsilon)\,\Delta a - a\,\Delta\varepsilon. \tag{41}$$

If $\varepsilon \sim 0$, we neglect terms in ε^2; using (39) and (40)

$$\begin{aligned} \Delta R_P &\sim \frac{2T}{n}\,\Delta t\left[(1-\varepsilon)(1-\varepsilon\cos\Phi) - \frac{\varepsilon-\cos\Phi}{1-\varepsilon\cos\Phi}\right] = \\ &= \frac{2T}{n}\,\Delta t\left(\frac{1-2\varepsilon\cos\Phi-2\varepsilon+\cos\Phi}{1-\varepsilon\cos\Phi}\right). \end{aligned} \tag{42}$$

At perigee, $\Phi = 0^0$, and with $\varepsilon \sim 0$

$$\Delta R_P \sim \frac{4\,T}{n}\,\Delta t. \tag{43}$$

We can give some numerical values to illustrate the order of magnitude of ΔR_P.

We take

$$n = \frac{2\pi}{5500}; \qquad T = \frac{F_D}{m} = \left(\frac{A}{m}\right) v^2 \varrho; \qquad \Delta t = \frac{\Delta s}{v};$$

then

$$\Delta R_P = \Delta h_P \sim 4\,\frac{2\pi}{5500}\left(\frac{A}{m}\right) v\,(\varrho \cdot \Delta s).$$

Taking $A/m = 0.1/20$; $v \sim 8$ km/sec

Δh_P/orbit ~ 500 m for $h_P = 150$ km, $h_A = 400$ km

~ 50 m for $h_P = 200$ km, $h_A = 450$ km.

The effect of a change in h_P as against our assumption of fixed h_P becomes important. Its effect on lifetime can be judged by examination of Fig. 15.

References

1. S. F. SINGER, Studies of a Minimum Orbital Satellite, Part I. Geophysical and Astrophysical Applications. Astronaut. Acta **1**, 171 (1955).
2. Any textbook on mechanics or theoretical physics, e.g. F. R. MOULTON, Introduction to Celestial Mechanics. New York: Macmillan Co., 1914.
3. E. SAENGER, and I. BREDT, A Rocket Drive for Long Range Bombers. German Aviation Research UM 3538, August 1944.
   K. A. EHRICKE, On the Descent of Winged Orbital Vehicles. Astronaut. Acta **1**, 137 (1955).

Buchbesprechungen — Book Reviews — Comptes rendus

Technisches Wörterbuch für Raketen- und Weltraumfahrt. Von G. PARTEL. Herausgegeben von der „Associazione Italiana Razzi". VI, 107 S. Roma: Istituto Poligraphico dello Stato G. C. 1955.

„Die Weltraumfahrt ist eine der modernen Tätigkeiten, bei der eine Mitarbeit der verschiedenen Länder notwendiger als je geworden ist. Man hat es darum für besonders nützlich gehalten, ein mehrsprachiges Wörterbuch der Fachausdrücke der Weltraumfahrt, sowie der Raketentechnik, die die Grundlage der ersteren darstellt, herauszugeben...."

Mit diesen Worten beginnt General Prof. CROCCO, Präsident der AIR, sein Vorwort zu dem von GLAUCO PARTEL herausgegebenen technischen Wörterbuch. Es dürfte offensichtlich sein, daß gerade eine Normierung der Begriffe in den verschiedenen Sparten der Astronautik, vor allem aber eine Gegenüberstellung der gleichbedeutenden Begriffe in den verschiedensten Sprachen von außerordentlicher Wichtigkeit ist. Aus diesem Grunde ist das Erscheinen dieses Wörterbuches sehr zu begrüßen. Dieses Unternehmen stellt damit den so wichtigen Beginn von Bemühungen dar, deren Weiterführung nicht nur dem Verfasser, sondern auch allen anderen einschlägigen Fachleuten aufs wärmste empfohlen werden kann.

Vol. 2 1956

Wie der Verfasser sicher selbst gerne anerkennt, ist diese Arbeit ein Beginn, und als solcher noch mit einigen kleinen Mängeln behaftet. Abgesehen von Druckfehlern, die ja jederzeit ausgemerzt werden können, sind einige Übersetzungen von Begriffen leider nicht ganz exakt. Dies ist aber nicht verwunderlich, da wegen der Heterogenität der astronautischen Wissenschaften eine ganze Reihe von Fachleuten an einem solchen Projekt beteiligt sein müßten, sollten die Fachausdrücke in all den angegebenen Sprachen vollkommen klar und eindeutig sein. Als Beispiel sei hier der Begriff „gasförmiges Atomtriebwerk, gaseous atomic reactor", aufgezeigt. In Wirklichkeit sollte dies wohl „gasgekühlter Reaktor, gas-cycle reactor", heißen. Ebenso sind Flächenmaße (trotz Langenscheidts Taschenwörterbuch) kaum „superficial measures", sondern eher „square measures" und „percentuale molare = molarisches Prozent" wird mit „Molprozent" übersetzt. Diese Bemerkungen sind jedoch keinesfalls als negative Kritik an der wirklich sehr schönen Arbeit des Verfassers zu werten, sondern wollen lediglich aufzeigen, in welcher Richtung eine Verbesserung und Weiterentwicklung dieses Wörterbuches erfolgen sollte. Die angeführten Mängel sind für den praktischen Gebrauch insofern nicht von wesentlicher Bedeutung, da sie ja mit Hilfe einschlägiger Wörterbücher vom Benutzer jederzeit ausgebessert werden können.

Aus diesem Grunde kann dieses technische Wörterbuch jedem Wissenschafter und Techniker, der mit den Gebieten der astronautischen Wissenschaften zu tun hat, wärmstens empfohlen werden. H. J. KAEPPELER, Stuttgart

F. Kohlrausch: Praktische Physik zum Gebrauch für Unterricht, Forschung und Technik. Herausgegeben von H. EBERT und E. JUSTI. Unter Redaktion von H. FRÄNZ, W. FRITZ, H. KORTE, E. RIECKMANN, A. SCHEIBE und U. STILLE. 20., vollständig neubearbeitete Auflage. Stuttgart: B. G. Teubnersche Verlagsgesellschaft. Band I: Mit 394 Abb., VIII und 646 S. 1955. Gln. DM 36.—. Band II: Mit 435 Abb., 133 Tab., XI und 765 S. 1956. Gln. DM 52.—.

Jedem Wissenschafter und Techniker, der physikalische Messungen ausführt, ist dieses Lehrbuch seit Jahrzehnten ein Begriff. Der altvertraute „Kohlrausch" hat mannigfache Umgestaltungen und Ausweitungen bis zu dieser 20. Auflage erfahren, die nunmehr fast 50 Teilbearbeitern, 6 Redakteuren und 2 Herausgebern ihr Erscheinen verdankt und eine gänzlich neue Fassung darstellt. Das zweibändige Werk bedient sich der übersichtlichen modernen 10er Numerierung. Der I. Band umfaßt folgende Teilgebiete der Physik: 1. Allgemeines über Messungen und ihre Auswertung; 2. Mechanik; 3. Akustik; 4. Wärme; 5. Optik. Die Abschnitte des II. Bandes sind: 6. Elektrizität und Magnetismus; 7. Korpuskeln und Quanten.

Die Darstellung ist die eines Kurzlehrbuches, manchmal beinahe die eines naturwissenschaftlichen Lexikons, wobei naturgemäß auf besondere Verfahren nur mit Literaturzitaten hingewiesen werden kann. Um Mißverständnissen vorzubeugen: Der „Kohlrausch" stellt kein physikalisches Praktikum oder Handbuch der Experimentalphysik dar und soll auch keines der üblichen Lehrbücher der Physik ersetzen. Vielmehr gibt das Werk auf zusammengedrängtem Raum eine Definition und Übersicht der Vielfalt der häufigst angewandten praktischen Meßverfahren und nimmt so einen gesicherten Platz in der physikalischen Literatur ein. Die Namen der Bearbeiter verbürgen die zeitgemäße Behandlung der Themen.

Auch dem in der Raketentechnik und Astronautik tätigen Physiker oder Ingenieur kann der Gebrauch dieses Werkes oftmals von Nutzen sein, wozu auch die 133 mathematischen und physikalischen Tabellen am Ende des II. Bandes beitragen.

F. HECHT, Wien

Errata

EHRICKE, K. A.: Aero-Thermodynamics of Descending Orbital Vehicles. Astronaut. Acta *2*, Fasc. 1, 1 (1956).

p. 12, Eq. (42), read: $\left(\frac{T_0}{T_1}\right)^{\omega}$ for: $\left(\frac{T_1}{T_0}\right)^{\omega}$;

p. 12, Eq. (45), read: $(\gamma + \cos 2\,\theta)$ for: $(\gamma + 2\cot\theta)$.

Herausgeber, Eigentümer und Verleger: Springer-Verlag, Wien I, Mölkerbastei 5. — Für den Inhalt verantwortlich: Prof. Dr. Friedrich Hecht, Wien VIII, Alserstraße 69. — Druck: Berger & Schwarz, Zwettl, N.-Ö.

The Uses of Artificial Satellite Vehicles[1]
Part I.

By

H. E. Canney, Jr.[2], AAS, and **F. I. Ordway, III[3]**, AAS

Abstract. Possible and probable uses of the artificial satellites are demonstrated and it is shown that the concept of the space station can be essential to nearly every field of scientific inquiry. It is believed that the satellite concept holds promise for significant achievements, specifically in the realization of space flight, and generally in the further unravelling of our knowledge of the universe.

Astronomical and astrophysical advantages of the artificial satellite are covered, and sections are included on the benefits to the biological and medical sciences deriving from a space station. The feasibility of the satellite laboratory for undertaking physical and chemical experiments, and the possibilities of utilizing the orbital vehicle as a site for investigations of the geosciences are then presented.

Zusammenfassung. Es werden die möglichen und wahrscheinlichen Anwendungen des künstlichen Satelliten erörtert. Dabei wird gezeigt, daß die Existenz einer Außenstation für nahezu alle Zweige der wissenschaftlichen Forschung von wesentlicher Bedeutung sein kann. Es ist anzunehmen, daß die Ausführung des Satellitenprojektes sehr wichtige Ergebnisse bringen wird, insbesondere für die Verwirklichung des Raumfluges und ganz allgemein für die weitere Klärung unseres Wissens über das Universum.

Im hier vorliegenden ersten Teil der Arbeit werden die astronomischen und astrophysikalischen Vorteile des künstlichen Satelliten betrachtet und weitere Abschnitte über den Nutzen einer Weltraumstation für Biologie und Medizin angeschlossen. Ferner wird die Verwendbarkeit des Satellitenlaboratoriums für physikalische und chemische Experimente beschrieben und werden die Möglichkeiten angegeben, die das Satellitenfahrzeug als Basis für Forschungen auf dem Gebiet der Geo-Wissenschaften eröffnet.

Résumé. L'article traite des usages possibles d'un satellite artificiel et montre que l'existence d'une station dans l'espace peut devenir essentielle pour toutes les branches de l'observation scientifique. Tout porte à croire que la construction d'un tel satellite sera une étape significative vers la réalisation des voyages dans l'espace et plus généralement vers un accroissement de notre connaissance de l'Univers.

Cette première partie de l'article considère les avantages qu'on pourra retirer de cette station, véritable laboratoire dans l'espace, pour chacune des sciences suivantes: biologie et médecine, physique et chimie, géophysique.

[1] This paper (Parts I and II) was presented as a whole at the Sixth I.A.F. Congress at Copenhagen, August 4, 1955, and has been shortened for presentation to publisher. First version dated June 30, 1955. Since it was prepared before the U.S. Earth Satellite Vehicle Program was announced, it obviously does not reflect development that occurred during the last year and a half. Readers are referred to satellite reports being carried in this journal.

[2] Engineering Division, Bell Aircraft Corp., Buffalo, N.Y., USA.

[3] Guided Missiles Division, Republic Aviation Corp., Hicksville, N.Y., USA. Both authors now with General Astronautics Corp., Oyster Bay, N.Y., USA.

Introduction

The idea of the artificial satellite is not new. It has been considered theoretically for at least 50 years. But for the first time the background of experimentation, as illustrated by late developments in rocket powerplant, guidance, missile and other fields, allows the scientist to seriously view the establishment of the artificial satellite as a project that can be undertaken today.

It is felt that a survey of the usefulness of the satellite vehicle will stimulate further work in the direction of showing why it should be established. That a satellite station is feasible is one thing; that it serves definite scientific purposes, that it can advance many branches of human knowledge, and that it perhaps represents the only possibility of spring-boarding the exploration of the Earth's celestial neighbors is quite another. Its establishment, imperative to the field of astronautical endeavor can be shown to be desirable to many, if not all, of the relevant specialized sciences. The paper gives a fairly detailed account of the variety of uses of the satellite, and comments are presented on their application to these sciences.

In general, the results of this investigation indicate that our scientific knowledge can be given a tremendous impetus following the establishment of even a small, unmanned satellite, and that lifetimes are such as to justify the existence of close orbit minimum vehicles.

The theme of the Sixth International Astronautical Congress, as at the Second in London, is the artificial satellite vehicle. At the earlier congress many papers were given on the satellite and all are either reproduced or abstracted in the proceedings of the congress, published in 1951 by the British Interplanetary Society in a booklet entitled *The Artificial Satellite*.

Mr. L. R. SHEPHERD, in a paper of the same title, sounded a keynote which is perhaps still just as true in the philosophical sense today. "The real value of the orbital vehicle," he said, lies in its importance as an essential springboard in the supreme adventure of interplanetary flight. This without doubt must be regarded as the main reason for the device; all other purposes being of secondary importance."

On philosophical grounds, and on long-range practical grounds, the logic of it is indisputable. On short-range practical grounds, however, it would seem imprudent to espouse this as a formal policy for relations between the IAF itself, the member societies and the public at large. What fires a man's imagination will not necessarily open his pocketbook, though it may help.

The man in the street is likely to have to pay for part or all of a satellite program, since it is hard to visualize any coalition of private corporations big enough to handle it, unless some fairly immediate profit results therefrom. Several related aspects of an early artificial satellite come to mind:

1. What you will consider a successful satellite.
2. What precautions you will take in case the satellite is not successful.
3. What will happen if these precautions fail.

It is not pleasant to contemplate failure, especially in a field already so difficult as to discourage many a man. But it is equally unwise not to be prepared for all reasonably possible outcomes of a line of action.

First, the matter of what you will consider a successful satellite. It is wise, perhaps, to attempt something modest at the outset. In the case of the artificial satellite, even the most unassuming task, if successful, represents a very laudable achievement. The simplest case would consist of a metal or metallized plastic sphere set in orbit, and could be used, by means of observation from the ground, for geodetic triangulation and for experimentation (at least) in the problem of passive communications repeaters, and for navigational reference. What is meant here, of course, is a single satellite, which is hardly enough for scheduled communications, but which should, with proper planning, serve several purposes at once. Geodetic triangulation, a proposition that commands international respect and cooperation, can surely be thought worthwhile as would any reliable aid to navigation. In view of the immediately practical results from such a satellite the third role, that of experimentation, should be highly defensible. Here we have the artificial satellite reduced to its simplest terms and capable of

immediate usefulness. Because of its simplicity it is easier of attainment. *Surely in astronautics, where we have done nothing yet but talk, write and speculate, a small success is better than a spectacular project that failed.* If you will consider a sphere which remains in an orbit for a reasonable length of time, say a few weeks, and which permits some preliminary practice in the applications mentioned, a successful satellite, it would be wise to be content with that for the first time.

This brings us to the second consideration; what precautions you will take in case the satellite fails to achieve or remain in orbit. It is by no means certain that we can now put even the simplest satellite into an orbit, though common sense tells us we can. It is not known, for example, whether the upper atmosphere has tenuous prominences or is essentially flat like the ocean. If prominences exist and are both numerous and large the prospects for a low orbit (200—500 miles) are not particularly bright.

This is a serious matter since the size of a step-rocket system grows rapidly with increasing altitude. Cost grows with size and so do the consequences of failure. Thus, in a sense, the problem is a choice, or, rather, a realistic compromise, between cost and surety. This is one consequence of failure: the discouragement of further backing.

The second source of failure is a malfunction of equipment. Since it is desirable that a satellite be placed in orbit as cheaply as possible, conservation of propellants prompts an attempt to get into the horizontal element of trajectory as soon as possible.

This introduces the possibility that malfunction might bring a rocket step (section) hurtling down on same city in your own country or in someone else's.

Admittedly, the proposition of a misadventure in launching a satellite leading to international incidents touches on a rather remote outcome, but it is at least technically possible, not because of the failure, but because of the circumstances of secrecy which would probably surround the attempt. There is, perhaps, the same remote possibility in the event of success, which begs the definition of success itself. As STEWART ALSOP has said: "The satellite may be harmless, but how would we *know*?" Thus we have at least a technically admissible possibility that the establishment of a satellite at the wrong psychological moment might prompt the attempt to destroy it.

The end of the satellite itself will probably be no serious matter, fortunately, if it is of the simplest type. The consensus visualizes the simple satellite as a metallic foil envelope inflated by a cartridge-fed balloon. Air friction will either ignite it or slow it down to a gentle descent so that serious damage and injury is very unlikely.

Some types of artificial satellites will be passive in nature, and may be any one of a class of simple objects built by man. The range of shape is not necessarily limited but such uses as passive radio communications and navigational references, and geodetic triangulators may, in addition to the mechanical requirements of transport and inflation, dictate that the shapes be simple such as spheres and ogives discharged from rockets. Expendable steps, parts or fragments of multi-section vehicles, may accidentally assume orbits and would thus also be artificial satellites. An expired final section of a rocket which was intended to assume an orbit would also be an artificial satellite. A meteor or planetoid, brought in to assume an orbit, not being an artifact, would not be an artificial satellite but a natural satellite artificially established.

It has been reported (though definitely not confirmed) that two meteoritic natural satellites of the Earth have been discovered. If so, their utility must be doubtful. Any objects that have taken so long to locate would be too difficult to use for geodesy or navigation.

Other types of satellites are active in nature. An active satellite vehicle would carry something, namely equipment and/or crew. It is generally thought of as operationally complete and something of an end in itself. Being active it is capable of sensing elements of its environment and special relationships, and may, further, transmit messages or objects to points distant from it.

In this sense we may include most of the roles popularly ascribed to it such as astronomical and geophysical observation; laboratory experimentation in such

important sciences as physics, chemistry, biology and medicine; and military reconnaissance and combat.

A third type of artificial satellite may be more appropriately thought of as a space station. It is a station in the sense of being a place where you stop *en route* to or from somewhere else, and also a service agency in the sense of a gasoline service station, where you stop for fuel and repair or to avail yourself of facilities enabling you to perform a duty not native to the space station *per se*, such as further travel or construction preliminary to it. If there are a number of satellite vehicles in the locality which depend on the vehicle for an orbital center, or other control and restraint, it may be regarded as a space station in so far as it performs a duty beyond its own immediate nature. If the satellite vehicle is a military base in the same sense as a submarine tender or aircraft carrier it could also be considered to be a space station.

Returning to the utility of the satellite, we see that we must concern ourselves with both use and usefulness, and make this our policy in dealing with the public. The eight sections of this paper which follow attempt to show that the satellite does indeed have utility and that its establishment would benefit both science and the man in the street.

Let us hope that the weapons argument does not carry its usual weight. The appeal to the survival instinct can probably carry if properly made. But then we would buy the space station at the same tragic price that we paid for atomic energy. The appeal that can best be made is commerce, and that the space station, developing the capacities of commerce, benefits the human race.

If we lived in a planetary *Plato*'s republic, we could make directly the appeal that we morally should and get immediate cooperation from the laymen. Since we do not, we must concentrate on applied research in the direction of commercial progress, with pure scientific research present but not dramatized. Obtaining money for pure research in any field is difficult enough. If we appeal directly for money for pure research in a *new* field, we are raising unnecessary obstacles in our path.

Our best appeal will not be easy. Historically the astronautical experts themselves differed as to the practicality of the device. That TSIOLKOWSKI, OBERTH, and NOORDUNG were convinced no one can doubt. All three men went into exhaustive studies on the matter. ROBERT ESNAULT-PELTERIE, a great astronautical scholar, was not so convinced of the satellite's utility. Referring to OBERTH's satellite he said: "Je dois avouer que, personnellement, je ne vois pas tres bien l'utilité de semblables stations." On the other hand, DAVID LASSER exhibited almost uncanny insight when he observed, back in **1936**, that "perhaps by **1950** the brilliant project of HERMANN OBERTH for a station in space may be interesting the world-wide attention of engineers. The proposal of OBERTH to build an artificial satellite of the earth, if found feasible, may provide the mental and physical stepping stone from our conquest of the earth to that of the solar system".

OBERTH's solar mirror was not taken seriously until it was recalled that mirrors can burn. Weapons again. Following the earlier work of the pioneer astronauts, only a rather small amount of literature dealt with the overall uses of the satellite.

Usefulness in the vehicle was usually glossed over completely or a single use was emphasized. This situation changed, however, following the world war, when the true significance of the German rocket effort became even more apparent. By **1949**, we find that several overall surveys of the satellite vehicle had appeared. K. W. GATLAND and H. E. Ross in England reviewed many of the uses in papers published at this time, and subsequently numerous books have appeared on the subject, including one by OBERTH, **30** years after his initial work. Perhaps the most significant, and certainly the most recent, attempt to emphatically demonstrate the usefulness of the satellite station appeared in the American Rocket Society's proposal to the National Science Foundation.

The society explained in the proposal that its charter did not permit formal experimentations under official ARS sponsorship but that it could and would encourage professional people to support and participate in the program. The ARS wisely stated in their proposal: "The satellite should serve useful purposes... purposes whic

can command the respect of officials who sponsor it, the scientists and engineers that produce it, and the community who pays for it."

This paper is not a proposal but an exploration of the general question of utility. Since this is not a proposal we are able to speculate, though, we trust, with restraint.

By virtue of context we may go further into some of the uses, such as astronomical observation, and to discuss other uses the ARS report could not in conscience and logic discuss at all, such as the space station as an aid to interplanetary flight.

Included within the meaning of satellites in this paper are passive artifacts, active vehicles, orbiting service agencies, probes, and way stations established in circumsolar orbits. The eight sections presented are not intended to be either definitive or encyclopedic. The attempt has been one of survey and speculation from the standpoint of utility and to attempt to deduce from it a utilitarian frame of reference from which we can appeal for real support. It is suggested that from such considerations as these we can find a way of approaching the world within the solid framework of commercial progress. The dignity of pure science and the high adventure of the conquest of space will be there. We can scarcely escape them in so colossal an enterprise. Right now we must be practical. To do this we must find a way of showing the world that space flight in general and the satellite in particular are themselves eminently practical.

Vol. 2 1956

A. Astronomical and Astrophysical Advantages of the Artificial Satellite

The advantage of a workable astronomical observatory beyond the atmosphere is almost immediately apparent to anyone having even an elementary knowledge of the science. The existence of particles of matter between an object and its observer reduces the reliability of observation by absorbing or scattering light energy *en route* to the observer. As the distance of transit or the density of the medium, or both, increase, the worse the problem becomes.

On the surface of a planet having an atmospheric envelope the reduction in visibility is very pronounced. This situation is aggravated by turbulence and lack of homogeneity in the atmosphere. These produce, in addition to the scatter caused by the mere presence of a medium, a phenomenon known as shimmer. Shimmer is a twinkling of point-light sources and a dimensional instability of large images caused by an accumulation of local air turbulences encountered by a beam of light on its way to the ground.

Larger activity in the atmosphere causes heavy to total obstruction in the form of cloud overcasts or by transport of smoke or other impurity. When feasible, therefore, astronomers place their equipment in localities where these troubles are consistently less serious... generally on dry deserts or atop high mountains. This is often inconvenient logistically, but is done when the importance of the work warrants it. More favorable climatic conditions permit the use of somewhat larger instruments, and we note that the largest and costliest are generally so situated.

Even in these places, visibility is but slightly improved. Images of Mars, one of our closest planetary neighbors, are so badly fogged that the nature of even major surface features is still in doubt. It is obvious that building larger mirrors and elevating them a mile or so into an atmosphere several hundred miles thick will not help matters much. What is needed is to place the observatory where all the obstruction to visibility is removed. This is impossible even in theory, since above the atmosphere there is still inter-stellar matter, but the atmosphere accounts for 99 per cent of our trouble.

A quick survey of what is to be observed may be considered first. Loosely, astronomical objects fall into five categories: 1. Galactic systems and nebulae;

2. Stars; 3. Planets and satellites; 4. Planetoids, asteroids, comets and meteors; 5. Dust and gas; 6. Auxiliary satellites (future).

The nearest astronomical object is under our feet, so a satellite vehicle viewing the Earth could be regarded technically as an astronomical observatory, provided it viewed the planet more or less as a whole planet. An observatory looking down at the Earth would have the same atmosphere to look through, but this would not be as serious at sea-level observation of Mars because the planet is closer and also conditions at sea-level are already known in considerable detail. Shimmer would not be lessened but it would be less damaging. This observation of the Earth as a planet is something of a technicality in the context of this paper, and we should return, for a moment, to continue our examination of the upward look through the atmosphere.

The atmosphere, as we know, leaves earth-bound astronomers partially "color-blind" [1, 2, 3], as it is virtually opaque to wide (and extremely important) bands of the spectrum in the ultra-violet and infra-red regimes. Filtration in another sense, the absorption of micro-meteorites, prevents astronomers from getting an accurate idea of meteor population in space. Cosmic rays also strike the top of the atmosphere with tremendous impact, producing a partial breakdown of molecular structure and a disintegration of the cosmic rays themselves. Present-day conclusions, based on what we can observe of these rays, may not be entirely accurate, although high altitude research rockets are continually adding to our knowledge. A number of other effects such as the aurora and zodiacal light deserve special consideration because of their possible relation to incoming radiations.

Gravity also takes its toll [2, 4]. Even if the atmosphere were not a problem, the stresses caused by twist and sag in large instruments, especially in large mirrors, suggest that the 200-inch telescope on Mount Palomar may be the biggest earthbound instrument ever to be constructed. This is a rather large statement, but there are grounds for it. Distortions caused by stress place some fairly serious restrictions on how much of the sky can be viewed without spoiling the images due to a twisted mirror. Telescopes must be rotated to "follow" the planets or stars, introducing varying loads to the structure. It may be said that, as things now stand, new rigidity requirements for larger telescopes will soon surpass the ability of materials to meet them.

Another element is cost. Size and location and (inevitably) complexity rise sharply with each attempt to increase performance. Obtaining the money to build the 200-inch telescope was difficult enough to suggest that we are nearing the limit of the private pocket book.

But there is yet another reason to reconsider the observatory. New instruments such as radio telescopes are providing important insights into the general problem of studying the Universe. New insights often lead to reappraisals of perspective, and it is just possible that our present astronomy, which views the Universe through a spectrographic keyhole, as it were, may be pursuing some wrong programs. Recall, if you will, what even the crude Galilei telescope did to Ptolemaic astronomy.

We may find in an extra-terrestrial observatory that we have been pursuing a cosmogonic blunder like Ptolemy's. If we are now faced with physical paradoxes, it may well be that they stem from a too-ready acceptance of such propositions as the absolute speed of light... imposing as that proposition is. It seems invincible now, but so did Ptolemaic astronomy, and it is not impossible that we deal today with a sophisticated descendent of that same type of

intellectual bureaucracy... not in the proposition itself but in a curious new philosophy of scientific sacrosanctity.

Briefly, we may be wise to investigate the satellite vehicle as an observatory before we spend any more big money on large earthbound instruments. It would be grossly unfair to suggest that Mount Palomar was a procedural mistake, but another Palomar telescope, at a time when we can get into space, might be.

The freight costs for placing telescopes outside the atmosphere are very high indeed, but special conditions there reduce the size of the expected rocket payload enormously. In the weightless condition of free fall, for example, a large telescope needs only enough structural strength to maintain its rigidity. It would be so fragile that at sea-level it would immediately collapse under its own weight. In general it would seem that we are approaching the time when we can place in orbit instruments equalling Palomar in power and with a vastly expanded spectrum range... at a price (including auxiliary equipment) which may eventually be comparable to the cost of another Palomar observatory.

The problem of where to place the extraterrestrial observatory is not quite as simple as merely placing it in a permanent orbit outside the atmosphere. As with the location of a sea-level observatory, many factors have to be weighed and balanced off against each other. To a certain extent, placement depends on what you plan to look at.

Observing the Earth may well consist chiefly of weather and geodesy at the outset, and any orbit which would permit these observations should suffice for preliminary observation of the Moon, Sun and Planets. We might have to be content with an Earth orbit for quite a while, since anything more presupposes another step in order of magnitude in space flight itself. However, this vehicle, which during the earliest days of a space station program will probably be an unmanned vehicle, suggests a general class of transponder called "probes" which observe the surfaces of our own and other planets at close range and telemeter coded and video information back to a home base. BURGESS and CROSS [5] discuss a probe to be used for exploring the planet Mars from a circum-Martian orbit. Probes are generally thought of as unmanned, but the presence of a crew would not alter the essential fact that these vehicles observe only and do not land.

Returning to an Earth orbit, it is naturally hoped that a large conventional telescope may be established. What we are after is resolving power to enable us to measure such things as "normal sized" star diameters. Similar qualities of super size and high resolving power are looked for in very large radio telescopes. In both cases good resolving power is bought by enormous size, possible and practical only under weightless conditions.

The telescope in space must be a remotely controlled affair, and should be located directly ahead or directly behind to vehicle housing the technical crew, or certain oscillations (natural to the orbit, however), will set in and render the telescope unmanageable [6]. Also there would be a tendency for the observatory to drift away from the satellite vehicle. This is due to classical orbital mechanics which would cause a cluster or particles released in an orbit to eventually surround the parent body in even distribution like asteroids around the Sun.

Thus it is a serious problem if it is not permitted to attach the telescope to the dwelling station. However, it may be possible to avoid both oscillation and separation by causing the observatory to assume an orbit around the space station... thus becoming a satellite vehicle to a satellite vehicle. The forces at work which could keep the observatory safely in this orbit are not particularly strong, and further, the observatory would find its view periodically blocked by the space station. In the other direction, a large part of the sky would be

obstructed by the huge disc of the Earth. No part of the sky would be permanently obstructed, of course, since the two vehicles are in a circumterrestrial orbit. The complex motions of the two stations together with orbital precession of the nodes and the general pattern of perturbations at large in the solar system may call for a rather awesome system of analog computers and servomechanisms to keep the telescope pointed reliably in the desired direction.

In addition to this, the two stations would be darting in and out of the shadow cast by the Earth, creating a serious problem of optical distortion due to heating and cooling of the mirror and other equipment. This problem may be readily solved by the use of some fairly conventional insulation techniques, but whether these could be applied to a space observatory is not at all certain.

The temperature problem would be eased somewhat if the two stations were put in an orbit around the Sun at a point located permanently in the Earth's shadow, but the presence of the Earth's atmosphere causes the shadow cast by our planet to be extremely fuzzy... so much so that "darkness" in the shadow is not completely dark. Venus would give only an annular eclipse for the same reason [7]. There would be too much local light present in each case.

Mercury, having no atmosphere, might qualify, but this is uncomfortably close to the Sun, which might blanket out all communications with its radiations. A location in an orbit behind Mars or some further planet is thus arrived at through elimination.

An observatory behind Mars, however, is rather far from home and we are faced with the additional problem that there will be times when the Earth would be not only behind the disc of Mars but also behind the Sun. Large distances are involved. It may be that transponders will be needed not only in both trojan points but conceivably in some intermediate circum-solar orbit or at the Earth's trojan points. With this many transponders, however, a means of selection would be necessary to avoid a confusion caused by the same messages arriving at slightly different times due to difference in distances travelled over different routes. It may well be that placing all these transponders is more trouble than they are worth and that placement at the trojan points alone would suffice. One of the two could always "see" the Earth.

Circum-solar orbital transponders seem inevitable if the observatory is for some reason to be located behind one of the outer planets. Trojan-point visibility of the Earth may not be quite enough.

The question naturally arises as to whether the added distance would actually lower solar interference enough to actually pay for the effort. One can conceive of an installation placed so far out that the sun is no brighter than first magnitude... a proposition reserved, no doubt, for the very remote future. The only excuse for this would seem to be the construction of a special optical or radio telescope of staggering dimensions and designed specifically for observation of the farthest galaxies.

The next order of magnitude, an orbit around the center of the galaxy, is too vast to have any significance. The distances involved, the computation of orbits, and the period of rotation are too formidable to mean anything to the human mind. Over and above the physical logistics of observatory placement, there obviously must be some identifiable bond between the work being done and the culture which it serves.

Having examined the various kinds of orbits, one turns to the question of how to get the equipment up there. During the early days of space flight the mere problems of transportation alone will be enough to tax the ingenuity of Man. How you get the equipment up there depends on what is needed, which

in turn depends on what you want to observe... or, more realistically, what you will be content to observe. At the present time the question of what orbit to select is highly academic since we are not finding it very easy to get any equipment anywhere in space in any fashion.

Balloons and rockets are now being used to observe cosmic rays and other visitors from space, the thought being that the higher we go the less pronounced will be the changes wrought by collision with the atmosphere. Balloons remain aloft for extended periods, but seldom exceed 100,000 feet. Rockets go much higher and can observe phenomena hidden to balloons but remain in space only for a matter of minutes. Balloons and rockets which carry passengers are rare indeed and the occupants are usually so busy with the mechanics of flying that they have little time for business-like observing. In neither case do passenger-carrying vehicles go high enough to help matters much. Rockets, because they go further into space than balloons, are accorded more attention with regard to instrumentation and telemetering, and there is widespread speculation that we have within our grasp right now the means for placing some kind of a vehicle in an orbit. One frequently heard voice on the subject is that of Dr. S. FRED SINGER.

Vol. 2 1956

SINGER has noted a long list of observations which could be made from a satellite vehicle placed in a 400-mile orbit [8]. Broadly, they are astronomical and geophysical in character. With proper telemetering (and this art has reached a remarkably high state) an unmanned vehicle at that altitude could gather and relay enormous quantities of data before orbital decay reached any appreciable value.

Instruments are now available to measure infra-red, ultra-violet, X-Ray and primary cosmic radiations. Spectroscopes and GEIGER counters are also found in today's rockets. The incidence of micrometeorites can be measured by examination of pits in a polished plate set into the skin of the rocket. WEXLER [9] has even suggested that if samples of meteoric dust could be captured in space, theories as to its influence on our weather could be tested.

SINGER visualizes his satellite vehicle, the MOUSE (Minimum Orbital Unmanned Satellite, Earth), chiefly as a solar observatory. The latest version is about one cubic foot in volume, and would be simply a special capsule ejected from the nose of the rocket that brought it up to altitude.

Observations of this type, while they do not satisfy our instinctive desire for visual images, can, together with the knowledge we have obtained with poor optical images, enable us to arrive at a large number of valid conclusions by deduction.

We thus see by inspection that where we go, what we send or bring aloft, or what we can do with them, are, for the time-being, at the mercy of limitations to rocket performance. Since there is no logical reason to doubt that, eventually, the rockets will carry very large payloads, we can legitimately turn to the broader aspects of how to get the proper equipment into orbit.

It does seem that the first astronomical satellite vehicle will be very much like SINGER's MOUSE. Following this, there may be a number of stages of development before a first-class observatory is permanently established in space, fully staffed, and producing results. The next step may be an Earth probe, at least partly protected from temperature fluctuations, and which sends optical images of the Sun, Moon, and planets down to sea level by television, or possibly radiofacsimile. The next important step would be the establishment of a manned observatory associated with a dwelling station at perhaps 1,200 miles. The problem of distortions caused by temperature fluctuations may be exaggerated,

but it seems likely that visibility at 1,200 miles will be so improved over sea-level observation that astronomers will sacrifice a number of things to gain what new information they can.

Mirrors measuring 60 inches or larger in diameter probably have too much bulk to be carried by any rocket we could conveniently afford to build, bearing in mind that this would be the smallest of several progressively larger stages. Even if this were not true, such large structures of glass would undoubtedly crack or break under strong accelerations. Several solutions have been suggested.

One is the use of a tesselated mirror... a large mirror consisting of a number of glass blocks fitted together in (probably hexagonal) mosaic like floor tile, bound, ground, figured, polished, silvered, disassembled, brought to orbit in twos and threes and reassembled into a large mirror in space. G. HORN D'ARTURO said, in a paper [10] written several years ago (in which he discussed a mirror built at Bologna Observatory) that "in spite of the gaps between our tesserae, the images we obtain with the tessellated mirror are comparable with those obtained by any of the more usual instruments". He feels that "perhaps a day will come in which tessellated mirrors, five meters in diameter, will be counted among the small ones".

A smaller mirror of perhaps 30 inches could probably be brought up in one piece without breaking, but the main problem out in space is to assure good resolving power. This means longer local length, which demands larger mirrors to gather more light demanded by the longer focal length. Budgetwise, the question is what is the optimum size of mirror considering the cost per pound of payload in a rocket.

Disregarding price, we have seen that large size is possible through the use of incredibly flimsy structures permitted by the free-fall condition, and aiming, for the same reason, will cause no internal stress in the mirror that would distort images. Thus there is no limit of traverse. So although we have probably reached the size limit for terrestrial telescopes, there is no reason why a 2000-inch telescope could not be erected in space with a focal length of some 600 feet. Recently [2] CROSS presented a plan for the construction of a 1,000 inch mirror, in free-fall, using a thermo-plastic material weighing perhaps 150 pounds.

Someone has even suggested telescopes whose focal lengths and mirror diameters were measured in miles. Here the mirror would be made of a very thin sodium foil, and would have no physical connection with the prime focus, although it does seem likely that such an arrangement would probably be co-ordinated by some sort of radar relay servomechanism system.

Conventional mirrors could be silvered in space (which would be an advantage) but there are serious problems to be dealt with in the free-fall space telescope as a whole. Being in free-fall, the observer, because of his bodily movements, could not ride within the telescope, or on it. He could not touch it physically nor come anywhere near it because of heat. The telescope would be chiefly a photographic instrument, as are the largest of the surface telescopes, and all the work of aiming, changing plates, opening shutters, and so on (which in themselves involve weight shifting) would have to be done by remote control.

The observatory itself would not spin, of course, but several authors, among them HERMANN NOORDUNG [11], suggested that the crew live apart from the telescope in a separate spinning station. Solar power would be used by a third element (the "Maschinenhaus") and all three would be connected by cables. Newer designs for space stations nearly all combine the sun power element with the living-area vehicle. Also, had NOORDUNG built his station, he might have found that the cables raised havoc with control over the telescope.

Meteorites, meteoritic granules and dust would make short work of the telescope unless it were suitably protected. If this means full protection by meteor bumper layers, the telescope would be prohibitively expensive. More likely, local protection of the mirror and the prime-focus unit will suffice. In large and very large mirrors it may be necessary to trust to the laws of chance or to try to locate the observatory so as to avoid as many of the showers as possible. A large meteorite, however, will probably destroy anything man could construct. With respect to dust etching of the silver surface, and puncture or destruction by heavy showers, the sodium-foil telescope seems hopelessly vulnerable. Even if all the other engineering problems connected with the erection and control of a foil telescope could be conquered, this vulnerability alone may be enough reason to prevent its ever being attempted. If some cheap solution to the problem could be found, such instruments could be regarded as expendable.

If micrometeorites did not destroy a conventional telescope, they might cause it to vibrate or rock seriously as showering particles arrived. Radio telescopes, however, having less frontal area would be consequently less vulnerable. The nature, intensity and distribution of micrometeorites have been treated at length [12—22], often in papers directly concerned with satellite and space vehicles. It is obvious that the existence of meteoric and micrometeoric material in space will influence the design of manned and unmanned stations, since the possibility of damage by meteorites to long-life satellites is sure to be considerable. Undoubtedly meteor bumper-protection techniques will be tried at first on small unmanned satellites to determine their effectiveness in terms of meteoric intensity, permitting the knowledge obtained to be later applied to larger, more heavily instrumented vehicles and manned stations.

New types of film will probably have to be developed. Film that is sensitive to a widely expanded radiation spectrum may pose a very serious packaging problem. X-Rays can easily penetrate conventional paper envelopes and certain bands of cosmic radiation may easily penetrate lead casing. How then can we keep wideband emulsions from fogging until we can get to use them?

A very large radio telescope, properly constructed in space, could, according to WHIPPLE of Harvard Observatory [6], cover the entire electro-magnetic spectrum from one Ångstrom unit (10^{-8} cm) to 10,000 kilometers. Those unfamiliar with astronomy may not realize it, but this increase in the usable spectrum is stupendous. Against such a range of frequencies, the entire spectrum of visible light is like one single board in a wooden fence stretching from here to Alpha Centauri! A radio telescope capable of apprehending this range is ambitious but the expanded range is so important that it would not be premature to begin theoretical studies on it now. "There is enough work to be done in spectroscopic observations of the stars at these frequencies", says Dr. WHIPPLE, "to keep several such observatories busy for generations".

Spectroscopic techniques in the satellite vehicle, he feels, will be adaptations of laboratory techniques now used *in vacuo* for ultraviolet, x-ray and gamma ray work. In space many electronic and photoelectric problems are solved.

LEY mentioned other uses of the satellite vehicle. The density of interplanetary gas, cosmic dust and micro-meteorites in the Earth's orbit could be better studied. He suggested that continued impact on the hull of a satellite vehicle or orbital rocket would steadily reduce its visual brightness (since it would reflect less and less radiant energy) and would heat up. The rate of temperature rise could be telemetered down to surface receiving stations. Loss of visual brightness could be viewed through telescopes, although the high speed

of transit might require special fast-tracking instruments. The difficulty here, of course, is how to distinguish between etching caused by micro-meteorites and that caused by interstellar particles of dust, ice and gas. These latter probably will not account for very much of the etching, however.

Singer wonders [23] about the shape of the particles, and whether or not they are aligned by some interplanetary magnetic field. If this is the case, mapping the alignments may help to account for any discrepancies or inconsistencies in observations made through the medium. These alignments which are partially responsible for the reddening of light, may conceivably be pronounced enough to give false readings on stellar velocity.

Aller [24] discusses the interstellar medium at great length, and the underlying question seems to be twofold: "How much are stars dimmed by the medium"? and "How much does the medium affect stellar spectra"? But there are others such as the question of how much polarization of light [26] can be measured and attributed to the medium. The interest here is how this matter affects our knowledge of galactic structure. We believe that "in the immediate neighborhood of the Sun (which falls in a spiral arm) the total mass of the interstellar medium is of the order of that of the stars themselves".

It would seem that studies (and perhaps sampling?) of the medium in the Earth's orbit would assist in the over-all investigation. On the other hand, if the dust and other components of the medium have a tendency to gather in space, the same forces of gravity may cause the Sun, Earth, and perhaps even the satellite vehicle on its small way, to create a serious tunnelling effect[1]. We have habitually associated tunnelling with certain types of large stars, but we cannot be entirely sure that this does not occur with smaller bodies. If true, we may think the average density of the interstellar medium to be far greater than it really is.

Other questions, which an astronomical space observatory can attempt to answer, are the following: what is the average density, composition, and kinetic temperature of interstellar gas? How much activity in the solar system can be attributed to solar radiation pressure? Is it possible that hard-to-believe values of red shift are due to an aging of light? — or to a deterioration in light rays after transit through a vast quantity of medium? — or some hitherto-unknown trick of optics not perceivable at the Earth's surface? Getting the right answer naturally depends on asking the proper question, but it is widely suspected that the nature and composition of interstellar matter holds the key to the origin and mechanics of the Universe.

The importance of an extra terrestrial observatory for making long-exposures for the studies of extra galactic nebulae has not gone unnoticed [3]. Such investigations will undoubtedly go a long way towards solving some of the problems of the metagalactic structure. Ovenden pointed out that the whole field of spectroscopic binaries will receive a tremendous boost, since the observatory unhindered by an atmosphere will provide vastly increased observational accuracy. Undoubtedly totally unknown binaries will be resolved and studies may lead to the discovery of extra solar-system planets. In this referenced paper, Ovenden also showed that stellar magnetism phenomenon may be successfully analyzed from outside our atmosphere.

The chief object of study by satellite observatories is likely to be the Sun, and for quite some time to come. The Sun is a reasonably representative and standard star. It is near at hand, as stars go, and a more effective study of the

[1] This ignores radiation pressure exerted on particles, of course.

Sun's composition and behavior permits more reliable extrapolations about stars in general. Solar activity has a profound influence on radio and wire communications, and research here would pay practical dollar dividends in increased efficiency of communications networks.

If the observatory concentrated on solar studies, small special equipment could be developed for the purpose. Corpuscular radiation measurement, and observation of solar prominences, flares and corona would be greatly enhanced. If the satellite were in a vertical orbit (latitudinal) it could carry on a continuous all-latitude surveillance of the solar ultra-violet and X-ray spectra.

SINGER has written on the investigation of the corona by means of rockets [23], and proposes a "follower" device which keeps solar observation instruments aimed at the Sun's disc regardless of the position of the vehicle. TOUSEY [25] has also reported a sun follower, and notes that several one-axis types have been utilized by the Naval Research Laboratory. In the ultraviolet, we know, the Sun acts much like a variable star. Scientists know a little about the changes that occur in the energy spectrum of primary cosmic radiation, which are tied in with Solar activity, but on the other hand, they know less about the emission of ionizing corpuscular radiation since it cannot be directly observed.

Vol. 2 1956

To measure solar ultra-violet and X-ray emission, a set of photon counters was proposed, each sensitive to a particular waveband, including, especially, the important LYMAN-alpha line of Hydrogen at 1216 Ångstrom units. Variations observed would then be correlated with simultaneous observations of the Sun, made at sea level [27]. TOUSEY [25] has discussed methods used by NRL for detecting solar radiation in the extreme ultraviolet, employing photon counters and a thermo-luminescent powder technique (phosphor, $CaSO_4 \cdot Mn$), which "thermo-luminesced strongly after exposure to extreme ultra-violet and X-rays"). As for the photon counters, they responded to the 1100—1350 Å spectral band at 70 kilometers, and "were approaching a maximum value asymptotically at 150 km", which was the limit of the rocket trajectory. While valuable information can be gained from one-shot rocket firings, values are representative only of one place, at one time and for a limited range of altitudes, all such restrictions will be removed by satellite observations.

Decreases in cosmic ray intensity often accompany magnetic storms on the Earth (or vice versa). It is useful to know whether the magnetic storm effect is explainable as an actual deceleration of particles or a decrease in intensity of a given energy level emission. The decreases are real [28], and occur even at the poles, showing that we are dealing with a real decrease (of some kind) in the vicinity of the Earth, and not, as has been supposed, a deflection away from the Earth by a ring-current thought to encircle the globe during periods of magnetic storms. OVENDEN [3] thought these currents to be "largely speculative", and felt that "their actuality" could be "confirmed or denied by electrical sampling by rockets".

Sudden increases on Earth are associated with solar flares, and a set of questions, analogous to those for decreases, come to mind: is a solar flare an acceleration of existing cosmic particles or an increase in the number of particles in a certain portion of the energy spectrum? Why do some flares cause increases and not others? Does the Sun generate additional rays? MENZEL [29] reports that RICHARDSON has "presented evidence that suggests the existence of a great corpuscular stream between the sun and the earth at the time of severe magnetic disturbance". Satellite observatories would establish the nature, intensity, and variations of the phenomenon.

Broadly, the question propounded by Dr. Singer may be interpreted as the following: is the Sun even capable of producing particles with energies as high as those observed in cosmic rays, or does some condition obtain in space to accelerate or decelerate them?

Elsewhere [30], Singer touches upon auroral particles (protons) known to be stopped by the upper atmosphere. He noted that a large increase of X-ray emission during solar flares in different regions of the energy spectrum, if they could be adequately observed, would provide valuable data on how energy is transferred from the Sun's surface to its own outer atmosphere, some 10,000 miles up. Hard X-rays and gamma rays are suspected solar emanations but we cannot observe them directly at sea level. Measurements of a 2.2 mev gamma ray resulting from the radiative nuclear capture of neutrons by protons have been made, and these suggest that there may actually be high-energy neutrons in the Sun.

Another example of the Earth's atmospheric filtration is mentioned by Aller in a discussion of planetary nebulae. The central stars often remain invisible, even on long exposures with special filters. "For a fixed bolometric magnitude" he says, "the hotter the central star, the fainter it will be photographically". This, of course, is because it shines in the far ultra-violet, to which our atmosphere is opaque.

Finally, the combination of solar and general cosmic ray activity has certain geophysical overtones noted by Singer [28]. In discussing an application of MOUSE for the study of the Sun, he proposed the use of ultra-violet and X-ray photon counters to measure cosmic rays as a function of latitude. Geiger counters were also suggested. Cosmic ray intensity was associated with magnetic variations on the Earth's surface again, but in a somewhat unexpected way. Instead of deflection of focusing of the cosmic rays by magnetic fields, which one might suspect because of the operation of cathode ray tubes, he suggested that corpuscular streams squeeze and shape the pattern of lines of magnetic force. Magnetometers should be able to detect these effects and determine if they are transmitted, to some extent, down through the ionosphere to sea level. Moreover, it is strongly suspected that the ionosphere itself generates magnetic disturbances which have repercussions at sea level. It is thus necessary, at sea level, to distinguish between the two. If we had a satellite vehicle located above the ionosphere for purposes of comparison, we could readily do this.

The problems of studying this Sun may be generalized and certainly expanded upon when you consider stars in general. Giants, dwarfs, variables, novae and supernovae and multiples each have their own peculiar problems. Overall considerations of composition, nature, process, and evolution apply to these stars. One question, raised by Whipple [6], concerns the interesting matter of determining the circulation of material in double star systems. Spitzer, like Aller, is interested in color-temperature measurement of hot stars, and also looks forward to an ability to make more accurate measurements of eclipsing binaries [31].

Planetary work can capitalize on telescopes with high resolving power in the 100 to 200 inch sizes for the study of the composition of atmospheres [6]. Here again, photography in the far ultra-violet will come to the rescue. In the case of analyzing planetary surface detail, infra-red light has been used somewhat successfully for Mars [32, 33] but in the case of Venus it "obtained completely negative results". Ovenden [3] emphasized that from a space observatory (he preferred using the Moon) planetary atmospheres could be studied accurately, and pointed out the difficulties we experience making our observations from

Earth. RICHARDSON described the astronomer's woes in "The Atmosphere of Mars" [34], and reviewed some of the techniques used to determine the compositions of planetary atmospheres. A thorough treatment of the Martian atmosphere has been given by DE VAUCOULEURS [35].

KUIPER has suggested an interesting method for attempting to penetrate the dense mantle of atmosphere surrounding Venus. Heat waves, rising up from the surface, should make themselves perceptible to cameras using film especially designed for those frequencies. Assuming that the heat rises more or less vertically, one could get an approximation of the land masses beneath. While this procedure is not strong on resolution of detail, the result will undoubtedly be more enlightening than present knowledge on the subject.

Cosmic rays arrive from space with energies of several billion electron volts and at very nearly the speed of light. These high-energy corpuscular radiations consist largely of protons, helium nuclei, and nuclei of heavier elements... so far as we have been able to determine. Where they come from, and what processes are at large in the Universe to produce such enormous particle velocities, are not known. ALLER thinks they are probably electromagnetic [24], and that perhaps there are magnetic fields in our galaxy which act as an accelerating force. Recent accounts of primary cosmic radiation have been prepared by VAN ALLEN [37] and SWANN [38].

Vol. 2 1956

We do not receive primary radiation at sea level, but detect only the results of primary radiation. Rockets get brief glimpses of these radiations, but what is needed is a continuous survey of the energy spectrum, from 0 to 90 degrees latitude. A satellite vehicle can do this excellently, measuring radiations directly as a function of latitude. Communications with the satellite vehicle itself will tell us much about communications in general, as affected by the ionosphere. The satellite would move with respect to a fixed ground station, and the number of electrons between them will increase and decrease as the vehicle pursues its orbit. Thus we obtain a change in the index of refraction introducing a measurable frequency shift.

Certain observations of our own planet will provide a basis for improved [39] extrapolations, where necessary, about other planets. Measurements of albedo and the Earth's solar heat intake could be measured. Our planet intercepts energy equal to the solar constant at the Earth's orbit times the cross section of the Earth... about 2 calories per square centimeter every minute [40]. Of all energy received, only a given amount is reflected in the visible range. This is about 35 per cent, and is thrown back largely by clouds (whose albedo is 100 per cent). The general percentage is lowered by land values of 15 per cent and ocean values of 4 per cent.

Net energy (incident minus reflected) heats the Earth's surface and atmosphere. Energy influx is balanced by heat loss from the surface and atmosphere according to classical radiation laws. Low temperatures (300 degrees Kelvin) indicate that radiations are in the far infra-red (about 10 microns). Visual albedo on which heat balance calculations depend, can be easily made from a satellite vehicle with photocells. The importance of these data, which will probably enable fairly long-range climatic predictions, is hard to overestimate.

In a recently published article "Horizons in Astronomy" [41], LYMAN SPITZER wrote that he thought the "next important instrumental step in astronomy" would be the space observatory. He went on to say that a modest 40 inch telescope would be able to "resolve objects only one-tenth as big as the smallest object which the 200-inch telescope can now resolve on a photograph", adding that the smaller telescope could pick up galaxies more than five times further

away. "Once astromers get into space", speculates Spitzer, "the whole subject of astronomy will be revolutionized". In astronomy, at least, there can be no doubt about the utility of the artificial satellite.

B. "Biology and Medicine and the Space Satellite"

Some questions in biology and medicine as applied to the satellite vehicle probably seem academic. A. C. Clarke, for example, wonders how micro-organisms would fare under conditions of zero gravity [42]. Would they become giant or freakish? A large amoeba would certainly be interesting to study, if low or zero gravity prompted rapid increase in size. Unfortunately, white blood cells are also somewhat like protozoa. If gravity reduction caused amoebae to grow very large, perhaps the white blood cells would also. This would not be serious unless they grew very large or got lazy. In many generations of human beings, the size of the human body may change if the zero-gravity state is continuous [43]. One can also imagine experiments with plants, observing their rate of growth under the zero-gravity state.

Clarke also thinks that this state would be less of a strain on heart patients. Convalescence and treatment would be more favorable, but the difficulty is the 5—6 G acceleration the patient would probably have to survive in order to get up there.

The mechanics of cell division are related to genetics. Observation of mitosis in zero gravity, perhaps also in the presence of primary cosmic radiation, might be revealing as to what it would tell us about human genetics.

Schaefer [44] and Krebs [45] are particularly interested in this matter of cell division. What effects, they ask, may be brought about by bursts of cell nuclei caused by primary radiation? Genetic repercussions of some kind seem inescapable. Proper shielding from cosmic and other radiation is a serious problem. True, the crews of satellite vehicles must be adequately protected, but lead shielding is heavy and freight costs on ferry rockets are appalling.

Ley [46] seems to be more interested in cellular growth at the tissue level. Would wounds heal more rapidly in free fall? What about amoeba splittings — would they be accelerated? Would mitosis be speeded up or slowed down? These and other questions suggest a wide avenue of research.

Oxygen cycling in the satellite vehicle may depend upon *chlorella algae*. This alga produces 50 times its own volume in oxygen in a hour when exposed to full sunlight [47]. If zero-gravity increases the rate of growth, to which the photosynthetic process is related, the output of oxygen may be increased. The question then arises whether free fall will affect all organs and organisms dealing with oxygen at the same rate in both the ecological and evolutionary sense. On an interstellar voyage, which way would the ecological balance be tipped? Could we rely on every ecology, however small, finding its own balance? Is Nature that friendly?

The photosynthetic part of space ecology, at any rate, is nothing new. Even Tsiolkowski speculated on oxygen cycling by photosynthesis over 50 years ago. What may be new is the possibility that photosynthesis may be either speeded up [48] or done artificially [49]. A recent discovery that adenosine triphosphate (ATP) could be made to operate outside green leaves has set off excited speculation that here is an answer to both the cycling and food problem. Independence of living plants may be an important step forward in the establishment of a reliable and stable cycling system. Large-scale oxygen and food production by this means may be forthcoming in the not too distant future.

Hydroponic gardening may also be possible, and garden leafage would, of course, assist with cycling. This may supplement rather than replace food from ATP. The whole problem of food supply in a satellite vehicle or space ship is a rather serious one because of the alarming volume of matter involved in such confined precincts. The perennial hope of science fiction, the meal in a pill, is very remote indeed, and, even if it were not, the lack of bulk might create serious changes in the human alimentary tract which would set up a dangerous dependence on bulkless food.

A vitally important region of study is that of orientation in the weightless condition. Accomplished at sea level chiefly by the vestibular system in the inner ear, and coordinated by connections to the cerebral cortex, it is assisted optically, and by a kinesthetic apparatus, which "consists of special receptors in the muscles, tendons, connective tissue, skin and viscera, etc." [50]. All related nervous circuits converge on the brain which makes integrations and decisions, and transmits commands to the body to maintain balance and co-ordinated action. Much of the process of orientation is probably based on habit engendered since time immemorial on the basis of gravity, and what might be described as a tension between the body and body's environment. In free fall, this does not obtain, or at least not as fully, and a variety of effects, such as disorientation and vertigo, result. Some elementary work has been done on this, by sending up mice and monkeys in rockets. It is not what we would desire, but it will have to do until science can establish a vehicle in an orbit.

Also, as HABER points out [51], a distinction must be made between real and apparent weight. A variety of forces such as lift, drag, tangential and centrifugal forces (in varying situations) come into play. It is convenient to consider the vehicle separately and assume its weight to be in "equilibrium with a resultant D'ALEMBERT force arising from the centrifugal and tangential forces of inertia". Safety to human vision becomes urgent beyond the atmosphere, as solar illumination there is of the order of 13,000 footcandles [52]. Goggles may have to be nearly opaque in order not to pose impossible demands on retinal adaptation. One of the questions that arises is whether man will be able to withstand abrupt changes in vision — light shocks, as it were.

Work already done on hull temperatures in the outer aeropause is important to the satellite vehicle, which faces an intensified version of most of the same problems. During weightlessness, and with no artificial ventilation, all convection of the air will cease, "and the exchange of the heat of the air, water vapor, respiratory gases, suspended matter, sputum, etc., will be determined entirely by the slow-acting process of heat convection and diffusion" [53]. BEUTTNER notes that the hull of the vehicle will assume equilibrium temperature under the influence of the following components of radiation: 1. Direct solar rays; 2. Reflected solar rays (clouds, Earth's surface, etc.); 3. Thermal radiation of the cosmos (negligible); 4. Thermal emission of the hull of the ship.

"Since about half the heat of the body is lost by evaporation and convection", and since free fall stops this, "the temperature differential between the skin and the environment must be approximately doubled". Inner wall temperatures of about zero fahrenheit are indicated.

These are not the only problems of the closed-cabin environment. Tolerance of the human being to pure oxygen is related to total pressure and to the percentages of water, nitrogen, and carbon dioxide present [54]. Over and above the necessity of maintaining a favorable pressure differential between the environmental air and the lungs, is the nightmare of explosive decomposition. Above

15 kilometers, man has about 15 seconds to live and less than that to save his life in the event of a serious decomposition.

Radiation, of course, is a classic consideration. Cosmic rays are definitely a hazard, as are those of infra-red and ultra-violet, though the degree of hazard has yet to be established. Schaefer [55] pointed out that the exposure hazard to cosmic radiation would be higher along the polar axis due to the weak deflection forces. If there are nuclear sources of power and propulsion in the vehicle, the problem is multiplied. Since the precise nature of primary cosmic rays is not known, it is not possible to guess intelligently as to whether man may fly in space for extended periods of time without receiving fatal dosages. Even if not, one may only surmise whether genetic effects will be induced which are detectable only in later generations [56, 57, 58][1].

Toxicology [59] in a closed environment, such as the cabin of a satellite vehicle, represents a situation not unlike that faced by the occupants of a submarine caught deep under water. In both cases, though precautions will always be taken, there is the constant danger of trouble. A relatively minor and often overlooked hazard in the satellite vehicle is pollution caused by fuel vapors and ozonization and other changes wrought by internal equipment. More rapid and serious are the metabolic surpluses of the human body. Bowel gases (methane and hydrogen) and carbon dioxide from the skin add their toxic products to lung exhalations. Urine and foeces contribute gaseous products and present serious distribution problems which are not entirely a matter of disposal, since their products may be required in some phase of the vehicular ecology. Garbage and used bath water together with unconvertible liquid and semi-liquid body surpluses present a serious disposal problem. Ejected from an airlock, they would explode into a fine mist and surround the satellite vehicle in an envelope.

Excretions from the skin include carbon dioxide, water, salt, urea, potassium and lactic acid, and would no doubt find their way somehow into the general toxic matrix threatening the life and health of the individual. There is also the possibility that harmless matter of certain types, perhaps certain types of living matter, when irradiated by cosmic or other rays filtering through the hull of the satellite vehicle, would generate or turn into toxic chemicals. Putrefactive bacteria are considered toxic.

If plant material is present, such as leafy plants or algae used for oxygen cycling, it should be remembered that they are also living matter and are also subject to the action of certain poisons. Since their action in cycling tends to reduce the general toxicity of an environment (by using in their own vital processes matter which is toxic to other classes of life) any danger to them is a danger to human beings which depend upon them.

In broad terms, we see that the field of biological and medical research performed in and by the satellite vehicle is concerned chiefly with orientation, hygiene, ecology, and medicine. It is unlikely that science can get any very exact data on orientation in free fall unless manned rockets are sent aloft for at least a matter of hours. This demands an orbit, which means a satellite vehicle.

---

[1] As time passes, it may not be necessary to fly in space to encounter significant radiations. Direct effects of the Hiroshima and Nagasaki bombs, added to the general effects of frequent testing of fission and fusion devices, accumulation of radioactive wastes from manufacture, natural radioactivity of the Earth's minerals, and other sources may produce an aggregate radioactivity capable of causing genetic difficulties in the planet's population, such that, perhaps, by the time Man enters space, the further addition of primary cosmic radiations may be less injurious to bodies already somewhat pre-conditioned to radiations.

Many phases of microbiology, microbotany and microclimatology can be dealt with at the Earth's surface, of course, but the presence of gravity introduces a large question mark if one attempts to extrapolate this into the free fall condition. Toxicology and ecology may be similarly treated, and with the similar reservation that gravity probably causes distributions of matter that would not be caused in free fall, especially in air convection.

Some may challenge the problem of zero gravity. The satellite vehicle may be made to spin, they say [60], and the problems associated with a lack of gravity, whether real or imagined, would not materialize. But in some roles, such as astronomical observation, the vehicle may not spin; or, if this were not the case, possibly something might cause the vehicle to stop spinning rapidly or slowly, and eventually stop. It might be hard to re-start, for some reason, and the problem, if not prepared for in advance, could prove fatal.

Since there are many potential hazards to the life and health of the individual in space, there is some wisdom in the philosophy of sending unmanned satellite vehicles aloft to measure such powerful phenomena as cosmic radiations. This, of course, means telemetering and all the sources of potential malfunction and breakdown associated with electronic material. Some suggest meeting the problem gradually by rocket-powered flights in progressively higher and higher trajectories, and insist that more data could be collected than with an unmanned vehicle (since there is less source of error and breakdown), and the vehicle could be returned to the ground to be re-used, repaired, or improved for the next trip. A compromise between cost and human safety will probably be arrived at when the final decision is made to place the first satellite vehicle in orbit. The nature of the compromise will be based on what the scientists will be content to do. Whether the compromise will lean toward the manned or unmanned vehicle remains to be seen.

The world consensus seems to be that an unmanned satellite will be established first, to scout the medium, and will be followed later by Man. Since the whole program would be costly, it is not likely that we will tolerate steps which are too small. The world could go bankrupt by being too cautious. In the manned vehicles, most of the work will bear rather directly on long voyages through interplanetary space, since any improvement in the performance of a space station will probably improve the preliminary design of space ships. And if life is possible on space satellites, a long step will have been made towards deep manned space voyages.

Interstellar flight is almost certainly in the remote future, but problems in such tremendously long trips may be studies profitable for perspective. The longer the trip, the more nearly a space ship must resemble a self-contained planet ecologically, and on a star ship, the post of Surgeon General (or equivalent) would be a vital one indeed. Ecology is the fundamental link with the satellite vehicle, and the fundamental factor in long voyages, even to near planets.

Space medicine is already a recognized entity in the United States, and the systematic study of phenomena specifically intended for, directly related to, the manned satellite vehicle is now underway. A few years ago this knowledge would cause surprise; today it surprises no one. However, space medicine is hampered by the fact that zero-gravity cannot be synthesized, and can be attained only for a matter of minutes, in actuality, in ballistic trajectory flights of rocket-powered aircraft. The only way to solve this problem that one can now visualize, is to establish a manned satellite.

In conclusion, then, it may be said that the biological and medical work done in the satellite vehicle performs two key functions... to determine the conditions

for, and to establish, the habitability of manned vehicles, and by so doing, to develop the medical and ecological knowledge required for long, practical voyages in space.

C. The Artificial Satellite as a Laboratory for Physical and Chemical Research

In view of the conditions of pressure, temperature and free fall which are available to researchers, one would expect the literature of astronautics to be rich in speculation upon what physical and chemical scientists could do in a space station. There is practically nothing on the subject.

Pressure and temperature in space are very close to zero absolute, and much closer than Man has ever been able to get in the best laboratories. By the concentration of light on the one hand, and blocking it completely on the other, extreme temperature values would be obtainable close to one another. Zero gravity doesn't exist anywhere in the Universe strictly speaking, but the condition of free fall, available conveniently in orbits not too distant from the surface of the Earth, is as good as zero gravity for all practical purposes.

A number of interesting possibilities do come to mind, which would bear further study... and they fall generally in those aspects of physics and chemistry which are not typical astronomical considerations, such as solar energy levels, which are closely related to both physics and chemistry. The temperatures of metallic and coated space vehicles in various orbits could be determined, and temperature drops could be observed as they passed into the shadow formed by Earth [1]. What materials could hold up on abrupt and continuing temperature changes? What influence would micro-meteoric bombardment have on the temperature shock resistance of such materials? Such practical problems could be worked out from an orbital space station.

Weights represented by flywheels, for example, tend to cause their shafts to concentrate their friction wearing on the bottoms of journal bearings if there are no applied loads in other directions. In free fall, again assuming no loads, the friction wearing would be evenly distributed around the bearings and the mechanism would last longer.

A practical analogy to this type of mechanism is the electric motor. The momentum of the armature is less pronounced, but in free fall the slightly reduced friction would probably result in a detectable increase in rate of rotation. If cooled slowly and allowed to float outside the vessel it might speed up considerably. Very low temperatures improve the conductivity of metals, or, to put it another way, reduce resistance to the flow of electrical current. At a given voltage, current flow rises as resistance is reduced. At zero absolute, resistance dwindles to zero and current flow is theoretically infinite. Since zero absolute is never quite attained, even in space, current flow will never be quite infinite, but could easily go high enough to burn out the windings.

In electronics we observe that large voltages are required in cathode-ray tubes to drive the stream of electrons to the screen. This may be "the nature of the beast", but do we know for certain that in the hard vacuum of space this might not be the case...? In any event, the ability to dispense with vacuum seals in space should simplify experimental procedures in a number of ways. Clarke [1] has spoken of large scale vacuum research laboratories in space, suggesting a wide variety of possible experiments, and involving large mean free paths, difficult or impossible to duplicate on Earth.

Low-carbon steel, at a temperature of $-450\ ^{0}\mathrm{F}$, is known to increase five times in strength (in terms of normal or room temperature), but it also becomes

very brittle. At the same low temperatures dielectric materials as sapphire will attain thermal conductivity some sixty times that of copper at room temperatures, while metals like gadolinium exhibit magnetic properties several times more ferromagnetic than iron at room temperatures. Incidently, this metal ordinarily shows no unusual magnetic properties.

Making weight measurements in terms of Earth gravity may appear a rather difficult matter, but there seems no reason why this could not be done by placing the item to be weighed in a special scale mounted in a centrifuge spun at an exact number of revolutions per minute. Also, some experiments may capitalize on some such equipment which would permit testing a certain effect at various gravitational equivalents.

In conventional chemistry, we may discover that gravity has an effect on the point at which certain salts go in or out of solution, or where certain reactions might or might not occur, depending on the strength of gravity. In free fall, crystals may be induced to grow larger... perhaps in new shapes (which would probably jolt the science of crystallography)... and, if so, new axes might be possible, and a new species of piezo-electricity, or an increased level of the old kind. A typical problem to be investigated here would involve the intermolecular forces of attraction and repulsion, and their relationship to gravitational attraction. LEY [12] thinks that in space the chemist may find out how zero-gravity affects molecular arrangement, which could result in new branches of science growing out of such findings.

If we mix together two chemicals, a strong acid and a strong base, we expect and get a brisk result. What happens if each is frozen solid to zero absolute (complete quiescence) and then brought together or, are these matters totally irrespective of temperature? What happens with two thoroughly frozen masses? Does the reaction refuse to start or start with local excitation?

D. The Geo-sciences and the Artificial Satellite

Inasmuch as the geo-sciences treat the agencies which pertain to the Earth and its atmosphere, this study, as applied to the satellite vehicle, may be regarded as a highly specialized type of astronomy dealing with the Earth as a planet, and may be thought to include, broadly, meteorology, geodesy, geology, geophysics and geomorphology.

In the meteorological aspect, geophysics verges on astronomy proper, since the outer reaches of the atmosphere are exposed to the conditions of interplanetary space. As noted in Chapter A, energy arriving from space, especially the Sun, impinges on the gaseous envelope, causing both physical and chemical changes. Cosmic radiations are believed to affect or be affected by the Earth's magnetic field, and this interaction causes a chain of effects felt even at the surface of the planet.

Measurement of densities of the upper atmosphere would be possible by observing the drag decelerations [30]. If the "top of the atmosphere" is essentially flat, the deceleration should be fairly regular; if wispy prominences extend vertically for many miles, the deceleration would be sporadic. This question may be rather important, for re-entry by ferry rockets built for atmospheric braking could be a hazardous affair if atmospheric prominences were large in size.

Changes in orbits could be studied. An elliptical orbit whose perigee grazes the atmosphere, for example, will slowly approach circularity. Knowing the type of orbit and the area and mass of the satellite, the rate at which the orbit approaches circularity could be computed.

Prof. SINGER, who suggested these orbital measurements, has also brought forward the proposition that a phenomenon known as the "twilight flash" could be more adequately observed with the aid of a satellite vehicle which exhausts a trail of sodium vapor.

This flash is observed as an emission, a yellow *D*-line of sodium in the spectroscope. Chemical reactions in the upper atmosphere induced by solar energy lead to the emission of light. At twilight, the lower atmosphere is dark while the upper is lit by the sun. Under these conditions, the few sodium atoms of the upper atmosphere, because of resonance radiation, exhibit the characteristic sodium line very strongly. Now, if a satellite vehicle were to exhaust sodium vapor into the upper atmosphere so as to produce a defined trail of sodium atmosphere, this trail would, in turn, exhibit a defined trail of sodium emission light. Since, as SINGER points out, the sodium atoms are subject to collision with other atoms, they will soon cool down and share their temperature. From the spreading of the trail, therefore, we would be able to deduce the existence of winds in these rarified regions.

Determination of mean free path is an important task in arriving at the true temperature for a given altitude. The mention of mean free path brings to mind the fact that gas molecules and atoms are continually escaping from the atmosphere. It may prove important to measure exactly the rate of escape for the planet as a whole. It is believed, for example, that free hydrogen atoms escape into interplanetary space at the rate of 10^8 per square centimeter per second [61].

SINGER's MOUSE vehicle, it would seem, could do all of these things, in addition to radiation and magnetometric observations. With the sodium trail gone, and the batteries dead, the empty hulk would still be useful in the computation of orbit changes. This 50-pound cylindrical vehicle is visualized as pursuing a 200-mile orbit with a 90-minute period for about one month. In its one-month stay, MOUSE would contact an airplane at the North Pole 16 times a day for three-minute periods. The information to be gathered is so important, says SINGER, that even if the MOUSE began to deviate after only a few circuits of the Earth, it would already have paid for itself.

Four thousand miles has been suggested by Dr. HARRY WEXLER of the United States Weather Bureau as the best altitude for a meteorological observatory [9]. Meteorology is chiefly a matter of prediction. Prediction is based on the three-dimensional state of the atmosphere as to pressure, temperature, wind, humidity, clouds, precipitation, etc. This is presently accomplished by a system of ground observing stations and the use of balloons... signals being sent back from the balloons as they ascend through the air levels. These are plotted in symbols on a chart to give an instantaneous picture of the area in question. Knowing this, weathermen can extrapolate future conditions. Unfortunately, there are large areas covered by oceans and wasteland which are incompletely observed.

A satellite vehicle, although contributing nothing by way of pressure, temperature, humidity and wind fields by direct measurement, would give a good bird's view of a large tract of the Earth's surface at any one time, and would act as a storm patrol by observing the Earth's surface and cloud formations. A major cyclonic storm cloud, visible from above, will be the warm front cloud from which the major portion of the storm's precipitation usually falls. Typical gradations and interpenetration of forms can be identified.

Although incipient storms will be hard to spot of themselves, the tendency of all cyclonic storms on the North American continent, for example, to arrange themselves in families with certain spacing and directions, will enable their

existence to be inferred from known patterns. Cloud "streets" of bright cumulus from two to eight miles in altitude can indicate the direction of winds. WEXLER outlines the desirable properties of a satellite weather station roughly as follows:

1. High enough to view an area the size of the North American continent and some of its adjacent oceans.
2. Low enough to permit geographical features to be recognized.
3. Move so that any cloud system can be viewed twice in each 24-hour period, to permit tracking of associated storms.
4. Move slowly enough that cloud systems can be related to terrain.
5. Cover the entire earth by daylight at least once daily.
6. Should have a westward component of motion for spotting new storms, which generally move from west to east.

Such a vehicle would circle the Earth every four hours and describe a series of curves as the planet turned under it. Assuming no external perturbations, the orbit would be preserved. Because of its special curved path, the rotation of the Earth would cause the vehicle to be over all latitudes at noon local time, as it proceeded northward. It would then cross the pole and proceed southward over all latitudes, local time, at exactly midnight, for the same reason. In 24 hours the vehicle would have returned to its starting point.

In preparing a typical chart from observed data, the meteorologist first enters the normal noontime illumination of the Earth's surface of the Sun. Next, brightness of the field of the Earth (before passage of reflected light up through the atmosphere) is obtained by multiplying local surface illuminations and albedoes. This is not easy, as there are many and subtle variations.

Next, values of the Earth's intrinsic brightness is established by determining the brightness of the Sun and subtracting from it the dimming caused by the atmosphere. Next is computing the atmospheric contribution to brightness of field at the vehicle, by estimating the downward diffusion of sunlight and the upward diffusion of earthlight by the same assumed fraction. The two brightness values... from the Earth and from the atmosphere... are added together to give a total brightness.

Color contrast of objects on the ground is suppressed by the selective scattering of blues by the atmosphere itself, and the dilution (whitening) of all colors by foreign particles in the air. In general, the ground would have a bluish tinge below, and at the horizon, gray near the ground (10,000 feet), a thin blue line (RAYLEIGH effect — scattering) and then black above that.

Having established nominal values for cover illumination, albedo, and atmospheric effects, and knowing the typical cloud albedoes from accumulated experience with the satellite vehicle, their brightness could be computed and these results plotted on the chart over the previously-determined brightness values for the ground over which the clouds lie.

The result will be a fairly reliable representation of light and dark areas from which cyclones, fronts, cloud "streets", and other classical phenomena can be inferred. Cyclones would be marked by cloud concentrations, and anti-cyclones (high pressure areas) would be quite clear. Cloud "streets" would be more numerous over seas than over land. Today these distributions are inferred from data taken at widely-scattered outposts by Dr. WEXLER and his colleagues, who prepare a series of weather maps by dint of sheer heroic patience, attention to detail, and dogged integrations and extrapolations. In the space station, if the method of developing plots of light values can be perfected (and there seems no reason why it could not) the advantage of the satellite vehicle for meteorological operations becomes abundantly clear.

Dr. WEXLER points out that there are pitfalls, however, even when one is equipped with such a weather station. The four-hour circuit of the Earth permits tracking of a well-defined storm. Three fixes could be obtained in a 12-hour period. But since clouds obscure ground details to associate them with, and hinder edge-tracking by the fact the masses may change shape or start dissipating from the edge you are sighting with, the accuracy may not be too good. This is compensated for by the fact that large storms move slowly whereas young storms, although they move more rapidly, cover less area and are easier to plot. The eyes of hurricanes, cold front, and line squalls are also easy.

Another element, the Earth's own orbit, will cause the vehicle to cross each latitude about four minutes earlier than the preceding day. In six months the station will have reversed its previous apparent motion with respect to a given area, going north at midnight and south at noon. Midway between these times the station will pass over this same given area at dawn and dusk. In view of these variations of efficiency, Dr. WEXLER suggests a cycle based on a noon-time base point of December 21st, permitting the best observation of the Northern Hemisphere during the winter time when it is most needed.

An unmanned vehicle could relay cloud pictures back to Earth by television. A manned station could add valuable geophysical and solar data such as Earth surface temperature, precipitation, and freezing-level heights which could be measured by radar. Thunderstorms could be spotted by lightning flashes at night or electronically by day. Solar radiations could be related to weather, if there be any relation. Long range albedo records could be correlated with variations of climatic change, and permit a more accurate estimate of the cycles of the ice ages and intervening warm periods. Collection of meteoric dust samples would permit testing the theory that this dust, entering the atmosphere, especially after meteoric showers, acts to seed terrestrial clouds and thus increase rainfall. In short, Dr. WEXLER concludes that a properly moving satellite would be of immense value as a weather patrol for short-range weather forecasting, and a long-term collector of data for solar and geophysical studies. And since on meteorological conditions depends the general appearance of the Earth [62, 39] a satellite vehicle would enable man to obtain an overall view of our world as a planet.

Related to the measurement of orbital changes suggested by SINGER is the proposition of geodetic triangulation of TOMBAUGH [63]. The period of a satellite in a circular orbit at 1075 miles would be known with extreme accuracy after a month's observation. The "satellite search" technique (similar to that used by the United States Government satellite detection project operating at White Sands and Mt. Wilson) would permit the determination of accurate distances and azimuth angles. With a complex triangulation network, positions of the station could be gotten to "within a few feet with respect to points thousands of miles apart". TOMBAUGH feels that this contribution to geodetic triangulation, alone, would justify the establishment of a small unmanned artificial satellite.

ROSEN shows that the satellite need not be expensive. In fact, he speculates that the first satellite will "consist merely of a large but lightweight hollow sphere, capable of being observed from the ground" [64]. Such a sphere, when tracked, would allow accurate measurements of the size of the Earth, its shape, and the intensity of the gravitational field. Outcomes of this, he suggests, are improved mapping and all-weather navigation at sea.

The average value of "*g*", the gravitational pull of the entire Earth, is unknown. The shape of the Earth, especially with regard to its oblateness, is still incompletely known. The two considerations are related. Objects at the

equator are lighter than at the pole by one pound in 290. This is due largely to the rotation of the Earth (centrifugal force) but also, slightly, to the fact that such objects are farther from the center of attraction (oblateness). "As the variation in the gravitational constant is known from the equator to the pole, the determination of one good value for "*g*" will permit the computing of acceptable values for any place on Earth" [65]. Geophysicists today explore and map the Earth's gravitational field with the aid of gravity meters. Local anomalies, manifest by the rate of change in acceleration, often help to locate oil deposits. An artificial satellite would help establish the exact gravitational constant. This would make local anomalies more significant and productive and result in the saving of millions of dollars new spent annually in exploratory digging.

LEVITT notes several practical outcomes of triangulation with the satellite vehicle using a search technique such as that proposed by TOMBAUGH. At 200 miles altitude (a much lower figure than any of TOMBAUGH's orbits) LEVITT figures that a ten-foot sphere of thin aluminum would appear as a first magnitude star. An ephemeris could be plotted from measurements taken against the background stars by the aid of computers, and once the orbit had been precisely determined, the vehicle could be used for triangulation over vast distances with vast savings of money. Today, expeditions are sent out to "run arcs", such as that to close the 30th Meridian last year, and are very expensive. A satellite beacon would reduce the costs to those of observation and time in the computing machines. Accuracy would be increased tenfold, he says, and would permit, for example, measuring the width of the Atlantic Ocean to within 100 feet. Similarly, vertical measurements of height above sea level, now complicated by the mutual attraction of the water and land, would be improved. Errors today may run between 45 and 180 feet.

Another field of Earth exploration is magnetometric surveying. Our planet is a large but irregular magnet whose intensity of field varies considerably from place to place. Magnetometers are used to measure these anomalies, some instruments sensing vertically and some horizantally [66]. Geologists put these meters to a variety of uses, notably petroleum prospecting.

The unit of intensity of the Earth's magnetism is a gauss, which is the intensity of a magnetic field that acts with a force of one dyne upon a magnetic pole. The gamma (1/100,000 gauss) is the unit used in magnetometric surveying. For oil or gas surveys, a magnetometer that measures vertical magnetic intensity is used. Variations from normal indicate the presence of certain characteristic geologic masses in the crust of the Earth [67]. A negative anomaly is where the magnetic vector is directed away from the Earth, and a positive anomaly where the vector is directed towards it. Rocks vary greatly in their susceptibility to magnetic flow and comparison of specific flux densities with a standard value permits a fairly reliable interpretation of local and regional magnetic anomalies.

Magnetometric surveys may be made aloft as well as on the ground, and this, of course, includes extreme altitudes represented by the orbit of a satellite vehicle. Here, however, some correction may be needed, as it has been suspected that there is some interaction between cosmic rays and the Earth's general magnetic field in such a way that changes or fluctuations may be transmitted down to lower altitudes and even to the surface. If this is the case, it will be necessary to establish the nature of the changes produced in order that readings taken in orbit may be converted to useful indications of deposits below. Work done in mapping gravitational anomalies at high altitudes and in orbit may

also be combined with magnetometric surveys to sharpen the accuracy of indications and further reduce the cost of prospecting for petroleum.

With careful planning, it should be possible to design a satellite vehicle of the unmanned type which could make systematic observations in several branches of geophysics at once. Some information could be telemetered to the ground receiving stations and other information inferred from triangulation readings taken upon it both before and after the internal power has expired. Even if the orbit were not permanent, it is easily appreciated that a vast amount of data could be collected before the vehicle finally came down. It need not be permanent to pay for itself.

References

In general, references have been keyed to as few sources as possible, and to sources readily accessible to the astronautical reader. In the case of space medicine, for example, while dozens of papers in such medical journals as the Journal of Aviation Medicine were consulted, in as far as possible the reader has been referred to papers in a compilatory book, i.e., one source.

1. A. C. Clarke, Interplanetary Flight. London: Temple Press Ltd., **1950**.
2. C. A. Cross, Extraterrestrial Observatories — Their Purpose and Location. J. Brit. Interplan. Soc. **14**, 137 (1955).
3. M. W. Ovenden, Astronomy and Astronautics. J. Brit. Interplan. Soc. **8**, 180 (1949).
4. A. C. Clarke, Exploration of Space. London: Temple Press Ltd., **1951**.
5. E. Burgess and C. A. Cross, The Martian Probe. J. Brit. Interplan. Soc. **12**, 72 (1953).
6. F. L. Whipple, Astronomy from the Space Station. Sky and Telesc. **12**, No. 6 (1953); J. Brit. Interplan. Soc. **12**, 10 (1953).
7. C. A. Cross, Orbits for an Extraterrestrial Observatory. J. Brit. Interplan. Soc. **13**, 204 (1954).
8. S. F. Singer, Research in the Upper Atmosphere with Sounding Rockets and Earth Satellite Vehicles. J. Brit. Interplan. Soc. **11**, 61 (1952).
9. H. Wexler, Observing Weather from a Satellite Vehicle. J. Brit. Interplan. Soc. **13**, 269 (1954).
10. G. Horn d'Arturo, The Tessellated Mirror. J. Brit. Astronom. Assoc. **63**, No. 2 (1953).
11. H. Noordung, Das Problem der Befahrung des Weltalls. Berlin: R. C. Schmidt & Co., **1928**.
12. W. Ley, Rockets, Missiles and Space Travel, 2nd Ed. London: Chapman & Hall Ltd., **1951**.
13. F. L. Whipple, Meteoric Phenomena and Meteorites. From: Physics and Medicine of the Upper Atmosphere — A Study of the Aeropause, ed. by C. S. White and O. O. Benson. Albuquerque: University of New Mexico Press, **1952**.
14. L. la Paz, Meteorids, Meteorites, and Hyperbolic Meteoric Velocities. See Ref. [13], Op. Cit.
15. M. W. Ovenden, Meteor Hazards to Space-Stations. J. Brit. Interplan. Soc. **10**, 275 (1951).
16. G. Grimminger, Probability that a Meteorite will Hit or Penetrate a Body Situated in the Vicinity of the Earth. J. Appl. Physics **19** (1948).
17. M. W. Ovenden, Meteors and Space Travel. J. Brit. Interplan. Soc. **10**, 176 (1951).
18. Possible Hazards to a Satellite Vehicle from Meteorites. RAND Corp., Santa Monica, **1946**.
19. N. H. Langton, Mechanical Penetration of Bumper Screens. J. Brit. Interplan. Soc. **13**, 286 (1954).

20. A. C. Clarke, Meteors as a Danger to Space-Flight. J. Brit. Interplan. Soc. **8**, 157 (1949).
21. M. W. Ovenden, Nature and Distribution of Meteoric Matter. J. Brit. Interplan. Soc. **6**, 157 (1947).
22. C. P. Olivier, Meteors. Baltimore: Williams & Wilkins Co., 1925.
23. S. F. Singer, Investigation of the Solar Corona by Means of Rockets. From: Rocket Exploration of the Upper Atmosphere. London: Pergamon Press Ltd.; New York: Interscience Publishers, 1954.
24. L. H. Aller, Astrophysics — Nuclear Transformations, Stellar Interiors and Nebulae. New York: Ronald Press, 1954.
25. R. Tousey, Solar Work at High Altitudes from Rockets. From: The Sun, ed. by G. P. Kuiper. Chicago: University of Chicago Press, 1953.
26. J. L. Greenstein, Physics of Cosmic Matter — Interstellar Matter. From: Astrophysics — A Topical Symposium, ed. by J. A. Hynek. New York: McGraw-Hill, 1951.
27. S. F. Singer, Astrophysical Measurements from an Artificial Earth Satellite. See Ref. [23], Op. Cit.
28. S. F. Singer, A Minimum Orbital Instrumented Satellite — Now. From: Space-Flight Problems. Biel-Bienne (Switzerland): Laubscher & Cie., 1955; J. Brit. Interplan. Soc. **13**, 74 (1954).
29. D. H. Menzel, Our Sun. Philadelphia: Blakiston Co., 1949.
30. S. F. Singer, Studies of a Minimum Orbital Unmanned Satellite of the Earth (MOUSE). Amer. Rocket Soc. Pre-print 195-55; Astronaut. Acta **1**, 171 (1955).
31. L. Spitzer, Astronomical Advantages of an Extraterrestrial Observatory. RAND Report, 1. Sept. 1946, cited by the J. Brit. Interplan. Soc. **9**, 140 (1950), News and Notes Section.
32. J. C. Turner, Planetary Photography in the Ultra-violet and Infra-red. Bull. Brit. Interplan. Soc. **2**, No. 1 (1947).
33. W. M. Sinton, New Findings about Mars. Sky and Telesc. **14**, No. 9 (1955).
34. R. S. Richardson, Exploring Mars. New York: McGraw-Hill, 1954.
35. G. de Vaucouleurs, Physique de la Planète Mars — Introduction a l'aéro-physique. Paris: Albin Michêl, 1951.
36. G. P. Kuiper (Ed.), The Atmospheres of the Earth and Planets, 3rd Ed. Chicago: University of Chicago Press, 1952.
37. J. A. van Allen, The Nature and Intensity of Cosmic Radiation. See Ref. [13], Op. Cit.
38. W. F. G. Swann, The Story of Cosmic Rays. Cambridge: Sky Publishing Corp., Harvard College Observatory, 1955.
39. A. Danjon, Albedo, Color and Polarization of the Earth. From: Earth as a Planet, ed. by G. P. Kuiper. Chicago: University of Chicago Press, 1954.
40. M. Nicolet, Solar Physics and the Atmosphere of the Earth. See Ref. [13], Op. Cit.
41. L. Spitzer, Horizons in Astronomy. Amer. Scientist, April 1955.
42. See Ref. [4], Op. Cit.
43. This notion dates back at least to Tsiolkowski. See, for example, A. Ananoff, L'Astronautique. Paris: Librarie Arthème Fayard, 1950.
44. H. Schaefer, The Biologic Effects of Cosmic Radiation. See Ref. [13], Op. Cit.
45. A. Krebs, The Biologic Effects of Laboratory Radiation; Methods of Assessing the Biologic Effects of Ionizing Radiations. See Ref. [13], Op. Cit.
46. See Ref. [12], Op. Cit.
47. J. Meyers, Annu. Rev. Microbiol. 1951.
48. J. F. Decker, J. Astronautics **2**, 71 (1955) (News and Notes).
49. Arnon, see Ref. [47], Op. Cit.
50. P. A. Campbell, Human Orientation During Travel in the Aeropause. See Ref. [13], Op. Cit.
51. H. Haber, Man in Space. London: Sidgwick & Jackson, 1953. See also H. Haber, Gravity, Inertia and Weight; see Ref. [13], Op. Cit.

52. P. A. Cibis, Retinal Adaptation Applicable to Visual Problems in Flight at Increasing Altitudes. See Ref. [13], Op. Cit.
53. K. Buettner, Thermal Aspects of Travel in the Aeropause — Problems of Thermal Radiation. See Ref. [13], Op. Cit.
54. U. Luft, Physiological Limitations in Cabin Environment and Human Adaptations. See Ref. [13], Op. Cit.
55. H. J. Schaefer, Exposure Hazard from Cosmic Radiation at Extreme Altitude and in Free Space. From: Probleme aus der Astronautischen Grundlagenforschung, ed. by H. H. Koelle. Stuttgart, 1952; J. Amer. Rocket Soc. **22**, No. 5 (1952).
56. J. Talbot, The Biological Effects of Power Plant Radiation. See Ref. [13], Op. Cit.
57. H. Muller, Genetic Effects of Cosmic Radiation. See Ref. [13], Op. Cit.
58. "Man's Survival in Space." Colliers, 28. Feb. 1953.
59. H. Specht, Toxicology of Travel in the Aeropause. See Ref. [13], Op. Cit.
60. E. Esclangon, La vie, serait-elle possible à bord de satellites artificiels de la terre ou de projectiles astronautiques? Extrait du „Mémorial de l'artillerie française", tome XXIII, 4e fasc. 1949. Paris: Gauthier-Villars, 1950.
61. J. Kaplan, The Chemosphere. See Ref. [13], Op. Cit.
62. C. T. Holliday, The Earth as Seen from Outside the Atmosphere. From: The Earth as a Planet, ed. by G. P. Kuiper. Chicago: University of Chicago Press, 1954.
63. C. W. Tombaugh, Proposed Geodetic Triangulation from an Unmanned Orbital Vehicle by Means of Satellite Search Technique. Jet Propulsion **25**, 232 (1955).
64. W. Rosen, The Viking Rocket Story. New York: Harper Brothers.
65. I. M. Levitt, Geodetic Significance of a Minimum Satellite Vehicle. J. Astronautics **2**, 1 (1955).
66. F. C. Lahee, Field Geology. New York: McGraw-Hill, 1941.
67. C. G. Lalicker, Principles of Petroleum Geology. New York: Appleton-Century-Crofts Inc., 1949.

Ascent of Orbital Vehicles[1]

By

Krafft A. Ehricke[2], ARS, AAS, IAS

(With 12 Figures)

(*Received January 20, 1956*)

Abstract. Ascent into a satellite orbit along a minimum energy ellipse (elliptic ascent) is compared with ascent along an arc of an elliptic trajectory (ballistic ascent) where the satellite stage is transferred into the orbit at or near the summit. Discussed are basic energy requirements (other than losses during powered ascent), thrust program, effect on the size of stages, visibility during ascent, and flight time. The general effect of ballistic ascent on vehicle design and booster recovery is assessed. The results show that more powerful satellite stages are required if ballistic, rather than elliptic ascent is used, even if the increase in overall energy requirement is small. Conversely, booster stages can, in many cases, be smaller than for elliptic ascent. Parachute recovery of booster stages appears to be facilitated, compared to elliptic ascent, both, from the viewpoint of frictional heating and of ground operations. If the complete ascent, including transfer into the orbit, is to be observable from the launching site or its immediate surrounding, then, for orbital altitudes above 200 n.mi. (360 km), the trajectory angle at cut-off for the ballistic ascent must exceed 20 degrees. Under the same conditions, the cut-off angle must be 30 degrees for an orbital altitude of about 800 n.mi. (1,440 km). The overall flight time into the orbit is greatly reduced, compared to the elliptic ascent. Principally, however, the ballistic ascent compares unfavorably with the elliptic ascent, because of the high transfer energy required at the summit point, resulting in the need for transporting comparatively large quantities of material and propellant into orbital distance. It is concluded that the elliptic ascent is more attractive for regular operations, leaving the ballistic ascent essentially restricted to occasional flights in response to special conditions or requirements, such as, for instance, observability of the ascent of an instrumental satellite, or perhaps rapid emergency ascents to manned satellites.

Zusammenfassung. Der Aufstieg in eine Satellitenbahn entlang einer Minimum-Energie-Ellipse (elliptischer Aufstieg) wird verglichen mit dem Aufstieg entlang einer elliptischen Geschoßbahn (ballistischer Aufstieg), in welchem Falle die Satellitenstufe am oder nahe dem Gipfelpunkt in die Satellitenbahn übergeführt wird. Diskutiert werden die grundsätzlichen Energieanforderungen (ausschließlich der Verluste entlang der Antriebsbahn), das Schubprogramm, der Einfluß auf die Stufengröße, Sichtbarkeit während des Aufstieges und die Flugzeit. Der allgemeine Einfluß des ballistischen Aufstieges auf Gerätekonstruktion und Rückgewinnung unterer Stufen wird berücksichtigt. Die Ergebnisse zeigen, daß größere Satellitenstufen benötigt werden, wenn der ballistische Aufstieg an Stelle des elliptischen gewählt wird, selbst wenn der Gesamt-Energiebedarf nicht viel größer ist. Umgekehrt können die unteren

[1] Originally presented, in slightly longer form, at the Fall Meeting of the American Rocket Society, El Paso, Texas, September, 1953.

[2] Chief of Preliminary Design and Systems Analysis, Convair-Astronautics Div., San Diego, Calif., USA.

Vol. 2 1956

Stufen in vielen Fällen kleiner sein als beim elliptischen Aufstieg. Fallschirmrückgewinnung der unteren Stufen scheint leichter möglich als beim elliptischen Aufstieg, vom Standpunkt der Reibungserhitzung sowohl wie der Bodenarbeiten. Wenn Beobachtung des gesamten Aufstieges, einschließlich des Einlenkens in die Satellitenbahn, gewünscht wird, und zwar von der Startstelle oder ihrer unmittelbaren Umgebung aus, dann muß der Brennschlußwinkel beim ballistischen Aufstieg zu Bahnhöhen über 200 n.mi. (360 km) größer als 20° werden. Für 800 n.mi. (1440 km) Höhe muß, unter den gleichen Bedingungen, der Brennschlußwinkel 30° betragen. Die Gesamtflugzeit zur Satellitenbahn ist im Vergleich zum elliptischen Aufstieg stark verringert. Grundsätzlich jedoch ist der ballistische Aufstieg gegenüber dem elliptischen unvorteilhaft wegen der am Gipfelpunkt erforderlichen hohen Einlenkungsenergie, aus der sich die Notwendigkeit ergibt, vergleichsweise große Mengen von Material und Treibstoff auf die Bahnhöhe zu heben. Die Schlußfolgerung ist, daß der elliptische Aufstieg für reguläre Operationen vorzuziehen ist. Der ballistische Aufstieg wird im wesentlichen auf gelegentliche Flüge unter speziellen Bedingungen oder Anforderungen beschränkt sein, wie zum Beispiel die Beobachtbarkeit des Aufstieges unbemannter Satelliten, oder vielleicht auf schnelle Notaufstiege zu bemannten Stationen.

Résumé. L'ascension à une orbite de satellite par une montée le long d'une ellipse d'énergie minimum est comparée avec l'ascension balistique suivie d'un transfert dans l'orbite au voisinage du sommet.

La discussion porte sur le bilan énergétique (à l'exclusion des pertes le long de l'arc de trajectoire propulsée), le programme de la poussée, la dimension des étages de la fusée, la visibilité pendant la phase ascensionnelle et le temps de vol.

L'incidence qu'a l'emploi d'une montée balistique sur le dessin de la fusée et la récupérabilité des fusées d'appoint est établie. Les résultats montrent que, comparée à la montée elliptique, la montée balistique requiert des étages plus puissants, même si l'accroissement d'énergie totale requise est faible. En contre-partie les fusées d'appoint peuvent souvent être réduites.

La récupération des fusées d'appoint par parachute semble être facilitée aussi bien du point de vue de l'échauffement cinétique que des opérations nécessaires au sol.

Si l'ascension complète et le transfert dans l'orbite doivent pouvoir être observés du point de lancement ou de ses environs immédiats l'angle que fait la trajectoire balistique au moment où la propulsion est coupée doit dépasser 20 degrés si l'altitude orbitale est supérieure à 360 km. Cet angle doit être d'environ 30 degrés pour une altitude orbitale de 1440 km.

Le temps de vol pour entrer dans l'orbite est considérablement plus faible que pour l'ascension le long d'une ellipse d'énergie minimum. Cependant le principal inconvénient de la montée balistique réside dans le grand transfert d'énergie requis au sommet, qui impose le transport d'un poids mort et d'une quantité de combustible importante jusqu'à l'altitude orbitale.

En conclusion la montée elliptique est plus attrayante pour un lancement normal, la montée balistique doit être réservée à des lancements occasionnels répondant à des exigences spéciales telles que la possibilité d'observation pour un satellite instrumental ou la rapidité de l'ascension dans un cas d'urgence.

Nomenclature

a	major semi-axis	v_c	circular velocity
e	numerical eccentricity	v_p	parabolic velocity
h	energy of orbit	x	distance along the surface or the cut-off circle
p	parameter of ellipse	y	altitude
r	radius vector; distance from center of the earth	γ	constant of gravity field
r_{00}	radius of the earth	δ	$180 - \eta$
T	period of revolution	η	true anomaly
t	time	θ	trajectory angle
v	velocity		

Subscripts:

n	normal to the radius vector	s	satellite orbit
r	radial	1	cut-off conditions

Superscripts:

* conditions at the summit point

I. Introduction

The orbital vehicle ascends from the earth to a satellite orbit, assumed here to be of approximately circular shape. The flight mechanics of orbital vehicles is concerned with various methods of ascent and their effect on a number of parameters, such as energy requirement, thrust program, size of stages, visibility during ascent, flight time, and others. Minimization of the overall energy requirement will always be of primary importance as long as propulsion energy is limited. However, other parameters may at times become important also, warranting a different type of ascent. In this case the energy penalty, compared to the minimum energy ascent, and the effect on thrust program and vehicle design must be assessed.

II. Types of Ascent

This paper is not concerned with the powered phase, but rather with the overall ascent. Therefore gravitational and drag losses will not be considered in detail. However, their effect will be taken into account qualitatively as a trend in the discussion of overall energy requirements and thrust programming.

Generally, three basic types of ascent can be defined (Fig. 1):

Powered-all-the-way ascent (PAW ascent)
Ballistic ascent
Elliptic ascent.

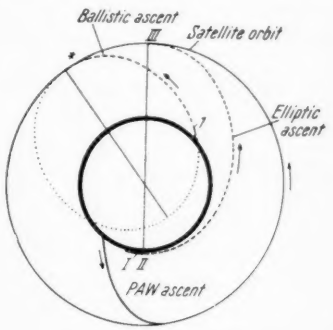

Fig. 1. Ascent into satellite orbit

During the PAW ascent the vehicle engines operate continuously. There is only one propulsion phase and its cut-off data are, at least theoretically, identical with the orbital data of the satellite with respect to altitude and velocity vector. The thrust does not have to be constant. Unless very low orbits, not far above the relevant portion of the atmosphere are considered (say, 100 to 200 n.mi. or 180 to 360 km), this type of ascent is much more expensive than either of the two subsequent ones, mainly because extended burning time against the gravitational pull of the earth is necessary, with a correspondingly large penalty in terms of gravitational loss. For lower altitudes where this ascent can gain practical significance, it is therefore necessary to optimize the deflection program in such a manner that these losses are minimized, that is, that for a given ideal velocity (or total propellant energy) the altitude at which circular velocity is attained, becomes a maximum. It is not the purpose of this paper to pursue this investigation. Therefore the PAW ascent presently will be excluded from further consideration.

The ballistic ascent uses trajectories similar to those of long-range guided missiles. These trajectories are essentially elliptic arcs about the center of the

earth. The vehicle is carried to the summit or apogee which lies in the satellite orbit. Upon approaching the summit, the vehicle must, in a second propulsion period, produce the velocity increment required for transfer into the orbit.

In the well-known elliptic ascent the vehicle first attains circular velocity at relatively low altitude (station I). Subsequently (either immediately or after a short interval) the vehicle is accelerated to the perigee velocity (II) of the transfer ellipse at whose apogee an additional short burst of power is required for entering the satellite orbit. For reasons of brevity the circular orbit at station I will subsequently be designated as perigee orbit. The numbers and symbols designating the stations in Fig. 1 will be used as subscripts in the analysis.

As is well known, the elliptic ascent is considered to require the smallest amount of energy for ascending into a given orbit. This is theoretically correct, though not necessarily always in practice (cf. Section III, below). In general, the ballistic ascent will require more energy. However, it is not immediately clear how much more energy will be needed. This depends a great deal on the orbital altitude and on the cut-off angle at station I which, in turn may strongly be affected by visibility (tracking) requirements. Aside from the gross energy, there are other changes, especially in vehicle design, connected with the selection of ballistic ascent. Finally, the ballistic ascent offers a number of features which may be considered attractive for some purposes:

Shorter Flight Time. — Obviously, the path length traveled during a ballistic ascent is shorter than for the elliptic ascent. Consequently, the time of unpowered flight (coasting time) will be correspondingly shorter. In general, this may not be too important, because the elliptic coasting time is not very long either. It will be seen that the differences are of the order of 15 to 35 minutes.

Visibility During Ascent. — The steeper ballistic ascent will under certain conditions permit optical or radar tracking of the vehicle up to the summit, from installations at or near the launching site. Thus, without the need for advanced tracking and guidance bases, the vehicle's actual flight path can be determined and the vehicle be monitored, if necessary. This can result in a considerable improvement of the accuracy of ascent, particularly in the case of instrumental satellites or automatic supply ships. The elliptic ascent has the practical disadvantage that the vehicle arrives at the apogee approximately on the other side of the earth, as seen from the launching site. Tracking, if necessary, must therefore be done by a number of widely distributed ground stations.

Booster Recovery. — From the viewpoint of booster recovery, the steeper powered trajectory of the ballistic ascent and the lower velocities, hence, smaller size of the booster stages, appears advantageous. The horizontal distance traveled by the booster from cut-off to impact is shorter. In the case of parachute recovery the salvaging operation is thereby simplified. The slow-down (release of parachute) begins before the summit point of the particular stage is reached, the point of release being determined by the most favorable compromise between deceleration requirements and greatest possible reduction of the thermal load on the parachute, due to frictional heating. During the residual ascent of the stage, the conditions will improve rapidly for the parachute, because of velocity decrease, due to altitude increase and due to the decrease in static pressure. Behind the summit excessive velocity gain is prevented, because parachute-braking is effective from the beginning of the descent. It should be pointed out, however, that the stage which has cut-off at station 1, will accompany the satellite stage to the summit point and will from there fall back into the atmosphere without a possibility of recovery. This could be prevented by separating the last stage prior to arrival at station 1, with the satellite stage providing the final impulse, then cutting off

and re-igniting near the summit. The operation of the satellite stage is thereby complicated, because its engines must be ignited twice. Moreover, in cases where the transfer impulse at the summit is very large, this method leads to a further increase of the already sizeable satellite stage. In elliptic ascent, stage recovery, especially of the second stage, must be attempted at very high speed which probably makes parachute recovery impractical.

III. Energy Requirements

From the standpoint of flight mechanics, the difference between the three methods of ascent lies in the different energy levels of the perigee orbits. Neglecting drag, and assuming an infinitesimal propulsion period, the optimum distance of the perigee orbit from the center of the earth is equal to the earth's radius. Kinetic energy, equivalent to the required perigee velocity, is accumulated without loss. This energy which weighs nothing, in contrast to propellant energy, is used by the vehicle to climb to the apogee point. In this sense the elliptic ascent is identical with the minimum energy ascent. In deviating from this minimum ascent, the perigee orbit can be moved either upward into space, or downward into the earth.

In the first case, the difference between perigee orbit and satellite orbit is decreased; but the vehicle must climb to a greater altitude initially. More energy must be carried up in the form of propellant weight. This invariably produces gravitational losses (at practical thrust-to-weight ratios) which overcompensate any relief derived from closer distance of perigee and satellite orbit. The extreme case is the PAW ascent, where the perigee orbit coincides with the satellite orbit, and the amount of propellant energy to be carried aloft becomes a maximum. A moderate upward deviation, which becomes necessary in practice, is the displacement of the perigee orbit into the outer atmosphere, some 300,000 to 500,000 ft (90 to 150 km) up, because of finite burning time, air drag, and guidance and control requirements.

A deviation toward negative altitude of the perigee orbit leads to the ballistic ascent. The energy difference between perigee and satellite orbits increases progressively, resulting in a lower energy level of the elliptic (ballistic) trajectory as compared to the elliptic (transfer) orbit. In the elliptic ascent all energy required to climb from perigee orbit to satellite orbit is produced in the most efficient form, namely as horizontal (or normal [to the radius vector]) velocity component Δv_{II} which represents the difference between the circular velocity v_I in the perigee orbit and the required perigee velocity $(v_I + \Delta v_{II})$. As the perigee orbit moves below the surface, the cut-off point can no longer coincide with the perigee point. The climb energy between cut-off point and satellite orbit is provided in the form of a vertical (or radial) velocity component, while the normal component becomes smaller. The radial velocity component is the least desirable form of energy, because it is lost entirely at the summit where the radial velocity is zero by definition. The steeper the ballistic ascent for a given orbital altitude and, to a lesser extent, the greater the orbital altitude for a given cut-off angle, the larger must the radial velocity component become. This reduces progressively that fraction of the total kinetic energy at the cut-off point, which is available in useful form, namely as horizontal velocity component.

To be sure, the loss in the form of radial velocity is of a different nature than the gravitational loss or the drag loss where energy is dissipated and cannot be recovered. The radial component can be recovered by falling back to the cut-off point distance, because the motion takes place in a potential field and involves

conservative forces only. A loss exists in the sense that the horizontal velocity component, the most useful form of kinetic energy, is not a maximum at cut-off. Outwardly, this is indicated by the steeper powered ascent in the ballistic case, introducing additional gravitational losses. The fact that the drag losses will be reduced contributes some relief; however, in large rockets with low initial thrust-to-weight ratio (1.2 to 1.5) the drag loss is only about 10 percent of the gravitational loss. Of greater help is the fact that the cut-off velocity (v_1) is smaller than in the elliptic case, yielding shorter burning time, at equal initial acceleration, and decreasing the gravitational loss proportionately.

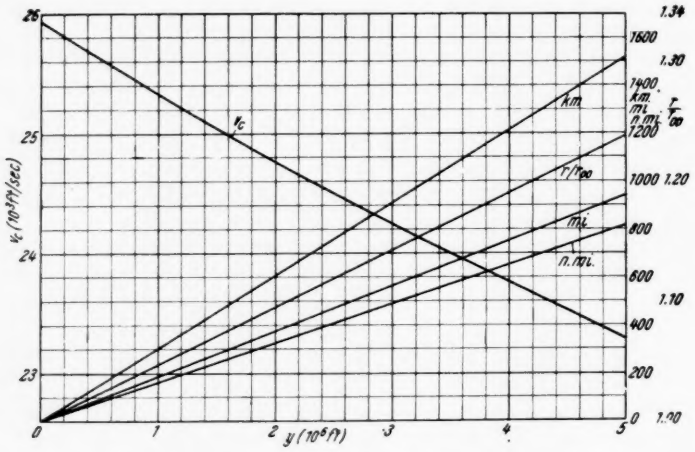

Fig. 2. Variation of circular velocity with altitude

A ballistic ascent with small cut-off angle (i.e. small radial component) will require only little increase in energy above the minimum energy ascent. In addition the effect of a slightly steeper ascent is compensated for (and in some cases even overcompensated) by shorter burning time and smaller drag loss, as pointed out before. On the other hand, practical cases of elliptic ascent require powered climb to a sufficiently high perigee orbit, as outlined before. Therefore, for not too high orbits, the ballistic ascent can be of equal, and in fact even of less energy expense than the elliptic ascent. The exact transition point to superior economy of the elliptic ascent depends on configuration and thrust program of the vehicles under consideration. However, the region of ballistic superiority is comparatively small, to be sure. For the frequently considered orbital altitudes of the order of 500 to 1,000 n.mi. (900 to 1,800 km), the elliptic ascent is certainly superior. This leaves the ballistic ascent essentially restricted either to special conditions, such as ascent of instrumental satellites to lower altitude, or to visibility requirements or other requirements, such as perhaps rapid emergency ascent to manned satellites and other cases where energy minimization is not of primary importance.

Fig. 2 shows the variation of circular velocity v_c and minimum velocity v_{min} with altitude. Here v_{min} is defined as the total velocity requirement $(v_I + \Delta v_{II} + \Delta v_{III})$ for the minimum energy ascent, that is $v_{min} = (v_c)_s \, [1 + 2 \, y_s/r_{00}]^{1/2}$ (for symbols cf. nomenclature). The ballistic ascent will be compared against this minimum velocity.

From the theory of elliptic orbits, the following relations are known or can easily be obtained (cf. Fig. 3 for nomenclature and definitions):

Polar equation

$$r = \frac{p}{1 + e\cos\eta} = \frac{p}{1 - e\cos\delta} \tag{1}$$

$$e\cos\eta = \frac{p}{r} - 1 = q - 1 \tag{2}$$

$$q = \frac{{v_n}^2}{g\,r} = \left(\frac{v}{v_c}\right)^2 \cos^2\theta; \tag{3}$$

eccentricity

$$e = \sqrt{(1-q)^2 + q^2\tan^2\theta} \tag{4}$$

where

$$\tan\theta = \frac{v_r}{v_n}$$

$$\tan\delta = \frac{q\tan\theta}{1-q}; \tag{5}$$

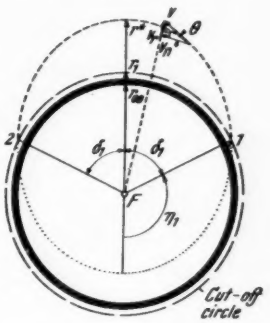

Fig. 3. Elliptic trajectory

radial velocity component

$$v_r = v_n \frac{e}{q}\sin\delta; \tag{6}$$

normal velocity component

$$v_n = \sqrt{v^2 - {v_r}^2} \tag{7}$$

where v ist the instantaneous flight velocity,

$$v = \frac{\sqrt{\gamma\,p}}{r\cos\theta} \tag{8}$$

and

$$\gamma = g\,r^2 = {v_c}^2 r = 1.4055 \cdot 10^{16}\ \mathrm{ft^3/sec^2} = 3.98 \cdot 10^5\ \mathrm{km^3/sec^2}. \tag{9}$$

If the subscript 1 designates cut-off conditions, the velocity at the summit is given by

$$v^* = {v_n}^* = v_{n1}\frac{r_1}{r^*} \tag{10}$$

where

$$\frac{r^*}{r_1} = \frac{q_1}{1-e}. \tag{11}$$

From the energy relation $h = v^2 - {v_p}^2 = v^2 - 2\,\gamma/r$ one also finds the alternate expression

$$v^* = \sqrt{{v_1}^2 - \frac{2\gamma}{r_1} + \frac{2\gamma}{r^*}}. \tag{12}$$

The range between cut-off point and summit point, measured along the cut-off circle, is given by

$$x_{1y^*} = \frac{\pi}{180} r_1\,\delta_1^{(0)} = r_1\,\delta_1^{(r)}. \tag{13}$$

Among the elliptic trajectories, one family is of special interest, because it yields maximum range for a given cut-off velocity (minimum energy trajectory,

or MET). Of all ellipses which pass through take-off point and impact point, the MET has the smallest eccentricity. Its energy constant h is a minimum. Since one can write

$$h = -\frac{\gamma (1 - e^2)}{p} \tag{14}$$

the term $(1 - e^2)/p$ must become a minimum. For $\eta = 90^0$

$$r = a (1 - e^2) = p \tag{15}$$

hence,

$$h = -\frac{\gamma}{a}. \tag{16}$$

This shows that for the MET the major semi-axis must be a minimum. At the cut-off point

$$r_1 = \frac{p}{1 - e \cos \delta_1}$$

whence

$$p = r_1 (1 - e \cos \delta_1) \tag{17}$$

or

$$r = \frac{r_1 (1 - e \cos \delta_1)}{1 - e \cos \delta}. \tag{18}$$

At the apogee ($\delta = 0^0$)

$$r^* = a (1 + e). \tag{19}$$

Thus, for the summit point, r in Eq. (18) can be substituted by $a (1 + e)$, yielding

$$a = \frac{r_1 (1 - e \cos \delta_1)}{1 - e^2}. \tag{20}$$

This equation defines the major semi-axis in terms of cut-off values. For a given range then, the major semi-axis becomes a minimum when the partial derivative of a with respect to e becomes zero,

$$\frac{\partial a}{\partial e} = e^2 - \frac{2 e}{\cos \delta_1} + 1 = 0$$

or

$$e_{min} = \frac{1 \pm \sin \delta_1}{\cos \delta_1}$$

whence, for $0 < \delta_1 < 180^0$,

$$e_{min} = \frac{1 - \sin \delta_1}{\cos \delta_1}. \tag{21}$$

The polar equation of the MET is therefore

$$r = \frac{p}{1 - \dfrac{1 - \sin \delta_1}{\cos \delta_1} \cos \delta}. \tag{22}$$

The trajectory angle at cut-off is obtained from

$$\tan \theta = \frac{v_r}{v_n} = \frac{dr/dt}{r\, d\eta/dt} = \frac{dr}{r\, d\eta} = \frac{dr}{r\, d\delta}$$

where, from Eq. (18),

$$\frac{dr}{d\delta} = \frac{r_1 (1 - e \cos \delta_1)\, e \sin \delta}{(1 - e \cos \delta)^2}$$

whence

$$\tan \theta_1 = \frac{e \sin \delta_1}{1 - e \cos \delta_1}. \tag{23}$$

From this general equation the MET cut-off angle $\theta_{1,min}$ is obtained by substituting e_{min} for e, which results in the simple relation

$$\tan \theta_{1,min} = e_{min}. \tag{24 a}$$

Thus, $\theta_{1,min} = 45^0$ is the boundary case for very short ranges, as e_{min} approaches unity (parabolic trajectory). The other boundary case is the circular orbit where e_{min}, hence also $\theta_{1,min}$, becomes zero. In between lies a region of decreasing cut-off angle as cut-off velocity and range increase. Since with the attainment of circular velocity the optimum cut-off angle becomes zero, one can show that

$$\tan \theta_{1,min} = \sqrt{1 - \left(\frac{v_1}{v_c}\right)^2} = \sqrt{1 - \frac{r_1 {v_1}^2}{\gamma}}. \tag{24 b}$$

The MET cut-off angle is shown in Fig. 4. It should be mentioned that consideration of finite burning time and drag losses lead to somewhat different cut-off angles for minimum energy.

From the energy relation and from Eq. (18) one obtains for the cut-off velocity

$$v_1 = \sqrt{\gamma \left(\frac{2}{r_1} - \frac{1}{a}\right)} \tag{25}$$

or, with the aid of Eq. (19),

$$v_1 = \sqrt{\gamma \left(\frac{2}{r_1} - \frac{1 - e}{r^*}\right)}. \tag{26}$$

The velocity at the summit follows from Eq. (12), whence the ratio of summit velocity to cut-off velocity becomes

$$\frac{v^*}{v_1} = \left[\frac{{v_1}^2 - \frac{\gamma}{r_1}\left(1 - \frac{r_1}{r^*}\right)}{\gamma \left(\frac{2}{r_1} - \frac{1 - e}{r^*}\right)}\right]^{\frac{1}{2}} \tag{27}$$

which is an alternate expression to Eq. (10). The latter can also be written in terms of r_1/r^* and θ_1,

$$\frac{v^*}{v_1} = \frac{r_1/r^*}{\sqrt{1 + \tan^2 \theta_1}}. \tag{28}$$

For the MET, Eqs. (27) and (28) become

$$\left(\frac{v^*}{v_1}\right)_{\text{MET}} = \left[\frac{{v_1}^2 - \frac{\gamma}{r_1}\left(1 - \frac{r_1}{r^*}\right)}{\gamma \left(\frac{2}{r_1} - \frac{1 - \sqrt{1 - (v_1/v_c)^2}}{r^*}\right)}\right]^{\frac{1}{2}} \tag{29}$$

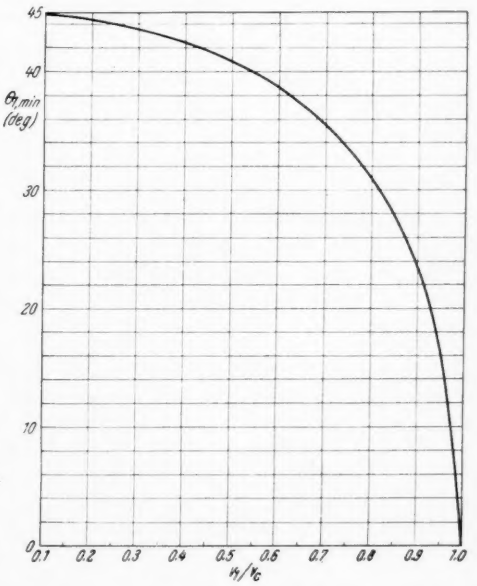

Fig. 4. Angle of departure for minimum energy trajectory

Vol. 2 1956

$$\left(\frac{v^*}{v_1}\right)_{\text{MET}} = \frac{r_1/r^*}{\sqrt{2 - \left(\frac{v_1}{v_c}\right)^2}}. \tag{30}$$

The required velocity increment at the summit for transfer into the satellite orbit follows then from

$$\Delta v^* = v_c^* - v^*. \tag{31}$$

From Eq. (11) the summit distance follows, in terms of r_1, v_1, θ_1 and e,

$$\frac{r^*}{r_1} = \frac{r_1 v_1^2}{\gamma (1 - e)(1 + \tan^2 \theta_1)} \tag{32}$$

or

$$\left(\frac{r^*}{r_1}\right)_{\text{MET}} = \frac{r_1 v_1^2}{\gamma (1 - e_{min})(1 - e_{min}^2)} = \frac{v_1/v_c}{\left[1 - \sqrt{1 - \left(\frac{v_1}{v_c}\right)^2}\right]\left[2 - \left(\frac{v_1}{v_c}\right)^2\right]}. \tag{33}$$

It is apparent from the general characteristics of the MET that the summit altitude must be very low at small cut-off velocities as well as at large cut-off velocities approaching circular velocity where the summit altitude approaches the cut-off altitude. In between, the summit altitude must reach a maximum which, therefore, marks the highest satellite orbit obtainable for ballistic ascent via MET. By differentiating in Eq. (33) r^*/r_1 with respect to $(v_1/v_c)^2$ and solving, the applicable solution is found to be

$$\left(\frac{v_1}{v_c}\right)^2 = 0.82884; \qquad \frac{v_1}{v_c} = 0.91038. \tag{34}$$

At this point

$$\frac{r^*}{r_1} = 1.2074. \tag{35}$$

Assuming, tentatively, a cut-off altitude of not less than 300,000 ft (about 90 km), the maximum MET summit altitude is approximately 765 n.mi. (1380 km).

The period of revolution follows from the well-known KEPLER equation,

$$T = 2\pi \sqrt{\frac{a^3}{\gamma}}. \tag{36}$$

Remembering KEPLER's second law, the general relation between time (counted usually from the perigee) and true anomaly can be written in the form

$$dt = \frac{r^2}{C}\, d\eta \tag{37}$$

where $C = r\, v \cos\theta$. Integration of this equation gives the flight time between two arbitrary stations 1 and 2 on the elliptic path

$$\Delta t = \int_{\eta_1}^{\eta_2} r^2\, d\eta, \tag{38}$$

the two stations being defined by the true anomalies η_1 and η_2. Because of Eq. (1) it follows

$$\Delta t = \frac{p^2}{C} \int_{\eta_1}^{\eta_2} \frac{d\eta}{(1 + e \cos\eta)^2}. \tag{39}$$

The solution of this integral is, generally,

$$\Delta t = \frac{\sqrt{\frac{p}{\gamma}}}{1-e^2}\left\{\sqrt{2\,p\,r_1 - r_1^2\,(1-e) - p^2} - \sqrt{2\,p\,r_2 - r_2^2\,(1-e) - p^2}\right.$$
$$\left. + \frac{p}{\sqrt{1-e^2}}\left[\sin^{-1}\left(\frac{r_2\,(1-e^2)-p}{e\,p}\right) - \sin^{-1}\left(\frac{r_1\,(1-e^2)-p}{e\,p}\right)\right]\right\} \tag{40}$$

and for the MET

$$(\Delta t)_{\text{MET}} = \frac{\sqrt{\frac{p}{\gamma}}}{\left(\frac{v_1}{v_c}\right)^2}\left\{\sqrt{2\,p\,r_1 - r_1^2\left(\frac{v_1}{v_c}\right)^2 - p^2} - \sqrt{2\,p\,r_2 - r_2^2\left(\frac{v_1}{v_c}\right)^2 - p^2}\right.$$
$$\left. - \frac{p}{\left(\frac{v_1}{v_c}\right)}\left[\sin^{-1}\left(\frac{r_2\left(\frac{v_1}{v_c}\right)^2 - p}{p\,e_{min}}\right) - \sin^{-1}\left(\frac{r_1\left(\frac{v_1}{v_c}\right)^2 - p}{p\,e_{min}}\right)\right]\right\}. \tag{41}$$

Thus, for a given ellipse whose parameter and eccentricity are known, the above relations yield the coasting time between two distances r_1 and r_2 somewhere

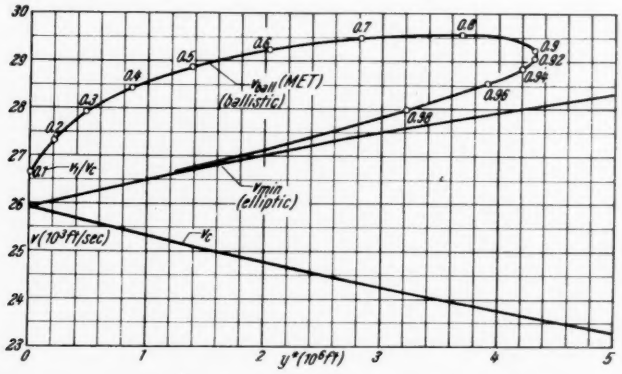

Fig. 5. Velocity required for elliptic and ballistic (MET) ascent

between perigee and apogee. For the ballistic ascent, where the end point is at apogee distance (at least approximately), the second square root term in Eqs. (40) and (41) becomes zero.

The energy required for the ballistic ascent is proportional to the cut-off velocity v_1 plus the velocity increment Δv^* (neglecting transition losses). The sum of these two velocities shall be designated shortly as ballistic velocity

$$v_{ball} = v_1 + \Delta v^*. \tag{42}$$

The difference between v_{ball} and v_{min} will shortly be termed ballistic excess.

Fig. 5 shows a plot of v_c, v_{min}, and v_{ball} for the MET. The corresponding ballistic excess is shown in Fig. 6. It can be seen that the ballistic excess reaches

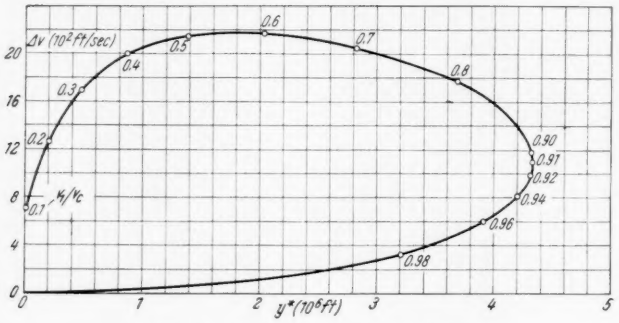

Fig. 6. Ballistic excess for MET

a maximum at $v_1/v_c \approx 0.55$, at which the MET leads to a summit altitude of about 280 n.mi. or 504 km. The ballistic excess is 2,200 ft/sec. Such an increment on top of the already high v_{min} causes an appreciable increase in take-off weight of a multi-stage vehicle.

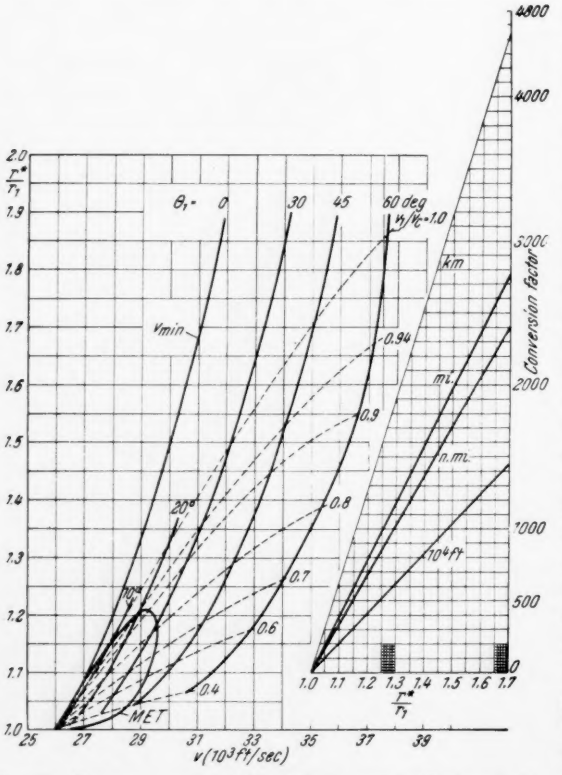

Fig. 7. Energy spectrum for elliptic and ballistic ascent

Although the ballistic excess decreases for higher velocities, v_{ball} remains about constant in the range $0.6 - v_1/v_c - 0.9$. Thereafter, the velocity falls off quickly, as conditions resembling those of elliptic ascent are approached. However, the altitude beyond a velocity ratio of 0.91 decreases also rapidly. At velocity ratios below 0.5, v_{ball} is still of the order of 27,000 to 29,000 ft/sec (8.25 to 8.85 km/sec), reflecting the increase in Δv^* which ultimately (at sufficiently low velocities) exceeds v_1. Most of the propellant content of the orbital vehicle must be carried to greater altitudes than in the elliptic case. Consequently, the satellite stage must progressively get bigger and ultimately will have to consist of more than one stage. These cases, however, are not of practical significance.

Fig. 7 presents a general energy spectrum for (minimum energy) elliptic ascent and for ballistic ascent, including MET. In an auxiliary graph on the right hand side, conversion lines are given for the different units. The velocity is seen to increase strongly with increasing angle of departure for a given satellite altitude r^*/r_1. The velocity increase is comparatively less pronounced, if the cut-off angle is kept constant while the altitude is increased. The dashed lines of constant v_1/v_c indicate how much of this velocity must actually be attained at cut-off. The MET indicates a comparatively high energy requirement, mostly corresponding to ellipses between 30 and 45 degrees cut-off angle. This shows that the MET does not occupy the same special position in the energy spectrum of ballistic ascent, which it holds in the energy spectrum of long-range ballistic trajectories. The reason for this is, of course, that the optimum condition for ballistic ascent is not minimization of the angular momentum of the ascending ellipse, but minimization of the radial velocity component at the cut-off point.

IV. Thrust Program and Stage Size

Consideration of the overall energy requirement, however, does not reveal the whole picture. The dashed lines of constant cut-off velocity in Fig. 7 permit a quick estimate of the transfer velocity Δv^* and they indicate a pronounced increase of Δv^* with decreasing altitude.

A more detailed picture of this tendency is presented in Fig. 8. At constant cut-off angle and decreasing altitude, the increase in Δv^* first is slow, but becomes progressively more pronounced. Another, for the vehicle design very important characteristic is that, for a given satellite altitude, an increase in cut-off angle not only causes the overall velocity requirement to go up, but most of the increase affects Δv^* rather then v_1.

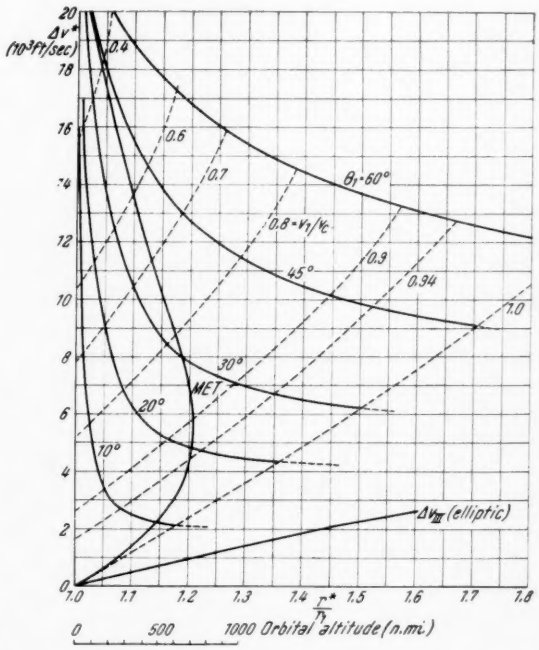

Fig. 8. Transfer velocity increment into circular orbit

A large Δv^* increases the size and weight of the satellite stage and the amount of propellant weight that must be carried into the orbit. If one compares Δv^* in Fig. 8 with Δv_{III} for the elliptic ascent, it becomes apparent that the implications of a large Δv^* in regard to staging and propulsion efficiency may well become more significant than the mere increase in overall energy. For instance, Fig. 7 shows that for $r^*/r_1 = 1.1$, v_{ball} for 10^0 cut-off angle is only about 300 ft/sec higher than v_{min}, and this difference will probably disappear when the ballistic

ascent is compared with a practical elliptic ascent, as pointed out before. However, inspection of Fig. 8 shows that Δv^* has gone up to 2,500 ft/sec, compared to Δv_{III} of about 500 ft/sec. The change from elliptic to the 10^0 ballistic ascent therefore goes deeper than the ballistic excess alone might indicate.

The particular significance of this trend depends, of course on the individual project conditions. However, it is apparent that for smallest weight of the satellite stage, elliptic ascent should be used, even if it makes little or no difference in the overall energy requirement. Small size and weight are particularly important for manned satellite gliders for reasons of simplifying the aerothermodynamic problems during the descent through the atmosphere.

V. Visibility

For the MET, the summit altitude is plotted in Fig. 9 as function of the cut-off velocity. At the same time δ_1 and $(r/r_{00})_{min}$ are shown, where $(r/r_{00})_{min}$ designates the minimum altitude at which the vehicle theoretically could just be seen on the horizon by an observer on the surface (that is, at zero elevation angle, $\beta = 0$).

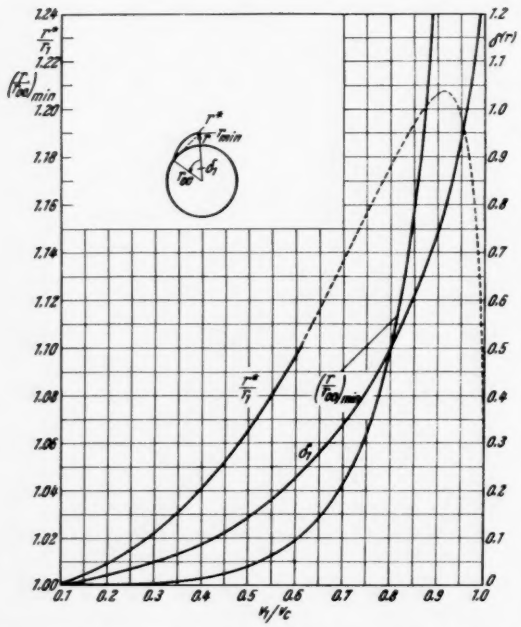

Fig. 9. Visibility during ballistic ascent along MET

The distance x on the surface from the point directly beneath the vehicle to the observer who sees the vehicle at an elevation β above the horizon, is given by

$$x = \frac{\pi}{180} r_{00} \cdot \left\{ \left[\cos^{-1} \left(\frac{r_{00}}{r} \cos \beta^0 \right) \right]^0 - \beta^0 \right\}. \tag{43}$$

For $\beta = 0^0$,

$$x = \frac{\pi}{180} r_{00} \cos^{-1} \frac{r_{00}}{r} \tag{44}$$

so that

$$\frac{r}{r_{00}} = \left(\frac{r}{r_{00}} \right)_{min} = \frac{1}{\cos \frac{180}{\pi} \frac{x}{r_{00}}} = \frac{1}{\cos \delta_1}. \tag{45}$$

In Fig. 9 the two curves δ_1 and $(r/r_{00})_{min}$ can be seen to intersect at $r/r_{00} = 1.1$. For greater altitudes the range increases at the same time to such an extent that the summit point is no longer visible from the launching site. This portion of the r^*/r_1 curve is therefore dashed. The "inaccessible region" therefore comprises, for the MET, all cut-off velocities in excess of about $v_1/v_c = 0.6$. For the most interesting parts of the MET, the visibility requirements could not be fulfilled.

Fig. 10 shows this fact in a different plot, namely as function of x_{1y^*}, so that other elliptic trajectories can be included. It can be seen that for interest-

ing orbital altitudes between 1.1 and 1.2, cut-off angles of at least 25 to 30 degrees are required. Since under actual optical conditions the vehicle when arriving at the summit point, should be visible at least under a small elevation angle of, say 10 to 15 degrees, it follows that visibility requirements from the launching site lead to rather high cut-off angles. In many cases it is therefore advisable to track the transition into the satellite orbit from a downrange station.

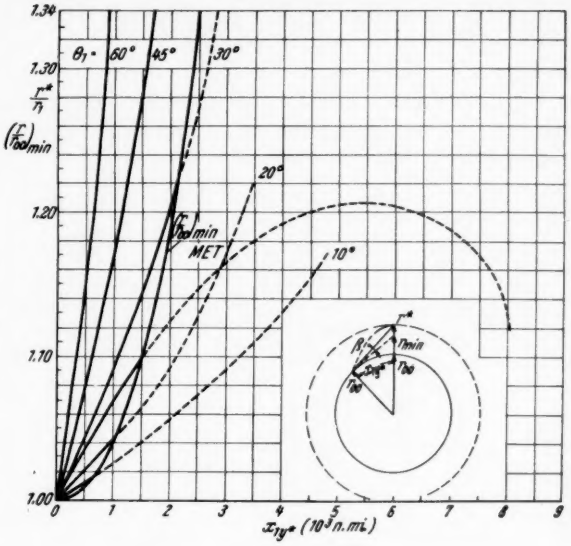

Fig. 10. Visibility during ballistic ascent

VI. Flight Time

The results of the flight time calculations are presented in Figs. 11 and 12, as function of cut-off velocity and altitude, respectively. It is seen that a com-

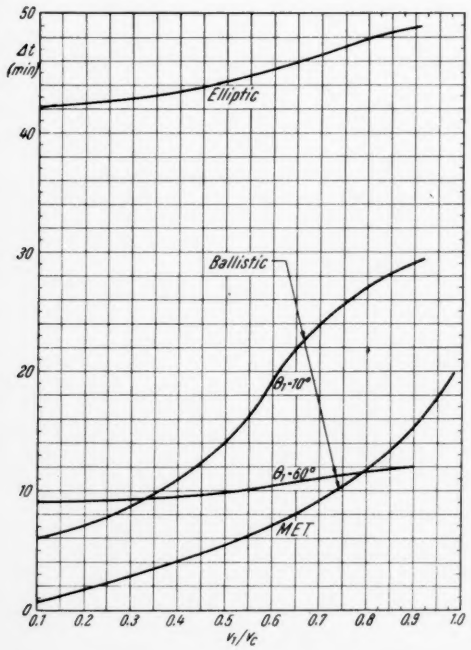

Fig. 11. Coasting time as function of cut-off velocity

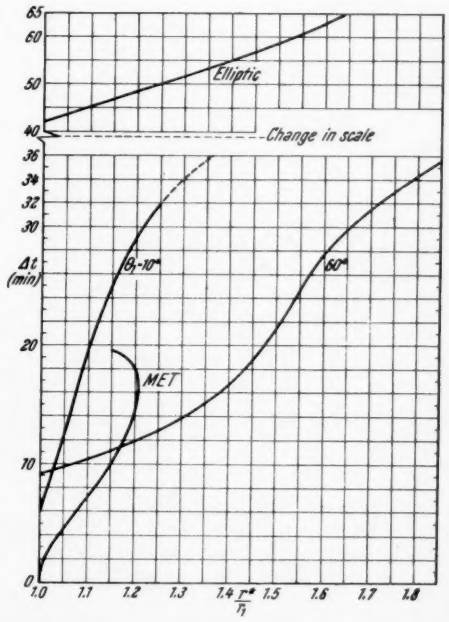

Fig. 12. Coasting time as function of summit altitude

paratively strong reduction in coasting time is obtained with the ballistic ascent.

However, in view of the comparatively short coasting time in the case of elliptic ascent, the reduction in time will not be significant for normal flight schedules; and, in view of the other unfavorable implications, there will be very few cases in which the time reduction is sufficient reason for selecting the ballistic ascent.

VII. Conclusion

Except for comparatively low altitude orbits at 200 to 300 n.mi. (360 to 540 km), the unfavorable characteristics of the ballistic ascent outweigh its attractive features to the extent that ballistic ascent will be considered only in special cases, involving exceptional conditions or requirements.

Über die Überbrückung interstellarer Entfernungen

Von

W. Peschka[1], ÖGfW

(Mit 5 Abbildungen)

(*Eingelangt am 16. März 1956*)

Zusammenfassung. Es wird gezeigt, daß Entfernungen bis zu ungefähr 25 Lichtjahren durch Photonenraketen einst erreichbar sein werden, wobei auch die Rückkehr gesichert ist. Die Reisegeschwindigkeit soll möglichst nahe an die des Lichtes im Vakuum heranreichen, weil dann die Zeitdehnung, die sich aus der speziellen Relativitätstheorie ergibt, bereits fühlbar wird. Ferner wird gezeigt, daß enorme Massenverhältnisse nötig sind, um diesen Zeitdehnungseffekt überhaupt zu erreichen.

Abstract. It is shown that distances up to about 25 light years, plus return voyage, may be attainable eventually by means of photon rockets. The transit velocity should approach as closely as possible the velocity of light, when the time dilatation, which follows from relativity theory, would become appreciable. It is demonstrated that enormous mass ratios would be required to exploit this effect.

Résumé. L'auteur montre que l'utilisation de fusées à photons permet d'envisager des rayons d'action de l'ordre de 25 années de lumière. La vitesse de croisière serait voisine de celle de la lumière dans le vide, la dilatation relativiste du temps devenant alors sensible. Des rapports de masse énormes seront nécessaires pour réaliser ces conditions.

Unter dem Titel „Die Erreichbarkeit der Himmelskörper" hat im Jahre 1925 WALTER HOHMANN eine Arbeit veröffentlicht, in der er unter vereinfachenden Annahmen Bahnkurven, Start und Landemanöver sowie die Rückkehrmöglichkeiten für Raumfahrzeuge berechnete. Reiseziele waren die Planeten unseres Sonnensystems, die mit einem Mindestaufwand an Treibstoff erreicht werden sollten. Die Reisegeschwindigkeiten lagen dabei — je nach dem Reiseziel — zwischen 20 km/sec und 40 km/sec. (Alle Geschwindigkeiten werden in dieser Arbeit auf den Schwerpunkt unseres Sonnensystems bezogen, sofern nicht ausdrücklich ein anderes Bezugssystem genannt wird.) Die Reisedauern zu den inneren Planeten unseres Sonnensystems, einschließlich der Rückreise, liegen dabei zwischen 2 und 5 Erdenjahren, während die Entfernungen Erde—Planet größenordnungsmäßig etwa 100 Millionen Kilometer betragen.

Diese Entfernungen sind verschwindend klein gegen die der Fixsterne, so daß die Frage nach deren Erreichbarkeit zunächst als Utopie erscheint. In der Tat, bei Reisegeschwindigkeiten von 40 km/sec — die man vielleicht einmal mit thermischen Atomraketen erreichen wird — und Entfernungen von 5 bis 100 Lichtjahren (der nächsten Fixsterne) ergeben sich Reisedauern, die natürlich völlig indiskutabel sind. Das hält aber die Helden in Zukunftsromanen nicht ab,

[1] Technische Hochschule, II. Institut für Allgemeine Mechanik, Wien IV., Karlsplatz 13, Österreich.

interstellare Entfernungen in phantastisch kurzen Zeiten zu durcheilen, weil es sich die Verfasser solcher „Romane, die einmal Wahrheit werden können" sehr leicht machen, indem die Reisegeschwindigkeit ihrer Fahrzeuge einfach beliebige Vielfache der Lichtgeschwindigkeit betragen soll. Noch dazu bringen es die Helden dieser Erzählungen fertig, mit der Startbasis in drahtloser Verbindung zu bleiben, trotzdem die Fortpflanzungsgeschwindigkeit drahtloser Signale gleich der des Lichtes ist und diese eine obere Grenzgeschwindigkeit darstellt.

Der Zweck dieser Arbeit ist es, zu zeigen, daß Sterne, die maximal etwa 25 Lichtjahre von uns entfernt sind, unter folgender Voraussetzung erreichbar sein werden:

Es soll möglich sein, Triebwerke zu bauen, die mit technisch realisierbarem Aufwand gestatten, der Lichtgeschwindigkeit beliebig nahe zu kommen.

Dies erfordert, daß die Ausstoßgeschwindigkeit der Treibmaterie relativ zur Rakete möglichst nahe an die Lichtgeschwindigkeit heranreichen muß, um nicht dadurch das Massenverhältnis schon untragbar hoch zu machen.

So hohe Ausstoßgeschwindigkeiten sind nur mit Ionen- oder Photonentriebwerken erreichbar. Leistungsfähige Triebwerke dieser Art kennt man heute noch nicht. Wenn es aber einst gelingen wird, thermonukleare Kettenreaktionen unter technische Kontrolle zu bringen, dann ist der größte Schritt bereits getan, weil sich dann wahrscheinlich die hohen Photonenstromdichten, die man benötigt, erzeugen lassen werden.

Die Ionenrakete würde Teilchenbeschleuniger für ebenfalls extrem große Stromdichten verlangen. Bei derart hohen Stromdichten ist es aber sehr schwierig, den Ionenstrahl im Apparat zusammenzuhalten, weil die abstoßenden Kräfte im Strahl enorm groß werden. Die spezielle Relativitätstheorie zeigt jedoch, daß diese abstoßenden Kräfte gegen Null gehen, wenn die Teilchengeschwindigkeit gleich der Lichtgeschwindigkeit wird. Je näher also die Teilchengeschwindigkeit an die Lichtgeschwindigkeit heranreicht, desto höhere Stromdichten sind erreichbar, weshalb eben auch bei der Ionenrakete die Ausstoßgeschwindigkeit möglichst der Lichtgeschwindigkeit nahekommen soll. Da die Reisegeschwindigkeit daher ebenfalls der des Lichtes beliebig nahekommen soll, kann nicht mehr mit der „klassischen Mechanik" gerechnet werden. Streng genommen ist hier die allgemeine Relativitätstheorie zuständig, weil die Rakete und unser Sonnensystem gegeneinander beschleunigte Bezugssysteme darstellen, solange das Triebwerk arbeitet. Die Näherung nach der speziellen Relativitätstheorie ist trotzdem zulässig, da der Einfluß des durch die Beschleunigung hervorgerufenen Gravitationsfeldes sehr gering ist und außerdem die Raum-Zeit-Intervalle noch klein genug sind.

Solange die Bewegung — bezogen auf ein LORENTZsches Bezugssystem — geradlinig ist, kann überhaupt mit der speziellen Relativitätstheorie gearbeitet werden.

Es seien nun kurz die wichtigsten Ergebnisse der speziellen Relativitätstheorie angeführt, weil sie dann später nötig sein werden (zitiert aus [1]).

1. Aufgabe der speziellen Relativitätstheorie ist es, Naturgesetze zu ermitteln, die sich invariant verhalten beim Übergang von einem Bezugssystem zu beliebigen, gegen dieses geradlinig gleichförmig bewegten Systemen.

2. Der NEWTONsche Begriff einer universellen Zeit ist unhaltbar, man muß vielmehr jeder Stelle in einem Bezugssystem ihre individuelle Zeitmessung (Uhr) zugeordnet denken (EINSTEINsches Zeitprinzip). Gerade dieses Zeitprinzip gestattet die Unabhängigkeit der Naturgesetze in gegeneinander gleichförmig geradlinig bewegten Bezugssystemen.

3. Prinzip von der Homogenität von Raum und Zeit.

4. Prinzip von der Konstanz der Lichtgeschwindigkeit:

Von allen gegen ein Grundsystem geradlinig gleichförmig bewegten Systemen aus betrachtet, pflanzt sich das Licht im Vakuum geradlinig und mit derselben konstanten Geschwindigkeit fort, unabhängig davon, ob die Lichtquelle mitgeführt wird oder nicht.

Die Ergebnisse dieser Postulate sind nun folgende:

Es seien zwei Raumzeitsysteme $L(x, y, z, t)$ und $L'(x', y', z', t')$ mit gemeinsamen Raumzeitanfangspunkten betrachtet, von denen das zweite sich mit der Geschwindigkeit $v > 0$ in Richtung der positiven x-Achse gegen das erste geradlinig gleichförmig bewege.

Im übrigen falle die x'-Achse dauernd mit der x-Achse zusammen, während die y- und y'-Achse und ebenso die z- und z'-Achse zueinander dauernd parallel bleiben.

Dann werden die Beziehungen zwischen den Raumzeitkoordinaten ein und desselben Ereignisses in diesen beiden Systemen durch folgende Gleichungen dargestellt:

$$\begin{aligned} x' &= K(x - v\,t), & x &= K(x' - v\,t'), & \frac{1}{K^2} &= 1 - \beta^2 \\ y' &= y, \quad z' = z, & y &= y', \quad z = z', & & \\ t' &= K\left(t - \frac{v}{c^2}\,x\right), & t &= K\left(t' - \frac{v}{c^2}\,x'\right), & \beta &= \frac{v}{c}. \end{aligned} \tag{1}$$

Vol. 2 1956

Längenvergleich: Ein Stab von der Länge l im „gestrichenen" System hat, wenn er senkrecht zur Bewegungsrichtung liegt, vom „ungestrichenen" System aus betrachtet dieselbe Länge l; liegt er hingegen parallel zur Bewegungsrichtung, dann hat er die Länge

$$l \cdot \sqrt{1 - \beta^2} \quad \text{und umgekehrt.} \tag{2}$$

Zeitvergleich: Von den beiden Uhren im Anfangspunkt 0 und 0′ unserer beiden Koordinatensysteme L und L', die im Augenblick der Koinzidenz (nach Voraussetzung) gleiche Zeit zeigten ($t_0 = t'_{0'} = 0$), bleibt jede hinter den Uhren des anderen Systems, an denen sie vorbeizieht, zurück: Es ist

$$t'_{0'} = t_{0'} \sqrt{1 - \beta^2} \qquad \text{und} \qquad t_0 = t'_0 \cdot \sqrt{1 - \beta^2}. \tag{3}$$

Ungenau ausgesprochen lautet dieser Satz: „Bewegte Uhren gehen langsamer als ruhende Uhren."

Als weiteres wichtiges Ergebnis sei hier noch das Additionstheorem der Geschwindigkeiten angegeben:

Bewegt sich ein Punkt, auf das „gestrichene" System bezogen, mit der Geschwindigkeit u' in der x-Richtung, so ist seine Geschwindigkeit u, bezogen auf das „ungestrichene" System:

$$u = \frac{u' + v}{1 + \dfrac{u'v}{c^2}}, \tag{4}$$

wo v wieder die Relativgeschwindigkeit der beiden geradlinig gleichförmig gegeneinander bewegten Systeme ist.

Aus Gl. (4) folgt unter anderem, daß Überlichtgeschwindigkeit nicht durch Superposition von Unterlichtgeschwindigkeiten erreicht werden kann.

Zuletzt seien noch zwei allgemein bekannte Beziehungen angeführt:

$$E = m \cdot c^2. \tag{5}$$

Zufolge Gl. (5) wird der Energie Trägheit, also Masse, zugeschrieben.

$$m = \frac{m_0}{\sqrt{1 - \beta^2}}. \tag{6}$$

Als wichtigste Folgerungen aus den beiden letzten Gleichungen sei nur angeführt, daß eine Masse nie Lichtgeschwindigkeit erreichen kann und daß die Ruhmasse der Lichtquanten (Photonen) gleich Null ist.

Es möge noch erwähnt werden, daß Gln. (5) und (6) schon vor der speziellen Relativitätstheorie bekannt waren.

Mit den Gln. (3) bis (6) können nun alle Fragen, die uns hier interessieren, geklärt werden.

Zunächst sei noch der Vollständigkeit halber die relativistische Raketengleichung angeschrieben (vgl. [2]):

Die Rakete möge sich bei Abwesenheit von äußeren Kräften (Schwerkraft) bewegen (Abb. 1). v sei ihre Geschwindigkeit bezogen auf ein Inertialsystem. u sei die Ausstoßgeschwindigkeit der Treibmasse bezogen auf die Rakete, u_1 bezogen auf das Inertialsystem.

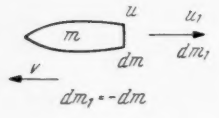

Abb. 1

Der Schwerpunktsatz (Impulssatz) ergibt:

$$d(m\,v) - u_1\,dm_1 = 0.$$

Mit Gl. (4) erhält man:

$$u_1 = \frac{u - v}{1 - \frac{u\,v}{c^2}},$$

und nach einigen Umformungen ergibt sich die Differentialgleichung

$$\frac{1 - \frac{u\,v}{c^2}}{1 - \frac{v^2}{c^2}} \cdot dv = -\,u\,\frac{dm}{m},$$

die leicht integriert werden kann. Man erhält

$$\left(\frac{1 + \frac{v}{c}}{1 - \frac{v}{c}}\right)^{\frac{c}{2u}} = \frac{M}{m\left(1 - \frac{v^2}{c^2}\right)^{1/2}} =$$

$$= \frac{M}{m_r} = \sigma_r. \qquad (7)$$

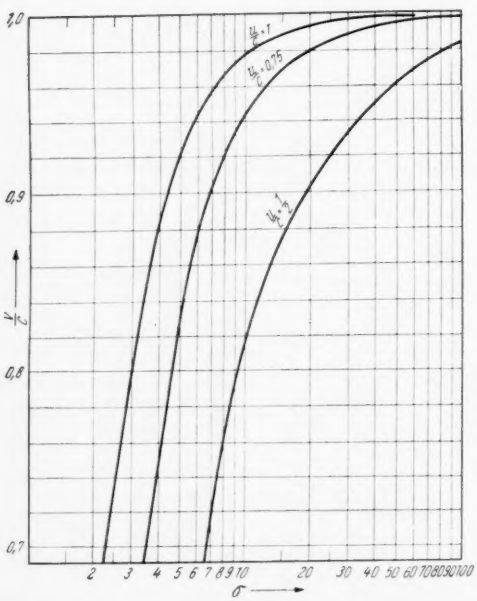

Abb. 2

M ist die Startruhmasse, m_r die jeweilige Raketenruhmasse und σ_r das dazugehörige Massenverhältnis. Löst man nach v auf, so erhält man:

$$\frac{v}{c} = \frac{\sigma_r^{\frac{2u}{c}} - 1}{\sigma_r^{\frac{2u}{c}} + 1}. \qquad (8)$$

Gl. (8) ist für verschiedene Verhältnisse u/c in Abb. 2 aufgetragen. Die später folgenden Betrachtungen sind für $u/c \doteq 1$ angestellt, also für die Photonenrakete oder die Ionenraketen, deren Ausstoßgeschwindigkeit nahezu Lichtgeschwindigkeit ist.

Ferner wird noch das Weg-Zeit-, Geschwindigkeits-Zeit- und Beschleunigungs-Zeit-Gesetz der Bewegung eines Massenpunktes, auf den eine Kraft wirkt, benötigt, wobei aber die Massenveränderlichkeit berücksichtigt werden soll.

Das Grundgesetz der Dynamik lautet (vgl. Abb. 3):

$$\frac{d(m\,\mathfrak{v})}{dt} = \mathfrak{P}; \qquad (9)$$

$\mathfrak{v}$ Geschwindigkeit, $\mathfrak{P}$ Kraft; $\mathfrak{v} = v \cdot \mathfrak{t}$, $v = |\mathfrak{v}|$ Betrag der Geschwindigkeit. $\mathfrak{t}$ Tangentenvektor an die Bahnkurve, $\mathfrak{n}$ Bahnnormale $|\mathfrak{n}| = 1$, $|\mathfrak{t}| = 1$, ϱ Krümmungsradius der Bahn; für m gilt $m = \frac{m_0}{(1-\beta^2)^{1/2}}$ nach Gl. (6).

Gl. (6) gibt mit Gl. (9) nach kurzer Umformung:

$$\mathfrak{P} = \frac{m_0}{\sqrt{\left(1-\frac{v^2}{c^2}\right)^3}} \cdot \frac{dv}{dt} \cdot \mathfrak{t} + \frac{m_0}{\sqrt{1-\frac{v^2}{c^2}}} \cdot \frac{v^2}{\varrho} \cdot \mathfrak{n}. \tag{10}$$

Nun mögen bezüglich eines Inertialsystems geradlinige Bewegungen betrachtet werden, also $1/\varrho \to 0$.

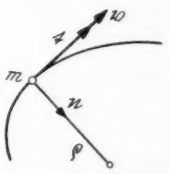

Abb. 3

Dann gilt

$$P = \frac{m_0}{\sqrt{\left(1-\frac{v^2}{c^2}\right)^3}} \cdot \frac{dv}{dt} \tag{11}$$

$$P = |\mathfrak{P}|.$$

$b = dv/dt$ ist die Beschleunigung des Massenpunktes.

Über diese Beschleunigung muß während des Fluges der Rakete eine Annahme gemacht werden. Es wird hier angenommen, daß der Schub der Rakete während des Fluges so geregelt wird, daß der Schwerefaktor $\varkappa$ konstant bleibt.

Mit Gl. (11) erhält man:

$$\varkappa = \frac{P}{m_0 g} = \frac{b}{g}\left(1-\frac{v^2}{c^2}\right)^{-3/2}. \tag{12}$$

Das $v(t)$ Gesetz lautet dann:

$$v = \frac{\varkappa g t}{\sqrt{1+\left(\frac{\varkappa g t}{c}\right)^2}} \tag{13}$$

für $t = 0$, $v = 0$.

Das $s(t)$ Gesetz ist:

$$s = \frac{c^2}{\varkappa g}\left[\sqrt{1+\left(\frac{\varkappa g t}{c}\right)^2} - 1\right], \tag{14}$$

oder nach t aufgelöst:

$$t = \frac{c}{\varkappa g} \cdot \sqrt{\left(\frac{\varkappa g s}{c^2}+1\right)^2 - 1} \tag{15}$$

für $t = 0$, $s = 0$.

Diese Ergebnisse sind nun auf unseren Fall anwendbar, wenn man von der gegenseitigen Bewegung der Fixsterne — in unserem Falle von der des Zielsternes gegen unser Sonnensystem — absehen kann, wenn also die Bahn der Rakete bezogen auf das Sonnensystem eine Gerade ist. Die Gln. (13), (14) und (15) geben dann die Beziehungen zwischen Geschwindigkeit, Weg und Zeit wieder, wobei die Rakete stets so beschleunigt werden soll, daß der Schwerefaktor $\varkappa$ konstant bleibt. Von der Wirkung des Schwerefeldes der Sonne kann vollkommen abgesehen werden, weil die parabolische Geschwindigkeit bezüglich der Sonne gegen die Reisegeschwindigkeit verschwindet (40 km/sec gegen angenähert 300 000 km/sec).

Für unsere Überlegungen wurde als Bezugssystem ein Koordinatensystem gewählt, dessen Ursprung mit dem Schwerpunkt unseres Sonnensystems zusammenfällt und auf dessen einer Achse der Zielstern liegt. Wird von der Bewegung des Zielsternes gegen den Schwerpunkt unseres Sonnensystems abgesehen — eine Vernachlässigung, die sicher erlaubt ist —, dann ist dieses Bezugssystem ebenfalls ein Inertialsystem. Die Anfangsbedingung $t = 0, s = 0$ würde verlangen, daß die Rakete vom Schwerpunkt unseres Sonnensystems anstatt von der Erde aus startet. Da aber die Dimensionen unseres Sonnensystems gegen interstellare Entfernungen verschwindend klein sind, kann man die Ergebnisse ohneweiters auch für den Start von der Erde oder irgendeinem anderen Planeten unseres Sonnensystems anwenden. Die Rakete bekommt zwar die Revolutionsgeschwindigkeit des betreffenden Planeten mit, aber die dadurch bewirkte Abtrift kann leicht während der Fahrt korrigiert werden.

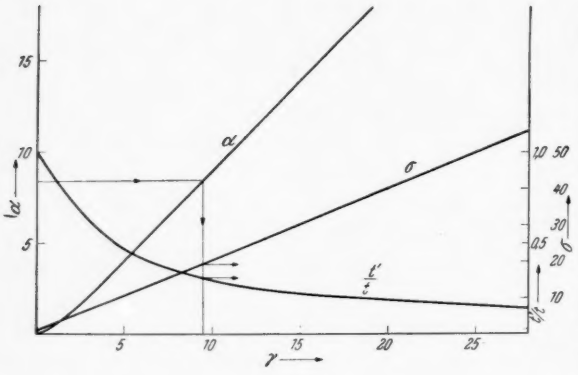

Abb. 4

In Abb. 4 sind nun die Gln. (13), (14) und die noch folgende Gl. (18) wiedergegeben.

Nimmt man ferner an, daß nach Durcheilen der halben Entfernung Erde-Ziel die Rakete um 180° gedreht wird, dann ist die dadurch bewirkte Verzögerung symmetrisch zur Beschleunigungsperiode. Man sieht, daß sich selbst bei Reisen mit angenähert Lichtgeschwindigkeit enorme Reisedauern — bezogen auf die Erde — ergeben.

Nun aber möge die Zeit berechnet werden, die eine Uhr in der Rakete anzeigen würde. Dies geschieht mit Gl. (3) $\Delta t' = \Delta t \cdot \sqrt{1 - \beta^2}$. Da hier die Geschwindigkeit v nicht konstant ist, muß zur Grenze übergegangen werden und man erhält:

$$t' = \int_0^t \sqrt{1 - \frac{v^2}{c^2}} \cdot d\tau. \tag{16}$$

Wird in Gl. (16) $v(t)$ aus Gl. (13) eingesetzt, so erhält man

$$t' = \int_0^t \frac{d\tau}{\sqrt{1 + \left(\frac{\varkappa g \tau}{c}\right)^2}} \tag{17}$$

und nach erfolgter Integration:

$$t' = \frac{c}{\varkappa g} \ln \left[\frac{\varkappa g}{c} \cdot t + \sqrt{1 + \left(\frac{\varkappa g t}{c}\right)^2} \right]. \tag{18}$$

Diese Zeit würde also eine Uhr im Raumfahrzeug anzeigen. Auch Gl. (18) ist in Abb. 4 wiedergegeben (Kurve t'/t).

Es kann nun gezeigt werden, daß t' zu einem Minimum wird, wenn entlang des halben Weges beschleunigt und dann spiegelbildlich verzögert wird. Sonst ist t' nur noch abhängig von $\varkappa$, dem Schwerefaktor, der so groß sein soll, als ihn ein Mensch dauernd ertragen kann. Aus Abb. 4 ersieht man aber auch sofort, daß dieses Minimum bei größeren Strecken nicht mehr erreicht werden kann, einfach weil das dazu erforderliche Massenverhältnis technisch nicht mehr realisierbar wird. Dies ist der Grund, warum Reisen in den interstellaren Raum bei Entfernungen von etwa 25 Lichtjahren ihre Grenze haben müssen.

In Tab. 1 sind die Daten für Flüge zu zwei näheren Fixsternen zusammengestellt.

Tabelle 1[1]

Stern (Sternbild)	Entfernung (LM)	$\varkappa$	$t \cdot 10^{-7}$ (sec)	$t' \cdot 10^{-7}$ (sec)	σ	Stufenzahl $\sigma_1 = 6$ $\sigma_2 = 8$	
Sirius (großer Hund)	8	2	56	17,6	400^2	~4	Gesamtreise
		2	28	8,8	400	~2	Hin-, bzw. Rückreise
		2, 0	60	48,8	100	2	Hin- und Rückflug; Antrieb nicht dauernd eingeschaltet
Wega (Leier)	25	2	171	24	3600^2	6	Gesamtreise
		2	85,5	12	3600	3	Hin-, bzw. Rückreise
		2, 0	216	179,2	100	2	Hin- und Rückflug; Antrieb nicht dauernd eingeschaltet

1 LM = 1 Lichtmeile = 10^{13} km = 1,05 Lichtjahre.
1 Jahr = $3{,}15 \cdot 10^7$ sec.

Die erste Zeile gibt in beiden Fällen die Daten für die Hin- und Rückreise. (Sirius und Wega sind nur gewählt worden, um die Verhältnisse näher zu illustrieren; es hätten ebensogut auch andere uns benachbarte Sterne gewählt werden können.)

Man sieht, daß für die Reise zur Wega das neunfache Massenverhältnis erforderlich ist wie bei der Reise zum Sirius, wenn entlang des halben Weges stets beschleunigt und entlang der zweiten Weghälfte stets verzögert wird. Tatsächlich ist das erforderliche Massenverhältnis unter diesen Umständen ungefähr dem Quadrat der Entfernung proportional.

In der zweiten Zeile sind die nötigen Daten für die Hin- oder Rückreise angegeben. Sollte es sich nämlich herausstellen, daß der Zielstern ein Planetensystem besitzt und sollte ferner der Fall eintreten, daß man dort die nötige Treibmaterie findet, dann liegt das Problem viel günstiger, da dann eben die Treibmasse für die Rückkehr nicht von der Erde aus mitgeführt werden muß. Das setzt natürlich voraus, daß mindestens ein Flug hin und zurück bereits gelungen und außerdem noch ein Planetensystem entdeckt worden ist.

[1] Für die Auffindung zweier numerischer Fehler ist der Verfasser Herrn Professor Dr. H. THIRRING sowie dessen Mitarbeiter Herrn Dr. BAUMANN zu Dank verpflichtet.

Die Gesamtreisezeit — bezogen auf die Erde — würde beim Flug zum Sirius ungefähr 19 Jahre betragen, bezogen auf die Rakete jedoch nur etwa 6 Jahre. Beim Flug zur Wega wären die Werte 57, bzw. 8 Jahre. Der Vorteil einer Reisegeschwindigkeit, die nur wenige Promille unter der des Lichtes liegt, ist ja gerade, daß die Mannschaft dabei wesentlich weniger altern würde. Dieser Vorteil muß aber dafür mit einem enorm großen Massenverhältnis erkauft werden.

In der dritten Zeile sind dann noch die Werte angegeben, die erforderlich sind, wenn für die Hin- und Rückreise mit einem Massenverhältnis von $\sigma = 100$ das Auslangen gefunden werden soll. Das bedingt natürlich, daß nur auf einem Teil der Reisestrecke der Antrieb eingeschaltet ist und daher ein Großteil der Strecke mit konstanter Geschwindigkeit durcheilt werden muß. Die Zeiten betragen dabei beim Sirius 20 und 16 Jahre, bei der Wega aber 70 und 60 Jahre, also Zeiten, die einer Raumschiffbesatzung niemals zugemutet werden können. Will man dennoch weiter entfernte Sterne aufsuchen, dann ist man eben gezwungen, mit Massenverhältnissen zu arbeiten, die so enorm sind, daß sie heute noch vollkommen absurd erscheinen. Es möge nun aber gezeigt werden, daß dem Massenverhältnis einer Mehrstufenrakete keine Grenze gesetzt ist, selbst wenn man vorschreibt, daß die Massenverhältnisse der einzelnen Stufen begrenzt sind.

Wenn σ das Verhältnis Anfangsmasse zu Endmasse der Stufenrakete ist, ferner σ_2 das Massenverhältnis jeder einzelnen Stufe — das bei allen Stufen gleich sein möge — und ferner σ_1 das Verhältnis von Masse der vollen ν-ten Stufe zur Masse der leeren ν-ten Stufe plus Masse aller folgenden Stufen, dann ist das Massenverhältnis σ einer n-stufigen Rakete durch σ_1 und σ_2 ausdrückbar, was man nach einiger Rechnung zeigen kann:

$$\sigma = \sigma_2 (1 + a)^{n-1} \qquad a = \frac{\sigma_1}{1 - \dfrac{\sigma_1}{\sigma_2}}, \qquad \sigma_1 < \sigma_2. \tag{19}$$

Löst man Gl. (19) nach n auf, so ergibt sich:

$$n = 1 + \frac{\ln \dfrac{\sigma}{\sigma_2}}{\ln (1 + a)}. \tag{20}$$

Gl. (20) ist in Abb. 5 aufgetragen. Damit wurde auch die Stufenzahl in Tab. 1 geschätzt.

Man sieht z. B., daß für $\sigma_1 = 6$, $\sigma_2 = 8$, $n = 4$ ein Massenverhältnis von $\sigma = 125\,000$ erreichbar wäre. Diese Rakete würde allerdings kosmische Dimensionen annehmen. Das wesentliche ist aber, daß man das Massenverhältnis σ beliebig groß machen kann und daß dabei trotzdem die Massenverhältnisse der einzelnen Stufen realisierbar bleiben. Platzmangel wird allerdings auf solchen „Raumschiffen der Asteroidenklasse" immer noch herrschen.

Es muß jedoch erwähnt werden, daß hier angenommen wurde, die Photonenrakete könne ihre gesamte Treibmasse in Form von Strahlung emittieren. Das ist sehr optimistisch. Ihren gesamten Massenvorrat in Strahlung zu verwandeln, das bringen nicht einmal die Fixsterne fertig. Und diese müßten wohl unsere Lehrmeister sein, wenn es einmal gelingen sollte, Photonenraketen zu bauen. Man kann gleichwohl annehmen, daß die nicht in Strahlung verwandelte Masse in Form von Ionen ausgestoßen werden kann, umso mehr als aus diesen und noch einigen in einer gesonderten Arbeit klarzulegenden Gründen ein kombiniertes Ionen-Photonentriebwerk das günstigste Antriebsmittel sein dürfte.

Der Start eines solchen Riesenfahrzeuges von der Erde aus wäre wegen der großen Gefahren sehr bedenklich. Man bedenke nur, welch fürchterliche Wirkung

ein Ionen-Photonenstrahl, dessen Schub in die Millionen Tonnen geht, haben würde — falls nicht etwa so hohe Strahlungsintensitäten schon aus physikalischen Gründen gar nicht erzeugbar sind.

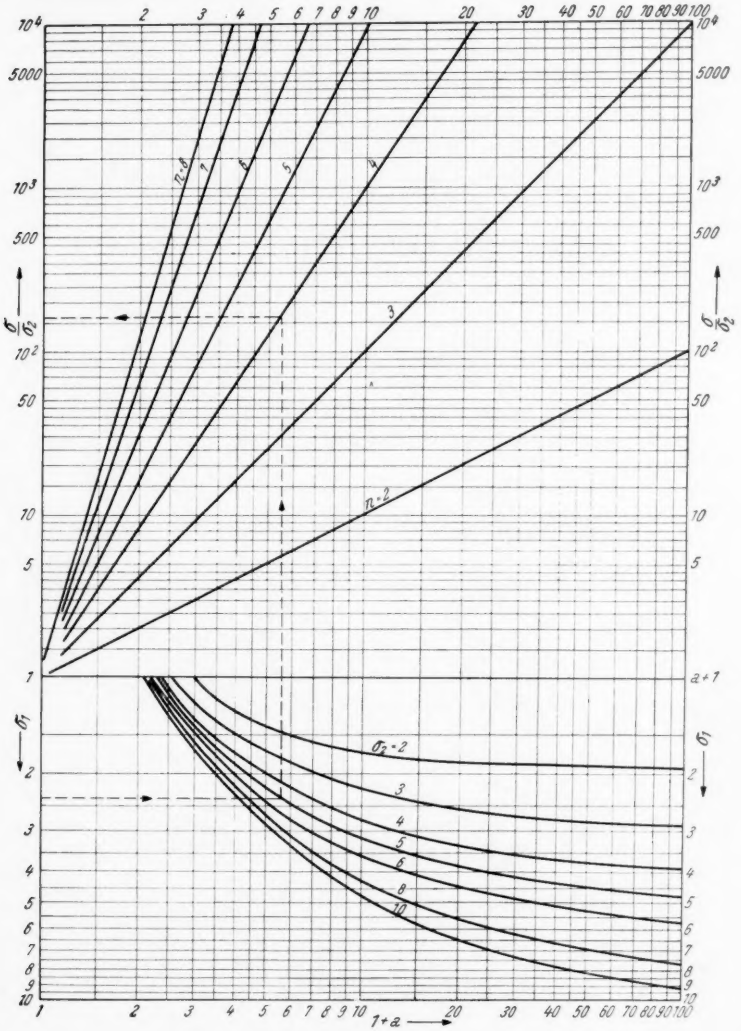

Abb. 5

Zusammenfassend kann also gesagt werden, daß die uns benachbarten Sterne erreichbar sein werden, wenn die Photonenrakete einmal existiert. Ein großes Glück für die bejammernswerte Besatzung eines solchen Himmelskörpers wäre es, wenn der Zielstern ein Planetensystem besäße: Diese Tatsache würde die Reise sehr erleichtern. Ferner wurde gezeigt, daß der Zeitmaßstab für die Rakete sehr gedehnt wird, wenn die Reisegeschwindigkeit nur wenig kleiner als die Lichtgeschwindigkeit ist, wodurch das Durcheilen dieser enormen Strecken für die Mannschaft überhaupt erst erträglich werden dürfte.

Es haben also auch die Verfasser von Zukunftsromanen und ähnlichen Geschichten es nicht nötig, ihre Helden und Heldinnen mit x-facher Lichtgeschwindigkeit durch den Raum fliegen zu lassen, um in fabelhaft kurzen Zeiten Millionen von Lichtjahren zurücklegen zu können. Solche Entfernungen werden uns immer verschlossen bleiben. Nur die allernächsten Sterne werden einst erreichbar sein.

Eine Möglichkeit hierzu ist die Photonenrakete.

Sie wird die einzige sein.

Literaturverzeichnis

1. E. R. NEUMANN, Vorlesungen zur Einführung in die Relativitätstheorie. Jena: G. Fischer, 1922.
2. J. ACKERET, Zur Theorie der Rakete. Helvet. Physica Acta **19**, 2 (1946).

Nachsatz

(eingelangt am 8. Oktober 1956)

Abschließend mögen einige Veröffentlichungen angeführt werden, die ebenfalls das Problem der Photonenrakete behandeln, aber nicht der vorliegenden Arbeit zugrundeliegen.

Da wäre zunächst eine Arbeit von R. ESNAULT-PELTERIE zu nennen, erschienen in L'Astronautique, Paris: Lahure, 1930.

Ferner Arbeiten von E. SÄNGER:

1. „Zur Theorie der Photonenraketen" (IV. Internationaler Astronautischer Kongreß in Zürich, 1953), unter demselben Titel erschienen in: Ingenieur-Archiv **21**, 213 (1953) und in: „Probleme der Weltraumforschung", Biel-Bienne: Laubscher und Cie., 1954. (Hier wird allerdings das Hauptaugenmerk auf Antriebsfragen gelegt.)

2. „Zur Mechanik der Photonenstrahlantriebe", Heft 5 der Mitteilungen aus dem Forschungsinstitut für Physik der Strahlantriebe e.V. Stuttgart, München: R. Oldenbourg, Januar 1956. Dort ist auch ein Literaturverzeichnis über einschlägige Arbeiten auf diesem Gebiet enthalten[1].

Des weiteren wäre noch eine Arbeit E. SÄNGERS zu nennen, die auch auf dem VII. Internationalen Astronautischen Kongreß in Rom (September 1956) unter dem Titel „Die Erreichbarkeit der Fixsterne" vorgetragen wurde und im wesentlichen dasselbe Gebiet bearbeitet wie die vorliegende Arbeit des Verfassers; schließlich ein (noch nicht veröffentlichter) Vortrag von E. SÄNGER in Freudenstadt/Schwarzwald (Februar 1956): „Zur Flugmechanik der Photonenraketen", der dem Verfasser bisher noch nicht inhaltlich bekannt geworden ist.

[1] Es möge noch erwähnt werden, daß sich der Verfasser der vorliegenden Veröffentlichung einigen Ergebnissen dieser zitierten Arbeit nicht anschließen kann.

Über einen photographischen Nachweis von Primären der kosmischen Strahlung in Erdbodennähe

Von

W. Strubell[1], GfW, PTA[2]

(Mit 1 Abbildung)

(*Eingelangt am 3. April 1956*)

Zusammenfassung. Es wird über eine seltene Sternfigur berichtet, die in Erdbodennähe registriert werden konnte.

Abstract. A very rare star figure is shown which was discovered near the ground.

Résumé. Présentation d'un cas extraordinaire de désintégration en étoile dans une émulsion photographique obtenue par exposition au rayonnement cosmique dans le voisinage de la surface terrestre.

Vol. 2 1956

Die Beeinflussung der kosmischen Strahlung auf lebendes Gewebe und Material zu kennen, ist für die künftige Weltraumfahrt wichtig, besonders deshalb, weil außerhalb der schützenden Atmosphäre mit Sicherheit außer Protonen und Elektronen auch schwere Kerne zu finden sind. Da nun vor allem die schweren Primären der kosmischen Strahlung durch Wechselwirkung in der Atmosphäre vernichtet werden, sind zur Erforschung dieser Teilchen stets große Höhen nötig.

Im folgenden wird über eine sehr seltene Sternfigur berichtet, die in einer Photoplatte in 150 m Höhe registriert wurde.

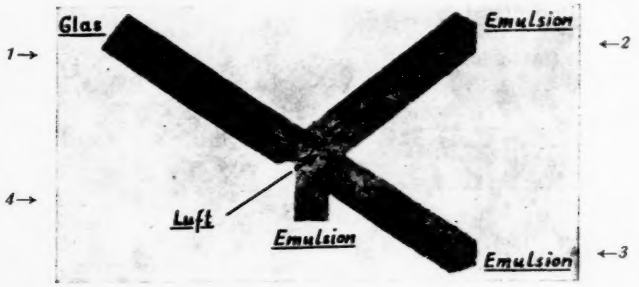

Abb. 1. Sternfigur aus 150 m Höhe über NN

Der Verfasser legte 1950 kernphysikalische Platten der Agfa, Typ K-1, in 150 m Höhe aus und fand bei der Durchsicht einer Platte die in Abb. 1 reproduzierte Sternfigur.

[1] Leipzig 0 5, Hermann-Liebmann-Str. 19 II, Deutsche Demokratische Republik.
[2] Polskie Towarzystwo Astronauticzne.

Dieser Stern ist insofern interessant, weil die Kernzertrümmerung selbst nicht registriert wurde. Sie muß also zwischen Platte und Verpackung mutmaßlich durch einen Fremdkörper hervorgerufen worden sein.

In Tab. 1 sind alle Daten für die in Abb. 1 gezeigte Kernzertrümmerung zusammengestellt.

Tabelle 1

Spur Nr.	Länge in μ	Anzahl der Körner	Mittlerer Kornabstand	Mittlere Korndichte	Ende der Spur
1	195	105	1,86	0,54	im Glas
2	183	39	4,8	0,21	in der Emulsion
3	163	37	4,4	0,28	in der Emulsion
4	17	8	2,1	0,48	in der Emulsion

Die Identifizierung der vier Spuren wurde auf Grund der bekannten Kornabstand-Reichweite-Beziehung und ihre Energie durch die Energie-Reichweite-Beziehung ermittelt, nachdem vorher die Platte mit Protonen und α-Teilchen geeicht worden war.

Zunächst sei gesagt, daß die Agfa K-1-Platte nur Protonen, α-Teilchen und schwere Primäre registrieren kann.

Die Bestimmung von Spur 1 ist unmöglich, da das Ende der Spur außerhalb der Emulsion im Glas liegt. Die Spur zeigt jedoch zum Ende hin eine starke Streuung, die mit der von Rückstoßprotonen in der K-1-Emulsion vergleichbar ist. Es liegt deshalb die Vermutung nahe, daß es sich um eine Protonenspur handeln könnte.

Die Spuren 2 und 3 sind beide als Protonenspuren auf Grund der Kornabstand-Reichweite-Beziehung identifiziert worden, während es sich bei Spur 4 um ein Teilchen von ganz geringer Energie, um ein α-Teilchen, handelt.

Auf Grund der Energie-Reichweite-Beziehungen, die durch Eichversuche mit Rückstoßprotonen und α-Teilchen in Agfa K-1-Platten ermittelt wurden, ergibt sich für die vier Bahnspuren das in Tab. 2 dargestellte Bild.

Bedauerlicherweise lassen die vier Bahnspuren keine Rückschlüsse auf das erzeugende Elementarteilchen dieses Sternes zu. Fest steht aber, daß keine der vier Spuren die Bahn des sternerzeugenden Teilchens zeigt; denn alle Spuren sind viel zu kurz, um daraus eine genaue Entscheidung treffen zu können. Bei Spur 2 könnte man vielleicht auf Grund der Zunahme der Kornzahl nach dem Zentrum hin schließen, daß es sich um die Spur des Primärteilchens handelt. Aber die nach außen hin zunehmende geringe, bei starker Vergrößerung gut erkennbare Streuung widerlegt diese Annahme. Außerdem liegt bei dieser Spur das Ende der Reichweite in der Emulsion, so daß auf Grund der Energiebilanz dieses Teilchen als Primärkomponente ausscheidet; denn die Energie des Primärteilchens muß ja bekanntlich gleich mindestens der Summe der Energie aller ausgesandten Teilchen sein. Aus der Summe der Energien (Tab. 2) läßt sich etwa auf einen Primären $Z = 12 - 20$ schließen.

Tabelle 2

Spur Nr.	Teilchenart	Energie
1	?	?
2	p	$4 \cdot 10^6$ eV
3	p	$3 \cdot 10^6$ eV
4	α	$4 \cdot 10^6$ eV

Personal Experiences during Short Periods of Weightlessness Reported by Sixteen Subjects[1]

By

S. J. Gerathewohl[2]

(*Received June 18, 1956*)

Abstract. A series of experiments on weightlessness was conducted using a Lockheed T-33 type aircraft for dives and parabola flights yielding practical weightlessness from 10 to 30 seconds duration. Records of the personal experiences of sixteen subjects during these states were obtained by interviews, pilot reports, and written statements.

Results: The majority of our subjects felt very comfortable during weightlessness; several subjects reported sensations of motion with no emotional involvement. A small group of subjects experienced discomfort, nausea, and severe symptoms of motion sickness.

Tolerance to weightlessness is discussed with regard to space flight. It is theorized that individuals differ significantly as to their susceptibility to sub- and zero-gravity and their adaptability to weightlessness. If the right persons can be selected and adapted, some earlier concepts about artificial acceleration or "quasi-gravity" of space vehicles can be revised.

Zusammenfassung. Ein Strahlflugzeug vom Typ Lockheed T-33 wurde für Versuche im andrucklosen Zustand verwendet, wobei im Sturz- und Parabelflug Andrucklosigkeit für die Dauer von 10 bis 30 Sekunden erzielt wurde. Einsicht in die Erlebnisse der Schwerefreiheit ergab sich durch Aussprachen und Interviews, Angaben des Piloten und schriftliche Berichte der Versuchspersonen.

Ergebnisse: Die Mehrzahl der Versuchspersonen erlebte den Zustand der Schwerefreiheit als angenehm; mehrere Personen berichten gefühlsneutrale Bewegungssensationen wie Fallen, Schweben und Drehempfindungen. Eine kleine Gruppe empfand den Zustand als unlustbetont und zeigte Symptome, die für die See- und Luftkrankheit charakteristisch sind.

Die Frage der Toleranz gegenüber der Schwerelosigkeit wird in Hinblick auf den Raumflug diskutiert. Es scheinen erhebliche Unterschiede zwischen den Individuen zu bestehen, sowohl was Toleranz als auch Anpassungsfähigkeit betrifft. Wenn man die geeigneten Personen auslesen kann, wird man auf die Einführung einer Dauerbeschleunigung oder „Quasi-Gravitation" bei Raumschiffen verzichten können.

Résumé. Une série d'expériences a été conduite à bord d'un avion Lockheed T-33 suivant une trajectoire parabolique ou de piqué en vue de neutraliser le champ de la pesanteur pendant une durée de 10 à 30 secondes. Les sensations éprouvées par seize sujets ont été recueillies soit par les rapports des pilotes ou par interviews et déclarations écrites.

---

[1] This paper was presented at the Seventh International Astronautical Congress in Rome, September 1956. — Opinions expressed herein are solely those of the author and in no way reflect the official views of the Department of Defense or the United States Air Force.

[2] School of Aviation Medicine, U.S.A.F., USA.

Résultats: La majorité des expérimentateurs ont trouvé la période de suppression de la pesanteur agréable; quelques uns ont éprouvé des sensations de mouvements sans réactions émotives. Un petit nombre s'est trouvé sujet aux symptomes caractéristiques du mal de mer et de vol: nausées et sensation d'incomfort.

La tolérance vis à vis de la suppression de la pesanteur est envisagée en relation avec le vol interplanétaire. Il semble que la réduction et la suppression de la pesanteur peut affecter les sujets de façons sensiblement différentes et que les capacités d'adaptation sont aussi variables. Si une sélection peut être faite en vue de l'adaptation certaines idées antérieures sur la nécessité d'une pesanteur artificielle dans les astronefs doivent être révisées.

In space flight operations, sub- and zero-gravity states will occur for considerable periods of time [1—8]. The psychophysiological condition associated with these states is designated as weightlessness and has been treated as a subject of scientific concern in numerous papers during the past seven years [9—17]. By and large, these treatises deal mainly with the phenomenon of weightlessness in a rather theoretical way, or they contain experimental data on alteration of performance during the weightless state. Only sporadically one finds reports about personal experience of weightlessness; and the few reports available from individuals having firsthand experience are almost shamefully hidden in an inconspicuous paragraph at the end of some research papers [13, 20, 23]. However, in the experience of every pilot or person, who was exposed to the weightless condition for at least a few seconds, there are certain symptoms that he interprets as weightlessness, and that manifest themselves as sensations being predominantly subjective in nature on the one hand, and as changes of performance on the other, the latter being chiefly distinguished by an overt and pronounced tendency of objectivation.

Before we attempt to demonstrate some of the problems involved in human behavior during the weightless state, we must discuss the problem of personal experience somewhat further. There can be no doubt that the differentiation between "sensations" on the one side, and "performance" on the other side, is an artificial one because both factors are so closely linked together and interrelated that any separation can serve as a working hypothesis only. It is mainly for the sake of a schematic classification of symptoms that we confine ourselves to the treatment of the "subjective" or personal experiences of weightlessness. Actually, changes in gravity, acceleration, and weight stimulate our mechanoreceptor organs which in turn discharge impulses to the brain. We have enough reason to assume that particular discharge patterns brought forth by changes of the weight of the otoliths induce harmless or even pleasant sensations as well as serious somatic disturbances associated with these changes. Thus, psychological and somatic effects of weightlessness may stem from the same labyrinthine source; and they may affect the well-being of the individual as well as his task performance.

The symptoms of weightlessness are manifested in many ways, and they are experienced so differently by man that thus far no clear picture about their effect has been obtained. Weightlessness nevertheless becomes an important environmental condition in the flight operation of tomorrow; and we must scratch together every bit of information available today. Unfortunately, it is true that it can be produced only in circumstances not very favorable for experimentation; and that zero-gravity can be achieved for only about 30 to 40 seconds at present. However, its importance cannot be ignored merely because of these limitations; and we believe that one can extrapolate more successfully and make valid predictions, the greater the amount of research data, and the

closer we inspect the variety of personal experiences obtained during the weightless state. An attempt is made in this report to present the existing data concerning subjective experiences during weightlessness, and to clarify some of the problems concerning human tolerance to exposure to short periods of reduced gravity.

Method

During the years 1955 and 1956, a series of experiments on weightlessness was conducted at the USAF School of Aviation Medicine. The study, performed by the Department of Ophthalmology in conjunction with the Department of Space Medicine, concerned eye-hand coordination under conditions of increased and decreased acceleration. In general, it was thought to study human behavior and to delineate the aeromedical implications of weightlessness.

Weightlessness, or at least a state of minimum gravity, was produced by flying the aircraft in a Keplerian trajectory or in a 40 degree dive. The aircraft used was a Lockheed T-33 A powered by a J-33 A-35 engine developing 4,600 pounds of thrust. The operational altitude for both flying maneuvers was between 20,000 and 17,500 feet. The pilot of the craft, Major HERBERT D. STALLINGS, USAF, flew the ascending arc of the parabola at full throttle, the descending part with about 75 percent r.p.m. in order to obtain weightlessness for about 25 to 30 seconds. During the dive, sub- and zero-gravity states of about 15 seconds were obtained. The study of eye-hand coordination consisted of a simple aiming test in the weightless state; and an additional experiment on stress was conducted by the Department of Pathology, School of Aviation Medicine, using some of the subjects and the same flight pattern in conjunction with our tests. Finally, a special experimental design was developed for assessing human tolerance during brief periods of weightlessness (see Appendix).

At the end of each sub- or zero-gravity flight the subject was asked to write a brief account of his experiences of weightlessness. He was told to describe rather casually his sensations including such phenomena as fall tendency or response, anxiety, and other emotional and autonomic reactions during reduced weight. Furthermore, the pilot and the flight surgeon who saw the subject during and after the flight, recorded symptoms of behavioral changes at the flight line. These data and the statements of the subject were collected at the end of the experiment and used for this study. Unfortunately, not all of the subjects complied with our request to furnish personal reports; and this is particularly true for those who evidently had shown adverse symptoms of weightlessness. Since not only interest and motivation but also age and flying experience may have some bearing upon the experience of reduced gravity, an abstract of the flight record of the individuals who participated in this study is given prior to the personal data. In all cases of subjective reporting, the story is given in the subject's own words. In the other cases, the observations are described as they were recorded by secondary sources and related to the particular individual. After all the data had been collected, they were classified with regard to the mode of personal experience.

Results

I. Sensations of Comfort and Pleasantness

1. Subject *H.D.S.*, pilot; age: 35; about 1,000 jet hours.

"During the experiment which involved numerous flights, over 200 parabolas and several different subjects, I had an opportunity to observe my personal reactions

as well as those of others. In the beginning of each parabola, the release of the positive pressure of the body against the air-frame tends to bring about a momentary dissociation between the pilot and the aircraft. As the zero-gravity state is continued, however, this mental condition seems to disappear. A slight change of pressure is noted in the ear drums but in no way impairs the hearing sense. A lifting sensation that resembles pressure on the lower portion of the eyeballs is felt but failed to prevent the eyes from functioning normally.

"Movements of the extremities is effortless and no trouble with muscular coordination was experienced. Orientation of aircraft in relation to the ground was unaffected. "Up" was still up, and "down" appeared to be still in the right direction.

"For my personal conclusion, the state of weightlessness is a pleasant feeling. There were no adverse effects to my sight, hearing, breathing, or muscular coordination during this condition. At first, there were slight errors in judgment as I reached out to change the power setting and to turn off the different fuel switches, but I found that automatic compensation took place during later parabolas. It would appear that from experience gained during this project, prolonged states of weightlessness would not impair the physical performance, physical condition, or mental well-being of the future pilots of space."

2. Subject *E.S.G.*, Captain, USAF (MC); age: **26**; flying and jet experience.

"On 21 September **1955** I participated in a T-**33** flight, during which time **9** parabolas were flown. Six were done while I was under the hood; the last three with the hood pushed back. My subjective reaction was essentially similar in both situations. During the actual period of weightlessness there was no unpleasant sensations. If anything, it was a mildly agreeable situation. My eye-hand coordination was only slightly impaired, if at all. If I had the opportunity of more practice under the weightless condition, I feel that my eye-hand coordination would rapidly become as good as under normal gravity. During the period of increased positive "*g*'s", I would start aiming for a point somewhat above the center, in order to hit the center of the target. If the "*g*'s" would decrease during this maneuver, my final mark would be somewhat above the central point. There was no similar necessity to aim for a point beneath the center of the target while undergoing the weightless condition."

3. Subject *R.S.F.*, Colonel, USAF (MC); age: **45**; long flying and jet experience.

"By constantly balancing the stilet in my hand and tossing it in the air I was able to detect rather accurately when entering the weightless state. In addition, a slight loosening of the seat belt caused me to rise from the seat and be held against the belt so that there was a total absence of "seat of the pants" sensation while in the weightless state. The mental sensation of weightlessness can best be described as one of incredulousness or even slight amusement. The incongruity of seeing objects and one's own feet float free of the floor without any muscle effort can only be described in those terms. It seemed that lifting my arms or performing movements with my hands had to be evaluated in the terms of resistance against overshooting."

4. Subject *R.M.R.*, 1st Lt, USAF; age: **31**; completed training as paratrooper in **1944**; flying experience; no previous jet experience.

"An initial reaction of acute anxiety and confusion lasting about five seconds followed by a marked feeling of well-being for the duration of the first parabola (six parabolas were executed). Upon entering the second parabola, a mild anxiety reaction lasting one or two seconds, followed by a feeling of well-being for the duration of the maneuver. Pleasant anticipation immediately preceding the remaining parabolas followed by the feeling of well-being. Little or no anxiety.

"The "feeling of well-being" is somewhat analogous to the relief experienced upon removing a heavy burden, such as a back pack, carried for a prolonged period. However, closer introspection seems to indicate that the sudden experience of "floating in space" temporarily allays or overcomes fear of falling; i.e., "I am weightless, hence I cannot fall". I have noted a similar paradoxical feeling of well-being during the experience of "weightless" free-falling in the course of parachute jumping.

"No visceral sensations were noted during zero-gravity. No subjective differences were noted between sensation of zero-gravity under the hood and with visual contact

Within the scope of the test described above, psychomotor adaptation to zero-gravity was extremely rapid. Normal gravity performance was obtained or excelled within 15 seconds of weightlessness."

5. Subject *J.B.B.*, A/2 C; age: 23; about 300 hours as passenger in conventional type aircraft; no previous jet experience.

"When we were over the testing area, Maj. STALLINGS told me to pull down the hood and prepare for the test. This I did. I held the stylus against the mask, and centered my eyes on the center of the target. My only thought at this time was to hear the signal to begin correctly. I first felt an increase in gravity, and then we went into zero-*g* condition. Maj. STALLINGS gave me the signal: zero-gravity, and I counted three, then I struck the target with a quick thrust. I was surprised at my close hit, because I had expected it would be difficult to hit. I had not previously spent any time in thinking where the hit was expected to be, but after the first seconds of zero-*g* I expected the hit would be high. I did not consciously try to compensate this expectation.

"During zero-*g* condition, I felt as if I were floating in the air, restraint only by the seat belt and shoulder harness. It seemed a rather pleasant sensation. I was not surprised or particularly impressed by the zero-*g* condition. When we recovered normal gravity, Major STALLINGS told me to change targets and he would tell me when I should strike the second target. The next five targets went by mechanically. I followed the same procedure as with the first target. I do not recall thinking about anything but concentrating intently on hearing correctly the instructions. When the six targets were finished, we did a roll to the right and then to left. I then raised the hood and Maj. STALLINGS demonstrated the zero-*g* procedure. I raised my hand under positive *g*'s and under zero-*g*. I had difficulty raising my hand when under positive *g*'s; and my hand seemed to float under zero-*g*."

6. Subject *W.J.Y.*, A/2 C; age: 22; about 300 flying hours; previous jet experience in 5 rides with B-57.

"Major STALLINGS gave me a final briefing on the test as we climbed to 20,000 feet. After we reached altitude, I pulled the hood over my section of the cockpit. We cleared the area and dropped off into a dive to gain airspeed. Major STALLINGS counted off the seconds before pullout so that again, as through the entire flight, I was forewarned of the maneuver.

"The pullout was about 3 *g*'s for a five second duration; then over the top and into the weightless condition. I made my strike and informed the Major. We then prepared for the succeedings runs and accomplished them in like manner. At the end of the last run we climbed to 20,000 feet and did our two rapid aileron rolls. One to the left and one to the right. The rolls didn't seem to have any effect on my sense of balance nor did I feel sick at any time. I kept track of the position of the aircraft by means of the artificial horizon.

"At the completion of the rolls I pulled the cockpit hood off and Major STALLINGS put the aircraft into a sustained parabolic path to give me a chance to mentally record my feelings and reactions while in a weightless condition.

"The weightless condition brought on an extreme feeling of well-being and comfort. At no time did I have the sensation of falling. The sensation of lack of physical support was also strangely missing. It was what I would suppose animated suspension might feel like. All my internal organs were comfortable, and I maintained normal mental activity. As the period of weightlessness lengthened I could feel my body relaxing. Actually, I've never been so bloody comfortable in all my life; and I think that if I had my choice of places to relax, a weightless condition would be definitely it. I must add though, that at no time did it have a drugging effect on me. I feel perfectly confident that I could carry out any assigned duty for the usual length of time without any interference other than teaching myself to coordinate my muscles under a weightless condition."

7. Subject *N.G.M.*, 1st Lt, USAF; age: 28; 1600 hours as fighter pilot; gunnery instructor since 1953 on T-33, F-80 A, B, C, F-84 G, and F-86 E and F.

The subject took a pad along during the flight and made short notes after the dives and parabolas. The flight pattern consisted of 4 dives, the first three with hood closed, and one series of four parabolas producing practical weightlessness up to about 30 seconds. The subject unfastened the safety belt during the parabolas and let himself float in the cockpit. He had no sensations of motion during the weightless state.

Here are his notes:

1. Dive: felt light (enjoyed it).
2. Dive: same feeling.
3. Dive: same feeling, no sensations (of motion, that is. The author).
4. Dive: no difference.
5. No difference (no belt).
6. No difference, enjoyed.
7. No difference, enjoyed.
8. No difference, enjoyed.

The subject supplemented his statements during the interview following his flight by telling about experiences of weightlessness during gunnery missions. He feels that jet pilots may have the best tolerance to sub- and zero-gravity.

8. Subject *L.A.K.*; Major, USAF (MC); age: 40; about 250 hours conventional type flying, including 6 weeks' flying training; 14 jet hours in T-33.

"During pushover (with hood closed and eyes open) slight but definite sensation of viscera being displaced upwards. No nausea, no disorientation with respect to cockpit environment. During weightless dive pleasant sensation of complete relief of muscular stresses. Part of this sensation might have been due to release of weights of clothing, chute, and helmet. No loss of motor coordination on attempted reaching for controls and instruments. Reaction effect of pushing against floor, raising arms, etc. not tested, as seat belt kept fastened. Pullout not remarkable.

"*Hood closed, eyes closed:* Physical sensations identical with dive 1. No sensation of disorientation or falling. Sensation of floating on air. No concept of orientation with respect to any external reference. No dizziness or nausea. Pleasant sensation of release of all muscular stress.

"*Dive 3: Hood open, eyes open.* Sensations same as for dives 1 and 2. No discomfort, no disorientation. Visual reference with ground provided no sense of illusion. No dizziness or nausea. No sense of falling or loss of support except as visual orientation demonstrated position and direction of movement with respect to plane of earth surface. Arms and legs were raised, and weightless state demonstrated with small free floating object in cockpit. I would describe the entire sensation as very pleasant.

"*Series of 4 consecutive ellipses:* During this phase of the flight, concentration was made on attempting to evaluate the effect of oscillating head motion (side to side) during zero-*g* ellipses and approximately 3-*g* pull-outs. During zero-*g* no untoward effects whatever were noted. During positive-*g* there developed, by about the last pull-out, slight sensations of nausea.

"During the ellipse the sensation was again one of pleasant lightness and stimulating release from some ubiquitous load. I had the feeling that once compensated by short training to operate in the zero-*g* medium coordinated movements might be much more rapid and accurate than under normal conditions. The alternation of zero- and positive-*g* produced no particular disorientation or vertigo inasmuch as ground reference was not lost.

"The letdown was performed rapidly, on the order of 5000 to 6000 fpm accompanied by much turning and banking. It was noted that even slight head movements under the conditions of continuous but changing degree of linear (dive brakes) and radial acceleration rapidly produced symptoms of motion sickness manifested by dizziness, sweating, and severe nausea, necessitating switch to 100% oxygen."

II. Sensations of Motion

1. Subject *J.R.W.*; A/2C; age 22; 250 flying hours during pilot training; 80 hours T-33.

"I felt no adverse effects during or after the zero-gravity period physically or otherwise. There was no symptom or change from the normal feeling that I noticed. As for subjective sensation and personal opinion, I like this state as a change from the ordinary, the floating feeling, at the weightless condition: it seems odd but not distasteful to be relieved of the task of holding up your own body and move without any effort."

2. Subject *J.M.Q.*, Major, USAF (MC); age: 42; about 400 flying hours; no previous jet experience.

"This afternoon I rode with Major STALLINGS in the SAM T-33 and experienced approximately 6 parabolic trajectory flights producing the short "zero-*g*" state.

"The most remarkable sensation was one of having begun a "back-flip" and becoming suspended with the back horizontal, face upward. I have done a fair amount of tumbling on gymnastic teams in high school and college. The sensation in the flight was one of having started a "back-flip" from a standing position and then becoming "hung-up" part way over — looking toward the sky but not completing the flip. It was important to note that there was no continuous feeling of motion once this feeling of a partial backward tumble reached the inverted position.

"There was no particular enjoyment nor dislike for the maneuver. Instead a feeling of indifference. No somatic sensations referable to viscera — such as sinking stomach, etc. Perhaps a longer flight with more runs would be indicated since there was no sensation of motion sickness from the few runs experienced.

"The flight was taken without a hood enclosing the cockpit so that visual references outside were available. However, I found myself ignoring the outside environment — not bothering to look for my orientation with reference to the ground."

3. Subject *S.J.G.*; age: 46; flying experience as glider pilot and passenger in conventional type aircraft; 1 jet hour.

"The one-hour familiarization flight in the T-33 included 3 parabolas with sub-gravity states lasting about 15 to 20 seconds each. The maneuver started with an increase in acceleration of about 3 *g*'s, then a short subgravity state of about 5 seconds during ascend and about 10 seconds during the dive after the pushover. During recovery, about 2—3 *g*'s were indicated.

"I had my eyes open during the first sub-gravity state. Nothing peculiar happened short of the feeling of hanging loose in the shoulder harness during the initial fall sensation which felt like that experienced during a sudden down-draft. I looked at the *g*-meter and saw the pointer on zero. There was also a short feeling of being slightly rotated around the lateral axis of the body like during a swan dive. This occurred during the push-over and may be due to the pitching movement of the airplane. No feel of up and down during the weightless condition; but pronounced weight sensation directed toward seat and feet during pull-out.

"I closed my eyes during the second sub-gravity maneuver. There was no apparent movement of the reddish lid background; but the eyes were closed after the zero-state had been reached. The orientation was completely lost during this phase but shoulder harness and safety belt furnished intermittently tactile clues as to suspension. The personal sensation associated with it was not unpleasant nor scaring; but uncomfortable feeling during the pull-out. This caused a slight attack of nausea; and I switched to 100% oxygen and had temperature lowered.

"I let the safety pin float during the third parabola, but it floated for 3—4 seconds only during the last part of the dive. During all three parabolas, the movement of the aircraft and slight accelerations served as orientational clues. The feeling of unpleasantness increased and I had slight attacks of motion sickness during the flight, was fatigued afterwards, and had headaches until about 3:00 p.m.

"The second flight of about 1 hour included four push-overs and sub-gravity for 15—20 seconds each. During the entry into the parabola, I felt a slight lift sensation with dangling in the harness and safety belt. There was a definite sensation of falling during the transition from increased to decreased gravity enhanced through the diving experience in the plane. Subjective sensation was not too pleasant.

Vol. 2 1956

"The third flight involving the aiming test was very comfortable, and I felt no unusual strain during and after the flight.

"No difficulties were observed during the sub-gravity state in flight test No. 4. The experiment was closed with two slow rolls in either direction. This caused an illusion of apparent motion just like in the BARANY chair. Furthermore, a slight dizziness and motion sickness spell was felt, so that I switched to 100% oxygen during the return home; but this may have been due to the increased acceleration during pull-out and the rolls, because I felt all right during the sub- and zero-gravity states.

"There was no sensation of being hindered during jabbing at subgravity. Moving the arm is very light since the arm tends to float during aiming and hitting. I had a scotoma for about 20 minutes 1 hour after landing."

The experiences in the additional flights can be summarized in that the weightless condition was neither a very pleasant sensation nor was it associated with severe symptoms of motion sickness. In some of the experiments the subject felt quite well, in others a slight dizziness, sweating, headaches, and fatigue were noticed. Concentrated insight during weightlessness with eyes closed yielded a feeling of backward rotation which started with the sensation that the head gets bigger and flips backward, and then the body follows as if one were in an inverted position. However, no sensation of falling or of moving with increased velocity was observed during this state.

III. Sensations of Unpleasantness and Psychosomatic Symptoms

1. Subject *J.R.K.*, Captain, USAF (MC); age: 31; about 1000 hours flight in conventional type aircraft; two hours jet flying including acrobatics in T-33.

"Following take-off climbed to 20,000 ft. and leveled off. Flew straight-and-level for several minutes prior to parabola flight. No apprehension — no evidence of motion sickness. Had previously flown in excess of 1000 hrs. including 2 hrs. in T-33 performing acrobatics (1 week ago) with no evidence of motion sickness.

"With hood in place pilot begun lst series of 6 parabolas with weightless or zero-gravity state produced for 10 to 15 seconds.

"Following 1st and 2nd parabolas had a feeling of discomfort — hunger sensations — uneasiness and slight fatigue. The feeling of nausea increased on fourth parabolic maneuver; switching to 100% oxygen brought no appreciable relief. Had sensation of increasing uneasiness and nausea. At the height of the parabolic arc it felt like my stomach was in my throat; I begun to look foreward to the plus *g* maneuver on pull-out at which time my stomach would feel like it were in proper position again. At the completion of the fifth zero-gravity state I knew it would only be a matter of time before an emesis would occur; I was aware of a slight regurgitation on the fifth. Fought the sixth maneuver desperately with continued swallowing, holding my mask in place, with burp bag in readiness. Had we continued the procedure one or two more times I would have been unable to retain the small breakfast I had consumed that AM.

"At the completion of the parabolas 2 rolls were performed with no increase in symptomatology. I noticed no unusual equilibrium disturbances during the flight.

"Following completion of flight felt uneasy and fatigued. Did not return to normal state until after a heavy noon meal."

The subject was flown in accord with our new flight pattern five months later. He reported the following experiences during the second experiment:

"Following take-off we developed a runway trim in full down position which was controlled after 5 minutes, and then climbed to 20,000 feet and leveled off. Unable to close instrument hood — wedged between seat and canopy — to simulate hood, I lowered visor and stared directly at cockpit instruments.

"First dive — normal sensations (eyes open). Second dive — sensation of floating out of seat and begin to turn in backward sommersault. Third — by looking outward

normal sensation of raising out of seat, falling weightless. Fourth — suspended arms and pencil in midair.

First parabola — looking at instruments: normal sensation of zero-gravity, floating out of seat, etc. Second parabola — moving head in vertical plane slowly — no unusual symptoms. Third parabola — moving head in horizontal plane — no vertigo. Fourth parabola — combining vertical and horizontal head movements — no disorientation.

"During last two parabolas switched to 100% oxygen; had slight "giddy" feelings in stomach but nothing to compare with previous flight. Two slow rolls to right and left — no untoward reactions. Had eaten a bowl of cereal and milk and slice of toast just prior to flight which may have helped to prevent nausea experienced on first flight."

2. Subject *C.P.D.*, Aviation Cadet, USAF; age: 20; active in flying training as pilot trainee; some jet experience in T-33.

The subject experienced the first troubles on the merry-go-round and on the Ferris wheel. He is highly motivated for flying. First symptoms of air sickness during primary flying. He vomited already in the Piper Cup. Later difficulties especially during stalls and acrobatics.

The subject flew parabolas with Major STALLINGS on August 10, 1955. He reported that he became motion sick through changes in acceleration. He observed no unpleasant feelings during sub- and zero-gravity, but the changes in stomach weight seemed to have produced symptoms of nausea. He let his arms float during the weightless state.

Vol. 2 1956

Major STALLINGS reported that the patient became sick during the weightless state; he observed him in the rearview mirror and cut the flight short because of the patient's complaints, which the latter described as 'getting hot', and feelings of nausea and the urge to vomit. The pilot flew two continuous slow rolls at the end after the patient had 100% oxygen and cold air.

3. Subject *A.G.B.*, T/Sgt, USAF; age: 35; 1500 pilot hours; several flights as passenger in jet type aircraft.

"At approximately 1100 hours, 11 October 1955, Major STALLINGS, Pilot, and I took off in T-33 for my first flight at zero-gravity. Upon reaching proper altitude I pulled the hood over rear cockpit, and awaited my instructions from Major STALLINGS. I had no visual reference with the horizon, nor anything outside of the cockpit. The first run at zero-gravity was uneventful, and I performed my task. During the second run, after I performed the task, I had a sensation of feeling that I was going over (float or fall) the instrument panel. I was not scared, but I wanted to place my hands on the instrument panel to catch myself, but I knew I was not going to move, and I kept my hands to my lap. After the third run I complained to Major STALLINGS that I was sweating and asked for lower temperature and better ventilation, and he adjusted same. I noticed a feeling of nausea. After the fourth run, and after performing task, the feeling of nausea increased. After performing the task on the fifth run I again had the sensation of going over the instrument panel, but again kept my hands in my lap. The nausea increased slightly, but the ventilation and decreased temperature had made me feel more comfortable. I switched to 100% oxygen temporarily, and tried to slow down or regulate my breathing in preparation for the sixth run. After the sixth run, my task was completed, the nauseated feeling increased again, and I explained this to Major STALLINGS, and he instructed me to go to 100% oxygen. I pushed the hood back, and Major STALLINGS performed one more run at zero-gravity, at which time I had visual reference with the horizon, and the nauseatic feeling was beginning to subside. At no time did I vomit nor have a feeling that I was at the verge of vomiting, although the nauseated feeling was there.

"I had an ill fit in my oxygen mask, and was quite uncomfortable while under the hood and subjected to 1.5 *g* and zero-gravity. For about two hours after the flight, and even though I had eaten lunch, my stomach had a mild upset feeling. Upon arising the morning of 12 October 55 my ears were plugged, with a very mild

occasional pain. This I believe to be due to 100% oxygen breathing, as it has previously been explained that this is a possible after-effect."

The subject repeated the zero-gravity experiment on November 2, 1955, but did not turn in a report about his personal experience during this flight. He felt "normal" according to his own statement and that of the pilot. Since the subject was under the effect of drugs (Benzedrin) at that time, the result is not conclusive.

4. Subject *F.G.H.*, A 2/c; age: 20. A few passenger hours, no previous jet experience.

The subject participated in an experimental zero-gravity flight on December 5, 1955 from 14^{55} to 15^{25} p.m. The flight consisted of dives rather than parabolas for obtaining zero-gravity yielding no noticeable increase of *g* during recovery. The subject developed extreme nausea after three zero-gravity states and vomited during the flight. He would not participate in further flights and did not turn in a report on his personal experiences during the weightless state. He was free of cold, allergy, etc., and had no medication in the last 24 hours before the flight.

5. Subject *F.N.R.*, Captain, USAF (MC); age 27; appr. 150 passenger hours in conventional type aircraft; no previous jet experience.

"During the first episode of weightlessness in which the canopy canvas was pulled forward and closed, I had the particular sensation of levitation. It was very easy to breathe, I had no sensation of nausea and everything seemed delightful.

"During the second weightlessness test in which my eyes were closed, I had the sensation that I was in nowhere particular due to the fact that I had lost the visual stimulus of the cockpit. However, I felt the same way, very light, as if floating in the air but there were no untoward effects.

"During the third episode of weightlessness I floated a burp cup suspended in the air and it was very easy again and pleasant to feel sensation.

„In the series of parabolas I had some sensation of nausea it seemed following each sensation of positive *g*. I felt no sensation of nausea during the positive *g*, but when I left the duration of positive *g* and entered the field of zero-*g*, I felt somewhat nauseated. However, there was no salivation although there was some slight generalized sweating. I was able to shake my head successfully very easy. No sensation of difficulty encountered in weightless period. Hard to shake head up and down under 3 *g*'s; no trouble to and fro.

"During the two rolls, one to the left and one to the right, I experienced the sensation that I was looking into a large spherical mirror but this did not seem to have any ill effects. My eyes were focused on the horizon and the clouds and I did not close them during any of the rolls.

"After finishing the rolls we flew for approximately ten minutes over the city of San Antonio and surrounding area and then returned home. When we made the initial dive to descend I began to feel somewhat nauseated and although we left 20,000 feet, by the time we hit 12,000 feet I began to have emesis. We then returned home and landed uneventfully.

"Immediately on going home I felt very limp and weak, somewhat tired and sleepy. I rested for approximately an hour and a half to two hours and ate some food and then felt much better. Throughout the afternoon following the flight I felt somewhat fatigued generally with occasional wave of nausea. However, I was able to carry out my work satisfactorily."

Discussion and Conclusions

To date, the experiences of 16 human subjects have been studied in controlled experiments yielding more than 300 dives and parabolas. During the brief exposures of 10 to 30 seconds of practical weightlessness, various degrees of tolerance to this state were observed; and some of the individuals' experiences varied when the experiment was repeated. From the reports given in the preceding paragraphs it appears that exposure time and practice seem to be of great importance for the behavior in and the adaptation to the weightless state.

However, it has been voiced that one cannot generalize from these short exposures because they do not permit extrapolations as to either adjustment of the organism to weightlessness, or to the aggravating effects of the autonomic disturbances observed. SIMONS [18] (1955) is somewhat critical in this respect by stating that the motion sickness syndrome normally needs some time to develop; and he writes in this connection:

"When the ocean suddenly becomes rough, it takes an appreciable time of exposure, something on the order of 15 to 20 minutes, before most neophyte passengers become thoroughly sick. Many hours later the seasoned sailors are still unaffected. There are many similarities between the factors producing motion sickness and its possible counterpart, space sickness. The differences are sufficient that there may or may not be the same 20-minute latent period upon initial exposure with acclimatization after repeated or prolonged exposure."

This situation is to some extent similar to that of about 50 years ago, when the WRIGHT brothers succeeded in maintaining their craft airborne for about the same period of time as we do today in the weightless state. There also were some doubts at that time as to whether the exposure of the human body to speed and acceleration would be harmful. Some of the differences between air sickness on the one hand, and "space" sickness on the other hand, are based upon the difference between conventional flying and space flight; and they must be considered with respect to the physiological and psychological factors involved.

The moment man travels in any kind of vehicle — train, car, boat or aircraft — he is exposed to motion. We know that individuals differ very markedly as to their motion sensitivity. The chain reaction of physiological events which lead to motion sickness is set off by changes in motion rather than by motion itself; especially if the person is susceptible and unaccustomed to stimulation of our gravireceptoric sense organs. Moreover, inconsistent sensations through the eye, the vestibular organ, and the proprioceptors may produce psychosomatic disturbances when a conflict arises between sensations closely related to the autonomic nervous system. If, on the other hand, the organism is under a heavy stress — for instance during high accelerations — the effect is not motion sickness but injury and collapse. All this can happen during conventional flights.

On the other hand, in space flight the state of zero-gravity will prevail, as already mentioned. In this case changes in motion or acceleration will not occur, but the gravireceptors may be in a state of stimulation, noticeable or subliminal. Moreover, if there is no sensation of motion and acceleration, the gravireceptors of the labyrinth and the peripherally located mechanoreceptors are more probably not stimulated at all. This is what actually happens in the weightless state: Practically all of our subjects reported sensations of rest or "floating"; a few persons observed sensations of motion during the transition phase. This seems to indicate that in the first case the otoliths do not register in spite of the fact that the subject is moving toward the center of the earth with an acceleration of 9.81 m per second, per second; and that in the second case they may discharge impulses at a rate which is characteristic for weightlessness, as SLATER hypothesized already in 1952 [19]. If, then, the individual finds himself in the gravity-free state, no further changes of acceleration or gravity will occur except those elicited by his own voluntary movements. But already BALLINGER has stated — and this was verified by our subjects — that voluntary head movements during weightlessness do not produce untoward effects [21].

This means that the critical phase appears to be the transition from one state into another; and as a matter of fact, we cannot identify the source of the

feelings of unpleasantness and the psychosomatic disturbances reported by some of our subjects very accurately as yet. There is some evidence that the adverse effects are brought about through changes. Hence, we have good reason to assume that persons who can stand the transition into zero-gravity will continue to feel all right during prolonged states of weightlessness. Those cases, moreover, which showed improvement through repeated exposure, indicate that tolerance to the transition phase can be increased by repetition. Since it was shown experimentally by HENRY, BALLINGER and others (1952) that the weightless state itself does not cause disturbances of the circulatory system, longer exposures may not include more hazards than short exposures [20, 21].

The psychological factors also seem to be of importance. According to STEELE (1956), motion sickness is more readily understood in terms of the information handling capacity of the brain; i.e., the effort expended by the individual to remain oriented, instead in terms of overstimulation [22]. Several of our subjects reported sensations of motion and position very different from the actual situation. They also agreed that they were completely disoriented when they closed their eyes and discarded the proprioceptive stimuli. Hence it seems that some of the motion sickness symptoms may be produced by the sensory inconsistencies and the final breakdown of the subject's frame of orientation.

In a similar way, SIMONS (1955) introduced the concept of "mental set for falling" into the discussion of motion sensitivity during space flight [18]. It seems now that some individuals may develop such set more easily than others, whereas certain persons do compensate for noticeable stimulation of the gravireceptors during the weightless state by means of rational reasoning. One of our subjects put it this way: "... I am weightless, hence I cannot fall." If we assume that the psychological factors associated with the experience of weightlessness are subjected to learning, we also may conclude that the individual will adjust better, the more he improves his ability to remain oriented.

The serious functional disturbances observed during our experiments occurred mainly with persons having a relatively low resistance to motion sickness. Patient *C.P.D.*, for instance, was found to be very susceptible to changes in acceleration. He was tested with the EXNER Spiral, and the after-effects of a 30-second exposure were relatively long (28, 37, and 25 seconds). The differences of the after-effects between right and left rotation in the BARANY chair were very pronounced (14.25 vs. 23.0) showing a high sensitivity to labyrinthine stimulation in one direction. He also reported hot and cold feelings after this test at 20 r.p.m. The general diagnosis through the Flight Surgeon was "chronic and severe motion sickness in a predisposed individual."

The other case of high motion sensitivity is Subject *F.N.R.*, who enjoyed the weightless state as an unusual environmental condition but developed the first symptoms of nausea already during the dives. We also saw subject *F.G.H.* coming back from his flight showing severe symptoms of nausea and motion sickness, which incapacitated him for the rest of the day. Although these cases do not permit definite conclusions as to the contribution of sub-gravity to the symptoms of motion sickness, there seems to be enough evidence to assume that persons who are particularly sensitive to stimulation of the gravireceptors will also be inclined to develop autonomic disturbances during weightlessness.

Summing up the discussion we can say that there are considerable differences among personal experience of the weightless state. While the majority of our subjects enjoyed being partly or practically weightless, a few cases reported symptoms of motion sickness, the reasons for which could not be determined as yet. If changes of gravity are the cause, transition from one state into another

will be critical; but no detrimental effects are to be expected in the zero-gravity state. If a hypersensitivity to unusual stimulation of the gravireceptors is the cause, prolonged states of weightlessness may aggravate these symptoms. Upon these premises one can assume that the first group can endure longer periods of sub- and zero-gravity without incapacitating attacks of "space sickness"; whereas the members of the last group will not be fit for space flying at all. This latter percentage does not seem to be alarming, however.

It seems to me that some progress has been made in attacking the problem of human tolerance to weightlessness since 1952, when SLATER presented his paper to the members of the Third International Astronautical Congress [19]. But a lot more remains to be done. The solution of our problem is quite important for the manning of space vehicles in the future. The crew of an artificial satellite, for instance, must live in the weightless state for days or even weeks. Space flight, on the other hand, including shuttle service to a satellite, will involve frequent changes of accelerative forces. Earlier calculations by GAUER and HABER (1950) and recent experiments by PRESTON-THOMAS, EDELBERG, HENRY, MILLER, SALZMAN, and ZUIDEMA (1955) indicate the high accelerations and their pronounced changes necessary to attain the escape velocity [4, 24]. The latter investigators presented evidence that "select crewmen can be expected to assist in the control of such a vehicle during the critical acceleration phases of the flight" [24]. Even if our evidence is by no means as clear cut as theirs, we nevertheless believe that selected crews will also be able to perform efficiently under sub- and zero gravity conditions.

Vol. 2 1956

The final word concerns the designer of the future space vehicles. Since physiological difficulties during weightlessness were expected, the introduction of a continuous slight acceleration as a sort of "quasi-gravity" was already mentioned by TSIOLKOVSKII and GANSWINDT at the end of the last century; and some of the modern engineers accepted this proposal as a necessity for their blue-prints. This, of course, is a complication which the designer wants to avoid; for every additional device and every kilogram load — not to speak of room and expenses — is a nuisance in a space craft more than in any conventional type of airplane. If we succed in solving the remaining problems of human tolerance to sub- and zero-gravity, we not only help the future space cadet to perform his job, but also the designer and the engineer by facilitating his task of constructing the hardware for the great venture.

Appendix

Instructions to the Subject on Experiment on Human Tolerance to Sub- and Zero-Gravity

1. This experiment is made to gather information about *your* experience of weightlessness. Read these instructions carefully and follow them through your flight.

2. There will be 4 dives from an altitude of 20,000 to 17,500 feet producing weightlessness for about 15 seconds. Pull the canvas in front of you during the first three dives and direct your attention exclusively to the sensations, feelings, and perceptions of weightlessness. Keep your eyes open during the first dive, have them closed during the second dive; and observe a floating object or your arms during the third one. Find out, how it feels to be weightless. This task requires insight and practice; that is the reason why we fly this maneuver three times.

3. Push the canvas back after the third dive and look outside during the fourth one. Does this make any difference to your perceptions and sensations in the weightless state?

4. There will be a short period of recovery during straight-and-level flying at 20,000 feet. If you are not sure about your experiences or want to try again under a certain condition, let the pilot know. The pilot will repeat the maneuver.

5. If you get motion sick or feel uncomfortable, communicate this to the pilot. He will adjust the temperature and return home. Switch to 100% oxygen.

6. If you feel comfortable, the pilot will fly a series of 3 parabolas, one after the other. This will produce practical weightlessness up to about 30 seconds in each parabola, and a radial acceleration of about 3 g's during each pull-out. Compare how this feels now. Shake your head slowly in the horizontal and vertical plane during the third period of weightlessness. Do you notice any changes in perception or even visual illusions during head movements?

7. If you should feel uncomfortable, direct your attention to exploring the cause. Is the feeling of unpleasantness enhanced during weightlessness or during the pull-out? If you get sick, tell the pilot; he will fly you home.

8. If you feel well and want to try, the pilot will conclude the flight by two slow rolls; one to the right and one to the left. Compare how this feels, and whether visual illusions occur during the maneuver.

9. Please render a written report about your personal experiences and your tolerance during the weightless condition. The more interesting experiences you can report, the better you can help us. If nothing seems of interest to you, sum your experiences up in about 4 or 5 phrases.

10. *Remember:* In a few years, people will have to live and work in sub- and zero-gravity for some hours and even days. Your contribution is essential for the exploration of space.

References

1. H. G. ARMSTRONG, H. HABER, and H. STRUGHOLD, Aeromedical problems of space travel. J. Aviat. Med. **20**, 383 (1949).
2. H. VON DIRINGSHOFEN, Medizinische Probleme der Raumfahrt. München: Oldenbourg, 1952.
3. S. J. GERATHEWOHL, Zur Frage der Orientierung im schwerefreien Zustand. From: Space Flight Problems (Sammlung Fachvorträge IV. Internat. Astronaut. Kongreß, Zürich 1953). Biel-Bienne: Laubscher & Cie, 1955.
4. O. GAUER and H. HABER, Man under gravity-free conditions. In: German Aviation Medicine World War II, Part I, Chapt. VI, pp. 641-644. Washington, D. C.: U.S. Government Printing Office, 1950.
5. H. HABER and S. J. GERATHEWOHL, Physik und Psychophysik der Gewichtslosigkeit. Weltraumfahrt **4**, 44 (1953).
6. H. HABER and F. HABER, Possible methods of producing the gravity-free state for medical research. J. Aviat. Med. **21**, 395 (1951).
7. H. STRUGHOLD, Space equivalent conditions within the earth atmosphere. Astronaut. Acta **1**, 31 (1955).
8. H. STRUGHOLD, Medical problems of space flight. Internat. Rec. Medicine **168**, 570 (1955).
9. ANONYMUS, Wie wird sich der menschliche Organismus voraussichtlich im schwerefreien Raum verhalten? Weltraumfahrt **2**, 81 (1951).
10. S. J. GERATHEWOHL, Physics and psychophysics of weightlessness: Visual perception. J. Aviat. Med. **23**, 373 (1952).
11. S. J. GERATHEWOHL, Comparative studies on animals and human subjects in the gravity-free state. J. Aviat. Med. **25**, 412 (1954).
12. H. J. A. VON BECKH, Experiments with animals and human subjects under sub- and zero-gravity conditions during the dive and parabolic flights. J. Aviat. Med. **25**, 235 (1954).
13. H. J. A. VON BECKH, Untersuchungen über Schwerelosigkeit an Versuchspersonen und Tieren während des lotrechten Sturzfluges. From: Space Flight Problems (Sammlung Fachvorträge IV. Internat. Astronaut. Kongreß, Zürich 1953). Biel-Bienne: Laubscher & Cie, 1955.
14. H. STRUGHOLD, Gravi-Receptors. 27th Annual Meeting Aero Med. Assoc., Chicago, 16-18 April 1956.
15. H. VON BECKH, Fisiología del Vuelo. Buenos Aires: Editorial Alfa, 1955.

16. L. Gougerot, Lois de Weber-Fechner et variations de la pesanteur apparante. Méd. aéronaut. **8**, 119 (1953).
17. S. J. Gerathewohl, H. Strughold, and H. D. Stallings, Sensomotor performance during weightlessness: Eye-hand coordination. 27th Annual Meeting Aero Med. Associat., Chicago, 16-18 April 1956.
18. D. G. Simons, Review of biological effects of subgravity and weightlessness. Jet Propulsion **25**, 209 (1955).
19. A. E. Slater, Sensory perceptions of the weightless condition. III. Internat. Astronaut. Congress, Stuttgart, 1-6 September 1952; and Annu. Rep. Brit. Interplan. Soc. **1952**, 342.
20. J. P. Henry, E. R. Ballinger, P. M. Maher, and D. G. Simons, Animal studies of subgravity states during rocket flight. J. Aviat. Med. **23**, 421 (1952).
21. E. R. Ballinger, Human experiments in subgravity and prolonged acceleration. J. Aviat. Med. **23**, 319 (1952).
22. J. E. Steele, The cause of motion sickness. 27th Annual Meeting Aero Med. Associat., Chicago, 16-18 April 1956.
23. H. von Beckh, Gravity changes in aircraft and ships. J. Brit. Interplan. Soc. **15**, 73 (1956).
24. H. Preston-Thomas, R. Edelberg, J. P. Henry, J. Miller, E. W. Salzmann, and G. D. Zuidema, Human tolerance to multistage rocket acceleration curves. J. Aviat. Med. **26**, 390 (1955).

Buchbesprechung — Book Review — Compte rendu

200 Miles Up. By J. GORDON VAETH. 2nd Edition. With 77 Figs., 261 pp. New York: The Ronald Press Company. 1956. $ 5.00.

The first edition of Mr. VAETH's book became one of the most useful and successful of the volumes dealing with the upper atmosphere. Part of the success can be attributed to the fact that this is still the most authoritative account of all phases of upper atmosphere research written in a simple, non-technical style. The other reason for its success is that in spite of its non-technical style the book is completely accurate and explains the new discoveries as well as the rocket and balloon vehicles used in upper atmosphere research. Last, but not least, there is the collection of excellent pictures (of which there are 77, most of them photographs). In this 2nd edition the author has revised his previous treatment, where necessary in the light of more recent developments, and has added a great deal of completely new material; in fact three new chapters. After bringing the Viking story up to date by adding a description of the most recent firings, the author discusses the future of upper atmosphere research, including the latest developments in the small rocket field, the *Rockoon* and the *Rockair*. One whole chapter is given over to discussion of minimum satellites and their application during the International Geophysical Year. The final chapter is given over to a brief discussion of space flight.

Among the many new features of the second edition one might mention the interesting discussion of the biological firings in which mice and monkeys were sent up beyond the atmosphere in *Aerobee* rockets and the implications of this work to space medicine.

S. F. SINGER, College Park/Md.

Errata

LEITMANN, G.: Stationary Trajectories for a High-Altitude Rocket with Drop-Away Booster. Astronaut. Acta *2*, Fasc. 3, 119 (1956).

p. 120: In the second line following eq. (1.1) it should read ... Auxiliary conditions are $s(0) = 0$, ...

p. 123: The simplified expression given by eq. (4.3) holds in vacuo only. The line following eq. (4.3) should read ... where $T = \int_0^s ds/v$ = time of flight.

Herausgeber, Eigentümer und Verleger: Springer-Verlag, Wien I, Mölkerbastei 5. — Für den Inhalt verantwortlich: Prof. Dr. Friedrich Hecht, Wien VIII, Alserstraße 69. — Druck: Berger & Schwarz, Zwettl, N.-Ö.